Contribution isotopique (δ13C, δ15N, δ18O, 87Sr/86Sr) à la connaissance de la mobilité, des pratiques pastorales et des rites dans les sociétés actuelles et anciennes de Mongolie

Nicolas Lazzerini

MUSÉUM NATIONAL D'HISTOIRE NATURELLE

École Doctorale 227
Sciences de la nature et de l'Homme : évolution et écologie

Année 2020 **N°attribué par la bibliothèque**
|_|_|_|_|_|_|_|_|_|_|_|_|

THÈSE

pour obtenir le grade de

DOCTEUR DU MUSÉUM NATIONAL D'HISTOIRE NATURELLE

Spécialité : Géochimie isotopique

présentée et soutenue publiquement par

Nicolas Lazzerini

le 8 juillet 2020

Contribution isotopique ($\delta^{13}C$, $\delta^{15}N$, $\delta^{18}O$, $^{87}Sr/^{86}Sr$) à la connaissance de la mobilité, des pratiques pastorales et des rites dans les sociétés actuelles et anciennes de Mongolie.

---

sous la direction de :	**Antoine ZAZZO**	**Directeur de recherche CNRS, UMR 7209.**	**Directeur de thèse**
	Sébastien LEPETZ	**Directeur de recherche CNRS, UMR 7209.**	**Directeur de thèse**
	Aurélie COULON	**Maître de conférences MNHN, UMR 7204 & 5175.**	**Co-encadrante de thèse**
devant le jury :	**Thomas TÜTKEN**	**Professeur, JG Université de Mainz (Allemagne)**	**Rapporteur**
	Robin BENDREY	**Maître de conférences, Université d'Edimbourg (Royaume-Uni)**	**Rapporteur**
	Valérie DAUX	**Professeure UVSQ, UMR 8212.**	**Examinatrice**
	Marjan MASHKOUR	**Directrice de recherche, CNRS, UMR 7209.**	**Examinatrice**
	Laurent SIMON	**Maître de conférences, UCBL, UMR 5023**	**Examinateur**

À mes grands parents

REMERCIEMENTS

Ce manuscrit de thèse ne serait pas complet sans que je remercie tous les gens qui m'ont accompagné, soutenu pendant ces trois années et demi.

Tout d'abord, je tiens à remercier particulièrement les membres de mon jury de thèse, mes deux rapporteurs Robin Bendrey et Thomas Tütken, ainsi que mes examinateurs Valérie Daux, Marjan Mashkour et Laurent Simon, pour avoir accepté d'évaluer ce travail de thèse plus ou moins proche de leurs thématiques de recherche.

Ensuite, je tiens absolument à remercier mes chefs Antoine Zazzo, Sébastien Lepetz et Aurélie Coulon pour leur soutien et leur encadrement tout au long de cette thèse. Je les remercie d'avoir accepté de me prendre en thèse sans me connaître vraiment et de m'avoir fait confiance pour cette longue aventure dans les steppes de Mongolie. Je remercie Antoine pour sa patience et sa pédagogie et ses conseils mais aussi pour sa disponibilité quotidienne tout au long de ces années afin de me guider, me former et m'apprendre à interpréter les résultats isotopiques, de me ramener régulièrement du beau matériel tout frais de Mongolie, mais surtout de ces longues randonnées au fin fond de l'Asie Centrale pour cueillir des fleurs indispensables pour ce travail de thèse. Malgré peu de restes archéozoologiques à se mettre sous la dent, je remercie Sébastien pour sa présence, ses remarques toujours constructives sur les résultats géochimiques et son aide inestimable en archéozoologie, pour un novice tel que moi. Enfin, je souhaite remercier Aurélie, qui a toujours été disponible, car bien qu'étant à Montpellier et moi à Paris, cela n'a jamais posé de problèmes de communication. R continuera à avoir de nombreux secrets pour moi mais grâce à elle, j'ai pu me dépatouiller avec mes innombrables données GPS et traitements statistiques.

Merci à Charlotte Marchina pour ses commentaires toujours pertinants et son aide inestimable en Mongolie, sans qui le terrain aurait été bien plus compliqué et de m'avoir fait découvrir une partie de la culture de ce si grand pays qu'est la Mongolie, pour lequel je garderai toujours un intérêt.

Je tiens aussi à remercier Laurent Simon et Vincent Balter pour leur investissement dans mes comités de pilotage, leur bienveillance et leurs remarques constructives qui m'ont aidé à faire le point et à avancer tout au long de cette thèse. Je les remercie de leur accueil lors de ces

nombreuses semaines passées à Lyon pour enchaîner les chimies et les encapsulages pour les nombreux échantillons que contient cette thèse.

Merci également à Denis Fiorillo, Michel Lemoine et Olivier Tombret qui grâce à leur expérience et leur bonne humeur m'ont aidé pour mes nombreux échantillons que ce soit dans leur préparation ou leurs analyses isotopiques. Je remercie également Aline Lamboux, Emmanuelle Alabalat, François Fourel et Philippe Telouk pour leurs expertises techniques à Lyon.

Merci aussi toutes les personnes d'AASPE, j'ai passé de joyeuses et enrichissantes années en découvrant une partie de l'histoire de l'humanité parmi vous. Merci également au pôle gestion et informatique, Isabelle Baly, Anne-Cécile Haussonne et Myriam Meziou, pour leur aide tout au long de cette thèse.

Un merci particulier aux éleveurs khazakhs pour leur accueil dans leurs magnifiques yourtes, pour le thé au lait et les beignets en abondance ainsi que le gras (ou viande grasse) et les pâtes fraîches. Merci à eux d'avoir accepté de poser ces colliers GPS sur leurs bêtes et à ces dernières d'avoir donné leurs corps à la science, même si un CAP boucherie aurait été un plus avant de commencer cette thèse.

Enfin, merci aux organismes qui ont permis de financer cette thèse, en premier lieu le CNRS LabEx BCDiv et le Muséum nationale d'Histoire naturelle, mais également le Ministère des Affaires Étrangères par le biais duquel j'ai pu aller en Mongolie.

Enfin, je tiens à rendre justice à tous ceux qui m'ont supporté que ce soit au labo ou en dehors, à ces compagnons de débats de société, de discussions scientifiques, de craquages nerveux ou tout simplement de café, de bière, de frites et de cinéma …

Je remercie tout particulièrement mes parents qui m'ont permis de faire des études longues et qui m'ont toujours soutenu dans les projets que j'entreprenais, malgré leurs doutes, en ayant une confiance sans faille.

Pour finir, je ne remercierai jamais assez Fanny Pagnat qui m'a toujours soutenue dans mes choix et qui a toujours été à mes côtés quoiqu'il arrive!

Merci pour cette thèse sur les biquettes, comme beaucoup d'entre vous le disiez.

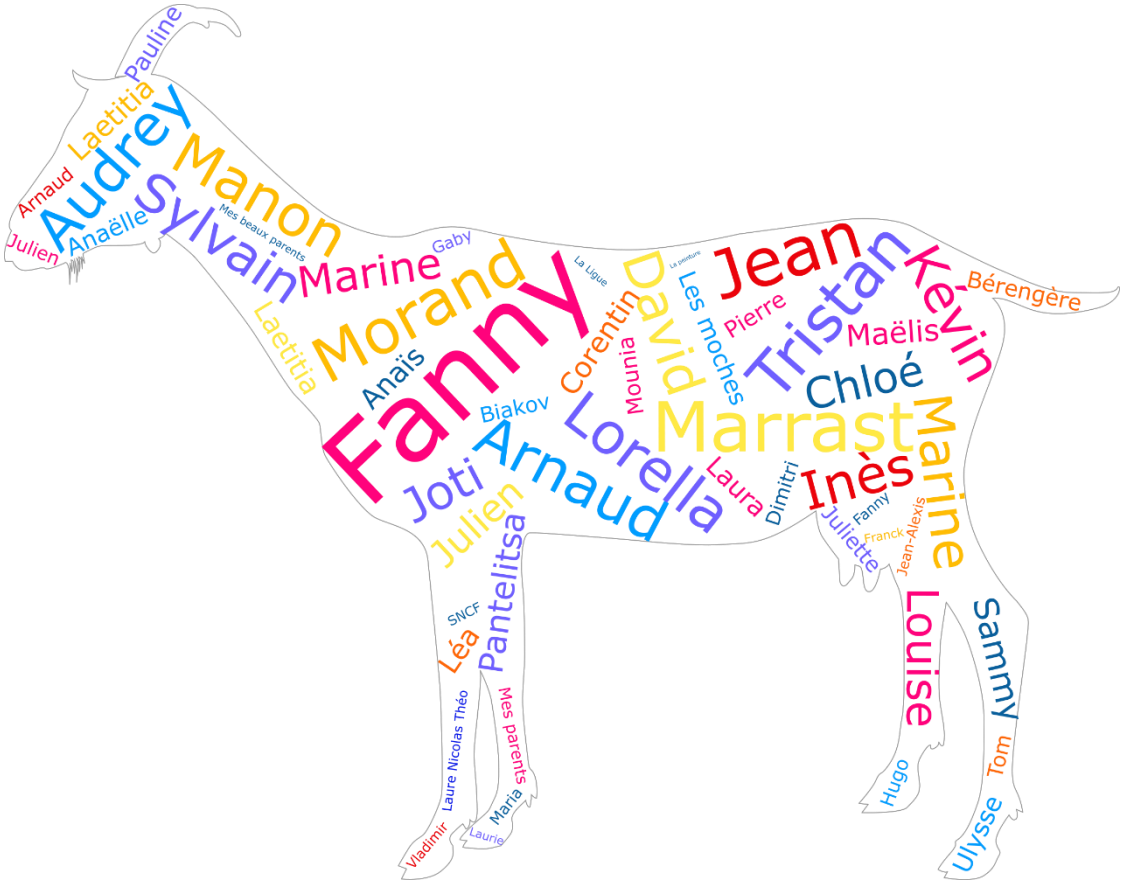
Pauline
Laetitia
Audrey
Manon
Arnaud
Sylvain
Anaëlle
Mes beaux parents
Julien
Gaby
Marine
Morand
Laetitia
Fanny
Anaïs
Bjakov
Joti
Arnaud
Julien
Pantelitsa
Léa
SNCF
Laure Nicolas Théo
Vladimir
Maria
Laurie
Mes parents
La Ligue
Corentin
Mounia
David
Lorella
Marrast
Laura
Dimitri
Les moches
Pierre
Jean
Tristan
Kévin
Bérengère
Maëlis
Chloé
Inès
Marine
Juliette
Fanny
Franck
Jean-Alexis
Louise
Hugo
Sammy
Tom
Ulysse

TABLE DES MATIERES

PARTIE I – INTRODUCTION GÉNÉRALE

Chapitre 1 – Généralités sur le pastoralisme extensif et la gestion des troupeaux

L'apparition des modes de vie agropastoraux, centrés sur une économie de production (agriculture et élevage), a constitué une véritable révolution pour l'humanité durant le Néolithique, impliquant un bouleversement social, technique, culturel et économique des sociétés (Vigne, 2017). Encore aujourd'hui, ce système de production est très répandu.

De façon générale, le pastoralisme regroupe les moyens de production consistant en une interconnexion de stratégies de gestion de troupeaux et de relations sociales qui se concentrent sur l'exploitation des ressources de ruminants domestiques (ovins, caprins, bovins, équins, camélidés) (Cribb, 2004; Little, 2015). En plus des ressources primaires que sont les troupeaux, les éleveurs peuvent obtenir des produits secondaires fournis par les animaux tels le lait, le fromage et le cuir. Le pastoralisme est donc caractérisé par une forte relation entre le bétail et les éleveurs. Les pasteurs emploient une large variété de pratiques/stratégies d'élevage dans le but de maintenir et éventuellement d'augmenter la production et la reproduction de leurs troupeaux. La saisonnalité est également un facteur important influençant diverses stratégies, que l'on retrouve au niveau de la disponibilité des ressources et de l'occupation des sites. En effet, l'un des principaux enjeux auxquels font face les éleveurs est de pouvoir maintenir l'accès pour leurs bêtes à des sources de pâturage suffisantes tant en quantité qu'en qualité nutritionnelle soit par la distribution de fourrage soit par le déplacement vers de nouvelles pâtures.

Les déplacements de troupeaux jouent un rôle central dans l'économie pastorale passée et présente. La mobilité pastorale est définie par une série de déplacements calculés qui varient en termes de temps, de distance et de durée, entrecoupés d'intervalles de sédentarité. Les schémas de mobilité vont de l'utilisation sédentaire de riches pâturages (peu de migrations), à la transhumance (migrations saisonnières d'une partie du groupe familial – Ferret, 2014), en passant par le semi-nomadisme (installation permanente du foyer) et le pastoralisme nomade (mouvement fréquent du foyer). Le rythme, les modes de déplacement, les degrés de mobilité et les territoires occupés dépendent d'une combinaison de paramètres tels que l'organisation socio-politico économique, l'environnement, le climat, le nombre et le type d'espèces élevées (Arbuckle and Hammer, 2018; Dong et al., 2011; Fernandez-Gimenez, 2000; Kerven et al.,

2006; Stépanoff et al., 2013). Les stratégies de mobilité pastorale couvrent un spectre entier, de la sédentarité totale à la mobilité extrême. Se déplacer permet aux éleveurs de récolter du fourrage dans une plus grande zone, d'utiliser avantageusement les ressources de différents types d'habitat (Fernández-Giménez et Febre, 2006) et éventuellement de gérer plus d'animaux que s'ils étaient sédentaires. La mobilité est aussi utile afin de réduire la probabilité d'être confronté aux aléas naturels comme la sècheresse, des hivers rigoureux ou à des problèmes politiques (Bassett, 1986).

Parmi les différentes formes que peuvent prendre ces déplacements, la mobilité verticale est une stratégie vitale communément utilisée par les éleveurs vivant dans des zones montagneuses (Finke, 2004). Le pastoralisme dans les environnements montagneux est largement répandu et se caractérise par une stratification des ressources selon l'altitude. Les éleveurs exploitent ainsi les variations de productivité des pâturages liées à l'élévation en déplaçant le bétail de pâture en pâture le long d'un gradient altitudinal afin de pouvoir faire paitre les animaux au mieux durant l'année sans épuiser les ressources. En effet, les différences de température et de précipitation entre les plaines et les hauteurs peuvent conduire à des pics annuels de productivité asynchrones. Généralement, les troupeaux sont placés dans les plaines en saison froide, moment où les conditions météorologiques et écologiques y sont favorables, et dans les alpages durant l'été dès que les températures deviennent plus avantageuses au développement de la végétation (Ferret, 2014; Marchina, 2019; Salzman, 2002). Cette mobilité saisonnière peut se dérouler selon diverses stratégies parfois très complexes. L'éleveur peut se déplacer une seule fois, rapidement, entre la plaine et les pâtures d'altitude ou réaliser une série de déplacements successifs avec des campements intermédiaires profitant alors de pâtures d'élévation moyenne. De plus, la fréquence des déplacements peut grandement varier selon la saison, l'accès aux pâtures, les conditions locales des pâturages, mais également les liens entre les différents éleveurs.

La question de l'abattage du bétail est un autre paramètre central de la gestion des troupeaux que nous allons aborder dans ce manuscrit. L'abattage d'un seul animal peut en effet fournir de la nourriture pour un petit groupe de personnes ou une famille sans gaspillage et sans épuiser de manière significative les ressources du troupeau. Généralement, les études portant sur l'abattage s'orientent vers la caractérisation de l'âge au décès, puisque ce dernier dépend de la nature de la production souhaitée. Ainsi, la production laitière intensive implique un sevrage précoce, s'accompagnant souvent de stratégies d'abattage axées sur les jeunes individus afin de maximiser les prélèvements de lait pour les éleveurs ; tandis qu'un système mixant production

de lait et de viande implique un sevrage moins intensif et un abattage différé (Payne, 1973; Vigne and Helmer, 2007). Mais cet abattage dépend par ailleurs d'autres critères, notamment saisonniers, liés aux pratiques pastorales, aux déplacements des groupes humains, aux habitudes alimentaires ou encore à la conservation des produits. Les éleveurs nomades de Mongolie, par exemple, voient leur consommation de viande augmenter pendant l'hiver parce qu'ils voudront éliminer les animaux plus plus faibles afin de garder la taille du troupeau à l'équilibre et de mieux le nourrir (Bruun, 2006; Fernández-Giménez et al., 2012). L'abattage hivernal du cheval permet, toujours en Mongolie, de faciliter la conservation de la viande. En outre, la viande équine est considérée plus énergétique et donc plutôt consommée à cette époque de l'année (Ferret, 2009; Marchina et al., 2017). Dans d'autres systèmes pastoraux, les animaux ne sont abattus que rarement et seulement pour des occasions rituelles et des fêtes d'importances particulières (Abu-Saad et al., 2001; Galvin and Little, 1999).

Malgré le rôle central du bétail dans le mode de vie pastorale, on sait relativement peu de choses concernant la mobilité et les stratégies de gestion des troupeaux par les éleveurs des sociétés passées, ainsi que sur l'influence de ces dernières sur la structuration des communautés. La recherche en archéologie s'est traditionnellement portée sur l'émergence de la domestication des animaux plutôt que sur la mise en place et la transformation des stratégies d'élevage de ces derniers. Ces différentes stratégies ont effet contribué à l'émergence de formes variées de pastoralisme et notamment du nomadisme que l'on retrouve globalement (p. ex. Lynch, 1983; Niamir-Fuller and Turner, 1999; Dong et al., 2011; Stépanoff et al., 2013; Liechti and Biber, 2016; Arbuckle and Hammer, 2018). Généralement, les sociétés complexes à grande échelle, où les communautés sont plus larges et plus intégrées, sont apparues après l'adoption de l'agriculture et d'un mode de vie sédentaire permettant des interactions plus régulières et intenses. Cependant, de nombreuses sociétés pastorales nomades, caractérisées par leur grande mobilité et leur faible densité ont présenté des caractéristiques d'organisation sociale complexe sans que l'on puisse comprendre comment une telle intégration et organisation a pu se former et se maintenir. L'identification et l'explication de la riche diversité des stratégies de subsistance et de la mobilité des pasteurs sont essentielles pour s'interroger notamment sur le rôle des animaux et des déplacements dans ces processus plus larges associés à l'émergence et à l'évolution de l'organisation sociale, des systèmes idéologiques et à l'établissement d'entités politiques dans certaines sociétés pastorales. (Hammer and Arbuckle, 2017; Honeychurch, 2015a, 2013; Honeychurch and Makarewicz, 2016; Houle, 2015; Makarewicz, 2011; Porter, 2012).

Cependant, identifier et interpréter les traces de ces groupes mobiles ainsi que leurs interactions avec leur bétail et leur environnement dans le registre archéologique est particulièrement difficile en raison des vestiges temporaires (p. ex. habitations, enclos) laissés par ces modes de vie. En effet, cette mobilité qui varie facilement dans le temps et dans l'espace n'offre que très peu de présence matérielle directe. Des vestiges de campements, de sites rituels tels que des monuments funéraires, de l'art rupestre ou encore des foyers sont les rares traces témoignant des modes de vie et des stratégies de gestion (p. ex. Agirre-García et al., 2018; Martín et al., 2016; Mashkour and Abdi, 2002). Les tentatives d'identification des mouvements passés se sont généralement concentrées sur la comparaison de la distribution spatiale des anciennes occupations pastorales avec celles observées dans les enregistrements ethnographiques ou les données zooarchéologiques qui évaluent la démographie et la structure des troupeaux (Arnold and Greenfield, 2017; Elliott et al., 2015). Afin de mieux comprendre la configuration spatiale, la motivation des déplacements et les liens sociaux au sein des communautés, une nouvelle approche est parfois utilisée qui se définit par le concept de « paysage pastoral » (*pastoral landscape*). La méthode consiste à porter un même regard sur les différents types de sites (campements saisonniers, sites d'art rupestre, monuments funéraires) qui constituent la zone où se déroulent les interactions entre les hommes et leurs bétails. Ces informations sont comparés avec des paramètres géographiques et la saisonnalité de productivité des pâtures dans le but de modéliser à partir des SIG les déplacements des éleveurs nomades sur la base de couloirs de déplacement potentiels moins coûteux (Frachetti, 2008; Frachetti et al., 2017; Seitsonen et al., 2014). Toutefois, ce genre d'approche se concentre sur les restes laissés par l'homme, ne représentant qu'une partie de l'occupation du territoire, alors que l'animal fait entièrement partie de ce paysage et en est un acteur majeur. Dès lors, la recherche zooarchéologique s'est beaucoup intéressée à certains des aspects des relations homme-animal comme celles liées à l'abattage ou à la production de produits carnés. Les approches concernant la reconstruction de la mobilité des pasteurs se sont, elles, basées sur des mesures largements indirectes, mentionnées précédemment. Elles ont permis de mieux comprendre les stratégies de subsistance des éleveurs et l'utilisation du paysage dans divers contextes environnementaux et sociaux. Malheureusement, l'étude seule des conditions de mort des animaux ne permet pas d'aborder l'ensemble des caractéristiques géographiques et saisonnières de la gestion des troupeaux. Or, l'étude des traits de vie de l'animal et leurs interactions avec leur environnement est une clé d'entrée essentielle pour comprendre les interactions homme-animal-environnement dans ces sociétés pastorales. C'est ce que permet l'utilisation des techniques d'analyse de la géochimie isotopique. Ces techniques livrent en effet

des informations sur l'histoire alimentaire, la mobilité et l'environnement des animaux contribuant à révéler les pratiques des hommes qui les ont élevés.

Chapitre 2 – L'apport des isotopes stables pour comprendre la gestion des troupeaux passés

2.1. Introduction aux isotopes stables et généralités

L'analyse de la composition des isotopes stables des restes archéologiques des animaux domestiques peut être utilisée pour déterminer différents paramètres des pratiques d'élevage, tels que la mobilité ou la saison d'abattage. Actuellement, les éléments majoritairement ciblés par les études archéologiques sont le carbone, l'azote, l'oxygène et e strontium dont les variations de compositions isotopiques sont influencées par le climat, la géologie, la végétation, l'alimentation et la physiologie des individus.

Les isotopes d'un élément chimique possèdent le même nombre de protons, mais diffèrent par leur nombre de neutrons. Un isotope avec un petit nombre de neutrons sera considéré comme l'isotope léger (commun) et à l'inverse l'isotope avec le plus grand nombre de neutrons sera l'isotope lourd (rare). Dans le cas du carbone, par exemple, il existe deux isotopes stables, le ^{12}C et ^{13}C avec respectivement 6 et 7 neutrons. La proportion d'isotopes lourds par rapport aux isotopes légers est définie par le rapport isotopique (R). Contrairement aux isotopes radioactifs (par exemple le ^{14}C), les isotopes stables ne se désintègrent pas avec le temps et les rapports se fixent et se conservent dans les milieux, reflétant les processus et environnements inorganiques et biogènes dans lesquels ils se sont formés. Toutefois, les rapports isotopiques peuvent varier en fonction des molécules et des réservoirs, en lien avec les transformations ayant lieu durant les processus physico-chimiques. Les différences dans l'abondance naturelle des différents isotopes sont généralement petites – mesurées normalement en partie par milliers (pour mille ou ‰). C'est pourquoi, afin de pouvoir comparer plusieurs rapports isotopiques (R) de façon précise, la notation delta (δ) a été proposée (McKinney et al., 1950).

$$\delta\ (‰) = \left(\frac{R_{échantillon}}{R_{standard}} - 1\right) \times 1000$$

La notation δ indique ainsi une différence mesurée par rapport à un standard (Sharp, 2007). Un δ positif correspond à un enrichissement de l'échantillon en isotopes lourds par rapport au standard. La différence de masse entre deux isotopes d'un même élément entraîne

des variations légères dans leurs propriétés chimiques et physiques, permettant, notamment, de les séparer par spectrométrie de masse pour mesurer leurs teneurs relatives.

Les différences dans la cinétique des réactions, ainsi que dans la composition à l'équilibre, peuvent entraîner un fractionnement isotopique au cours des processus physico-chimiques, lorsque des éléments sont incorporés dans des systèmes vivants ou participent à des réactions chimiques inorganiques (Sharp, 2007). Au cours des processus biogéniques (c'est-à-dire l'assimilation et les processus métaboliques), le fractionnement se produit généralement en raison de l'utilisation ou de l'incorporation préférentielle d'un isotope par un organisme par rapport à un autre. Ainsi les proportions moyennes en isotopes stables peuvent être altérées entre l'alimentation et les tissus biologiques du consommateur. Cela peut influencer les valeurs isotopiques de différents tissus à différents degrés (Deniro and Epstein, 1981; DeNiro and Epstein, 1978). Les rapports isotopiques peuvent varier entre les espèces et les individus en raison de leurs métabolismes et compositions biochimiques différents.

L'application de l'analyse de la compostion isotopique des tissus des animaux se base sur le principe que le milieu environnant, la nourriture et l'eau ingérées au cours de la vie de l'individu laissent des signatures chimiques dans les tissus corporels. De nombreuses études expérimentales contrôlées ont confirmé que les compositions isotopiques des tissus biologiques reflètent celles des régimes alimentaires (p. ex. Ambrose, 2002; Ayliffe et al., 2004; Sponheimer et al., 2003b, 2003a; Zazzo et al., 2007). Dans le registre archéologique, les tissus les plus couramment analysés sont les os, l'émail et la dentine et plus rarement la kératine (poil et corne). Certains de ces tissus animaux (dent, poil, corne) ont une croissance continue ou prolongée au cours de la vie de l'individu et deviennent chimiquement inertes après leur formation. Les analyses isotopiques de ces tissus, le long de leur axe de croissance, peuvent donc fournir des informations temporelles des compositions isotopiques de l'environnement (type de nourriture ou d'eau consommée, lieu de vie) éprouvées par l'animal et donc être interprétées en termes d'histoires de vie avec un degré variable de résolution temporelle selon le tissu (p. ex. Balasse et al., 2019; Balasse and Tresset, 2002; Bendrey et al., 2017; Pellegrini et al., 2008; Trentacoste et al., 2020; Ventresca Miller and Makarewicz, 2017; Zazzo et al., 2015). Il faut souligner que les profils d'isotopes stables observés au niveau individuel sont le produit d'une interaction entre des processus écologiques, physiologiques et biochimiques. Un effort est nécessaire pour comprendre les processus d'incorporation du signal isotopique dans les différents tissus et l'influence du métabolisme de l'animal ainsi que des processus de formation des tissus (amélogénèse, kératogénèse) (p. ex. Ambrose, 1991; Fuller et al., 2004;

Hoppe et al., 2004; Passey and Cerling, 2002). De nombreuses études ont été conduites sur des animaux modernes afin de documenter l'intégration du signal isotopique dans les tissus des animaux (p. ex. Ayliffe et al., 2004; Bendrey et al., 2015; Cerling and Harris, 1999; Flockhart et al., 2015; Green et al., 2018b; Lewis et al., 2017; Podlesak et al., 2008; Zazzo et al., 2010, 2007) ainsi que l'influence des stratégies d'élevage sur les compositions isotopiques (p. ex. Balasse et al., 2001, 2002, 2012; Makarewicz and Tuross, 2006; Tornero et al., 2018). Cette approche est cruciale afin d'interpréter les données isotopiques et de pouvoir identifier différentes stratégies de gestion des troupeaux via les enregistrements isotopiques des restes archéologiques. De plus, comprendre les signatures isotopiques saisonnières obtenues à partir des tissus des animaux nécessite une connaissance détaillée de leurs sources et de leurs variations saisonnières locales, et donc une connaissance des conditions environnementales du site d'étude.

Dans ce chapitre, nous commencerons par aborder la formation de l'émail dentaire et de la kératine des poils - deux tissus à la base de ce travail de recherche – ainsi que la manière dont ils intègrent le signal isotopique. Dans un second temps, nous aborderons l'utilité de différents systèmes isotopiques (carbone, azote, oxygène, strontium) pour étudier la mobilité, mais également la saison d'abattage des animaux. Nous aborderons à cette occasion les limites de ces méthodes. Toutefois, ces aspects seront plus détaillés dans les chapitres **4 à 9**.

2.2 Principaux tissus biologiques étudiés : formation et enregistrement du signal

Les séries chronologiques des variations isotopiques éprouvées au cours de la vie d'un animal peuvent être déduites à partir de l'analyse des tissus à croissance progressive qui ne se remodèlent pas après leur formation, comme les tissus dentaires ou les phanères (tissus kératinisés).

2.2.1 L'émail dentaire

L'émail est le tissu le plus fortement minéralisé chez les mammifères et est constitué presque essentiellement d'hydroxyapatite – ou bioapatite, un phosphate de calcium ($Ca_{10}(PO_4)_6(OH)_2$) (Elliott, 2002). Un groupement carbonates (CO_3^{2-}) peut substituer un groupement phosphate (PO_4^{3-}) ou un groupement hydroxyle (OH^-). Les groupements carbonate de la bioapatite, extraits de l'émail dentaire sont plus couramment analysés pour leurs compositions isotopiques car ils enregistrent à la fois les valeurs de $\delta^{13}C$ et $\delta^{18}O$. De plus, le

strontium est incorporé en concentrations importantes lors de la formation de la bioapatite en tant que substituant du calcium permettant l'analyse du rapport $^{87}Sr/^{86}Sr$.

L'émail dentaire est inerte métaboliquement et une fois formée sa composition isotopique reste inchangée. Dans le cas des ongulés (p. ex mouton, chèvre, cheval) avec des dents à couronne haute (hypsodontie), il est aisé d'échantillonner séquentiellement l'émail le long de la couronne dentaire. Avec un tel prélèvement sérié, il est possible de reconstituer l'histoire isotopique individuelle durant la période de formation de la dent qui peut se réaliser sur une durée de plusieurs mois à plusieurs années selon l'espèce.

Le développement de l'émail (amélogenèse) est un processus progressif et discontinu qui se réalise en deux étapes distinctes. Dans un premier temps, l'émail est déposé – phase d'apposition - sous forme d'une matrice organique faiblement minéralisée (~25% de teneur) suivie par une phase prolongée de maturation, pendant laquelle il y a une perte progressive de la fraction organique et acquisition du taux de minéralisation final (Robinson et al., 1995; Suga, 1982) (**Figure 1**). Durant l'apposition, la minéralisation commence au niveau de la surface occlusale de la dent et progresse vers la racine. La surface d'une nouvelle apposition forme un angle faible par rapport à la jonction émail-dentine (EDJ), de telle sorte que les couches d'apposition séquentielles s'imbriquent (**Figure 1**). Ainsi, dans l'émail pleinement minéralisé, le front d'apposition est enregistré par des bandes de croissance progressive, appelées stries de Retzius (Hillson, 2005). De même façon que l'apposition, la maturation de l'émail progresse de la surface occlusale vers la racine, mais par le biais de vagues de minéralisation successives dans différentes directions à travers la couche d'émail entre la surface de l'émail et la jonction émail-dentine (Suga, 1982; Suga et al., 1970).

Ce délai et cette géométrie de minéralisation ont des conséquences importantes sur l'interprétation des séquences isotopiques mesurées par prélèvement sérié. Généralement, l'émail est échantillonné séquentiellement avec une fraise, ou par laser, perpendiculairement à l'axe de croissance. L'endroit où un échantillon est prélevé est lié à la croissance physique de la dent et peut être associé à une date calendaire approximative. Cependant, les valeurs isotopiques de l'échantillon ne se rapportent pas à la même période de temps, mais couvrent une période de minéralisation beaucoup plus longue, pendant laquelle l'émail continue d'intégrer les signaux isotopiques environnementaux. Ainsi, chaque échantillon, prélevant partiellement ou entièrement l'épaisseur de l'émail, représente un signal moyenné dans le temps, intégrant des intervalles de minéralisation et d'apposition distincts (**Figure 1**). Ainsi, les variations

enregistrées le long de la couronne dentaire sont atténuées par rapport aux variations isotopiques éprouvées par l'animal durant la minéralisation de la dent (Balasse, 2003; Hoppe et al., 2004; Passey and Cerling, 2002; Podlesak et al., 2008; Zazzo et al., 2012, 2005). Autrement dit, l'échantillonnage classique impliquant le prélèvement de matière perpendiculairement à l'axe de croissance de la dent, amène à mixer des signaux isotopiques temporellement différents. Cette atténuation est inversement proportionnelle au temps d'exposition d'un nouveau signal environnemental ou alimentaire (Passey and Cerling, 2002; Zazzo et al., 2010, 2005).

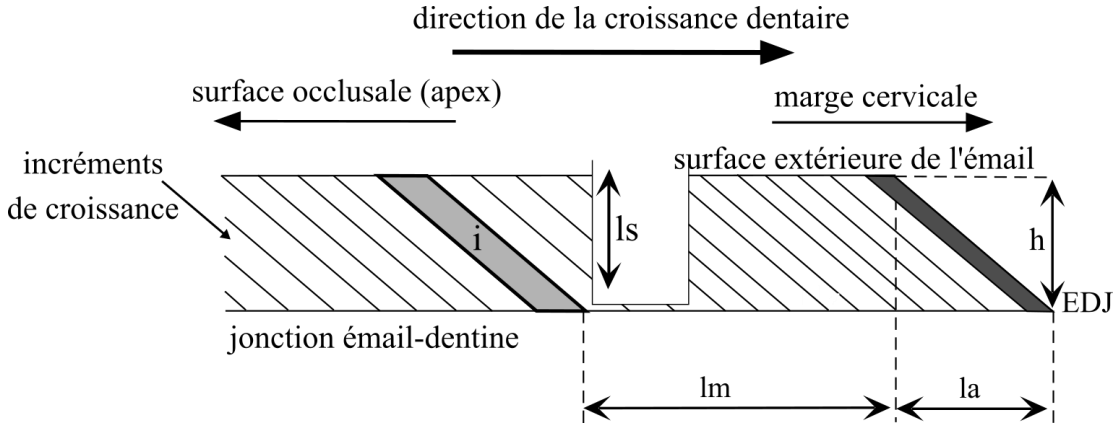

Figure 1: Diagramme schématique des paramètres de maturation de l'émail. La longueur d'apposition *la* est la longueur sur laquelle la matrice initiale hautement organique est déposée, ou la distance entre l'endroit où la couche d'apposition entre en contact avec la jonction émail-dentine et l'endroit où elle entre en contact avec la surface extérieure ; la longueur de maturation *lm* est la longueur sur laquelle l'émail se minéralise ; *h* est l'épaisseur de la couche d'émail ; *ls* est la profondeur d'échantillonnage perpendiculaire à l'axe de croissance de la dent. Modifié d'après Zazzo et al. (2012).

Par exemple, un faible changement sur une longue période de temps sera plus visible qu'un changement important des valeurs isotopiques sur une courte période de temps (Zazzo et al., 2010). Par conséquent, des changements de court terme (quotidien à hebdomadaire) des valeurs isotopiques sont difficilement indétectables. L'atténuation va également dépendre de la durée du processus de minéralisation, spécifique à chaque espèce, et qui est d'environ 3-4 mois chez les moutons et chèvres (Zazzo et al., 2010) et d'environ 6 mois pour les chevaux et bovins (Balasse, 2002; Hoppe et al., 2004). De plus, le processus de minéralisation n'est pas constant le long de la dent, avec la partie haute de la couronne qui minéralise plus vite que la partie basse (Bendrey et al., 2015; Zazzo et al., 2012). Cependant, des études où le régime alimentaire était contrôlé, ont confirmé que malgré un certain décalage dans le temps et une atténuation du signal isotopique, les modifications du régime alimentaire peuvent être reconstituées à partir de l'analyse isotopique du carbone de l'émail (Balasse, 2002; Passey and Cerling, 2002; Zazzo et al., 2005). La compréhension du schéma et du moment de l'incorporation de différents éléments

ou isotopes stables dans l'émail en développement est fondamentale pour l'interprétation de ces signaux (Passey et al., 2005; Passey and Cerling, 2002; Tafforeau et al., 2007; Zazzo et al., 2005). Cependant, actuellement des doutes subsistent concernant la synchronicité des variations de chaque système isotopique mesurées dans la dent, notamment pour le strontium qui semble avoir un temps de résidence dans l'organisme plus long que des éléments plus légers (C, O) amenant à une plus grande atténuation du signal isotopique (Montgomery et al., 2010).

2.2.2 La kératine des poils

La kératine est la protéine majoritaire du poil et de la corne. Le poil est largement utilisé comme support des analyses isotopiques dans les études portant sur l'écologie des mammifères, car il peut être prélevé de manière non invasive, est métaboliquement inerte une fois formé et est facile à stocker. La fibre capillaire se forme dans le follicule pileux. À mesure que la fibre capillaire continue de croître, les cellules vivantes subissent une différenciation terminale pour former une structure kératinisée dure qui finit par émerger de la peau. La caractéristique importante de la croissance du poil est l'activité cyclique du follicule pileux, pendant laquelle plusieurs phases se succèdent. Pendant la phase anagène, le follicule pileux est en croissance pendant une période continue de plusieurs années. Cette phase est alors suivie d'une courte période de repose appelée catagène qui dure environ quelques semaines, avant que le follicule ne soit progressivement résorbé pendant la phase télogène pendant quelques mois, conduisant finalement à la perte du poil pendant l'exogène (Ebling, 1988; Wilson and Tobin, 2010).

Une fois que le cheveu est kératinisé pendant sa croissance, il ne subit plus aucun changement biogène et présente donc un enregistrement chronologique de la chimie corporelle qui peut être reconstitué par la suite. Étant donné que les poils poussent rapidement et continuellement, l'analyse de la composition isotopique de sections permet d'examiner les variations de court terme enregistrées par ces poils, de restituer un enregistrement chronologique des paramètres environnementaux et alimentaires sur une durée de plusieurs saisons, voir de plusieurs années, et de les interpréter en terme de mobilité, de régiment alimentaire ou de changement environnemental (p.ex. Auerswald et al., 2011; Cerling et al., 2009, 2006; Chau et al., 2017; Männel et al., 2007; Rysava et al., 2016; Schnyder et al., 2006; Wittemyer et al., 2009). En effet, des études d'alimentation contrôlée sur des animaux domestiques ont montré que la composition isotopique du carbone d'un nouveau régime alimentaire est rapidement enregistrée dans le poil et permet de détecter dans l'alimentation des changements dans l'alimentation de court terme, de l'ordre de quelques jours. Cette rapidité

d'enregistrement offre une plus haute résolution temporelle que celle d'autres tissus biologiques (Ayliffe et al., 2004; West et al., 2004; Zazzo et al., 2008, 2007).

La rareté de leur préservation en contexte archéologique n'empêche en rien l'intérêt de leur utilité comme une archive haute résolution de l'environnement géochimique pour reconstruire l'environnement, la diète et l'origine des individus. Ainsi, dans certains cas les poils peuvent être utilisés comme une alternative aux dents hypsodontes (p. ex. Cerling et al., 2004; Frei et al., 2009; Iacumin et al., 2006, 2005).

2.3 Les isotopes stables : indicateurs de la mobilité

Depuis un peu plus d'une décennie, de plus en plus d'études se penchent sur le potentiel des isotopes stables à identifier la mobilité d'animaux modernes et anciens (p. ex. Arnold et al., 2013; Balasse et al., 2002; Britton et al., 2009; Chau et al., 2017; Copeland et al., 2016; Henton et al., 2017b; Julien et al., 2012; Makarewicz et al., 2017; Tornero et al., 2018; Viner et al., 2010) et notamment dans le cas du pastoralisme en milieu montagnard où cette mobilité est liée à l'altitude (p. ex.. Balasse and Ambrose, 2005; Bentley and Knipper, 2005; Dufour et al., 2014; Fisher and Valentine, 2013; Hermes et al., 2017; Knockaert et al., 2018; Makarewicz, 2017; Makarewicz et al., 2017; Mashkour, 2003; Mashkour et al., 2005; Tornero et al., 2018, 2016).

Les isotopes de l'oxygène, du carbone, de l'azote et du strontium sont les principaux systèmes isotopiques utilisés afin de retracer la mobilité des animaux, car les valeurs de $\delta^{18}O$, $\delta^{13}C$, $\delta^{15}N$ et $^{87}Sr/^{86}Sr$ varient dans les écosystèmes terrestres en fonction de divers paramètres environnementaux et géographiques (p. ex. Amundson et al., 2003; Bentley, 2006; Craine et al., 2009; Diefendorf et al., 2010; Koch et al., 2007; Kohn, 2010; Szpak, 2014; Tieszen, 1991). Les signaux isotopiques enregistrés dans les tissus animaux fournissent un signal spatialement intégré.

2.3.1 Le $^{87}Sr/^{86}Sr$ et la mobilité

Le $^{87}Sr/^{86}Sr$ est le système isotopique le plus communément utilisé en archéologie pour mettre en évidence la mobilité d'animaux sauvages ou domestiques (p. ex. Balasse et al., 2002; Bendrey et al., 2009; Britton et al., 2009; Copeland et al., 2016; Glassburn et al., 2018; Meiggs, 2007). La teneur isotopique en strontium trouvé dans un écosystème dépend généralement du substratum rocheux sous-jacent et va varier localement en fonction de l'âge, de la composition chimique de la roche et du taux d'érosion du substrat (Bentley, 2006; Koch et al., 2007). Le

strontium se substitute au calcium dans les tissus végétaux et animaux et son intégration n'entraine pas de fractionnement entre la source et le tissue (Flockhart et al., 2015). Par conséquent, le rapport isotopique en strontium mesuré dans les tissus des animaux représente directement celui de la zone géologique où l'animal a pâturé pendant la formation du tissu.

Ainsi, le $^{87}Sr/^{86}Sr$ mesuré dans les tissus biologiques peut être utilisé pour déterminer la provenance géologique d'origine. En archéologie, les profils de séries temporelles de $^{87}Sr/^{86}Sr$ de l'émail des dents d'ongulés, échantillonnées séquentiellement par fraisage, ont été souvent utilisées pour enquêter sur l'origine géographique et la mobilité saisonnière du bétail en comparant les variations de $^{87}Sr/^{86}Sr$ avec les variations spatiales de $^{87}Sr/^{86}Sr$ au sein de la zone d'étude, permettant ainsi d'estimer l'emplacement du bétail à différents moments de sa vie (p. ex. Bendrey et al., 2009; Chase et al., 2018; Makarewicz et al., 2018; Towers et al., 2010). Cette méthode a également été appliquée sur des animaux sauvages (p. ex. Britton et al., 2009; Copeland et al., 2016; Gigleux et al., 2019). Bien souvent, l'interprétation des valeurs isotopiques se limite à définir si un individu est 'local' ou 'non local'. Bien que ces études aient permis d'éclaircir d'importantes questions archéologiques, la cinétique de l'incorporation du rapport isotopique du Sr de l'environnement dans l'émail dentaire pendant sa minéralisation est encore mal comprise (Montgomery et al., 2010), du fait des rares expérimentations avec une alimentation contrôlée (Anders et al., 2019; Lewis et al., 2017), limitant la précision temporelle des estimations de la mobilité. De plus, l'échantillonnage séquentiel par fraisage collecte l'émail perpendiculairement à l'axe de croissance sur toute l'épaisseur de l'émail, amenant à réaliser une moyenne temporelle (~3-4 mois chez les moutons et chèvres) et à amortir le signal isotopique par rapport aux variations isotopiques de l'environnement éprouvées par l'animal (Balasse, 2002; Blumenthal et al., 2014; Passey and Cerling, 2002; Zazzo et al., 2012, 2010). Cette méthode classique d'échantillonnage peut ne pas convenir pour suivre une mobilité fréquente des troupeaux. De plus, le rapport isotopique du strontium peut s'avérer difficile à interpréter dans les zones montagneuses à cause d'une géologie potentiellement complexe et variée amenant à de fortes ou de faibles variations dans la distribution de strontium biodisponible. Ces fortes ou faibles variations peuvent masquer les mouvements de petite échelle typiques de la mobilité pastorale verticale et être masquées par le processus de minéralisation de l'émail dentaire.

Malheureusement, peu d'études ont évalué la représentativité des profils de variations de $^{87}Sr/^{86}Sr$ dans l'émail des dents, par rapport au schém de mobilité, en travaillant sur des animaux d'élevage dont la mobilité est connue et les variations de $^{87}Sr/^{86}Sr$ de leur

environnement immédiat déterminées. De rares études réalisées sur des animaux sauvages migrateurs modernes, dont les lieux de reproduction et d'hivernage étaient connus, ont toutefois montré que le strontium peut être un outil fiable pour détecter la migration saisonnière des troupeaux sauvages, et que les valeurs de $^{87}Sr/^{86}Sr$ des dents correspondent à celles attendues dans les zones d'habitat saisonnier (Britton et al., 2009; Glassburn et al., 2018). Mais, alors que les résultats isotopiques suggèrent des histoires de vie différentes pour les membres des troupeaux, les informations précises sur la mobilité géographique au niveau individuel n'étaient pas disponibles dans ces études (Britton et al., 2009 ; Glassburn et al., 2018). Ceci peut s'expliquer par les coûts relativement plus élevés et plus complexes des méthodes de préparation et d'analyse des isotopes du strontium par rapport aux autres systèmes isotopiques.

2.3.2 Le $\delta^{18}O$ et la mobilité

Les approches se basant sur le $\delta^{18}O$ pour examiner le mouvement des animaux s'appuient sur les variations géospatiales dans la distribution de la composition isotopique de l'eau météorique. La composition isotopique de l'oxygène des tissus biologiques reflète le $\delta^{18}O$ de l'eau ingérée, provenant de l'eau météorique essentiellement, mais également de l'eau des plantes. Les rapports de ^{18}O et ^{16}O de l'eau sont influencés par de nombreux processus environnementaux via des fractionnements isotopiques (c-à-d une séparation des isotopes lourds et légers), donnant pour chaque zone une signature isotopique typique (**Figure 2**)

Le $\delta^{18}O$ de l'eau est influencé par les températures, le niveau d'aridité, la quantité de précipitation, l'altitude et la continentalité (Dansgaard, 1964; Gat, 1996; Pederzani and Britton, 2019; Rozanski et al., 1993), des facteurs qui doivent être pris en compte lors de la construction d'ensembles de référence isotopiques. La latitude et l'altitude sont deux paramètres qui font varier le $\delta^{18}O$ des précipitations en lien direct avec la température de surface. L'augmentation de l'altitude tout comme le passage des basses latitudes vers les hautes latitudes s'accompagnent d'une baisse progressive de la température de l'air. Cette baisse de la température entraine une condensation de la vapeur d'eau et provoque des précipitations qui continue au fur et à mesure de la baisse de température et qui sont associées à des valeurs de $\delta^{18}O$ de plus en plus négatives. On observe donc une diminution du $\delta^{18}O$ en s'éloignant de l'équateur (Fricke and O'Neil, 1999; Rozanski et al., 1993) ou avec l'augmentation de l'altitude (Gat, 1996; Gonfiantini et al., 2001; Poage and Chamberlain, 2001a). Cependant, la relation entre altitude, latitude et le $\delta^{18}O$ des précipitations varie selon la géographie, la topographie et

les conditions spécifiques de chaque région (Kern et al., 2014; Poage and Chamberlain, 2001b; Rozanski et al., 1993).

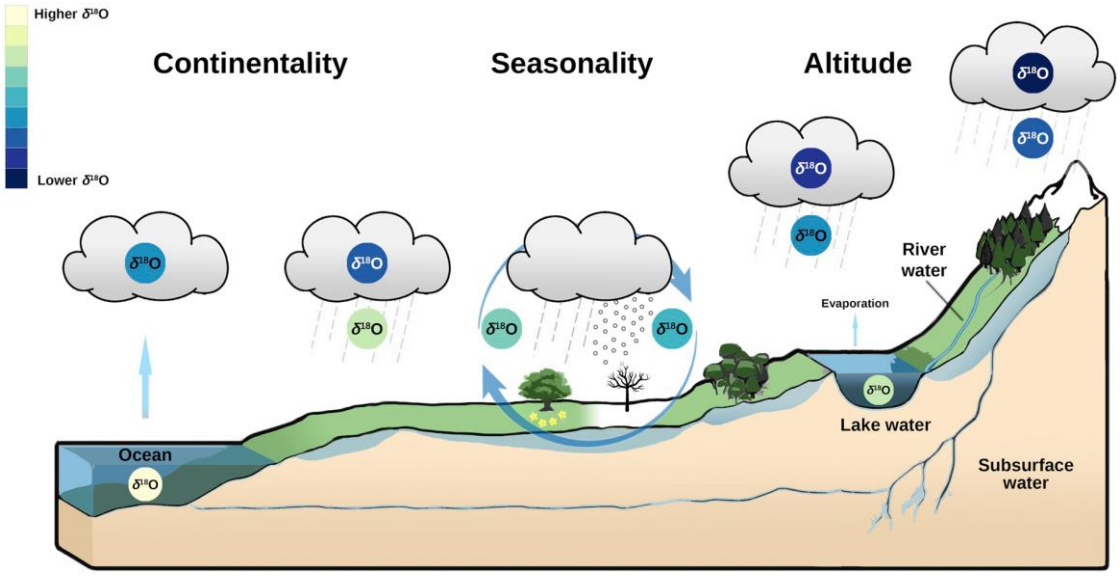

Figure 2: La variation isotopique de base est introduite dans le cycle hydrologique, car le $\delta^{18}O$ de l'eau est modifié par les processus de précipitation et d'évaporation, ce qui entraine des effets à grande échelle liés à la continentalité, la saisonnalité et l'altitude, ainsi que de la température, la quantité de pluie et l'humidité relative. (Figure de Pederzani et Britton 2019).

Les valeurs du $\delta^{18}O$ sont couramment utilisées conjointement avec d'autres systèmes isotopiques comme le $^{87}Sr/^{86}Sr$ ou la composition isotopique en carbone ($\delta^{13}C$). Leur utilisation permet de fournir un contexte saisonnier, car les valeurs du $\delta^{18}O$ varient cycliquement et peut donc fournir un repère saisonnier aux informations obtenues via les autres mesures isotopiques. Toutefois, l'observation seule des changements des variations des valeurs de $\delta^{18}O$ peut également être utilisée pour déterminer une mobilité (p.ex. Britton et al., 2009; Henton et al., 2017b; Hermes et al., 2017). Il s'agit d'un sujet faisant encore l'objet de recherches méthodologiques. La mobilité des troupeaux, domestiques et sauvages, se réalise afin d'éviter les extrêmes climatiques et environnementaux de l'hiver et de l'été en particulier dans les environnements difficiles comme les déserts ou les montagnes. Ainsi, dans de telles zones, les extrêmes climatiques sont évités en se déplaçant sur de longues distances, tels les animaux migrateurs, ou en changeant d'altitude. En été, les animaux se déplacent vers des régions ou altitudes plus douces en température, caractérisées par des valeurs de $\delta^{18}O$ plus faibles comparativement à celles qui auraient été observées s'ils n'avaient pas bougé. Par conséquent, les tissus biologiques des troupeaux, ayant une mobilité altitudinale ou une mobilité de longue distance, doivent dans ce cas enregistrer un cycle saisonnier des valeurs de $\delta^{18}O$ réduit en amplitude (Britton et al., 2009). Cette approche a été utilisée sur du matériel archéologique

(Birch et al., 2016; Henton, 2012; Henton et al., 2014; Pellegrini et al., 2008). Cependant, une approche alternative repose sur l'étude de la variabilité interindividuelle des valeurs de $\delta^{18}O$ au sein d'un groupe : une plus grande variabilité interindividuelle est interprétée comme un indicateur d'ingestion d'eau en dehors de la zone 'locale' et comme indicateur d'une mobilité verticale par certains individus (Mashkour, 2003; Mashkour et al., 2005). Il reste des difficultés inhérentes à cette méthode pour identifier la mobilité d'animaux passés. Récemment, quelques auteurs se sont concentrés sur la forme des courbes de $\delta^{18}O$ enregistrées par les tissus afin d'identifier la mobilité verticale en utilisant des modèles théoriques se basant sur les données environnementales et les variations spatiales des valeurs de $\delta^{18}O$ pour prédire les variations isotopiques (Henton et al., 2017b; Hermes et al., 2017). Toutefois, le potentiel du $\delta^{18}O$, seul, semble limité pour estimer la mobilité des animaux. Il est possible qu'une mobilité rapide puisse générer des ruptures dans les profils saisonniers du $\delta^{18}O$ enregistrés par les tissus biologiques. Mais au vue des variations spatiales des valeurs de $\delta^{18}O$ le long d'un gradient altitudinal (Hermes et al., 2017) ou latitudinal (Bendrey et al., 2017; Stacy, 2009), une mobilité devrait couvrir plusieurs milliers de kilomètres ou avoir un dénivelé de plusieurs milliers de mètres en peu de temps afin de générer un changement potentiellement visible dans les séquences temporelles des valeurs de $\delta^{18}O$. Or, généralement, les stratégies de mobilité de nombreuses sociétés pastorales reposent sur un mouvement graduel avec des campements intermédiaires entre les campements d'été et d'hiver, qui serait difficilement détectable.

2.3.3 Influence de l'altitude sur le $\delta^{13}C$

Dans les environnements terrestres, il existe deux principaux types de plantes qui se différencient selon leur voie photosynthétique utilisée pour fixer le carbone : les plantes en C_3 et les plantes en C_4. Ces deux types de plantes ont des valeurs moyennes en $\delta^{13}C$ différentes avec une valeur moyenne de -26 ‰ pour les plantes en C_3 et de -12 ‰ pour les plantes en C_4 (Kohn, 2010; O'Leary, 1988 - **Figure 3**).

Les plantes en C_4 sont favorisées par des températures élevées, une aridité importante avec un fort ensoleillement tandis que les plantes en C_3 sont majoritaires dans les environnements tempérés, plus humides et ombragés (Ehleringer, 2005; Kohn, 2010). Ces tolérances environnementales respectives entrainent des variations spatiales et temporelles de leur répartition et donc une distribution latitudinale et altitudinale des plantes en C_3 et C_4.

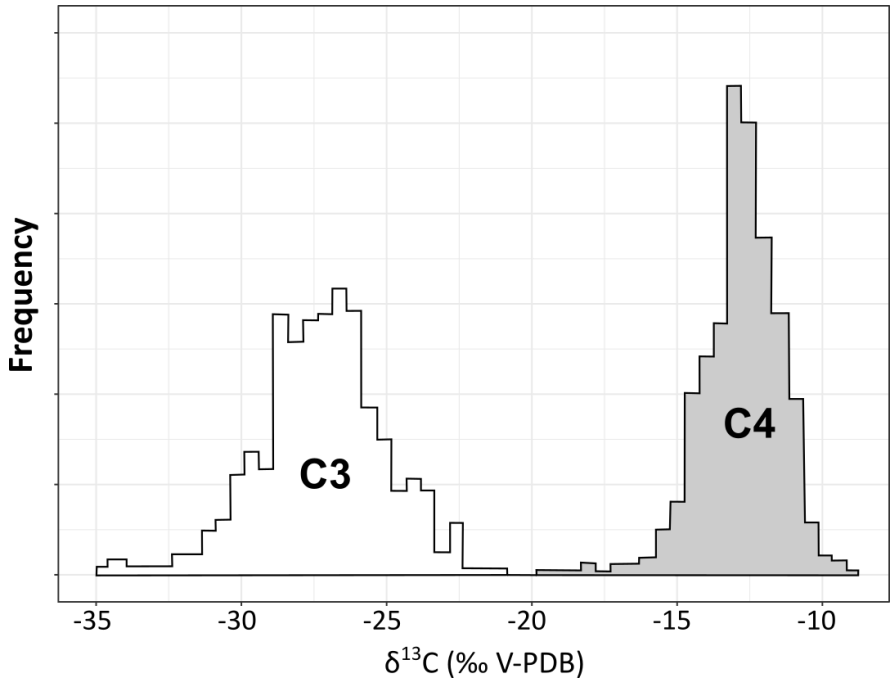

Figure 3: Histogramme montrant la distribution des valeurs de $\delta^{13}C$ des plantes C_3 (blanc) et des plantes C_4 (gris) d'après O'Leary (1988). Notez que comme les données brutes de O'Leary (1988) n'étaient pas disponibles et que l'axe y original n'a pas été conservé, les zones C_3 et C_4 ne montrent que la fréquence relative des valeurs $\delta^{13}C$ des plantes.

Avec l'augmentation de la latitude et de l'altitude, on observe une augmentation de la proportion relative des C_3 par rapport aux C_4 déclenchant une diminution des valeurs moyennes de $\delta^{13}C$ des communautés de plantes (Cavagnaro, 1988; Li et al., 2009; Tieszen et al., 1979). Dans ce contexte, une mobilité altitudinale peut être détectée en analysant les variations de $\delta^{13}C$ des tissus des animaux car celles-ci reflètent celles de l'alimentation et donc des plantes ingérées par le bétail. Ces changements d'alimentation peuvent être liés aux changements de pâtures et donc refléter les variations d'altitude (Balasse et al., 2002; Balasse and Ambrose, 2005; Dufour et al., 2014; Goepfert et al., 2013; Makarewicz, 2017).

En revanche, dans les environnements dominés par les plantes en C_3, i.e. essentiellement les milieux tempérés (Still et al., 2003), où il y a et il y a eu une forte présence d'une économie pastorale, la gamme des variations isotopiques est plus restreinte. Au sein de chaque groupe de plantes, les conditions climatiques affectent également le $\delta^{13}C$ des plantes terrestres, avec des variations saisonnières, notamment des valeurs hautes en été, en raison du stress hydrique et de l'intensité lumineuse (Farquhar et al., 1989; Kohn, 2010; Körner et al., 1991; Smedley et al., 1991). Ces facteurs environnementaux varient également avec l'altitude et plusieurs études ont documenté une relation entre les valeurs de $\delta^{13}C$ des plantes en C_3 et l'altitude mais cette relation peut être soit positive (Körner et al., 1988; Liu et al., 2016; Morecroft and Woodward,

1990) soit négative (Liu et al., 2016; van de Water et al., 2002). Ainsi cette relation potentielle du $\delta^{13}C$ avec l'altitude doit être déterminée pour chaque zone d'étude. De rares études ont pu observer ce type de relation enregistrée dans les valeurs de $\delta^{13}C$ des tissus du bétail (Männel et al., 2007). Toutefois, il est important de préciser que, dans un contexte d'élevage, le $\delta^{13}C$ des tissus des animaux domestiques peut varier suite à une intervention humaine dans l'alimentation (i.e. affouragement, compléments alimentaires) et peut venir masquer le signal d'une mobilité (Marie Balasse et al., 2012; Makarewicz and Tuross, 2006; Makarewicz, 2015).

2.3.4 Couplage du $\delta^{13}C$ avec le $\delta^{18}O$ pour détecter la mobilité altitudinale

Récemment, plusieurs auteurs se sont intéressés à l'utilisation conjointe des variations de la composition isotopique de l'oxygène et du carbone dans l'émail dentaire des ongulés, sauvages et domestiques, dans le but d'identifier une mobilité verticale caractérisée par une utilisation des pâtures d'altitude en été et des pâtures de plaine en hiver (Fisher and Valentine, 2013; Knockaert et al., 2018; Makarewicz, 2017; Makarewicz et al., 2017; Tornero et al., 2018, 2016).

Généralement, une covariation entre les profils de $\delta^{13}C$ et de $\delta^{18}O$ mesurés dans l'émail dentaire est attendue pour des herbivores stationnaires dans des environnements tempérés et semi-arides (Balasse et al., 2009, 2002; Fraser et al., 2008) avec des valeurs élevées durant la saison chaude et des valeurs basses durant la saison froide (**Figure 4A**). Cependant, une anticovariation (**Figure 4B**) entre les variations intra-dent des valeurs de $\delta^{13}C$ et de $\delta^{18}O$ a été observée dans plusieurs cas (Fisher and Valentine, 2013; Makarewicz et al., 2018, 2017; Makarewicz and Pederzani, 2017; Tornero et al., 2018, 2016). Cette anticovariation a été interprétée comme reflétant une mobilité entre des pâtures d'altitude durant l'été, où la proportion de plantes en C_4 dans l'alimentation est plus faible, et des pâtures d'hiver en plaine, où il y a une plus forte proportion de plantes en C_4 dans le régime alimentaire. Cette explication a été proposée pour décrire des schémas de mobilité aussi bien chez des ongulés sauvages (Fisher and Valentine, 2013; Tornero et al., 2016) que domestiques (Makarewicz, 2017; Makarewicz et al., 2017; Tornero et al., 2018).

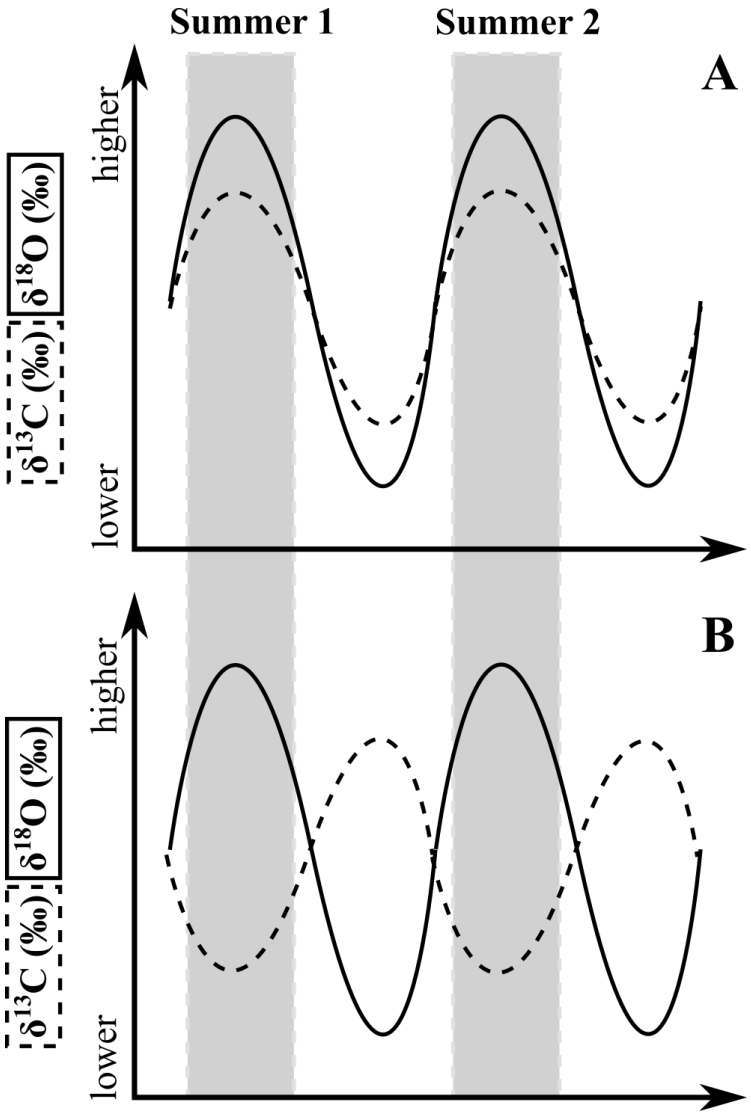

Figure 4: Représentation schématique des variations des valeurs de $\delta^{13}C$ et de $\delta^{18}O$ enregistrées par les dents dans le cas (A) où l'animal est stationnaire on observe une covariation et dans le cas (B) où l'animal a une mobilité altitudinale : on observe une anticovariation.

Cependant, dans le cas de systèmes pastoraux, une deuxième interprétation a été proposée. Celle-ci suggère une intervention de l'homme dans le régime alimentaire des animaux, par la distribution de fourrage. L'augmentation des valeurs de $\delta^{13}C$ pendant l'hiver serait le résultat de la distribution de fourrage riche en C_4 récolté pendant l'été. Une étude le documente sur le bétail moderne (Makarewicz and Pederzani, 2017) et cette interprétation a été utilisée pour décrire des pratiques pastorales passées (Makarewicz and Tuross, 2006; Makarewicz, 2017; Makarewicz et al., 2018; Winter-Schuh, 2017).

Ces interprétations conflictuelles sont en partie dues à la rareté des ensembles de données de référence modernes. Seules deux études ont exploré l'influence du fourrage (Makarewicz and Pederzani, 2017) et de la mobilité altitudinale (Tornero et al., 2018) sur des

animaux modernes mais n'impliquant que peu d'individus et sans qu'il n'y ait de groupe contrôle (c'est-à-dire non nourri ou sédentaire).

2.3.5 Influence de l'altitude sur le $\delta^{15}N$

Les isotopes de l'azote, qui sont typiquement utilisés pour étudier les changements de niveaux trophiques des régimes alimentaires des mammifères (entre carnivores et herbivores), sont aussi utiles pour étudier les variations du régime alimentaire au sein des herbivores (Balasse and Tresset, 2002; Makarewicz, 2015, 2014; Sponheimer et al., 2003b). Les valeurs de $\delta^{15}N$ des tissus des herbivores sont déterminées en partie par la composition en azote des plantes ingérées par l'animal qui, elle, est influencée par les conditions climatiques. Notamment, il existe une corrélation positive entre le $\delta^{15}N$ et la température (Amundson et al., 2003; Martinelli et al., 1999), et une corrélation négative entre le $\delta^{15}N$ et la disponibilité en eau (dont les précipitations) (Handley et al., 1999; Hartman and Danin, 2010; Murphy and Bowman, 2009). Plusieurs études ont ainsi documenté une diminution des valeurs de $\delta^{15}N$ des sols et des plantes en fonction de l'altitude (Amundson et al., 2003; XianZhao Liu et al., 2010; Liu and Wang, 2010; Männel et al., 2007; Szpak et al., 2013). Cette tendance est attribuée à de plus faibles températures et des précipitations plus importantes à haute altitude (Amundson et al., 2003; Garten, 1993; Handley et al., 1999; Liu et al., 2007; Liu and Wang, 2010). En revanche, Yi et al. (2006) et Vitousek et al. (1989) ont obtenu une tendance à l'augmentation avec l'altitude. Mais des tendances plus complexes ont également été observées. Ainsi, dans les Andes, Szpak et al. (2013) précisent que la relation entre $\delta^{15}N$ et altitude disparait quand l'altitude est supérieure à 2000 m et que les précipitations annuelles sont supérieures à 400 mm. Et Liu et al. (2010), dans les monts Dongling au nord de Pékin, ont observé en dessous de 1350 une corrélation négative entre le $\delta^{15}N$ des plantes et l'altitude, et influencée par les précipitations ; et au-dessus de 1350 une corrélation positive et influencée par les températures.

Ces différentes relations avec l'altitude peuvent varier selon les espèces de plantes, surement en raison de différents processus d'incorporation de l'azote, que l'on ne détaillera pas ici. Cette complexité est expliquée par le fait que l'azote des sols est affecté par les processus physiologiques et biogéochimiques des plantes et pas seulement par le microhabitat local (Craine et al., 2015, 2009). Les mécanismes de variation altitudinale du $\delta^{15}N$ restent ainsi incertains. Toutefois, Männel et al. (2007) ont pu montrer que si une relation entre le $\delta^{15}N$ des plantes et l'altitude est observée alors celle-ci s'enregistre dans les tissus des animaux (poils du

bétail dans leur étude). Cependant, encore peu d'études ont essayé d'utiliser les valeurs de $\delta^{15}N$ des tissus des animaux pour retracer leur mobilité altitudinale (p. ex. Dufour et al., 2014; Samec et al., 2018).

2.3.6 Isotopes stables et mobilité : synthèse

Chaque système isotopique ($\delta^{13}C$, $\delta^{15}N$, $\delta^{18}O$, $^{87}Sr/^{86}Sr$) a un potentiel pour inférer la mobilité des animaux, quelle soit longitudinale ou altitudinale. Les études utilisant le rapport isotopique du strontium, seul système ne dépendant que de la géographie, sont de plus en plus nombreuses, mais beaucoup sont contraintes par des échelles d'analyses grossières, limitant les interprétations sur les origines 'locales' ou 'non locales' des individus échantillonnés, sans pouvoir réfléter les schémas de mobilité qui peuvent être complexes, même à une échelle locale. Le $\delta^{18}O$, seul, semble limité pour définir des mobilités pastorales qui ne se déroulent pas nécessairement sur des grandes échelles et avec des mobilités très rapides. Son association avec le $\delta^{13}C$, ou même le $\delta^{15}N$, peut aider à inférer une exploitation des pâtures d'altitude et donc une mobilité altitudinale saisonnière. Cependant, l'interprétation d'une telle mobilité se restreint souvent à deux mouvements dans l'année (été et hiver) sans pouvoir réussir à refléter l'existence de campements intermédiaires ou encore d'autres formes de mobilité plus complexes. De plus, les nombreuses études s'appuient sur les différences du $\delta^{13}C$ entre les plantes en C_3 et C_4 alors que de nombreux environnements pastoraux sont essentiellement composés de plantes en C_3 avec une variabilité des valeurs de $\delta^{13}C$ plus faible. Pour définir précisément les modes de mobilité des sociétés pastorales anciennes, il est nécessaire de connaître les variations isotopiques spatiales du paysage afin d'utiliser les systèmes isotopiques appropriés. De plus, à ce jour, seul un petit nombre d'études basé sur du matériel des animaux domestiques modernes ont développé et évalué les méthodes isotopiques avant de les appliquer à des échantillons de faune archéologique afin d'explorer leur mobilité. Ces quelques études ne permettent pas de couvir tous les environnements, où la mobilité pastorale a lieu, mais également ne permettent pas de couvir la complexité et la variété des modes de mouvement utilisés dans les nombreuses sociétés pastorales.

2.4 Les isotopes stables : indicateurs de la saison d'abattage

Comme nous l'avons mentionné précédemment, le moment et le rythme de l'abattage des animaux domestiques, ou même sauvages, sont des paramètres importants pour comprendre

les interactions entre les hommes et leur environnement, la gestion de leurs troupeaux, mais également la saisonnalité d'occupation d'un site. Actuellement, les approches utilisant les restes des animaux pour estimer une saison d'abattage reposent très rarement sur l'analyse des isotopes stables.

Brièvement parlant, les approches communément utilisées analysent les dents et se basent soit sur (i) le stade d'éruption dentaire et les schémas d'usure dentaire, (ii) la cémentochronologie, l'analyse histologique du cément dentaire qui se dépose en couches périodiques (i.e. alternance de bandes claires et sombres) ou (iii) la micro-usure dentaire. Ces méthodes ont leurs avantages, mais également leurs limites, notamment le recours à des hypothèses de base couteuses comme avoir la connaissance de la période de naissance dans le cas de la méthode (i) ou du type de plantes consommé pour la méthode (ii). De plus, toutes ces méthodes ne permettent d'estimer la période de mort souvent que de manière large, de l'ordre de la demi-année ou au mieux de la saison sans pouvoir différencier finement des animaux morts au sein d'une même saison.

L'approche isotopique peut être utilisée pour aborder cette question de temporalité d'abattage en se basant sur les isotopes stables d'émail dentaire échantillonnée séquentiellement, cette méthode se base sur la variabilité saisonnière des compositions isotopiques de l'oxygène (Fricke and O'Neil, 1996; Koch et al., 1989). L'approche a d'abord été utilisée sur les défenses de proboscidiens, des dents à croissance continue poussant tout au long de la vie de l'animal, en s'intéressant à l'allure du profil des variations de $\delta^{18}O$ dans la partie de la dent la plus récemment formée (Koch et al., 1989). Ainsi, un profil avec une diminution des valeurs du $\delta^{18}O$ correspond à un individu mort en hiver. À l'inverse, une séquence, dont les valeurs à la base de la dent augmentent, est reflète un individu mort en été. Cette méthode a été étendue aux dents hypsodontes des ongulés herbivores, qui sont des dents à croissance prolongée. À cet effet, seules des dents en cours de minéralisation (i.e. phase d'apposition) à la mort de l'animal peuvent être analysées car une fois que la dent a fini de se former, l'émail est inerte et le signal isotopique environnemental ne s'incorpore plus. Quelques études se sont ainsi basées sur les analyses de $\delta^{18}O$ de dents immatures, particulièrement l'allule de la fin des profils, pour déterminer si certains d'assemblages archéologiques se sont formés suite à un évènement catastrophique ou par attrition (Julien et al., 2015; Knipper et al., 2008). Toutefois, ces études sont également restées sur une approche qualitative (été *vs* hiver ; comparaison interindividuelle relative) de la détermination de la saison de mort des animaux

sans pouvoir estimer de différences fines dans la saison de mort entre des animaux dont la tendance des profils isotopiques se ressemble.

Une détermination numérique de la période de mort, avec une erreur associée, se basant sur les profils saisonniers des valeurs de $\delta^{18}O$ est possible. En effet, Balasse et al. (2017, 2012) ont mis au point une méthode se basant également sur la séquence du cycle saisonnier enregistrée dans les deuxièmes molaires (dent dont la croissance débute à la naissance) afin de déterminer la période de naissance de l'animal avec une précision de l'ordre de quelques mois. L'estimation se fait via une modélisation de la séquence saisonnière sinusoïdale, en calculant le rapport entre la position (en mm) de la valeur optimale du $\delta^{18}O$ sur la couronne dentaire et la période du cycle saisonnier. Une méthode similaire pourrait être utilisée pour estimer numériquement, avec une erreur associée, la période de mort des animaux à partir de la séquence saisonnière du $\delta^{18}O$ enregistrée dans l'émail dentaire et cela avec une meilleure résolution que les méthodes précédemment citées. Toutefois, la méthode isotopique ne pourrait remplacer complètement les autres méthodes, car celle-ci ne peut s'effectuer que sur des dents en cours de croissance, limitant le nombre d'individus analysables. La mise en place d'une telle méthode requiert la constitution d'un jeu de donnée moderne avec des individus morts à différentes périodes de l'année et dont les dents sont en cours de croissance à la mort de l'animal. pour chaque espèce du fait des variations interspécifiques dans le processus de minéralisation des dents (Green et al., 2017; Hoppe et al., 2004; Zazzo et al., 2005).

Chapitre 3 – Objectifs et cadre d'étude

Cette thèse analyse le potentiel des isotopes stables et de l'échantillonnage séquentiel des tissus biologiques, particulièrement l'émail dentaire, mais également les poils, pour reconstruire les mouvements saisonniers et la date de mort des animaux domestiques retrouvés en contexte archéologique afin de mieux comprendre les pratiques d'élevage et de mobilité des pasteurs des sociétés passées. Comme nous venons de le voir, ces méthodes se basent sur le principe que les isotopes ($\delta^{13}C$, $\delta^{15}N$, $\delta^{18}O$ et $^{87}Sr/^{86}Sr$) peuvent être utilisés comme traceurs et que les tissus biologiques enregistrent au cours de leur croissance les signatures isotopiques de l'environnement de vie de l'animal.

Malgré les nombreuses études isotopiques réalisées au cours des dernières décennies pour retracer les pratiques d'élevage et de mobilité des sociétés pastorales passées, il existe un clair manque d'études s'appuyant sur des référentiels actuels robustes. Ces études de cas modernes sont importantes car elles permettent de tester les méthodes isotopiques par rapport à des comportements ou situations connus, et dans le meilleur des cas, variés, en utilisant des matériaux (dent, poil) se trouvant en contextes archéologiques. L'échantillonnage et l'analyse des matériaux modernes permettent de comprendre comment s'enregistrent les pratiques d'élevage et la mobilité dans ces tissus, avant de les appliquer aux matériaux archéologiques. En d'autres termes, « le présent est la clé du passé » (Ellenberger, 1996). Ce travail se basant sur des animaux domestiques modernes est précieux et permet de parvenir à une compréhension plus approfondie et plus largement applicable des isotopes stables dans les tissus animaux, afin d'interpréter au mieux les analyses sur des restes archéologiques.

Les objectifs principaux de cette recherche sont :

- D'explorer le potentiel de l'analyse isotopique ($\delta^{13}C$, $\delta^{15}N$, $\delta^{18}O$, $^{87}Sr/^{86}Sr$) et de l'échantillonnage séquentiel de deux tissus (dents et poils) de bétail moderne pour reconstruire les schémas de mobilité pastorale, en particulier altitudinale, sur une échelle restreinte.
- D'évaluer si les valeurs de $\delta^{13}C$ des tissus biologiques peuvent être utilisées pour caractériser l'exploitation des pâtures d'altitude dans un environnement dominé par les plantes en C_3.

- De déterminer si l'anticovariation entre les valeurs de $\delta^{18}O$ et $\delta^{13}C$ est présente chez les animaux ayant une mobilité altitudinale et si la variabilité de cette anticovariation est liée à la variabilité des schémas de mobilité altitudinale.
- De modéliser les séquences cycliques du $\delta^{18}O$ de dents en cours de minéralisation du bétail moderne afin d'établir un jeu de données de référence pour déterminer numériquement la date de mort des animaux modernes.
- De proposer une application sur des restes archéologiques de la même zone que les animaux domestiques modernes, afin de déterminer leurs schémas de mobilité et période d'abattage.

Cette thèse propose un nouveau référentiel moderne composé de bétail pour évaluer le potentiel de l'analyse isotopique de l'émail et des poils pour l'inférence des mouvements durant la vie de l'animal et de sa date de mort. Pour cela, les données isotopiques des tissus séquentiellement échantillonnés sont comparées à la mobilité, connue précisément grâce à l'utilisation de colliers GPS, et à la date de mort de l'animal, également précisément connue. Cela a déjà été fait pour des animaux sauvages (p. ex. Cerling et al., 2009). Mais la comparaison des données isotopiques aux données GPS est pour la première fois utilisée pour du bétail et donne lieu à une meilleure compréhension du potentiel de ces approches isotopiques pour la reconstruction des pratiques pastorales des sociétés anciennes.

Pour réaliser cette étude, des animaux domestiques (chevaux, moutons et chèvres) appartenant à des troupeaux de cinq éleveurs nomades de Mongolie occidentale ont été choisis (**voir annexes**). Ils présentent des parcours de mobilité différents en termes d'altitude et de fréquence. Dans cette zone, située sur les contreforts de l'Altaï, l'élevage est extensif avec plusieurs nomadisations pendant l'année. Celles-ci s'appuient sur la stratification verticale des ressources des différentes pâtures causée par la présence de reliefs escarpés (**Figure 5 et 6**).

La Mongolie est connue comme le centre culturel et géographique des empires nomades, le plus connu étant celui de Genghis Khan au 13ème siècle de notre ère. Mais avant l'Empire mongol, d'autres Empires comme celui des Xiongnu (3ème siècle avant n.e.-2ème siècle de n.e), Türk (6ème-8ème siècle de n.e.) ou Ouïgour (8ème-9ème siècle de n.e.) ont également dominé les steppes eurasiennes. Comment et pourquoi des organisations régionales complexes ont émergé

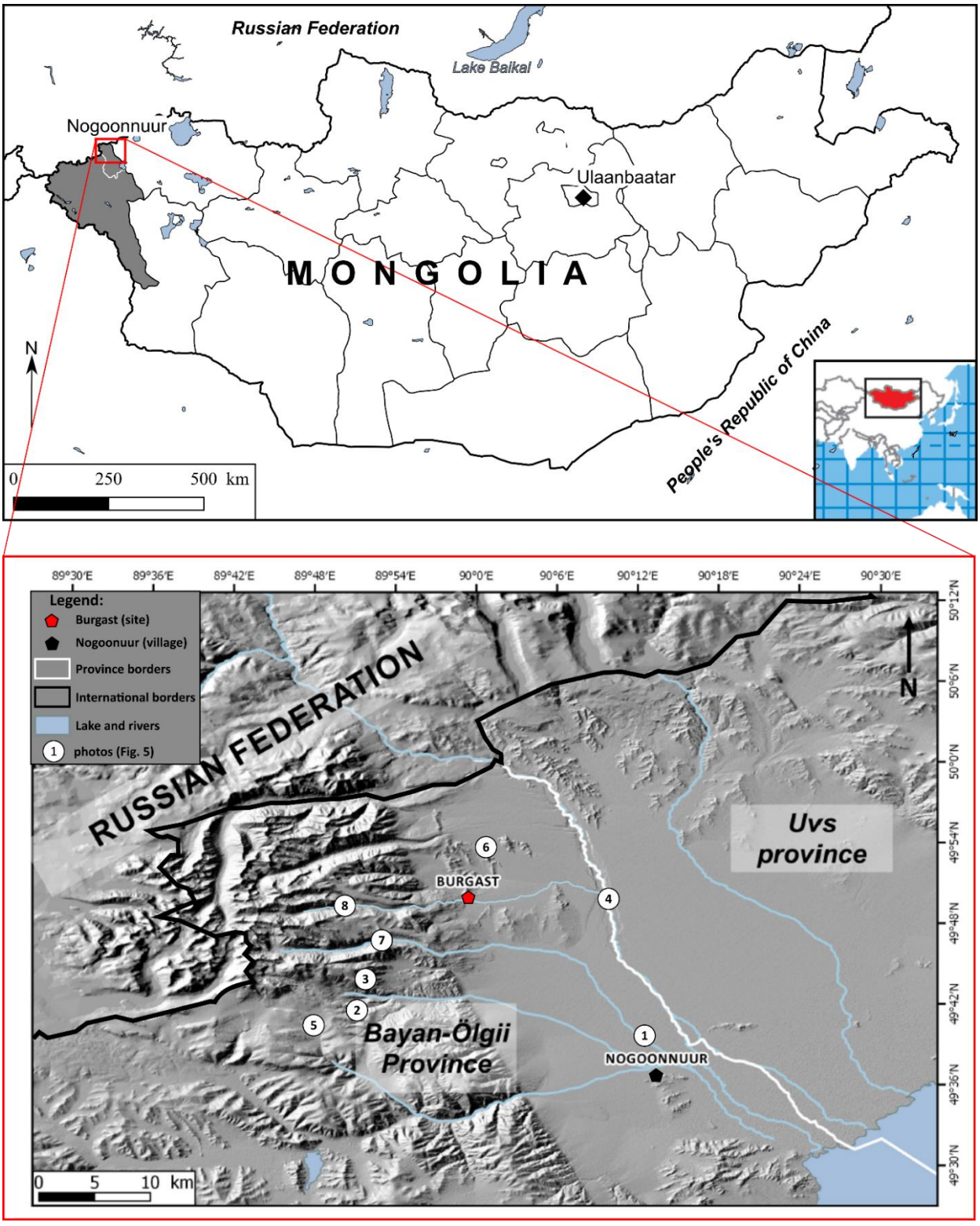

Figure 5: Le terrain d'étude se situe dans le district (*sum*) de Nogoonuur (fin trait blanc de la carte supérieure), près du village homoyme, au nord de la province (*aimag*) de Bayan-Ölgii à l'ouest de la Mongolie (province grisée sur la carte supérieure) proche de la province de l'Uvs et de la frontière avec la Russie (cf. carte du bas). Le figuré rouge situe le complexe funéraire de Burgast, d'où proviennent les restes de chevaux archéologiques analysés dans cette thèse. Les numéros figurant sur la carte inférieure font référence aux paysages de la figure 6.

Figure 6: Photos illustrant les différents environnements autour de la zone de Burgast. (**1**) pâture riche en zone humide proche du village de Nogoonnuur (Septembre 2016 - N. Lazzerini). (**2**) Vallée encaissée en altitude (~ 2200 m) où quelques arbres poussent (Septembre 2016 – N. Lazzerini). (**3**) Panorama des pâtures d'altitude avec en arrière plan la limite entre la plaine et la montagne (Septembre 2016 - N. Lazzerini). (**4**) pâture de zone fluviale avec une plus forte densité d'arbres (Septembre 2016 - A. Zazzo). (**5**) pâturage de haute altitude (~ 2600 m - Juin 2015 - A. Zazzo). (**6**) Panorama sur les steppes à l'est de Burgast (Septembre 2016 - A. Zazzo). (**7**) vallée de haute altitude (~2400 m) où l'éleveur Dl (voir annexe) installe son campement plusieurs fois par an (Septembre 2016 - C. Marchina) (**8**) vallée de haute altitude (~ 2400 m) où l'éleveur Kj installe son campement.

parmi les peuples nomades est l'une des questions de recherche les plus importantes dans l'archéologie mongole aujourd'hui (Honeychurch, 2015a, 2013). La connaissance des stratégies de mobilité et des pratiques pastorales de ces peuples fait partie des informations nécessaires pour comprendre le développement d'organisations sociales complexes telles que ces empires des steppes. Pendant des millénaires, les montagnes de l'Altaï ont constitué une importante zone de transition entre les steppes mongoles et kazakhes. De plus, l'Altaï est traditionnellement considéré comme étant le berceau des peuples türks.

Cependant, les périodes Xiongnu ou Türk sont assez méconnues dans l'Altaï. Les vestiges de la période Türk sont connus et étudiés, surtout dans l'Altaï russe ou Kazakhstanais (p. ex. Konstantinov et al., 2018) tandis que les vestiges de la période Xiongnu sont beaucoup présents en Mongolie centrale (p. ex. Houle and Broderick, 2011; Polosmak et al., 2008). C'est dans ce contexte que depuis 2014 plusieurs structures funéraires ont été fouillées dans l'Altaï Mongol, plus particulièrement dans le district de Nogoonnuur (**Figure 6**) dans le cadre de la Mission Archéologique Française en Mongolie (http://mission-archéologique-française-en-mongolie.fr), dirigée par Sébastien Lepetz. Ces fouilles ont permis de mettre au jour différentes structures datant de l'âge du Bronze mais également de la période Türk. Ainsi, dans cette thèse, les approches isotopiques mises en place sur le bétail moderne dans un premier temps sont appliquées dans un second temps aux restes archéologiques de chevaux datant de l'âge du Bronze et de la période Türk, du site funéraire de Burgast. Ce site se trouve dans la même zone que les troupeaux modernes étudiés. L'étude des chevaux archéologiques offre une meilleure connaissance de la mobilité de ces animaux domestiques ainsi que de leur date d'abattage en lien avec ces structures funéraires à différentes périodes.

Ce manuscrit s'articule en deux parties :

La première partie aborde les différentes méthodes pour déterminer et caractériser la mobilité, en particulier la mobilité altitudinale grâce à l'analyse de la composition isotopique. Cette partie est composée de quatre chapitres.

Le chapitre 4 aborde l'analyse séquentielle du $\delta^{13}C$ et du $\delta^{15}N$ des crins de chevaux et afin d'estimer l'influence des divers paramètres environnementaux et géographiques sur les variations isotopiques observées.

Le chapitre 5 est consacré à l'étude du $\delta^{18}O$ et $\delta^{13}C$ dans les dents de caprinés et de cheval et propose d'estimer l'influence de la mobilité altitudinale et de la résidentialité moyenne

altitudinale sur la corrélation entre les valeurs de $\delta^{18}O$ et $\delta^{13}C$, mais également sur les valeurs moyennes de $\delta^{18}O$ et $\delta^{13}C$.

Le chapitre 6 propose d'estimer si les variations intra-dent et la moyenne du $^{87}Sr/^{86}Sr$ permettent de caractériser l'origine et la mobilité spatiale fréquente des troupeaux suivis par GPS. Pour cela, le $^{87}Sr/^{86}Sr$ est mesuré le long de la couronne dentaire par ablation laser continue et est comparé à une modélisation attendue des variations intra-dent obtenue à partir des données GPS et des variations isotopiques spatiales de la zone d'étude.

Le chapitre 7 présente la mise en application des méthodes abordées dans le chapitre 5 et 6, aux dents des chevaux de l'âge du Bronze et Türk pour comprendre leur origine mais également leur mobilité et l'occupation du territoire par les groupes humains à ces périodes.

La deuxième partie aborde la question de la détermination de la saison d'abattage grâce à l'outil isotopique. Elle est divisée en deux chapitres.

Le chapitre 8 présente le référentiel moderne composé de jeunes caprinés dont les dates de mort, connues précisément, sont comparées aux dates de mort estimées à partir d'une modélisation des séquences des cycles saisonniers enregistrés dans les dents par le $\delta^{18}O$ afin d'évaluer la résolution temporelle d'une estimation de la période de mort à partir de l'analyse isotopique.

Enfin, le chapitre 9 est consacré à l'estimation de la période de mort des chevaux archéologiques en les comparant à un référentiel composé de chevaux modernes.

PARTIE II – RETRACER LA MOBILITÉ DU BÉTAIL

Chapitre 4 – Suivi de la mobilité altitudinale par l'analyse isotopique ($\delta^{13}C$ et $\delta^{15}N$) des crins de chevaux

Nous avons pu voir que l'inférence de la mobilité des animaux domestiques peut être d'un grand intérêt pour comprendre les pratiques d'élevage des sociétés passées et leur évolution au cours du temps. Les nomadisations fréquentes et rapides, telles que peuvent encore de nos jours les pratiques les éleveurs mongols, empêchent les tissus à croissance lente et prolongée, comme l'émaim dentaire d'enregistrer ce schéma de mobilité. Cette mobilité peut en revanche potentiellement être enregistrée dans les poils et les cornes. Mais la kératine est un matériel rarement utilisé parcequ'elle n'est généralement pas conservée dans les contextes archéologiques ; dans certains contextes particuliers, cependant (climat très sec ou sol gelé) elle nous parvient parfois. L'objectif de ce premier chapitre propose d'évaluer l'effet de l'altitude sur les variations de composition isotopique du carbone et de l'azote ($\delta^{13}C$ et $\delta^{15}N$) le long des poils des chevaux, ainsi que la relation avec la végétation des pâtures en contexte montagnard.

4.1 Résumé de l'étude

La composition isotopique en carbone ($\delta^{13}C$) et azote ($\delta^{15}N$) des tissus des herbivores reflète celles des plantes consommées. Cette dernière varie largement et systématiquement à travers le globe en fonction des différences environnementales et climatiques et peuvent donc offrir la possibilité de retracer la mobilité des animaux dans un environnement isotopiquement contrasté. L'analyse séquentielle de la composition isotopique en $\delta^{13}C$ et $\delta^{15}N$ des tissus à croissance continue (poils, émail) est couramment utilisée pour reconstituer les variations temporelles de l'alimentation des animaux actuels et passés. Dans les régions montagneuses, la mobilité altitudinale est un élément clé de l'écologie des animaux. Cependant, les effets de cette mobilité sur les valeurs de $\delta^{13}C$ et $\delta^{15}N$ des tissus des animaux reste difficile à prédire du fait des nombreuses variables (température, disponibilité en eau, type de sol) entrant en jeux et de leurs effets complexes contribuant aux variations de ces compositions isotopiques. Parmi ces tissus, le poil a probablement le meilleur potentiel, car il pousse rapidement et continuellement et devient biologiquement inactif une fois formé, permettant d'enregistrer des variations du régime alimentaire de courte durée et par conséquent d'explorer l'écologie spatiale des mammifères.

Ainsi cette étude vise à explorer le potentiel des variations de $\delta^{13}C$ et $\delta^{15}N$ des poils pour retracer la mobilité altitudinale des mammifères herbivores, en particulier dans un environnement dominé par les plantes en C_3 où les valeurs de $\delta^{13}C$ ont une plus faible variabilité. Pour cela, nous avons, entre juin 2015 et juillet 2018, équipé de colliers GPS six chevaux domestiques appartenant à quatre éleveurs mais vivant en liberté dans l'Altaï mongol. Ces chevaux exploitent tout au long de l'année des pâtures à différentes altitudes. En raison de son système de gestion extensif, le cheval mongol est un bon modèle pour étudier les pratiques d'élevage du passé. Nous avons fait l'hypothèse que les changements de pâture, qui sont liés à l'altitude, engendrent des changements des valeurs de $\delta^{13}C$ et $\delta^{15}N$. Tous les ans, nous avons échantillonné les crins de queue de chaque animal. Ces crins ont été lavés puis analysés séquentiellement à l'aide d'un analyseur élémentaire couplé en flux continu avec un spectromètre de masse de rapport isotopique (EA-IRMS). Les variations temporelles de $\delta^{13}C$ et $\delta^{15}N$ ont été comparées à la mobilité altitudinale connue précisément grâce aux données GPS. Pour cela, dans un premier temps, nous avons calculé un taux de croissance constant pour chaque poil. Dans un second temps, les valeurs de $\delta^{13}C$ et $\delta^{15}N$ du crin ont été converties en compositions isotopiques du régime alimentaire ($\delta^{13}C_{diet}$ et $\delta^{15}N_{diet}$). Ensuite, nous avons comparé les changements significatifs de la dérivée des variations de $\delta^{13}C_{diet}$ et $\delta^{15}N_{diet}$ aux changements de pâture inférés par GPS. Enfin, des modèles GAMM (generalized additive mixed models) ont été utilisés pour modéliser l'effet des facteurs géographiques (altitude, latitude, longitude) et environnementaux (NDVI, température) sur les valeurs de $\delta^{13}C_{diet}$ et $\delta^{15}N_{diet}$ en fonction du temps.

Durant la période de suivi, les chevaux des différents éleveurs ont eu des mobilités diverses. Mis à part un individu, ils ont montré une forte et fréquente mobilité altitudinale. Mais seule la moitié des changements de pâtures est marquée par une variation importante de la composition isotopique du carbone et de l'azote. On observe par eilleurs que de nombreuses fortes variations isotopiques importantes ne sont pas concomitantes des changements de pâture observés via les données GPS.

Malgré des schémas de mobilité différents, les chevaux présentent des variations de $\delta^{13}C_{diet}$ et $\delta^{15}N_{diet}$ similaires au cours du temps. Les valeurs de $\delta^{13}C_{diet}$ diminuent pendant l'été et augmentent en hiver et sont négativement corrélées au NDVI. Quant aux variations de $\delta^{15}N_{diet}$, elles sont caractérisées par une augmentation et diminution rapides pendant l'été, avec des valeurs minimales en milieu d'été, et des faibles valeurs plus stables en hiver. Les modèles

GAMM sur les valeurs de $\delta^{15}N_{diet}$ montrent une corrélation avec l'altitude et une faible influence des données de NDVI.

Ces variations similaires, indépendantes du schéma de mobilité des chevaux, suggèrent que des facteurs, autres que l'altitude, influencent la composition isotopique des plantes. Que ce soit pour les valeurs de $\delta^{13}C_{diet}$ ou de $\delta^{15}N_{diet}$, nous proposons que la disponibilité en eau des sols, en particulier en été via la fonte des neiges et les précipitations en altitude, ainsi que la disponibilité saisonnière des plantes fixatrice de l'azote atmosphérique ($\delta^{15}N \sim 0‰$), ont principalement influencé les variations de $\delta^{13}C_{diet}$ et $\delta^{15}N_{diet,}$ supplantant l'influence de l'altitude.

Ces résultats ont permis de montrer que la mobilité altitudinale n'est pas le seul facteur à l'origine des variations de $\delta^{13}C$ et $\delta^{15}N$ enregistrées par les crins des chevaux, mais que les variations saisonnières et les préférences alimentaires jouent également un rôle important. Il est donc risqué d'interpréter les variations de $\delta^{13}C$ et $\delta^{15}N$ des tissus des animaux vivant en milieu montagnard uniquement en terme de mobilité altitudinale, au moins dans les environnements dominés par les plantes en C_3 comme pour les steppes arides de l'Altaï, et de négliger la complexité des facteurs contrôlant les variations isotopiques.

Article I: Grazing high and low: Can we detect horse altitudinal mobility using high-resolution isotope ($\delta^{13}C$ and $\delta^{15}N$ values) time series in tail hair? A case study in the Mongolian Altai

Nicolas LAZZERINI, Aurélie COULON, Laurent SIMON, Charlotte MARCHINA, Bayarkhuu NOOST, Sébastien LEPETZ, Antoine ZAZZO

Published in *Rapid Communications in Mass Spectrometry 33*(19), 1512-1526
DOI: 10.1002/rcm.8496

Abstract :

Rationale - Carbon and nitrogen stable isotope time series performed in continuously growing tissues (hair, tooth enamel) are commonly used to reconstruct the dietary history of modern and ancient animals. Predicting the effects of altitudinal mobility on animal $\delta^{13}C$ and $\delta^{15}N$ values remains difficult as several variables such as temperature, water availability or soil type can contribute to the isotope composition. Modern references adapted to the region of interest are therefore essential.

Methods - Between June 2015 and July 2018, six free-ranging domestic horses living in the Mongolian Altaï were fitted with GPS collars. Tail hairs were sampled each year, prepared for sequential C and N isotope analysis using EA-IRMS. Isotopic variations were compared with altitudinal mobility and Generalized Additive Mixed (GAMMs) models were used to model the effect of geographic and environmental factors on $\delta^{13}C$ and $\delta^{15}N$ values.

Results - Less than half of the pasture changes were linked with a significant isotopic shift while numerous isotopic shifts did not correspond to any altitudinal mobility. Similar patterns of $\delta^{13}C$ and $\delta^{15}N$ variations were observed between the different horses, despite differences in mobility patterns. We propose that water availability as well as seasonal availability of N_2 fixing type plants primarily controlled horse hair $\delta^{13}C$ and $\delta^{15}N$ values, overprinting the influence of altitude.

Conclusion - Our study shows that altitudinal mobility is not the main factor that drives the variations in horse tail hair $\delta^{13}C$ and $\delta^{15}N$ values and that seasonal change in the animal dietary preference also plays an important role. It is therefore risky to interpret variations in $\delta^{13}C$ and $\delta^{15}N$ values of animal tissues in terms of altitudinal mobility alone, at least in C_3–dominated environments.

4.2 Introduction

Nomadic pastoralism is a husbandry practice which consists in moving livestock between different pastures in order to provide herd animals with a continuous source of fresh graze (Wright and Makarewicz, 2015). In mountainous regions, exploitations of pastures located at different elevations is commonly observed in order to take advantage of seasonal variation in pasture productivity. In general, highland pastures are exploited during the summer months, when still easily accessible, and lowland pastures during the winter months. Comfort can also drive mobility patterns, as herders can chose to move to valley bottoms during winter to protect themselves from the cold winds (Finke, 2004). This basic model is of course flexible and can change over time and space under the influence of various ecological, environmental and socio-political factors such as graze availability, access rights, water availability or pasture stocking rate (Kerven et al., 2016; Lkhagvadorj et al., 2013; Marchina, 2019). Therefore, documenting modern and ancient mobility patterns of domestic animals is fundamental to understanding the evolution of herding practices.

Animal mobility can be tracked by telemetry, *e.g.* with GPS devices set on the animals. But this method remains expensive and restricted to modern animals. An alternative approach consists in the isotopic analysis of animal tissues. C and N isotopes are the most commonly used isotopic systems. The $\delta^{13}C$ and $\delta^{15}N$ values of plants vary widely and systematically across the globe in response to environmental and climatic differences. They are incorporated into animal tissues through diet, thus offering the possibility of tracing the provenance of animals in isotopically contrasting environments. When analysed sequentially in continuously growing tissues (i.e. hair, horn, teeth), stable isotope time series can provide a quantitative method to study the mobility of modern and ancient organisms both domestic and wild (Cerling et al., 2009; Hobson, 2008; Ventresca Miller and Makarewicz, 2017; West et al., 2004). Among these tissues, hair has probably the best potential because it grows rapidly and continuously and is biologically inactive once formed. Controlled feeding experiments have shown that it is possible to detect short-term (daily) changes in diet (Ayliffe et al., 2004; West et al., 2004; Zazzo et al., 2008, 2007). Therefore, temporally resolved hair isotope records have been used to explore fine-scale spatial ecology of mammals.(Burnik Šturm et al., 2016; Cerling et al., 2009; Männel et al., 2007) Under specific conditions, keratin, the protein constitutive of hair, horn and hooves, can be preserved over several thousands of years and be used for palaeoenvironmental and palaeocological reconstructions (Iacumin et al., 2006).

Altitude has an important impact on climatic and soil conditions and thus on primary production (Raich et al., 1997; Zhang et al., 2014) and plant degradation (Coûteaux et al., 2002; Drewnik, 2006) and consequently influence the C- and N- isotope composition of soils and plants (Craine et al., 2009; Wang et al., 2015). Below, we briefly review the extant literature regarding the effect of altitude on plant C and N isotopic values and its potential to reconstruct animal vertical mobility.

The major mechanism influencing the $\delta^{13}C$ values of terrestrial plants is the photosynthetic pathway used for fixing carbon: plants using the C_3 pathway have an average $\delta^{13}C$ values of -26‰, while plants using C_4 pathway have an average $\delta^{13}C$ of -12‰ and plants using CAM pathway vary between those values (Kohn, 2010; O'Leary, 1988). While CAM plants are not of high importance in Mongolia, the vegetation is dominated by C_3 plants, followed by C_4 plants, especially in southern Mongolia (Pyankov et al., 2000). C_4 plants dominate in arid environments characterized by high temperatures and brightness, thanks to a higher water use efficiency, while C_3 plants dominate in temperate, humid and shaded environments (Ehleringer, 2005). Those differences trigger an increase of the relative proportion of C_3 vs C_4 plants with altitude (Makarewicz et al., 2017; Tornero et al., 2016). This vertical stratification of vegetation has been exploited to determine altitudinal mobility of modern and past livestock through isotopic analyses of tooth enamel with ingestion of C_4 plants in lowlands during winter and C_3 plants in highlands during summer (Balasse and Ambrose, 2005; Henton et al., 2017b; Makarewicz et al., 2017; Tornero et al., 2016). It is noteworthy that in the case of domestic herbivores, the increase in $\delta^{13}C$ values during winter can also be driven by the ingestion of ^{13}C-enriched fodder provided by the herder and is not necessarily caused by altitudinal mobility (Makarewicz, 2014; Makarewicz and Pederzani, 2017; Winter et al., 2016). In C_3-dominated environments, the range of isotopic variations is more restricted. Nevertheless, several studies have documented an increase in C_3 plants' $\delta^{13}C$ values with altitude (Körner et al., 1991, 1988; Li et al., 2006, 2009, 2007; Morecroft and Woodward, 1990; Szpak et al., 2013). This pattern is related to high carboxylation rates relative to stomatal conductance at high altitudes resulting in lower ^{13}C discrimination (Li et al., 2007; Szpak et al., 2013). This positive correlation can be recorded in the $\delta^{13}C$ of animal tissues, like hair (Männel et al., 2007). An opposite pattern was reported in SW US and in China (Liu et al., 2016; van de Water et al., 2002). The higher plant $\delta^{13}C$ values measured at lower altitude were explained by increased drought stress at lower elevations in these arid and semi-arid regions. Finally, several authors proposed that local climatic factors could modulate the effects of water availability and hence

locally complicate the relationship between $\delta^{13}C$ values and altitude (Liu et al., 2007; Morecroft and Woodward, 1990).

Several studies have documented a decrease in plant and soil $\delta^{15}N$ values with altitude (Amundson et al., 2003; Liu et al., 2007; Liu and Wang, 2010; Szpak et al., 2013). This trend was attributed to the decrease of mineralization and lower net nitrification rates at higher altitudes induced by lower temperature and higher precipitation (Amundson et al., 2003; Garten, 1993; Handley et al., 1999; Liu et al., 2007; Liu and Wang, 2010). However, more complex trends have also been observed. Indeed, Liu et al. (2010) showed that the correlation between plant $\delta^{15}N$ values and altitude is negative below 1350 m above sea level (asl) and positive above 1350 m asl. They explained this result by the fact that plant $\delta^{15}N$ values are controlled by precipitation below 1350 m asl, and by temperature above 1350 m asl. More recently, Szpak et al. (2013) showed that the negative relationship between $\delta^{15}N$ and altitude observed in Andean plants disappears above 2000 m asl and when precipitation exceeds 400 mm per year. This complexity is explained by the fact that soil nitrogen is affected by plant physiological and biogeochemical processes, and not only by local microhabitat(Craine et al., 2009).

This brief overview highlights the difficulty in predicting the effects of altitude on plant $\delta^{13}C$ and $\delta^{15}N$ values as several variables such as temperature, water availability or soil type can play a role. Moreover, animal seasonal dietary preferences (Duncan, 1992; Putman et al., 1987; Slivinska and Kopij, 2011) or manipulation of the diet by the herder can further obfuscate this relationship. In order to infer modern and past animal mobility based on isotopic variations measured in their tissues it is therefore important to build a modern reference for the region of interest. We investigated this question by analyzing the $\delta^{13}C$ and $\delta^{15}N$ variations in tail hair of domestic horses living in the Altai mountains of Western Mongolia. We hypothesized that $\delta^{13}C$ and $\delta^{15}N$ variations in horse tail hair are correlated to mobility between pasture areas and altitude. The studied animals were fitted with GPS collars, which allowed to monitor their movements and to confront these observations to isotopic variations. The primary purposes of this paper were (i) to test this hypothesis in a C_3-dominated environment and (ii) decipher the effects of altitudinal mobility and other environmental and ecological factors on C and N stable isotope variations in tail hair, to better understand under which conditions these isotope tracers can give information on altitudinal mobility.

4.3 Experimental

4.3.1 Study area and sample collection

The study area is located at the northernmost part of the aimag (province) of Bayan-Ölgii in the sum (district) of Nogoonnuur (**Figure 7**). Elevations range from 1500 to more than 4000 m asl. A north-south fault splits the landscapes in half with a lowland plain to the east and the Altai mountains to the west. The climate is strongly continental with long, cold winters and short, hot summers. During the study period (June 2015 to July 2018), monthly temperatures averaged + 18.0°C during summer (June-August) and – 17.6°C during winter (December-February) with extremes ranging from + 34 to -44°C. Average annual rainfall is 131 mm with a maximum of precipitation occurring during summer (meteorological station based at Nogoonnuur village- **Figure 7** – http://fr.climate.org). In the winter, there is very low snowfall and most of the time no snow cover at all. Open water is rare, and consists of few intermittent streams. The vegetation consists of semi-arid and alpine steppes and is mainly composed of grasses, with a few forbs and bushes exclusively near rivers in lowlands and valley exit. It is dominated by Asteraceae such as *Artemisia* spp., Fabaceae such as *Caragana* spp. and Poaceae, all of them using the C_3 photosynthetic pathway.

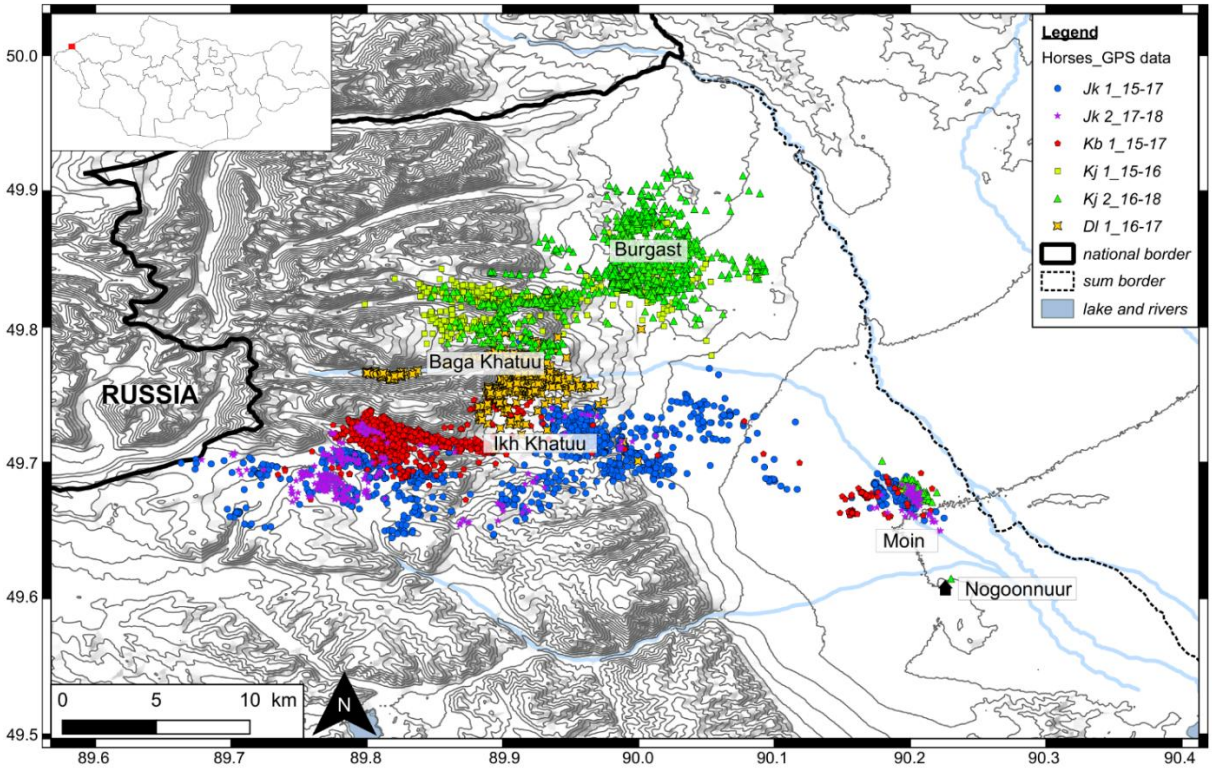

Figure 7: Map of the study area and its location in Mongolia (top left) with GPS fixes of the 6 monitored domestic horses and toponymy of interest.

Six horses (5 males and 1 female) were equipped with Globalstar© GPS collars (Lotek Wireless Inc. - http://www.lotek.com/) between June 2015 and July 2018 (**Table 1**). Collars were programmed to record their position every 13 hours. They also provided altitude and temperature data. GPS monitoring lasted on average 580.5 d (min = 244, max = 896). Monitoring was interrupted for a few months for two individuals, due to technical problems (**Supplementary Figure S4.1** – see supporting Information).

Table 1: Characteristics of the GPS and hair data of the six study horses with GPS based mobility of six study horses. MCP area is the Minimum Convex Polygon estimate of pasture area. [1] sampled when a horse was not equipped with a GPS collar. One-way ANOVA with Tukey's post-hoc HSD was used to compare the means of altitude between horses. N = number. *** = the average altitude of the individual is significantly (p-value < 0.05) different from that of all other horses. Detailed mobility pattern are provided in Supplementary Figure S1.

Horse id		Jk 1	Jk 2	Kb 1	Kj 1	Kj 2	Dl 1
Year of birth		2010	2009–2010	2007	1998	2013	2003
Sex		M	F	M	M	M	M
Start GPS		16/06/2015	30/11/2017	17/06/2015	19/06/2015	08/09/2016	16/09/2016
End GPS		29/11/2017	31/07/2018	08/08/2017	08/09/2016	29/07/2018	26/11/2017
N days		896	244	781	446	689	427
N GPS data		1299	421	1395	771	1256	775
Hair sampling date		16/06/2015 05/09/2016 30/11/2017	 30/11/2017 30/07/2018	17/06/2015 18/09/2016 19/11/2017	 19/06/2015 08/09/2016	08/09/2016 27/11/2017 30/07/2018	16/09/2016 17/11/2017 23/07/2018[1]
Altitude (m.asl)	Mean ± SD Max Min	2115 ± 476*** 2916.2 1449.5	2580 ± 477 3215.6 1446.8	2433 ± 432*** 3156.6 1205.2	2278 ± 459*** 3154.2 1468.1	2014 ± 356*** 3103.1 1428.6	2366 ± 138*** 2813.8 1698.0
N pasture		6	5	4	4	5	3
N pasture changes		23	5	11	14	15	4
N pasture changes/year		9.4	7.5	5.1	11.5	8	3.4
Total MCP area used (km^2)		434	237	328	104	164	65
Mean MCP area used by pasture (km^2)		27.8 ± 24.3	27.1 ± 24.8	21.3 ± 17.9	11.6 ± 6.9	24.8 ± 24.0	14.1 ± 11.1
Average (± SD) nb days on pasture		36 ± 26	54 ± 58	59 ± 78	31 ± 18	43 ± 39	85 ± 80

The horses belong to four different families of Kazakh-Mongolian nomadic pastoralists, with different mobility patterns. They moved freely and were only brought back to the camp occasionally, when needed. When palatable plants become scarce, horses move towards other pastures, either by themselves, or directed by the herder. Herders always keep the herd accessible in order to avoid robbery and to milk the females during summer and fall. During winter, horses may be supplemented with fodder (usually harvested in August-September). It was not possible to plan in advance which animals would be supplemented. However, we recorded the periods where the surveyed animals were foddered through interviews conducted yearly with the herders. Three out of the six animals were never complemented during the study period, while the other three were occasionally given some fodder for limited periods of time (**Supplementary Figure S4.1**). Tail hair from each horse was collected during immobilization

operations on four different occasions (June 2015, September 2016, November 2017 and July 2018 – **Table 1**). Tail hairs were stored in plastic bags (MiniGrip©) until analysis.

4.3.2 Hair sample preparation and stable isotope ratio analysis

Heavy and long tail hairs were selected and cleaned following the protocol published by O'Connell et al.(O'Connell et al., 2001) for keratinous tissues. Each hair was sonicated twice for 10 min in a solution of methanol and chloroform (2:1, v/v), rinsed with distilled water and oven-dried over night at 50°C. Individual hairs were serially sectioned into 7.5 mm samples in order to maximize temporal resolution while keeping enough material for C and N isotope analysis. The 610 individual hair segments generated were weighted in ultralight tin capsules (mass range 151-499 µg) and combusted in an elemental analyser (PyroCUBE Elementar, Hanau, Germany) coupled in continuous flow with an Isoprime isotope ratio mass spectrometer (Isoprime Ltd., Cheadle Hulme, UK) for C and N stable isotope analysis. In-house standards of casein calibrated against secondary international standards from the International Atomic Energy Agency, Vienna, Austria (IAEA-CH3, IAEA-CH6, IAEA-N1, IAEA-N2) were analysed every twelves samples as quality control. The long-term precision (SD) for the internal laboratory standard was better than 0.20 ‰ (C) and 0.11 ‰ (N). Isotope data are presented in δ notation [$\delta = (R_{sample}/R_{standard}) - 1$], with R the isotope ratio ($^{13}C/^{12}C$, $^{15}N/^{14}N$) of the sample or international standard (V-PDB, V-AIR).

4.3.3 Data Analysis

4.3.3.1 GPS-based inference mobility

GPS data were corrected for outliers and failed GPS readings. Horse mobility was detected using the Lavielle's method (Lavielle, 2005, 1999), a method of segmentation of time series of observations implemented in the R package adehabitatHR (Calenge, 2006) . This method discriminates series of successive locations ("segments") during which movements happen at the same spatial scale but between which movements happen at different spatial scales. This allows determining changes in animal movement, and hence discriminating between small-scale movements (within each pasture, in this study) and large-scale movements among pastures. Due to the nature of the landscape and after trials (where segmentation was based on x or y coordinates), segmentation was based on altitude and each segment was considered as a pasture, after visual validation. Pasture area was estimated as the size of the

95% MCP (Minimum Convex Polygon) of the corresponding segment (i.e. area of the smallest polygon joining 95% of the innermost locations of a segment).

4.3.3.2 Isotopically-based inference of mobility

Hairs may grow at different rates within and between individual horses. In order to compare isotopic and GPS data for different individuals, it was first necessary to convert hair length measurements into time (i.e. calendar dates). Growth rates ($mm.d^{-1}$) were determined for each individual horse by looking at overlapping patterns of stable isotope variations in the hairs collected at the different sampling periods. We divided the length between the root and the match zones of the hairs by the period of time between collection dates (Wittemyer et al., 2009). The apical and basal boundaries of the match zone provided respectively maximum and minimum estimates of growth rates. We assumed that growth rate was constant during the study period (Ayliffe et al., 2004; Wittemyer et al., 2009).

The isotope ratios of horse hair ($\delta^{15}N_{hair}$, $\delta^{13}C_{hair}$) were converted into diet isotopic compositions ($\delta^{15}N_{diet}$, $\delta^{13}C_{diet}$) using the isotope turnover model developed by Ayliffe et al. (2004). This model assumes that hair isotope values represent dietary inputs from three pools with different half-lives (0.5, 4 and 138 d) and fraction contributions (41, 15 and 44%). We used the same turnover parameters and a 3‰ diet-hair enrichment factor for both elements (Ayliffe et al., 2004; Sponheimer et al., 2003b). Moreover, hair does not immediately record the isotope composition of the new diet once formed, but only after the new hair follicle reaches the skin surface (Zazzo et al., 2008). This time lag can vary from 6 to 15 d depending on the animal age and species (Jones et al., 1981; Zazzo et al., 2008). In the case of horses, as the duration of this time lag had not been documented, we subtracted 7 d following (Zazzo et al., 2008).

We used one-way ANOVAs with Tukey's post hoc HSD to compare the means of $\delta^{15}N_{diet}$, $\delta^{13}C_{diet}$ variations between horses, between seasons and between months separately.

We investigated animal mobility from isotopic temporal variations by calculating the first derivative of carbon and nitrogen isotope compositions, $d(\delta^{13}C_{diet})$ and $d(\delta^{15}N_{diet})$ in ‰/day (see **Supporting Information Figure S4.2**). We considered that $d(\delta^{13}C_{diet})$ or $d(\delta^{15}N_{diet})$ larger than 1σ (standard deviation, estimated over the whole time-series of $d(\delta^{13}C_{diet})$ and $d(\delta^{15}N_{diet})$ indicated a significant mobility (Cerling et al., 2009). We compared those $d(\delta^{13}C_{diet})$ and $d(\delta^{15}N_{diet})$ – inferred mobilities with the changes of pastures inferred by the analysis of the GPS

data. We considered that isotope-inferred mobility matched GPS inferred mobility when a significant shift was simultaneous with a change of pasture inferred by GPS. In the case of a significant isotopic shift which covers several samples, we only considered the first sample of the series.

4.3.3.3 Testing the effects of mobility and the environment on isotopic values

We investigated the effect of geographic and environmental variables on isotopic variations. Based on GPS data, we calculated the means of different variables over each horsehair segment: altitude, latitude, longitude, temperature; we also estimated 10-day averaged values of NDVI (Normalised Difference Vegetation Index) as a proxy of photosynthetic activity. (Pettorelli et al., 2006) The NDVI raster had a 300 m resolution, and was freely generated by the land service of Copernicus, the Earth Observation program of the European Commission ("European Commission Copernicus Land Monitoring Service - Global Component. Accessible at: https://land.copernicus.eu/global," 2018). In each raw raster, all flag values (Missing, Cloud/Shadow, Snow/ice, Water) were replaced with NA values. A Pearson's correlation matrix was computed with R to assess dependency between variables. This test triggered the exclusion of longitude and temperature from the predictive variables. All the other correlations were lower than 0.23. Generalized Additive Mixed Models (GAMMs) were used to model the effect of geographic and environmental factors on the spatio-temporal variations of the stable isotope composition of diet using Gaussian distribution. Non-linear relationships were used to reveal cyclic seasonal variation of $\delta^{13}C_{diet}$ and $\delta^{15}N_{diet}$ values. GAMMs were implemented in R using the package gamm4 (Wood and Scheipl, 2017). Models explaining $\delta^{13}C$ and $\delta^{15}N$ variations of diet were fitted with the following predictor variables, Julian day (using a cyclic spline), altitude, latitude, NDVI. To account for inter-individual variations, models included 'individual' identity as a random effect. We also included an autoregressive model for errors (argument *correlation* = corARMA to the gamm function (package: mgcv) to account for the presence of temporal autocorrelation in the isotopic data. We rescaled data because some predictor variables were on different scales. We checked the normality of our data. We proceeded to a backward model selection based on AIC (Akaike information criterion). Histograms and QQ plots were used to inspect residuals for normality and independence. All data analyses were conducted in R (version 3.4.4).

4.4 Results

4.4.1 Altitudinal mobility inferred by GPS

Lavielle's segmentation of GPS data indicated that horses moved between 3.4 and 11.5 times per year during the study period (mean = 7.5, s.d. = 2.9). The study animals spent between 31 and 85 d on each pasture (mean = 51.3 d, s.d. = 19.6, median = 30 d), and used a mean area ranging from 65 to 434 km² (mean = 221.9 km², s.d. = 140.2) (**Table 1**). All the horses but one (Dl 1) displayed an East-West spatial movement pattern (**Figure 7**) with sharp altitudinal mobility between the eastern depression (1205 – 1468 m asl) and the western mountain pastures (up to 2800 – 3215 m asl). Horse Dl remained at a high altitude of 2366 ± 138 m asl during the study period (see **Supplementary Figure S4.1** for detailed data).

2.4.2 Tail hair carbon and nitrogen isotope ratios

Tail hair growth rate varied between 0.50 and 0.85 $mm.d^{-1}$ with a mean of 0.69 ± 0.11 $mm.d^{-1}$ (see **Supplementary Table S4.1**). As a result, the 7.5 mm increments taken on each tail hair represented an average period of 11.1 ± 1.9 d (ranging from 8.8 to 15 d).

Summary statistics are given in **Supplementary Table S4.1**. $\delta^{13}C_{diet}$ values were not statistically different among horses (Tukey HSD p-value > 0.05). Intra-individual variability ranged between 3.2‰ (Dl 1) and 6.0‰ (Kb 1) (**Supplementary Table S4.1**). We observed a very good agreement in $\delta^{13}C_{diet}$ values between different hair from the same individual (**Figure 8**) and limited (≤ 2 ‰) differences between hair from different horses from the same herder (Jk 1 vs Jk 2, Kj 1 vs Kj 2). Overall, the annual variability in $\delta^{13}C_{diet}$ values was 6.0‰ (between -30.2‰ and -24.2‰, **Supplementary Table S4.1**). Summer $\delta^{13}C$ values were significantly lower compared to the other seasons (-27.9 ± 0.7‰; p-value < 0.001; n = 149; 21st June to 20th September), with a minimum value in August (-28.3 ± 0.7‰, p-value <0.05, n = 37 – results not shown). On average winter showed the highest $\delta^{13}C$ values (-27.2 ± 0.6‰) but did not significant differ from spring (-27.3 ± 1.0‰) and autumn (-27.4 ± 0.8‰).

There was no statistical difference in $\delta^{15}N_{diet}$ values between the different individuals (Tukey HSD; p-value > 0.05). There was a good agreement in N-isotope values between hair from the same individuals (Jk 1, Kb 1, Dl 1, Kj 2 – **Figure 9**) and also between different individuals of the same herd. Intra-individual variability of $\delta^{15}N_{diet}$ values varied between 4.6‰ (Jk 1) and 10.6‰ (Dl 1). Overall, the annual variability in $\delta^{15}N$ values was 10.6‰ (between -2.1‰ and +8.5‰, **Supplementary Table S4.1**). N isotope composition was not statistically

different between seasons. The lowest $\delta^{15}N_{diet}$ values were recorded in July (+2.1 ± 1.8‰, p value <0.05, n = 55 – results not shown) and were surrounded by the highest $\delta^{15}N_{diet}$ values, measured in May and September.

4.4.3 Correlation between isotopic shifts and altitudinal mobility

In total, GPS tracking allowed the detection of 80 altitudinal mobilities. 53 significant carbon isotopic shifts were identified for all horses (**Table 2**), including 18 that matched a change of pasture inferred through the GPS data. The analysis of $d(\delta^{13}C_{diet})$ hence allowed to detect 22.5% of the 80 changes of pasture inferred by the GPS data for all the horses, ranging from 0% (Jk 2) to 34.8% (Jk 1) (**Table 2**). The analysis of $d(\delta^{15}N_{diet})$ also identified 54 significant isotopic shifts for all horses, sixteen (20%) shifts were linked with an altitudinal mobility inferred by the GPS data for all the horses, ranging from 0% (Dl 1) to 38.5% (Kj 1). C and N isotopic shifts were synchronous on 14 occasions. The combination of $d(\delta^{13}C_{diet})$ and $d(\delta^{15}N_{diet})$ allowed the detection of 38.8% of the 80 changes of pasture recorded in all individuals, varying individually from 18.2% (Jk 2) to 69.2% (Kj 1). Among the 107 isotopic shifts detected by either C or N isotope ratios, 76 (71%) were not linked with an altitudinal mobility.

Table 2: Summary of isotopic vs GPS inferred mobility. Each ratio represents the number of mobilities inferred through a significant isotopic shift over the number of changes of pasture inferred by GPS tracking. The number of significant isotopic shifts not associated with a change of pasture is also given. The analysis was done for each horse and for each herder (who had more than one horse monitored). Detailed results are provided in Supplementary Figure S2.2.

Horse	Significant shift of $\delta^{13}C$ values linked with mobility	Significant shift of $\delta^{15}N$ values linked with mobility	Significant shift of $\delta^{13}C$ and $\delta^{15}N$ values linked with mobility	Number of significant isotopic shifts not linked with change of pasture	
				For $\delta^{13}C$ values	For $\delta^{15}N$ values
Jk 1	8/23 (34.8%)	3/23 (13.0%)	9/23 (39.1%)	4	13
Jk 2	0/11 (0%)	1/11 (9.1%)	1/11 (9.1%)	7	9
Kb 1	2/10 (20%)	3/10 (30%)	4/10 (36.4%)	6	4
Dl 1	1/4 (25%)	0/4 (0%)	1/4 (25%)	2	3
Kj 1	4/13 (30.8%)	5/13 (38.5%)	9/13 (69.2%)	6	3
Kj 2	3/19 (15.8%)	4/19 (21.1%)	7/19 (36.8%)	10	6
Total	18/80 (22.5%)	16/80 (20%)	31/80 (38.8%)	35	38
Total without pastures < 11 days	17/71 (23.9%)	14/71 (19.7%)	29/71 (40.8%)	-	-
Herder					
Jk	8/29 (27.6%)	4/29 (13.8%)	10/29 (34.5%)	11	18
Kj	6/27 (22.2%)	9/27 (33.3%)	14/27 (51.9%)	16	9

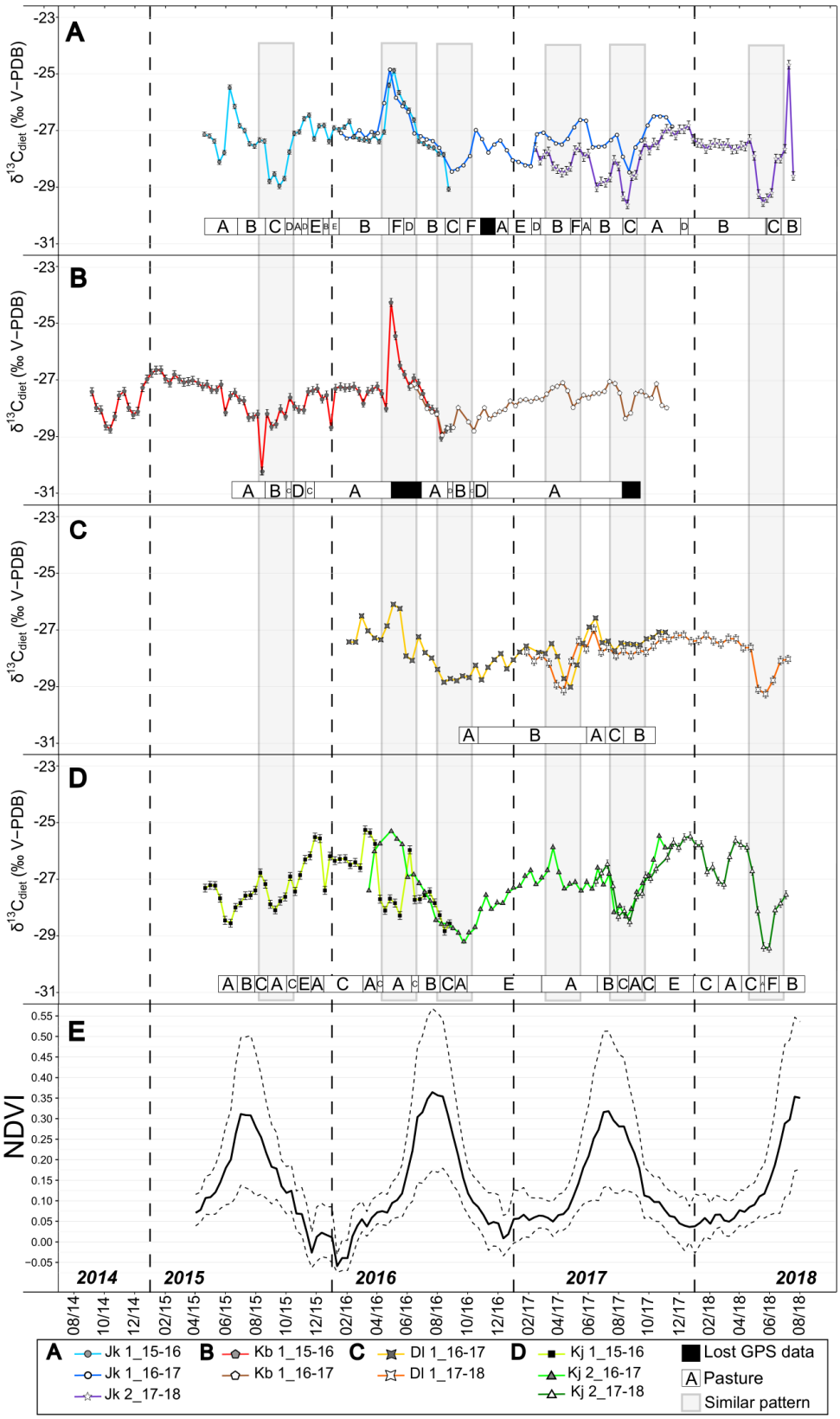

Figure 8: Panels A to D: Diet carbon isotope profiles of tail hair of six GPS-monitored horses. Each panel represents a different herder (A to D), each color a different tail hair and each symbol a different horse. To ease comparison, pastures identified by Lavielle's segmentation of altitudinal data are also reported, with letters at the bottom of each panel (one letter = one pasture). Panel E: Mean NDVI (black line) temporal variations in the study area, with standard deviation (dashed line). Grey shadings represent similar patterns in several hair profiles.

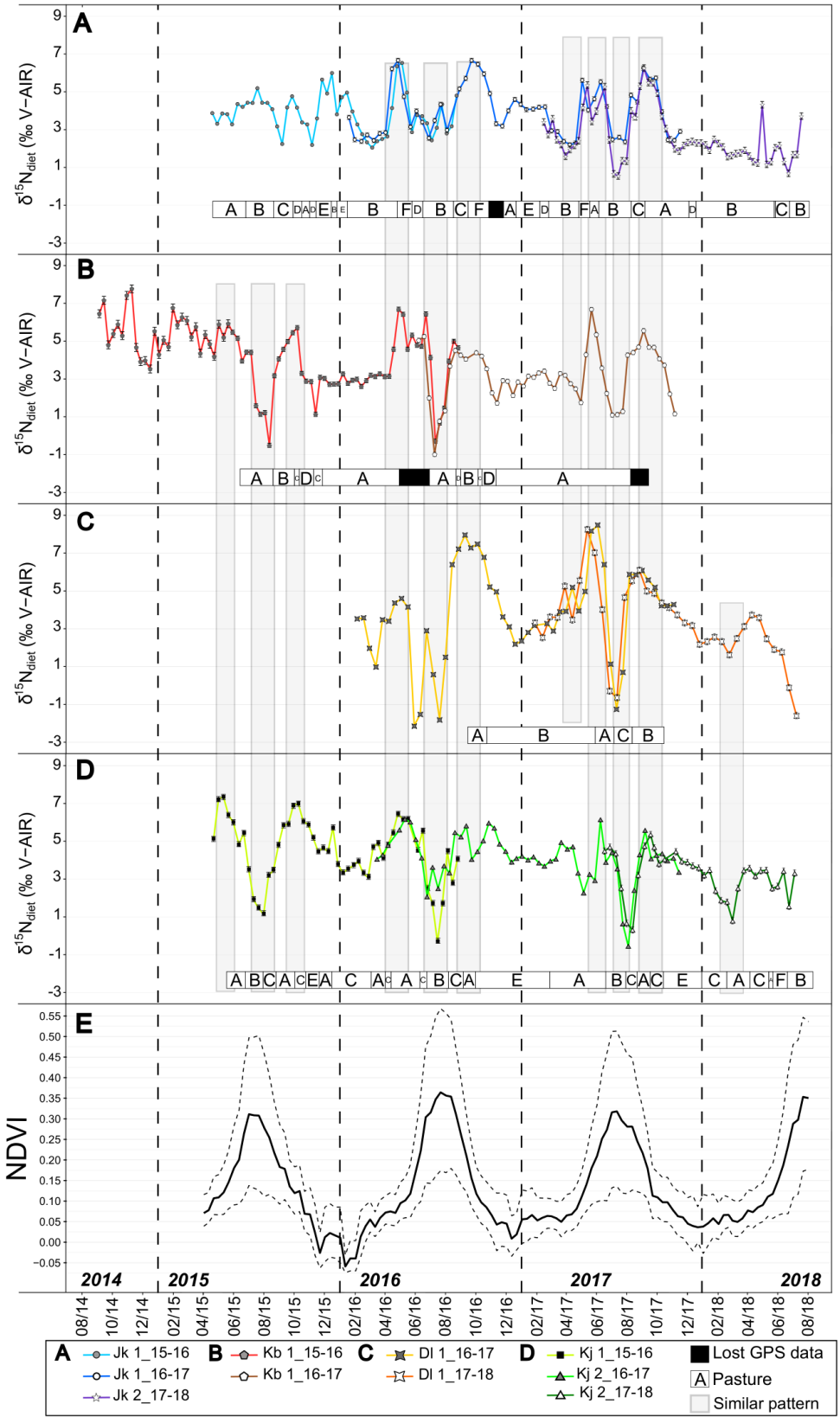

Figure 9: Panels A to D: Diet nitrogen isotope profiles of tail hair of six GPS-monitored horses. Each panel represents a different herder (A to D), each color a different tail hair and each symbol a different horse. To ease comparison, pastures identified by Lavielle's segmentation of altitudinal data are also reported, with letters at the bottom of each panel (one letter = one pasture). Panel E: Mean NDVI (black line) temporal variations in the study area, with standard deviation (dashed line). Grey shadings represent similar patterns in several hair profiles.

4.4.4 Factors influencing carbon and nitrogen stable isotopes

The stable isotope values measured along tail hairs and their corresponding date, latitude, longitude, altitude, NDVI and temperature are provided in **Supplementary Table S4.2**. The AIC scores of the different GAMM models are provided in **Supplementary Table S4.3**. The autoregressive model for temporal autocorrelation was not selected in the final models.

The best GAMM model investigating variation in $\delta^{13}C_{diet}$ values in tail hair included Julian day, Latitude and NDVI as only predictors (**Table 3**). The cyclic smooth term on Julian day was significant (**Figure 10A, Table 3**). The predicted values of Julian day on the $\delta^{13}C_{diet}$ values showed a strong annual cycle (**Figure 10A**) with inter-annual variability. This seasonal cycle was characterized by a rapid summer (June-September) decrease followed by a slow autumn to spring increase in $\delta^{13}C_{diet}$ values, with the exception of winter 2017/2018 where the $\delta^{13}C_{diet}$ increase was rapid. Finally, $\delta^{13}C_{diet}$ values were positively correlated with latitude (**Figure 10B**) and negatively correlated with NDVI (**Figure 10C**).

Table 3: Summary of GAMMs investigating the effects of geographical, temporal and environmental variability in δ13Cdiet and δ15Ndiet. The estimates and significance of terms are shown for the best model fit.

	Parametric coefficients				Approximate significance of smooth terms					
Model terms	Estimate	SE	t	p	Df	Rank	F	p	R^2	AIC
$\delta^{13}C_{diet}$										
Intercept	−0.05	0.15	−0.33	0.74					0.47	708.4
Latitude	0.28	0.12	−2.41	0.02						
NDVI	−0.08	0.10	−0.83	0.41						
s (Julian date, k = 30)					19.47	19.47	10.02	<2e-16		
$\delta^{15}N_{diet}$										
Intercept	−0.02	0.14	−0.18	0.86					0.45	702.18
Altitude	−0.19	0.06	−2.93	0.004						
NDVI	−0.02	0.10	−0.24	0.81						
s (Julian date)					27.64	27.64	5.11	5.7e-14		

The best GAMM model investigating variation of $\delta^{15}N_{diet}$ values in the tail hairs included 'Julian day', altitude and NDVI as predictors (**Table 3**). The cyclic smooth term on 'Julian day' was significant (**Figure 11A, Table 3**). The predicted values of $\delta^{15}N_{diet}$ showed an annual cycle (**Figure 11A**) with inter-annual variability. This annual cycle was characterized by important summer variations (amplitude ~2-3‰), with a rapid decrease from June to mid-summer and followed by a strong increase from mid-summer to September. Winter and autumn were mainly characterized by low $\delta^{15}N_{diet}$ values with little variations. The predicted effect of

NDVI on $\delta^{15}N_{diet}$ values was weak (**Figure 11C**). Finally, $\delta^{15}N_{diet}$ values were negatively correlated with altitude (**Figure 11B, Table 3**).

4.5 Discussion

C- and N- stable isotope ratios of tail hair recorded several significant variations over the study period. However, less than 40% of animal altitudinal movements were correlated to either C or N isotopic shifts, and the majority (71%) of the significant isotopic shifts were not correlated with altitudinal mobility. A significant isotopic change is hence not necessarily related to altitudinal mobility. Moreover, despite differences in the horse mobility histories we observed similarities in their pattern of C and N isotope variations (**Figures 8 & 9**), suggesting that factors other than altitude alone, such as weather events, influence plant isotopic composition. Despite this, a negative correlation was found between $\delta^{15}N_{diet}$ values and altitude including the one horse (Dl 1) with a reduced vertical mobility (<200 m), (**Figure 11B**). In the discussion below, we will first focus on the potential error on growth rate, which can affect the time assignment of our data. Then we will discuss the different factors driving change in $\delta^{13}C$ and $\delta^{15}N$ values of tail hair.

4.5.1 Time assignment and resolution of the isotopic record

We measured a mean tail hair growth rate of 0.69 ± 0.11 $mm.d^{-1}$ (**Supplementary Table S4.2**). This range of values is similar to those previously reported in domestic horses or wild equids (Ayliffe et al., 2004; Burnik Šturm et al., 2015; Dunnett, 2005; Sharp et al., 2003; West et al., 2004). Potential variability in the growth rate of a unique hair could deteriorate the temporal precision of chronologies, given the high frequency of mobility of some individuals, as well as the correlation between different hairs, dampening the peaks of existing seasonal patterns. Auerswald et al. (2011) showed that season and animal age had an impact on the tail hair growth of cattle. They found that growth rate was slower in winter than in summer and decreased with increasing age. This is in contradiction with the results of other studies showing that hair growth rate could be considered as constant over a year with no clear seasonal signal (Dunnett, 2005; West et al., 2004; Wittemyer et al., 2009). In our study, growth rates were calculated independently for each hair. We observed an agreement between the isotopic profiles from different individuals from the same herd (and the same mobility pattern e.g. Jk 1 & Jk 2), but also for horses from different herds (**Figures 8 & 9**). This suggests that the assumption of

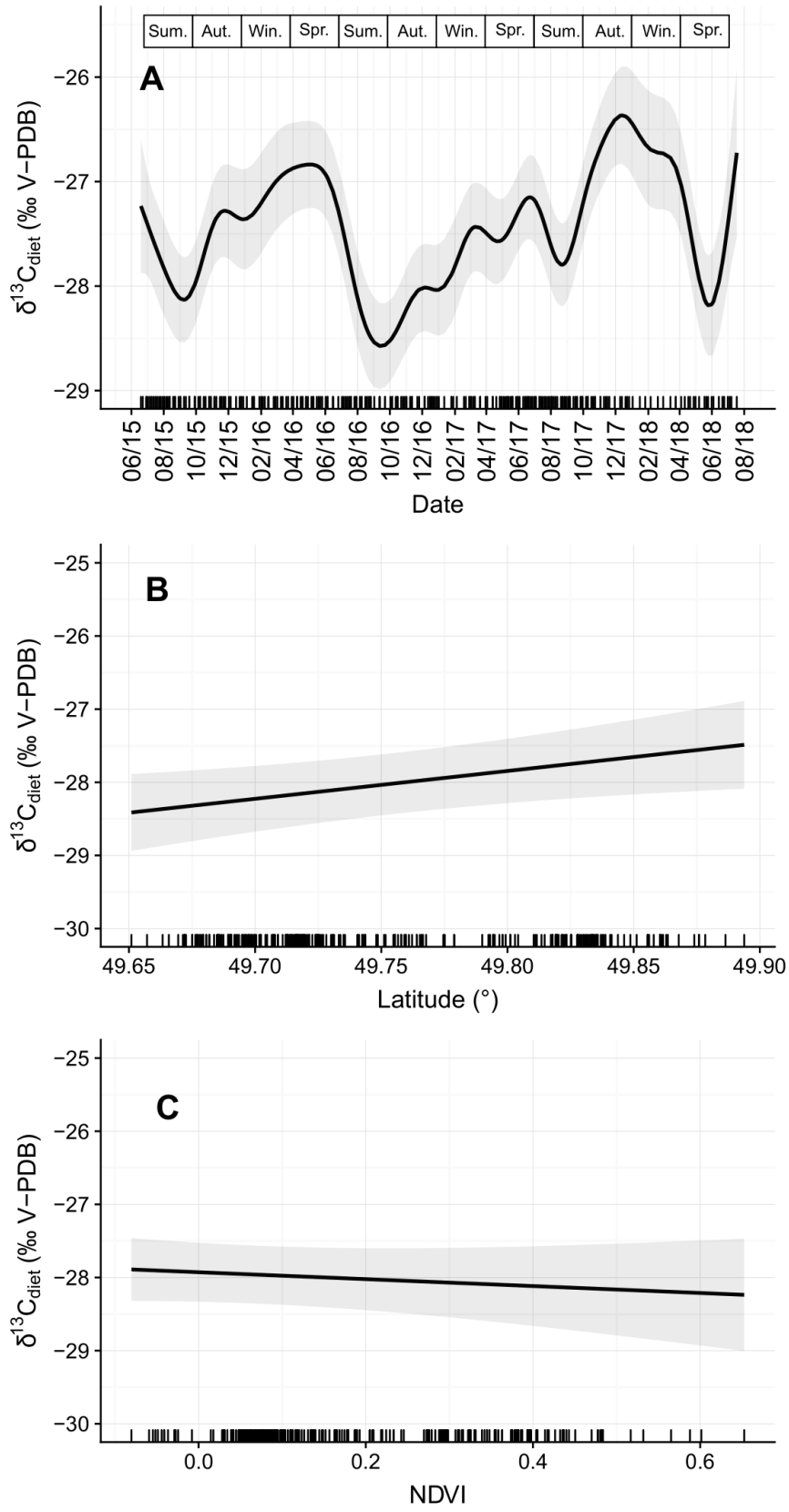

Figure 10: Smoother plots showing the relationships between predicted of δ13Cdiet values from the GAMM model and Julian day (A – smooth term), Latitude (B) and NDVI (C). Grey shadings represent the 95% confidence interval. Tick marks at the bottom of each graph indicate sample points.

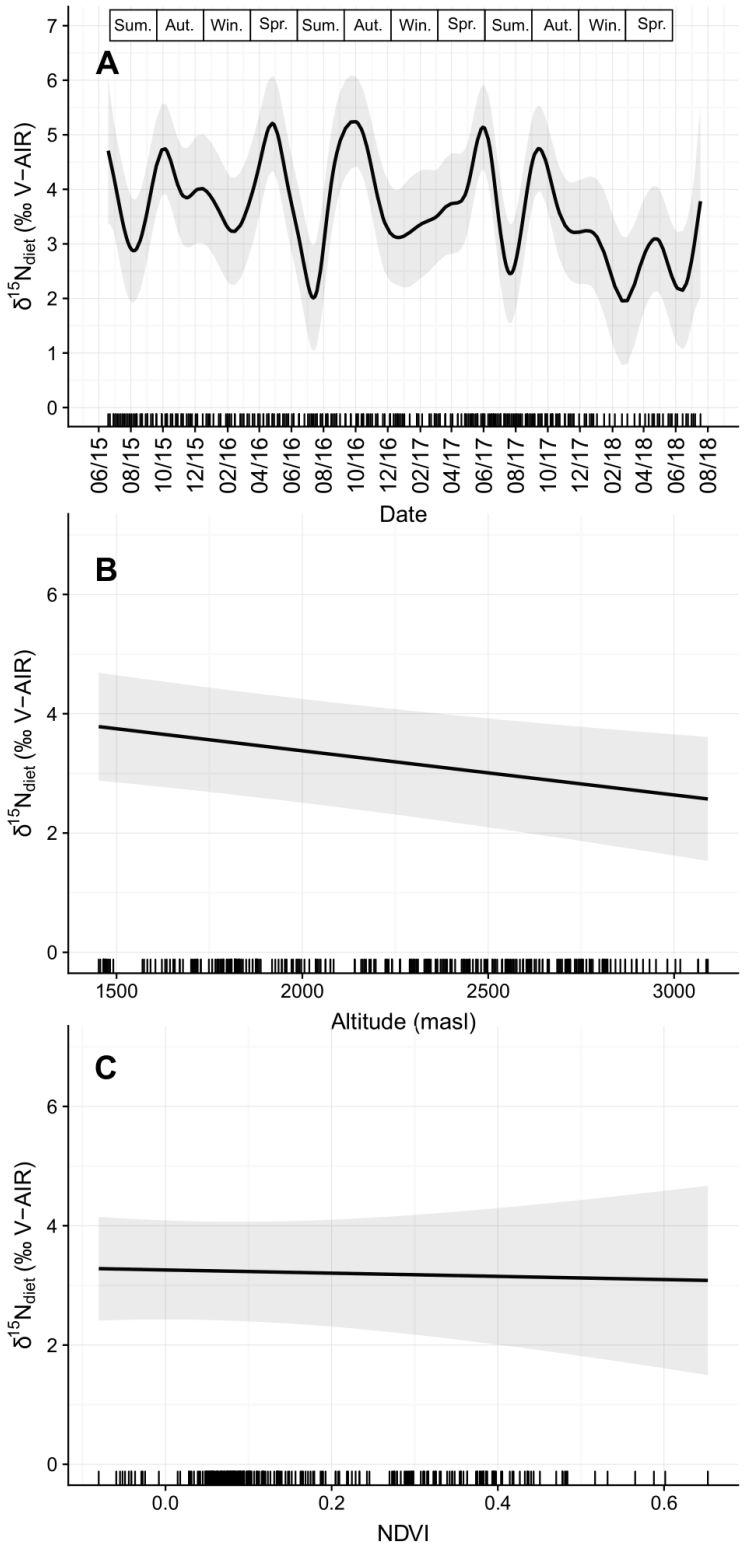

Figure 11: Smoother plots showing the relationships between predicted of $\delta^{15}N_{diet}$ values from the GAMM model and Julian day (A – smooth term), Altitude (B) and NDVI (C). Grey shadings represent the 95% confidence interval. Tick marks at the bottom of each graph indicate sample points.

a constant growth rate at the individual hair level is reasonable, regardless of the time of year or the age of the animal, and that this parameter has little impact on the temporal accuracy of our time line.

In addition to hair growth rate, the temporal resolution of our isotopic records (i.e. the timespan represented by each hair fragment) is mainly determined by the length of each fragment. Because a minimum sample mass is needed for isotopic analyses, the fragment length chosen was ~ 7.5 mm. The variability in growth rate between hairs of the same individuals (West et al., 2004) precluded the combination of multiple hairs (which would have allowed a reduction of fragment length for the same mass). However, the duration of the stay in most pastures (median = 30 d) was larger than the isotopic resolution (11.1 ± 1.9 d) and only nine pastures were used for a duration shorter than or equal to 11 d. The removal of these short-term pastures only marginally increased the proportion of pasture changes identified by isotopic shifts (**Table 2**). We are therefore confident that the temporal resolution of our isotopic records was appropriate to detect pasture changes.

4.5.2 Environmental control on variations in $\delta^{13}C$ hair values

We did not find any influence of altitude on the variation in $\delta^{13}C_{diet}$ values. This result is somewhat surprising because several studies have shown the existence of an altitudinal gradient in the carbon isotopic composition of plants (Körner et al., 1991; Li et al., 2009; Liu et al., 2016, 2007; Männel et al., 2007; van de Water et al., 2002). However, this is in good agreement with Burnik Šturm et al. (2016) (**Supplementary Table S4.2** and personal communication, May 13, 2019) , who did not find any altitudinal effect on $\delta^{13}C$ of C_3 plants (*Artemisia* sp. and *Stipa* sp. - from 1600 to 2800 m.asl) in the Dzungarian Gobi in South Western Mongolia. In arid and semi-arid regions, drought stress is the most significant factor controlling plants $\delta^{13}C$ values, with higher drought stress in lowland than in high altitude, leading to a decrease of plant $\delta^{13}C$ values with altitude (Liu et al., 2016; van de Water et al., 2002; Wang et al., 2016). We propose that animal feeding ecology could mask the relationship between plant $\delta^{13}C$ values and altitude. Indeed, the horse's diet is very selective and can vary seasonally (Salter and Hudson, 1979; Slivinska and Kopij, 2011). It is mainly composed of grasses, but can also include trees and shrubs. When domestic horses were grazing in lowland pastures, they remained preferentially near rivers or humid areas (i.e. Moin in **Figure 7**) and had access to grasses, trees and shrubs. On the contrary, when at high altitude they only had access to grasses. The relationship between plant $\delta^{13}C$ values and altitude seems less

pronounced for grasses than for trees or forbs, and this could also explain our results (Körner et al., 1988). Finally, the observed influence of latitude on $\delta^{13}C_{diet}$ values could also be explained by local differences in water availability between the northern and southern ends of the lowland areas. Indeed, higher $\delta^{13}C_{diet}$ values (mean = -27.1 ± 0.1‰) were measured for the two horses (Kj 1 & Kj 2; mean latitude = 49.83 ± 0.03°), which spent more time near Burgast than for the other four horses (mean = -27.6 ± 0.3‰ - **Supplementary Table S4.1**) located further south in Moin (mean latitude = 49.71 ± 0.03°).

Horse tail hairs showed a cyclic seasonal pattern characterized by high winter and low summer $\delta^{13}C_{diet}$ values (**Figure 10A**). This pattern has been described elsewhere in the literature, and is often interpreted as reflecting a seasonal change in the relative proportion of C_3 vs C_4 plants in the diet, either through direct consumption of perennial C_4 plants during winter (Burnik Šturm et al., 2016; Henton et al., 2017b), C_4 winter foddering (Makarewicz, 2017; Makarewicz et al., 2018; Makarewicz and Pederzani, 2017), or because of animal altitudinal mobility and the decrease in the relative abundance of C_4 taxa with increasing elevation (Makarewicz and Tuross, 2012; Makarewicz, 2017; Makarewicz et al., 2017; Tornero et al., 2018). Here, average $\delta^{13}C_{diet}$ values range between -30.2‰ and -24.2‰ suggesting that the horses' diet was essentially composed of C_3 plants as expected for a mountainous steppe environment in Central Asia (Pyankov et al., 2000; Still et al., 2003). Thus, we cannot invoke the influence of C_4 plants in the diet to explain the seasonal pattern observed in the domestic horses of the Mongolian Altai. In a C_3 environment, several factors influence the carbon isotopic composition of plants. C-isotope ratios of C_3 plants vary on a seasonal scale (1-2‰), with the highest values occurring during the warm/dry season and the lowest values occurring during the wet/cold season (Diefendorf et al., 2010; Fraser et al., 2008; Smedley et al., 1991). In a semi-arid environment, like the Eurasian steppe, water availability is the main factor controlling plant $\delta^{13}C$ values, with more negative values associated with higher water availability (Ehleringer and Dawson, 1992; Flanagan and Farquhar, 2014; Hartman and Danin, 2010; Kohn, 2010; Liu et al., 2007; Murphy and Bowman, 2009). Indeed, during periods of water stress, C_3 plants limit water losses by closing their stomata involving a decrease in CO_2 fixation, leading to a ^{13}C enrichment of the leaves (Cernusak et al., 2016; Ehleringer and Dawson, 1992; Farquhar et al., 1989, 1982). When water availability increases, water use efficiency decreases and this results in a decrease in leaf $\delta^{13}C$ values.(Farquhar et al., 1989, 1982; Kohn, 2010) In Western Mongolia, most of the precipitations occur during summer and are accompanied by snowmelt from high altitude, which begins in late spring at the same time

as the growing season (NDVI – **Figure 8E**). This could explain the minimum $\delta^{13}C_{diet}$ values recorded in summer. Moreover, during periods of active growth, photosynthesis is more efficient at using the ^{13}C isotope which causes an increase of $\delta^{13}C$ values.(Farquhar et al., 1989) The increase observed in April/May, simultaneous with rapid increase of NDVI, before summer precipitation, could therefore be explained by this mechanism. The increase in $\delta^{13}C_{diet}$ during winter cannot be explained by the lack of water availability, as there is no more photosynthesis (NDVI near 0 – **Figure 8E**). A strong decrease in photosynthetic capacity occurs during plant senescence. No difference in $\delta^{13}C$ between senescent leaves and green leaves has been established so far, so plant senescence (observed in winter) cannot explain this pattern either (Cloern et al., 2002; Wooller et al., 2003). However, different parts of a plant may differ in $\delta^{13}C$ values (Badeck et al., 2005; Codron et al., 2005) with roots and stems being more ^{13}C-enriched than leaves (Badeck et al., 2005). During winter, horses cannot be as selective as they are during summer and possibly have to eat the stems by digging through snow with their sharp and strong hooves, hence potentially explaining the increase *in* $\delta^{13}C_{diet}$ values during this period.

We also observed inter-annual variability in $\delta^{13}C_{diet}$ values with a larger amplitude in 2016 than in 2017 (**Figure 10A**). If water availability is the main factor of variations in $\delta^{13}C$ values, these results should translate into inter-annual variations in the precipitation patterns with more precipitation in 2016 (larger ^{13}C depletion in 2016 than 2017). The amount of rain at the Nogoonnuur station was not larger in 2016 (118 and 169 mm in 2016 and 2017 respectively – available at: http://www.infoclimat.fr), but snow cover was much higher in March 2016 than in March 2017 (995 mm vs 5 mm respectively). This difference in snowfalls could lead to higher water input into rivers and soils during summer 2016 and ultimately to lower plant $\delta^{13}C$ during summer but also the following winter. Interviews with herders confirmed this inter-annual difference in climate and vegetation growth between the two years (data not shown). However, we are aware that the survey period is too short to build strong inferences and that more work would be needed to ascertain this conclusion.

4.5.3 Environmental control on seasonal variation in hair $\delta^{15}N$ values

The large and synchronous variations measured in tail hair $\delta^{15}N$ values indicate that this tissue is able to record seasonal variation in plant isotopic composition at the regional scale. Plant $\delta^{15}N$ values are highly sensitive to variations in environmental factors and plant physiology, such as water and N availability, pathway of N assimilation, source of nitrogen and whether N is acquired directly from the soil or through symbiotic relationships with mycorrhiza.

As a result, $\delta^{15}N$ values can vary drastically between different microhabitats (Codron et al., 2005; Craine et al., 2009; Handley et al., 1999; Szpak, 2014). The water input from snowmelt occurs during late spring and early summer and is synchronous with the start of the growing season (NDVI – **Figure 9E**). Snowmelt may bring an important water supply in soil, increasing water at both valley bottoms and rich pastures soils at higher altitude. Increased water availability in soils increases soil denitrification and N loss, driving the overall ecosystem $\delta^{15}N$ values upwards. This could explain the increase in $\delta^{15}N$ values measured in spring, synchronous with the decrease in $\delta^{13}C_{diet}$ values. In turn, the general decrease in tail hair $\delta^{15}N$ between October and December could be explained by soil mineralization and nitrification in relation with a decrease in water availability (Craine et al., 2015; Hartman and Danin, 2010). It is noteworthy that the observed ^{15}N-enrichement in late winter/early spring could also be explained by animal weight loss during this time period (Fuller et al., 2005; Rysava et al., 2016), but since we did not monitor this parameter it is not possible to test this hypothesis.

The sharp (ca. 3-5 per mil) decrease in $\delta^{15}N$ values, observed for all animals in May-June (followed by an increase of the same magnitude in July-August) is somewhat more complicated to explain. In July, all the animals were grazing in high altitude pastures, and the low $\delta^{15}N$ values measured are responsible for the negative correlation between $\delta^{15}N_{diet}$ values and altitude (**Figure 11B**) in line with conclusions from other studies (Liu et al., 2007; Männel et al., 2007; Samec et al., 2017; Szpak et al., 2013). However, this spike is also recorded for the one horse (Dl 1) with no or very limited vertical mobility (< 200 m) and is rapidly (ca. one month later) followed by a sharp increase in $\delta^{15}N_{diet}$ values, not observed in $\delta^{13}C$ values.

Climatic factors are not likely to explain this phenomenon because it is too rapid and it would also affect plant $\delta^{13}C$ values. Therefore, this isotope spike, which occurs when pasture productivity is at its highest (**Figure 9E**), seems more related to the fact that all animals had access to a different type of plants for a limited period of time in June-July rather than to mobility between different pastures itself. In order to explain this abrupt decrease of diet $\delta^{15}N$ values, we propose that the horses had access to N_2 fixing plants (e.g. such as Fabaceae) during early-summer as the $\delta^{15}N$ values of plants that rely on N_2 fixation are usually near 0‰ reflecting atmospheric isotopic values (Craine et al., 2009). Preferential consumption of plants of the Fabaceae family during summer has been observed in the Przewalski's horse living in eastern Europe (Slivinska and Kopij, 2011). It is noteworthy that several species belonging to the N_2 fixing plant family Fabaceae such as *Caragana spinosa, Caragana bungei or Caragana pygmae* were identified in the study area (preliminary identification by Prof. Oyuntsetseg Batlai

personal communication). Isotopic analysis of four *Caragana* sp. samples taken during the June 2015 fieldtrip ($\delta^{15}N$ = 0.8±1.8‰) confirms their N_2 fixing status. Other Fabaceae, such as *Medicago* sp., *Thermopsi*s sp., *Glycyrrhiza* sp. and *Oxytropis aciphylla* are also consumed by horses in summer (Dash, 1966; Sambuu, 1945). *Medicago* sp. (clover) is abundantly consumed by horses, and can be found in the Mongolian Altai (Dash, 1966; Sambuu, 1945). N isotope values close to zero are measured in every horse, and thus, an important increase in the proportion of N_2 fixing plants in the horse's diet during a short period of maximum productivity could explain the decrease observed in tail hair $\delta^{15}N$ values. Direct observation of the horse dietary preferences would be necessary to confirm this hypothesis.

4.6 Conclusion

Despite the fact that Mongolian horse tail hair exhibit seasonal variability in $\delta^{13}C$ and $\delta^{15}N$ values, few significant isotopic shifts matched with changes of pasture, showing that a significant isotopic change is not necessarily related to an altitudinal mobility in the strong continental climate and C_3 dominated environment of Western Mongolia. At first order, we propose that variations in $\delta^{13}C$ and $\delta^{15}N$ values were influenced by seasonal change in soil moisture rather than altitudinal mobility or winter foddering as proposed in the literature. We also found a correlation between $\delta^{15}N$ values of tail hair and altitude but because a similar pattern of low summer $\delta^{15}N$ values was found for a horse with no or very little altitudinal mobility, we propose that short-term diet switches occurring at high altitude rather than altitudinal mobility *per se* is responsible for the observed N isotope shift. Hair has received increased interest as an archive of past animal life cycle. Because of its extensive management system, the Mongolian horse is a good animal model to study past herding practices provided that the complexity of the factors driving the isotope record is not overlooked.

ACKNOWLEDGEMENTS

We are deeply indebted to all the herders who kindly participated to the study and accepted to host two of us (AZ and CM) during the 2017 winter and 2018 summer fieldtrips. We are thankful to Prof O. Batlai (Natl Univ Mongolia) for her help with plant identification. We would like to thank A. Pinhède (Direction de l'Archéologie de Chartres Métropole.) who created map of the study area and Ts. Turbat (Institute of History and Archaeology, Mongolian Academy of Sciences) for the logistics and assistance during the fieldwork. We are grateful to K. Auerswald and two anonymous reviewers, whose constructive comments helped improving the manuscript. Fieldwork was supported by the French archaeological mission in Mongolia (CNRS, MNHN, MAEDI, director: SL) and by the CNRS. This

research was funded by a Ph.D. grant to NL from the French National Research Agency LabEx ANR-10-LABX-0003-BCDiv, in the context of the “Investissements d’avenir” n°ANR-11-IDEX-0004-02 and an Inalco Early Career Research Grant 2017 to CM.

SUPPLEMENTARY INFORMATION OF CHAPTER 4

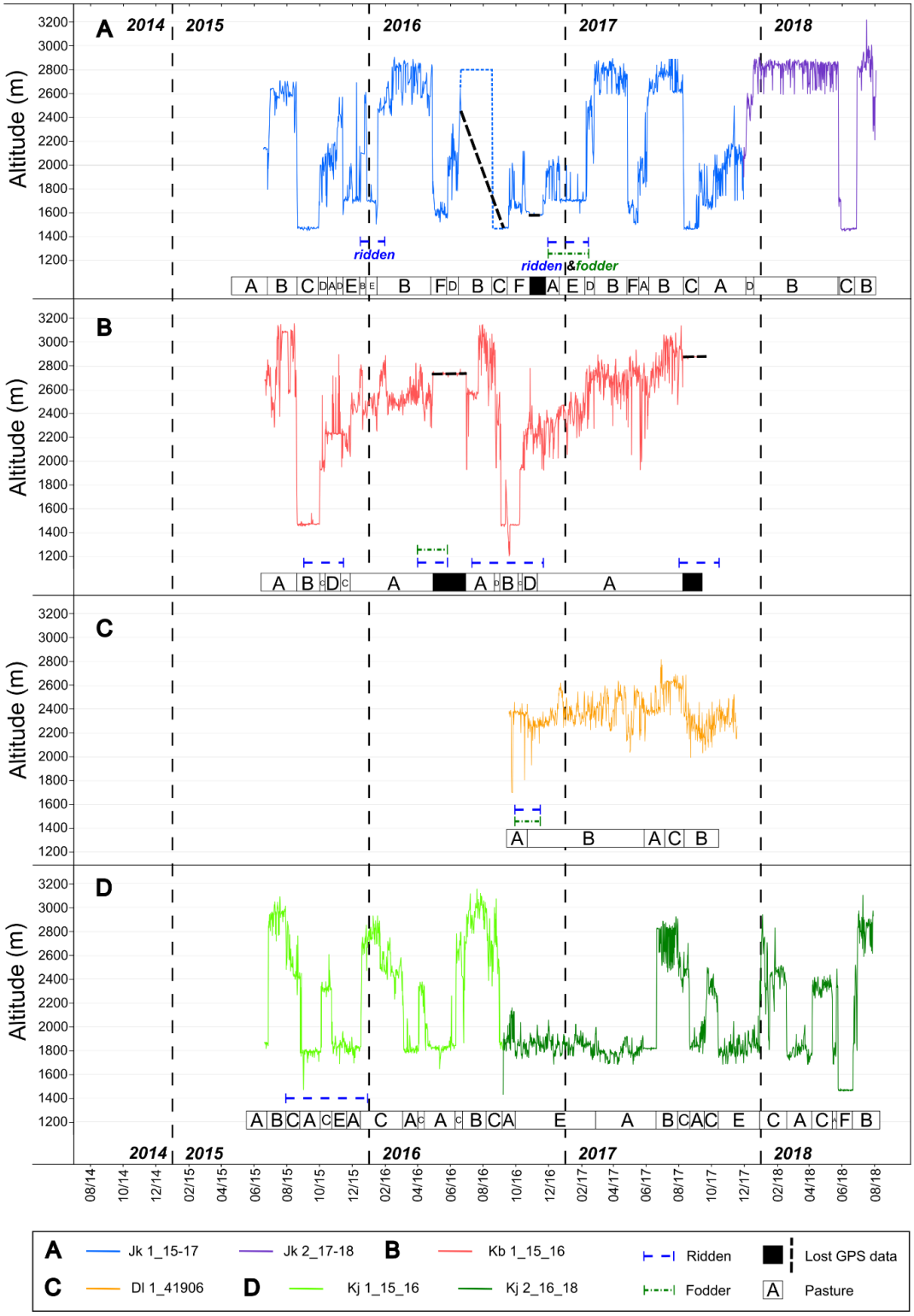

Supplementary Figure S4.1: (previous page) Temporal altitudinal variations of GPS-monitored horses. Each panel represents a different herder (A to D), each color a different horse. Pastures identified by Lavielle's segmentation of altitudinal data are represented with letters at the bottom of each panel (one letter = one pasture). Interruption of GPS monitoring are represented by black boxes.

Supplementary Figures S4.2

First derivative was calculated by the following equation: $d(\delta_i) = (\delta_{i+1} - \delta_{i-1})/(t_{i+1} - t_{i+1})$ where δ is the isotopic composition of the sample i of the hair and t is the date of the hair sample calculated from the hair growth rate.

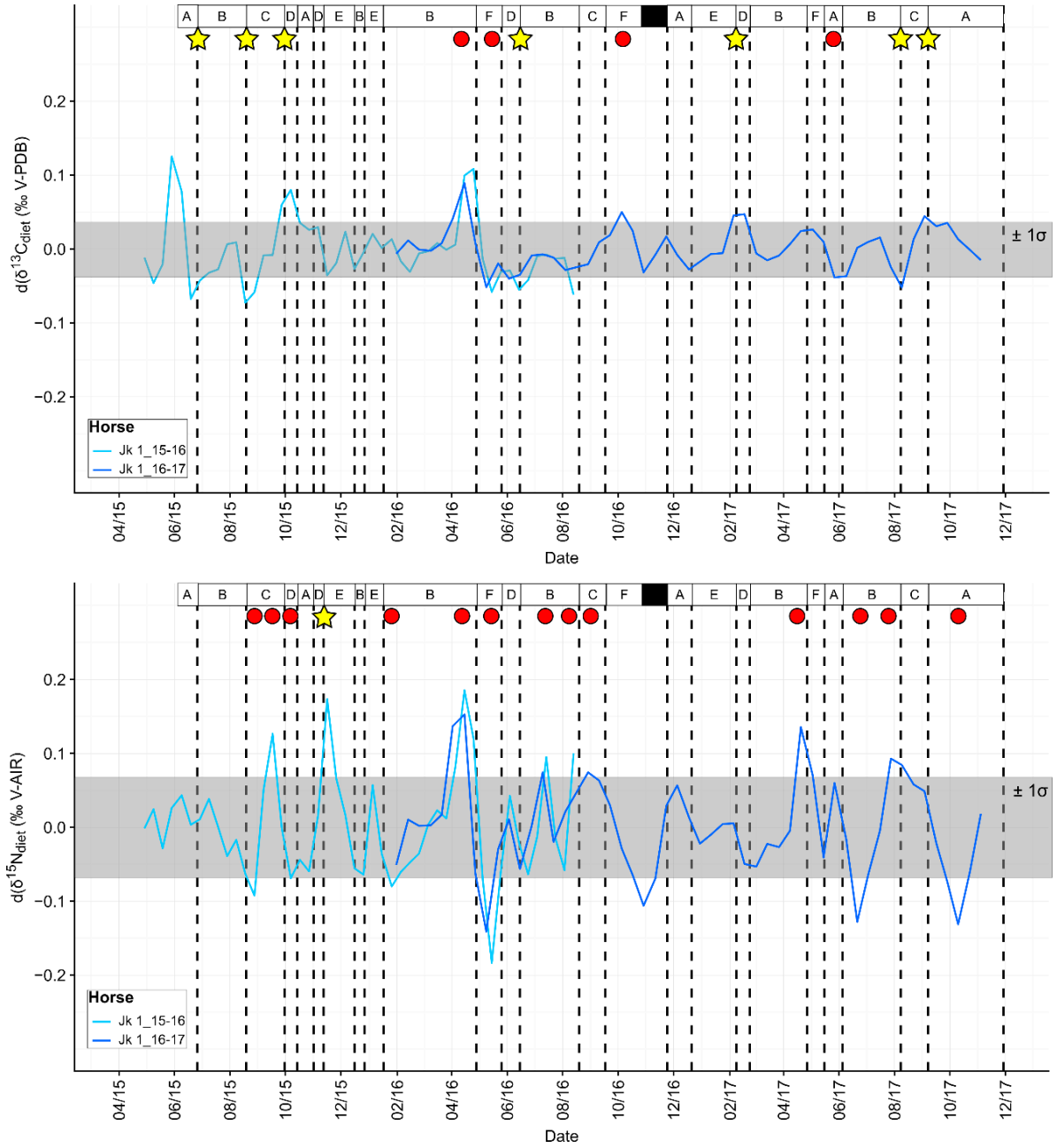

Figure S4.2.A: First derivative of $\delta^{13}C_{diet}$ (Top) and $\delta^{15}N_{diet}$ (Bottom) of horse Jk-1 ($d(\delta^{13}C_{diet})$ and $d(\delta^{15}N_{diet})$; (units are ‰/day). Vertical dashed lines represent changes of pasture determined by GPS, named with capital letters (same names as in Fig.8A & 9A). Black squares represent loss of GPS data. The different colors represent the two tail hairs sampled. Yellow stars mean that an important isotopic shift (i.e. which exceeded = one standard deviation of the time-series of isotopic values) matched with a change of pasture identified by GPS. There were 7 changes of pasture where the $d(\delta^{13}C_{diet})$ exceeded 1σ value and 1 for $d(\delta^{15}N_{diet})$. On the contrary, 4 significant $\delta^{13}C_{diet}$ shifts and 13signficant $\delta^{15}N_{diet}$ shifts were not linked with a change of pasture (red circles)

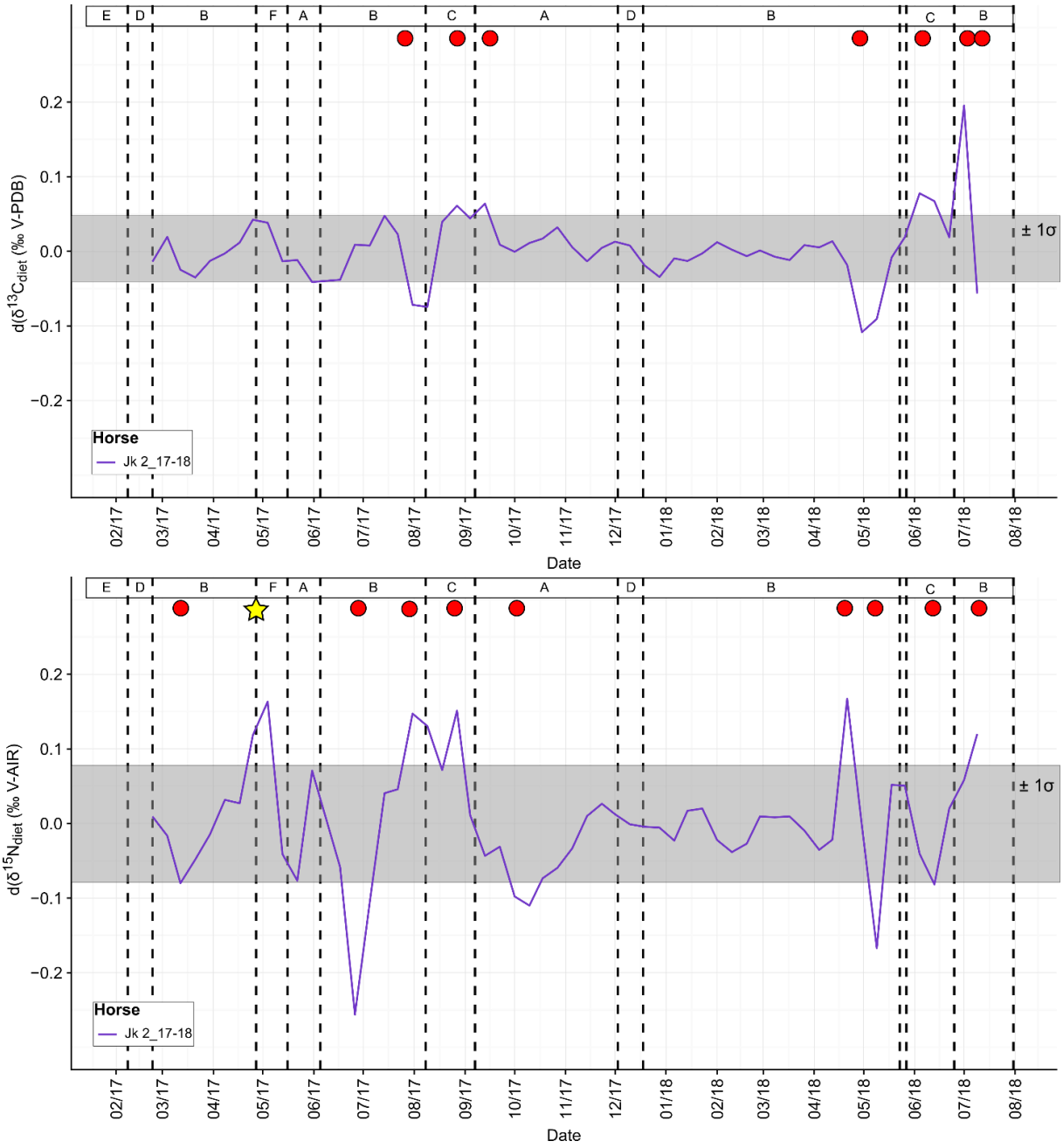

Figure S4.2.B: First derivative of $\delta^{13}C_{diet}$ (Top) and $\delta^{15}N_{diet}$ (Bottom) of horse Jk-2 ($d(\delta^{13}C_{diet})$ and $d(\delta^{15}N_{diet})$; (units are ‰/day). Vertical dashed lines represent changes of pasture determined by GPS, named with capital letters (same names as in Fig.8A & 9A). Black squares represent loss of GPS data. The different colors represent the two tail hairs sampled. Yellow stars mean that an important isotopic shift (i.e. which exceeded = one standard deviation of the time-series of isotopic values) matched with a change of pasture identified by GPS. There were 0 changes of pasture where the $d(\delta^{13}C_{diet})$ exceeded 1σ value and 1 for $d(\delta^{15}N_{diet})$. On the contrary, 7 significant $\delta^{13}C_{diet}$ shifts and 9 significant $\delta^{15}N_{diet}$ shifts were not linked with a change of pasture (red circles)

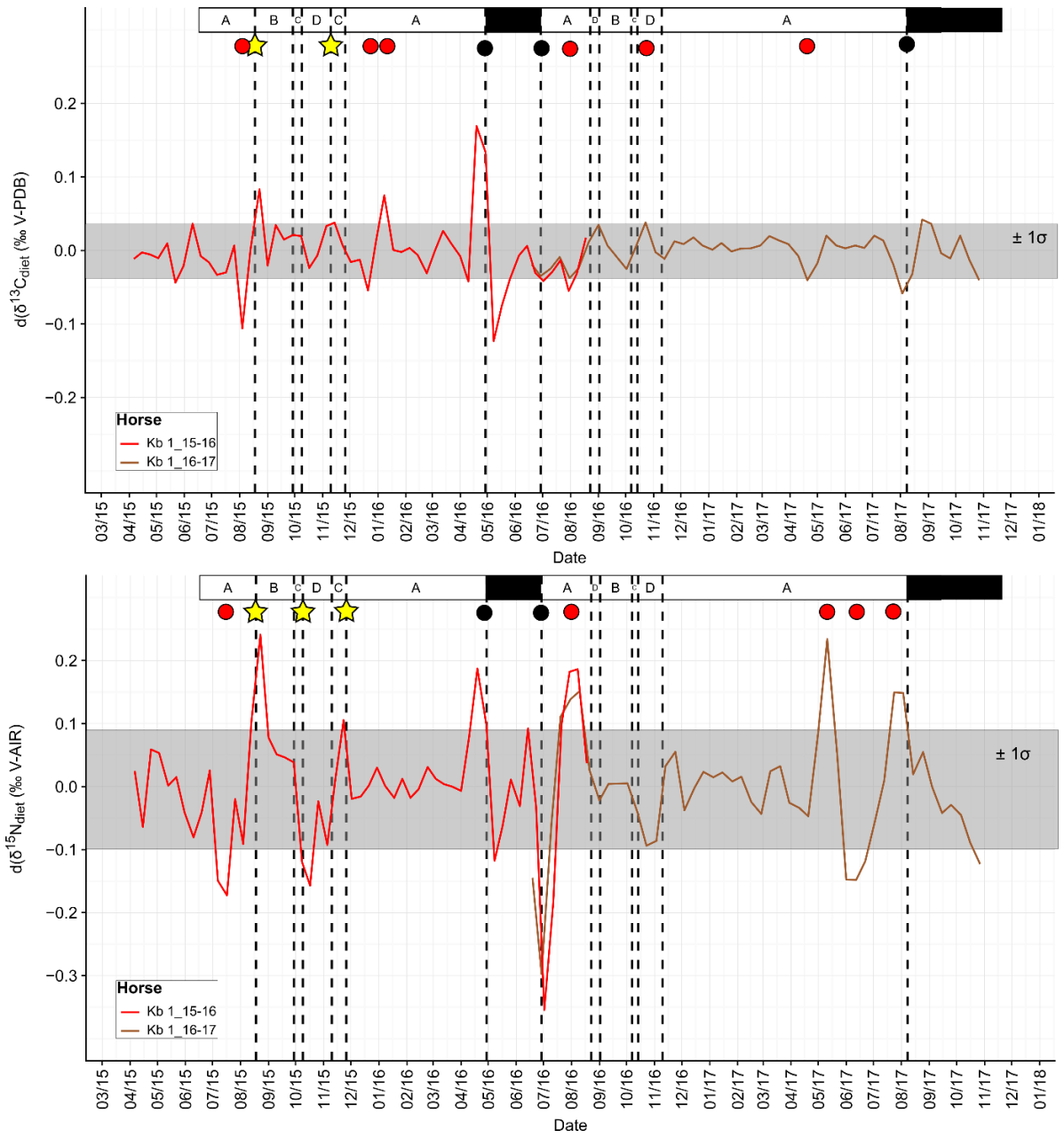

Figure S4.2.C: First derivative of $\delta^{13}C_{diet}$ (Top) and $\delta^{15}N_{diet}$ (Bottom) of horse Kb 1 ($d(\delta^{13}C_{diet})$ and $d(\delta^{15}N_{diet})$; (units are ‰/day). Vertical dashed lines represent changes of pasture determined by GPS, named with capital letters (same names as in Fig.8B & 9B). Black squares represent loss of GPS data. The different colors represent the two tail hairs sampled. Yellow stars mean that an important isotopic shift (i.e. which exceeded = one standard deviation of the time-series of isotopic values) matched with a change of pasture identified by GPS. There were 2 changes of pasture where the $d(\delta^{13}C_{diet})$ exceeded 1σ value and 3 for $d(\delta^{15}N_{diet})$. On the contrary, 6 significant $\delta^{13}C_{diet}$ shifts and 5 significant $\delta^{15}N_{diet}$ shifts were not linked with a change of pasture (red circles)

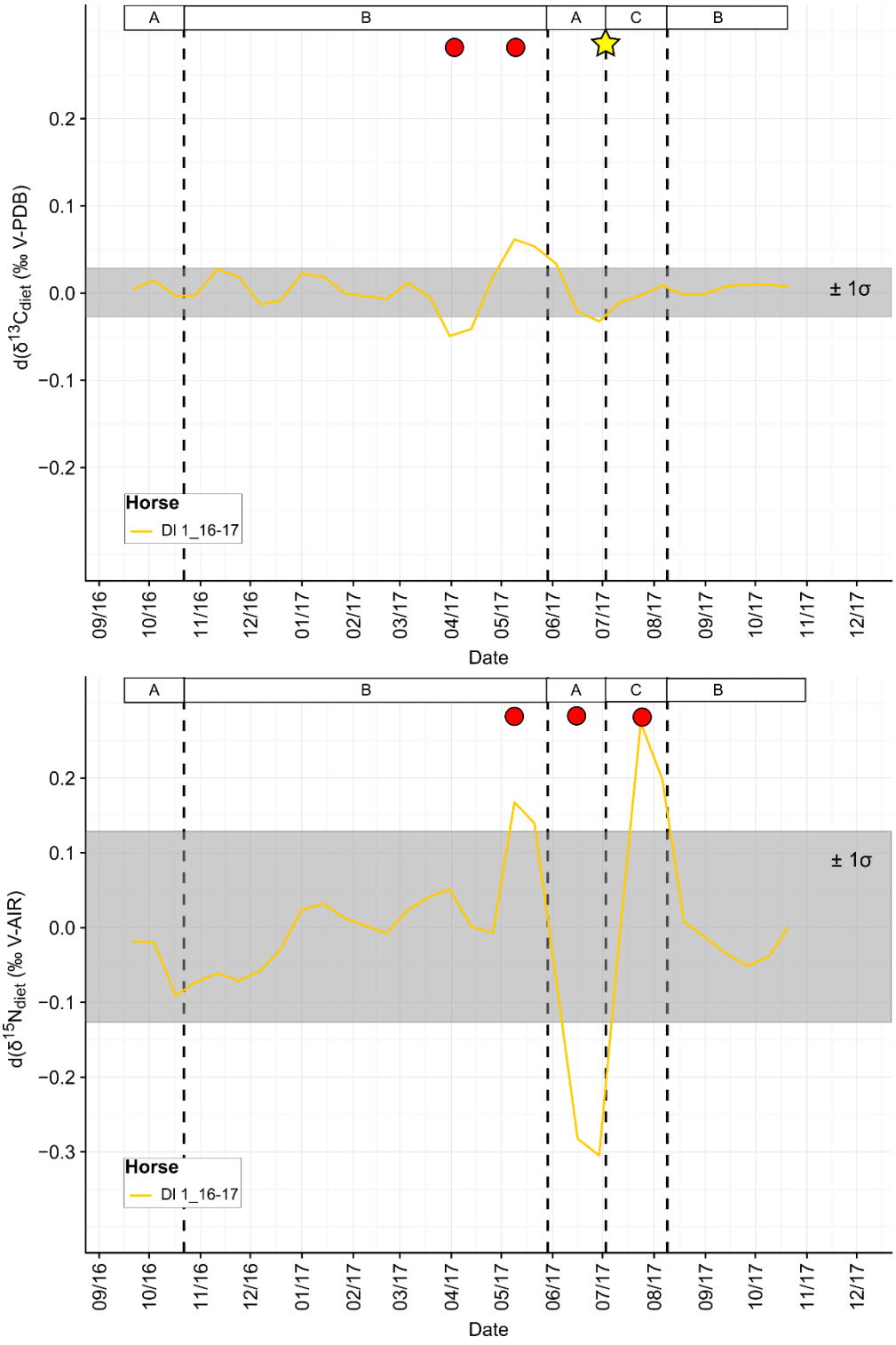

Figure S4.2.D: First derivative of $\delta^{13}C_{diet}$ (Top) and $\delta^{15}N_{diet}$ (Bottom) of horse Dl 1 ($d(\delta^{13}C_{diet})$ and $d(\delta^{15}N_{diet})$; (units are ‰/day). Vertical dashed lines represent changes of pasture determined by GPS, named with capital letters (same names as in Fig.8C & 9C). Black squares represent loss of GPS data. The different colors represent the two tail hairs sampled. Yellow stars mean that an important isotopic shift (i.e. which exceeded = one standard deviation of the time-series of isotopic values) matched with a change of pasture identified by GPS. There were 1 change of pasture where the $d(\delta^{13}C_{diet})$ exceeded 1σ value and 0 for $d(\delta^{15}N_{diet})$. On the contrary, 2 significant $\delta^{13}C_{diet}$ shifts and 3 significant $\delta^{15}N_{diet}$ shifts were not linked with a change of pasture (red circles).

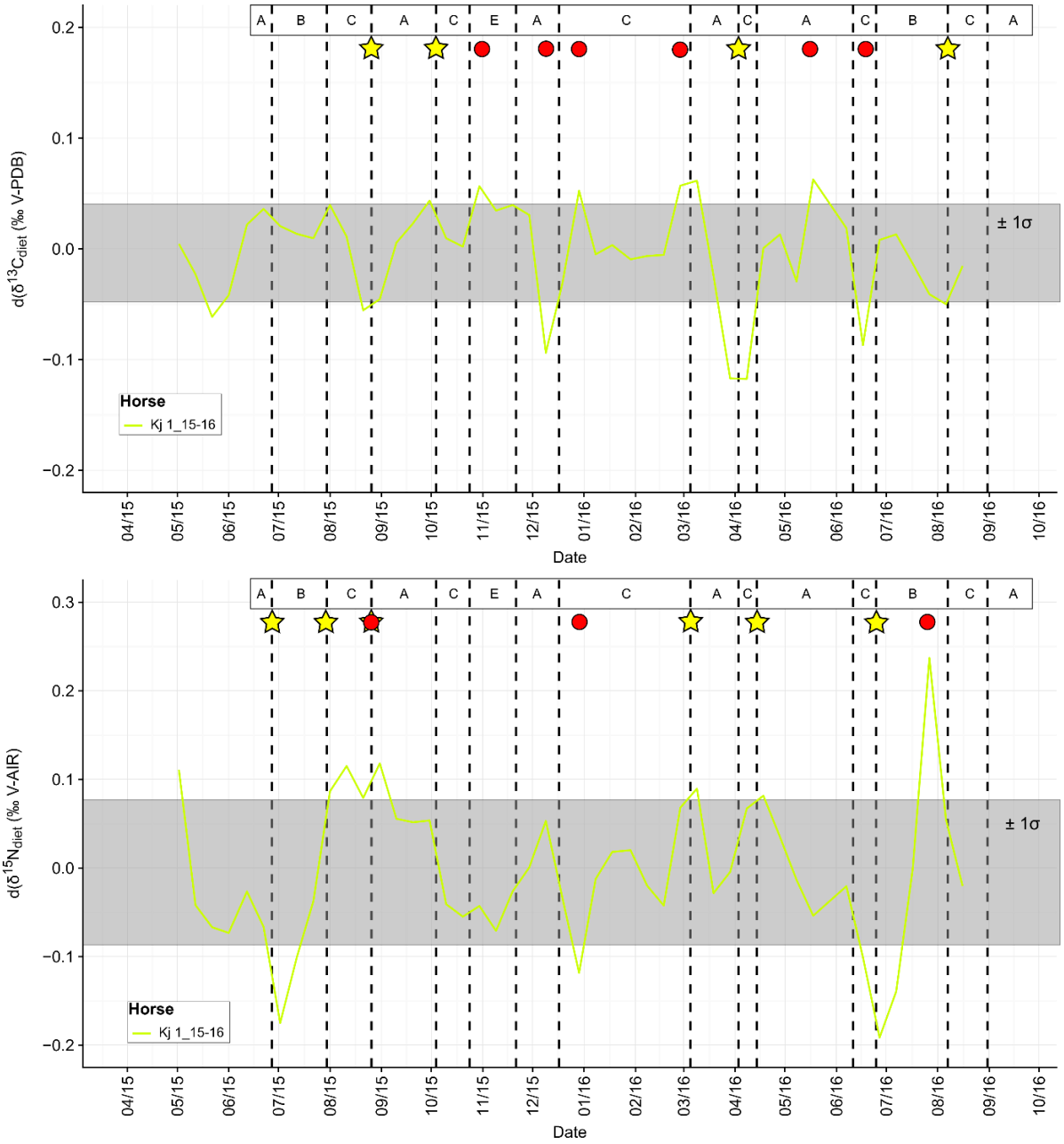

Figure S4.2.E: First derivative of $\delta^{13}C_{diet}$ (Top) and $\delta^{15}N_{diet}$ (Bottom) of horse Dl 1 ($d(\delta^{13}C_{diet})$ and $d(\delta^{15}N_{diet})$; (units are ‰/day). Vertical dashed lines represent changes of pasture determined by GPS, named with capital letters (same names as in Fig.8D & 9D). Black squares represent loss of GPS data. The different colors represent the two tail hairs sampled. Yellow stars mean that an important isotopic shift (i.e. which exceeded = one standard deviation of the time-series of isotopic values) matched with a change of pasture identified by GPS. There were 4 changes of pasture where the $d(\delta^{13}C_{diet})$ exceeded 1σ value and 5 for $d(\delta^{15}N_{diet})$. On the contrary, 6 significant $\delta^{13}C_{diet}$ shifts and 4 significant $\delta^{15}N_{diet}$ shifts were not linked with a change of pasture (red circles).

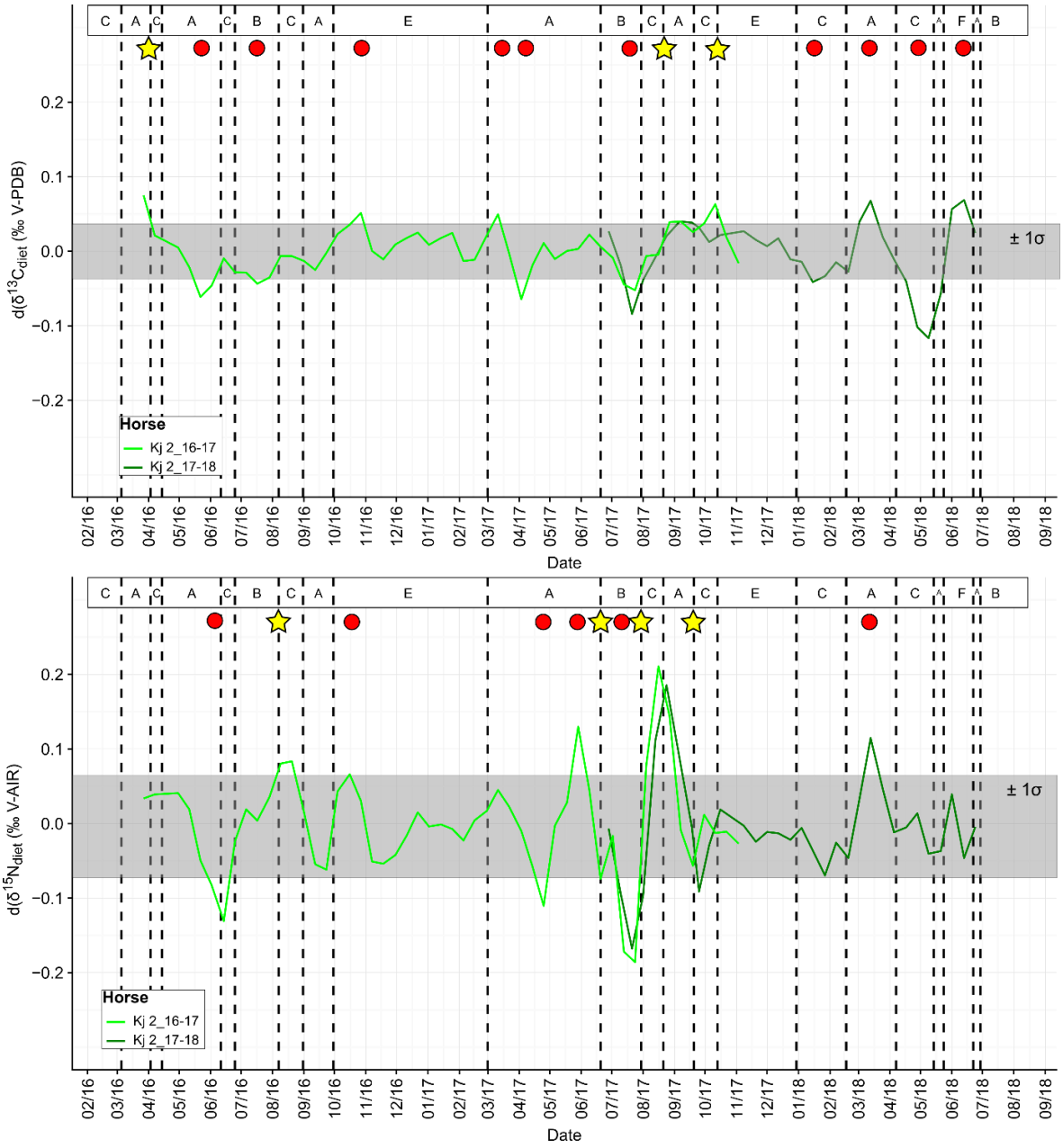

Figure S4.2.F: First derivative of $\delta^{13}C_{diet}$ (Top) and $\delta^{15}N_{diet}$ (Bottom) of horse Dl 1 ($d(\delta^{13}C_{diet})$ and $d(\delta^{15}N_{diet})$; (units are ‰/day). Vertical dashed lines represent changes of pasture determined by GPS, named with capital letters (same names as in Fig.8D & 9D). Black squares represent loss of GPS data. The different colors represent the two tail hairs sampled. Yellow stars mean that an important isotopic shift (i.e. which exceeded = one standard deviation of the time-series of isotopic values) matched with a change of pasture identified by GPS. There were 3 changes of pasture where the $d(\delta^{13}C_{diet})$ exceeded 1σ value and 4 for $d(\delta^{15}N_{diet})$. On the contrary, 10 important $\delta^{13}C_{diet}$ shifts and 6 significant $\delta^{15}N_{diet}$ shifts were not linked with a change of pasture (red circles).

Supplementary Table S4.1

Mean stable isotope ratios and growth rates of tail hairs of the six study horses and mean stable isotope ratios by season.

Horses	Year	Sample #	Growth rate ($mm.d^{-1}$)	$\delta^{13}C_{diet}$ (‰ V-PDB)			$\delta^{15}N_{diet}$ (‰ V-AIR)			*N*
				Mean ± SD	max	Min	Mean ± SD	max	min	
Jk 1	2015-2016	Al16-123	0.75	-27.2 ± 0.9	-24.9	-29.1	3.9 ± 1.1	6.5	2.0	50
	2016-2017	2017-148	0.61	-27.3 ± 0.7	-24.9	-28.5	4.0 ± 1.3	6.7	2.2	54
Jk 2	2017-2018	2018-65	0.85	-27.9 ± 0.8	-24.7	-29.6	2.6 ± 1.4	6.2	0.5	59
Kb 1	2015-2016	Alt16-343	0.81	-27.6 ± 0.8	-24.2	-30.2	4.2 ± 1.7	7.8	-0.5	79
	2016-2017	2017-82	0.71	-27.8 ± 0.5	-27.0	-28.9	3.2 ± 3.2	6.7	-1.0	49
Kj 1	2015-2016	Alt16-171	0.75	-27.2 ± 0.9	-25.7	-28.8	4.5 ± 1.7	7.3	-0.3	49
Kj 2	2016-2017	2017-126	0.67	-27.2 ± 1.0	-25.2	-29.2	4.1 ± 1.3	6.2	-0.6	54
	2017-2018	2018-62	0.66	-27.0 ± 1.1	-25.5	-29.4	3.2 ± 1.2	5.3	0.3	34
Dl 1	2016-2017	2017-60	0.59	-27.7 ± 0.7	-26.1	-29.0	3.9 ± 2.5	8.5	-2.1	50
	2017-2018	2018-33	0.50	-27.8 ± 0.6	-27.0	-29.3	3.3 ± 2.1	8.3	-1.6	36
All	2015-2018	-	0.69 ± 0.11	-27.5 ± 0.9	-24.24	-30.2	3.7 ± 1.7	8.5	-2.1	514
SEASON										
Autumn				-27.4 ± 0.8	-25.5	-29.2	4.0 ± 1.3	7.5	1.1	103
Winter				-27.2 ± 0.6	-25.3	-28.6	3.3 ± 1.1	6.8	0.8	116
Spring				-27.3 ± 1.0	-24.2	-29.5	4.1 ± 1.7	8.5	-2.1	146
Summer				-27.9 ± 0.7 ***	-24.7	-30.2	3.4 ± 2.1	8.0	-1.8	149

Supplementary Table S4.2

https://drive.google.com/open?id=1MrpPA9rUTcaKnGSZeGnlRUCXei0yYt3A

Supplementary Table S4.3

Table S4.3.A: Results and AIC score of the different GAMM models investigating the effects of geographical, temporal and environmental variability in $\delta^{13}C_{diet}$ values. Signifiant codes : *p<0.001 = *** ; p<0.01 = ** ; p<0.05 = **

Model terms	AIC	Parametric coefficients				Approximate significance of smooth terms			
		Estimate	SE	*t*	*p*	*df*	Rank	*F*	*p*
Model 1									
Intercept	712.58	-0.05	0.14	-0.336					
Altitude		-0.09	0.06	-1.42					
Latitude		0.23	0.11	2.08	*				
NDVI		-0.13	0.11	-1.17					
s(Julian date, k=30)						20.63	20.63	9.86	***
Model 2									
Intercept	795.74	-0.0004	0.14	-0.003					
Altitude		-0.12	0.05	-2.199	*				
Latitude		0.33	0.10	-3.335	***				
s(Julian date, k=30)						22.03	22.03	13.13	***
Model 3									
Intercept	712.15	-0.03	0.13	-0.23					
Altitude		-0.13	0.06	-2.01	*				
NDVI		-0.22	0.10	-2.17	*				
s(Julian date, k=30)						21.49	21.49	9.93	***
Model 4									
Intercept	709.63	-0.03	0.15	-0.208					
NDVI		-0.17	0.10	-1.82	.				
s(Julian date, k=30)						20.08	20.08	9.97	***

Table S4.3.B: Results and AIC score of the different GAMM models investigating the effects of geographical, temporal and environmental variability in $\delta^{15}N_{diet}$ values.

Model terms	AIC	Parametric coefficients				Approximate significance of smooth terms			
		Estimate	SE	*t*	*p*	*df*	Rank	*F*	*p*
Model 1									
Intercept	706.32	-0.03	0.13	-0.22					
Altitude		-0.18	0.07	-2.73	**				
Latitude		0.07	0.11	0.67					
NDVI		-0.006	0.11	0.06					
s(Julian date, k=85)						27.69	27.69	4.95	***
Model 2									
Intercept	702.18	-0.02	0.14	-0.18					
Altitude		-0.19	0.06	-2.93	**				
NDVI		-0.02	0.10	-0.24					
s(Julian date, k=85)						27.64	27.64	5.11	***
Model 3									
Intercept	773.89	-0.05	0.12	-0.39					
Altitude		-0.23	0.05	-4.23	***				
s(Julian date, k=80)						30.62	30.62	5.61	***

Chapitre 5 – Identifier la mobilité et l'exploitation altitudinale par l'analyse isotopique ($\delta^{13}C$ et $\delta^{18}O$) de l'émail des dents

Nous avons vu dans le chapitre 4 qu'en raison de la croissance rapide du crin de cheval, les variations isotopiques du carbone et de l'azote enregistrées par ce tissu sont difficiles à relier précisemment aux changements de pâtures effectués par les chevaux lorsque ceux-ci sont fréquents.

Ce cinquième chapitre est consacré à l'étude de la capacité de la composition isotopique ($\delta^{18}O$ et $\delta^{13}C$) de l'émail dentaire à inférer la mobilité altitudinale d'animaux géolocalisés. L'émail dentaire est plus généralement utilisé dans les études archéologiques, car ce matériau est plus résistant aux processus diagénétiques, mais la résolution temporelle des variations isotopiques de l'émail est plus faible que le poil à cause du processus de minéralisation qui atténue et moyenne dans le temps les variations environnementales. L'objectif de cette étude est d'explorer le potentiel de la composition isotopique de l'émail à estimer la mobilité résidentielle altitudinale et les stratégies d'exploitation du milieu montagnard des animaux domestiques. Et de fournir notamment un référentiel permettant de questionner les facteurs contrôlant l'anticovariation des valeurs de $\delta^{18}O$ et $\delta^{13}C$ de la dent, dont l'interprétation ne fait pas consensus.

5.1 Résumé de l'étude

L'identification des signatures isotopiques de la mobilité altitudinale et de l'exploitation des prairies alpines dans les dents des animaux domestiques a des implications importantes pour la compréhension de l'évolution des stratégies de subsistance des éleveurs. La composition isotopique de l'oxygène ($\delta^{18}O$) et du carbone ($\delta^{13}C$) de l'émail dentaire échantillonné séquentiellement, utilisée séparément ou de manière combinée, est couramment employée en archéologie pour étudier les pratiques d'élevage anciennes. Toutefois, la pertinence de ces méthodes pour la reconstitution des mouvements du bétail fait débat, en partie en raison de la rareté des référentiels modernes.

Pour pallier ce manque, nous proposons donc ici un nouvel ensemble de références, composé de moutons, de chèvres et de chevaux suivis par GPS en Mongolie occidental. Les objectifs sont de chercher à savoir si le $\delta^{13}C$ et $\delta^{18}O$ de l'émail sont influencés par l'altitude

résidentiel moyenne et si la covariation entre les valeurs de $\delta^{18}O$ et $\delta^{13}C$ de l'émail est influencée par la mobilité altitudinale. Dans cette optique, des molaires de 12 caprinés dont la croissance est contemporaine du suivi GPS et les molaires de 5 chevaux, non géolocalisés, ont été séquentiellement échantillonnées et leur composition isotopique a été analysée par spectrométrie de masse. Le $\delta^{13}C$ moyen des crins des chevaux géolocalisés (données issues du chapitre 4) a été inclus pour comparaison avec les valeurs de $\delta^{13}C$ des dents des 5 chevaux.

Nos données mettent en évidence une corrélation négative entre la valeur moyenne de $\delta^{13}C$ du régime alimentaire et (i) l'altitude moyenne de pâturage ; (ii) la proportion de temps passé dans les prairies alpines. Ce résultat est en bon accord avec la corrélation négative existante entre le $\delta^{13}C$ des plantes et l'altitude, causée par l'augmentation de l'humidité avec l'altitude. Cette relation, appliquée aux données des dents de chevaux modernes, non géolocalisées, a permis d'estimer une exploitation altitudinale similaire à celle des chevaux suivis par GPS (chapitre 4) validant l'approche pour l'estimation de l'exploitation altitudinale. Concernant les valeurs moyennes de $\delta^{18}O$, acune corrélation n'est observée avec l'altitude moyenne de pâturage. En revanche, nos données mettent en évidence une corrélation entre l'amplitude intra-dent du $\delta^{18}O$ et l'écart type de l'altitude moyenne de pâturage (i.e. reflétant la fréquence de la mobilité altitudinale). Ce résultat indiquerait la consommation de sources d'eau isotopiquement diverses, en raison de la mobilité altitudinale des animaux, comparé à des animaux se déplaçant très peu.

La corrélation entre les valeurs de $\delta^{18}O$ et $\delta^{13}C$ de l'émail est négativement corrélée avec la fréquence de la mobilité altitudinale. On observe une covariation pour les animaux pâturant toute l'année à une altitude équivalente et une anticovariation pour ceux ayant une mobilité altitudinale régulière et prononcée. Ce résultat vient confirmer que l'anticovariation entre les séquences de $\delta^{18}O$ et $\delta^{13}C$ de l'émail peut en effet être interprétée comme résultant d'une mobilité verticale avec un régime alimentaire ayant des valeurs plus basses en $\delta^{13}C$ pendant les mois d'été, reflétant possiblement une consommation d'arbustes pour les animaux mobiles comparés aux animaux ayant une faible mobilité altitudinale. De plus, pendant l'hiver, les animaux ayant une mobilité altitudinale pâturent plus souvent à basse altitude, consommant des plantes enrichies en ^{13}C, par rapport à l'herbe des alpages, ayant poussé en milieu plus aride durant l'été.

Cette étude a permis de compléter le référentiel moderne, trop réduit jusqu'à présent, concernant l'identification de la mobilité et exploitation altitudinale grâce à l'analyse de la

composition isotopique en C et O de l'émail dentaire des animaux, validant leur utilisation pour inférer ces pratiques d'élevage dans le registre archéologique. Cependant, il est nécessaire de prendre conscience que cette étude est restreinte à une région particulière et cette approche gagnerait à être étendue à d'autres zones climatiques. Pour finir, bien souvent dans la littérature, l'interprétation de l'anticovariation entre les valeurs de $\delta^{18}O$ et $\delta^{13}C$ se limite à une mobilité bi-modale de type transhumance avec un mouvement vers l'alpage en été et une descente en plaine pour l'hiver. Or, comme nous venons de le voir avec notre zone d'étude, cette anticovariation est à interpréter plus comme une préférence altitudinale haute pendant l'été et basse pendant l'hiver, mais cela peut recouvrir des stratégies de mobilité bien plus complexe avec de nombreux aller-retours entre les pâtures de plaine et d'altitude pendant l'été sans que cela soit soit forcément détectable.

Article II: The isotope record ($\delta^{13}C$, $\delta^{18}O$) of high pasture exploitation and altitudinal mobility by livestock: a case study in the modern Altai Mountains, Mongolia.

Nicolas LAZZERINI, Aurélie COULON, Charlotte MARCHINA, Noost BAYARKHUU, Tsagaan TURBAT, Denis FIORILLO, Sébastien LEPETZ, Antoine ZAZZO.

In preparation for submission in *Archaeological and Anthropological Sciences*

Abstract:

Identifying the isotopic signatures of altitudinal mobility and alpine meadows exploitation in domesticated animal teeth has important implications for understanding the subsistence strategies used by herders through history. The oxygen ($\delta^{18}O$) and carbon ($\delta^{13}C$) isotopic composition of sequentially sampled tooth enamel, used alone or combined to investigate the pattern of correlation between $\delta^{18}O$ and $\delta^{13}C$ profiles, are commonly used to investigate these husbandry practices. However, there are conflicting interpretations of the outcomes of these methods. This is due in part to the paucity of modern reference datasets. In this study, we propose a new reference set, composed of GPS monitored sheep, goats and horses from Western Mongolia, to investigate the influence of vertical mobility and mean grazing altitude, on the C and O isotopic composition of sequentially tooth enamel. $\delta^{13}C$ values of diet exhibited a negative correlation with the mean grazing altitude and time occupation of alpine meadows. This is consistent with the similar relationship observed in the study area between the $\delta^{13}C$ values of plants and the altitude. These data suggest that C and O isotopic analyses are useful for identifying mobility practices and alpine meadows exploitation in archaeological samples in this region. However, no correlation was found between the average $\delta^{18}O$ values of teeth enamel and mean grazing altitude. But livestock with important altitudinal mobility showed higher intra-tooth variability of $\delta^{18}O$ values compared to livestock grazing all the time at the same altitude. Indicating the ingestion of more isotopically diverse source of water outside of the 'local' range of lowlands for livestock with an important altitudinal mobility. The correlation between carbon and oxygen isotope values of tooth enamel was negatively correlated with the standard deviation of the animal altitudinal residency. This suggests that the anti-covariation between $\delta^{13}C$ and $\delta^{18}O$ sequences can indeed be interpreted as evidence for vertical mobility. The lower $\delta^{13}C$ values during summer months reflect probable higher consumption of shrubs and forbs by mobile livestock, which exploited highlands and lowlands

during this period. During winter, they exploited only lowlands and consumed grass with higher $\delta^{13}C$ values that grew in arid environment during summer.

Keywords: Sequential isotope analysis; Vertical mobility; sheep and goat; horse; herding strategies; bioapatite; plants; Mongolia

5.2 Introduction

Human-directed mobility of domesticated livestock between different pastures is a key element of the resource management strategy of pastoral systems. It aims to provide access to a continuous source of fresh graze throughout the year for livestock in patchy and low-productivity environments (Little, 2015; Wright and Makarewicz, 2015). Mobile pastoralism is practiced largely in the drylands and highlands of the world, from South America to North-East Asia (e.g. Lynch, 1983; Niamir-Fuller and Turner, 1999; Dong et al., 2011; Stépanoff et al., 2013; Liechti and Biber, 2016; Arbuckle and Hammer, 2018). Pastoral mobility can take various forms such as pasture rotation, transhumance, and nomadism, depending on a combination of different parameters such as environmental conditions, species and number of herd animals, economic and political context, social structures, and household life (e.g. for Inner Asia (Fernandez-Gimenez, 2000; Kerven et al., 2006).

In mountain areas, where the environment is characterized by a vertical stratification of resources, altitudinal mobility is a common strategy used by herders to maximize the exploitation of pastures situated along an elevation gradient. Not only does it provide a stable buffer against seasonal fluctuations in the quality and quantity of graze, but it also offers protection against winds and snowfalls, especially in extreme continental climatic conditions (Marchina, 2019). In such environments, herds usually graze in low elevation pastures during the cool season and in high elevation pastures during the warm season.

It has already been shown that mobile pastoralism may have structured political life, fostered social organization and large-scale political communities (Frachetti et al., 2017; Honeychurch, 2013; Lynch, 1983; Porter, 2012). Consequently, identifying the use of highland pastures, being able to detect the origin and characterize the extent of vertical mobility, is of paramount importance to describe subsistence economies and social interactions in past pastoralist communities. However, direct identification of past vertical mobility by archaeologists remains challenging.

When analysed sequentially in continuously growing tissues (i.e. tooth, hair, horn), carbon ($\delta^{13}C$) and oxygen ($\delta^{18}O$) stable isotope time series offer a quantitative method to study livestock husbandry strategies, including mobility. The oxygen isotopic composition from sequentially sampled tooth enamel has been regularly used to infer altitudinal mobility. Indeed, oxygen isotopes in herbivore tooth enamel record the $\delta^{18}O$ of ingested water, deriving from meteoric water, which is itself influenced by temperature, continental positioning, rainfall amount, humidity and seasonality (Dansgaard, 1964; Gat, 1996; Kohn and Welker, 2005; Rozanski et al., 1993). Altitude also has an important influence on $\delta^{18}O$ of meteoric water through two parallel phenomena: (1) the progressive rainout along mountain slopes, which preferentially removes ^{18}O-enriched water from clouds; (2) cooler temperatures. Both result in ^{18}O-depleted precipitation at high altitudes and ^{18}O-enriched precipitation at low altitudes (Gat, 1996; Gonfiantini et al., 2001; Poage and Chamberlain, 2001a). However, the relationship between altitude and $\delta^{18}O$ of precipitation varies according to geography, topography, and region-specific conditions (Ambach et al., 1968; Kern et al., 2014; Liu et al., 2014; Poage and Chamberlain, 2001a; Rozanski et al., 1993). Identification of animal's altitudinal mobility is based on the interpretation of the amplitude of $\delta^{18}O$ variations recorded within tooth enamel. An altitudinal mobility would lead to a reduction of the 'local' isotopic amplitude recorded by tooth enamel, because the animal avoids climatic extremes, comparing to an animal staying at the same location throughout its life (Britton et al., 2009; Henton, 2012; Henton et al., 2017b, 2010; Pellegrini et al., 2008). However, an alternative approach to determine vertical mobility proposed to rely on the higher inter-individual variability in enamel $\delta^{18}O$ values as an indicator of ingestion of water from outside the 'local' range of lowlands (Mashkour, 2003; Mashkour et al., 2005). However, there are difficulties inherent to this method for identifying past animal's mobility. Depending of the local topography, hydrography and climate, some differences of interpretations are expected due to differences in amplitude. These difficulties may reflect the influence of confounding factors such as the ingestion of buffered water sources (i.e. lakes or groundwater), the variability of drinking behavior or the ingestion of important proportions of ^{18}O-enriched leaf water in semi-arid/arid environments (Dufour et al., 2014; Knockaert et al., 2018; Makarewicz and Pederzani, 2017). These factors can lead to similar isotopic patterns in mobile and non-mobile animals. As a consequence, some authors have chosen instead to specifically focus on the shape of the $\delta^{18}O$ curve to identify vertical mobility by taking into account environmental isotopic variations and use theoretical models in order to predict isotopic variations. (Henton et al., 2017b; Hermes et al., 2017). However, these models are based on the $\delta^{18}O$ of meteoric water alone and do not consider the effects of delayed enamel maturation,

dampening and averaging $\delta^{18}O$ signal (e.g.Passey and Cerling, 2002; Balasse, 2003; Zazzo et al., 2012). Besides, because of the duration of the mineralization process, only a large and rapid movement between two isotopically distinct areas is able to generate a detectable change in the curve.

The carbon isotopic composition ($\delta^{13}C$) of herbivore tissues (i.e. tooth, hair, horn) reflects the $\delta^{13}C$ value of ingested plants and can be used to track animal dietary changes associated with seasonal changes in pasture composition, mobility or human interference (Balasse et al., 2002; Barbosa et al., 2009; Fisher and Valentine, 2013; Henton et al., 2017b; Knockaert et al., 2018; Männel et al., 2007; Ventresca Miller et al., 2017; Winter-Schuh, 2017). Several factors influence the $\delta^{13}C$ values of terrestrial plants. The dominant influential is the photosynthetic pathway used for fixing C. Indeed, plants using the C_3 pathway have an average $\delta^{13}C$ value of -26‰, those using the C_4 pathway exhibit an average $\delta^{13}C$ value of -12‰, and those using the CAM pathway show intermediates between the values of the C_3 and C_4 plants (Kohn, 2010; O'Leary, 1988). Other factors are associated with environmental conditions such as water availability. Water-use efficiency increases when water availability decreases, leading to a ^{13}C enrichment in plant carbon (Farquhar et al., 1989, 1982; Rao et al., 2017; Stewart et al., 1995). Generally, plants adapted to dry environments show higher $\delta^{13}C$ values. Finally, climatic conditions also affect the $\delta^{13}C$ values of terrestrial plants: increasing temperatures during hot seasons induce higher $\delta^{13}C$ values of plants due to the reduction of stomatal conductance to decrease water losses (Farquhar et al., 1989; Hartman and Danin, 2010; Smedley et al., 1991). Inversely, plants in wets areas or during wet/growth season tend to have high water losses and thus show lower $\delta^{13}C$ values Lavielle et(Kohn, 2010; Körner et al., 1991; Smedley et al., 1991). Thus, moving herbivores sampling the change of plant communities in space and time would the change of $\delta^{13}C$ value accordingly. Due to the ecological differences between C_3 and C_4 plants,an increase in the relative proportion of C_3 vs C_4 plants with altitude is observed, triggering a decrease of plant communities $\delta^{13}C$ values (Cavagnaro, 1988; Li et al., 2009; Tieszen et al., 1979). In C_3-dominated environments, the range of isotopic variations is more restricted. Nevertheless, several studies have documented an increase in the $\delta^{13}C$ values of C_3 plants with altitude (Körner et al., 1988; Li et al., 2006, 2009, 2007; Liu et al., 2016; Morecroft and Woodward, 1990) that can be recorded in the $\delta^{13}C$ values of livestock tissues (Männel et al., 2007). This pattern was explained by the high carboxylation rates relative to stomatal conductance at high altitudes, resulting in lower ^{13}C discrimination (Li et al., 2006, 2009, 2007; Morecroft and Woodward, 1990). However, the opposite pattern was reported in SW USA and

in China (Liu et al., 2016; van de Water et al., 2002), and was explained by increased drought stress at lower elevations in these arid and semi-arid regions. Finally, several authors proposed that local climatic factors could modulate the effects of water availability and hence locally complicate the relationship between $\delta^{13}C$ values and altitude (Liu et al., 2007; Xiaoning Liu et al., 2010; Morecroft and Woodward, 1990). The variations in $\delta^{13}C$ values of plants along altitudinal gradients hence may not be explained by a single factor but rather may be a result of an interaction between different factors and should be characterized for each site.

Given the limits of the O and C isotope systems alone, recent attempts at detecting altitudinal mobility have relied on the combined use of both tracers analysed together in tooth enamel. Generally, a co-variation of both $\delta^{18}O$ and $\delta^{13}C$ intra-tooth variations is expected for stationary herbivores in temperate and semi-arid environments (Balasse et al., 2009, 2002; Fraser et al., 2008), with high values during the hot season and low values during the cold season. However, an anti-covariation between $\delta^{18}O$ and $\delta^{13}C$ intra-tooth variations has been observed in different cases (e.g. (Fisher and Valentine, 2013; Makarewicz et al., 2017; Makarewicz and Pederzani, 2017; Tornero et al., 2018, 2016). This anti-covariation has been interpreted as reflecting movements between highland pastures in summer (with less C_4 plants in the diet) and midland/lowland pastures in winter (with more C_4 plants in the diet). This explanation has been proposed to describe the mobility patterns of wild (Fisher and Valentine, 2013; Tornero et al., 2016) and domestic caprines (Makarewicz, 2017; Makarewicz et al., 2017; Tornero et al., 2018). However, a second explanation was proposed in the case of domestic animals where diet manipulation by the herder cannot be excluded. In this case, higher winter $\delta^{13}C$ values have been interpreted as resulting from winter foddering of livestock with a C4-rich diet harvested during summer. This was documented for modern domesticated sheep from Mongolia (Makarewicz and Pederzani, 2017) and proposed as an explanation for archaeological livestock (Makarewicz and Tuross, 2006; Makarewicz, 2017; Makarewicz et al., 2018; Winter-Schuh, 2017). A third explanation was proposed by Chazin et al. (2019) to explain lower summer $\delta^{13}C$ values recorded in the teeth of domestic animals from Bronze Age Caucasus, involving the increase of ^{13}C-depleted shrubs and forbs in the diet (Dodd et al., 1998; Smedley et al., 1991). This proposition is supported by the observation of the increase of forbs in summer diets of wild and domestic sheep from the desert-steppe of Mongolia (Wingard et al., 2011).

These conflicting interpretations are in part due to the paucity of modern reference datasets. Only a few modern reference studies have explored this anti-correlation signal in order to constrain its origin, either through fodder (Makarewicz and Pederzani, 2017) or vertical

mobility (Tornero et al., 2018), involving few individuals and without any control group (i.e. non-foddered or sedentary). In this study, we propose a new reference set to investigate the influence of vertical mobility on the C and O isotopic composition of tooth enamel and to determine the influence of altitude on $\delta^{13}C$ values of plant communities and on $\delta^{13}C$ values of animal's tissues. To do this, we analysed the $\delta^{18}O$ and $\delta^{13}C$ variations in tooth enamel of domestic caprines (sheep and goats) of Kazakh-Mongolian herders from the Altai Mountains of western Mongolia, where nomadic pastoralism is characterized by vertical mobility (Finke, 2004). We also included a comparative analysis of previously published $\delta^{13}C$ variations in tail hair of horses belonging to the same herds. All these animals were fitted with GPS collars to monitor their daily movements for three consecutive years and vegetation was sampled at different localities in order to estimate $\delta^{13}C$ variations with altitude and influence of C_4 in the diet. Our aims were to test the hypothesis that (i) the correlation between $\delta^{18}O$ and $\delta^{13}C$ values of tooth enamel vary with the altitudinal mobility patterns of livestock in a C_3-dominated environment (with a positive correlation when livestock has a residential mobility); (ii) the highland pasture exploitation can be tracked by the $\delta^{18}O$ and $\delta^{13}C$ values of animal's tissues, with expected negative correlation between isotopic composition and mean grazing altitude.

5.3 Materials

5.3.1 Burgast: topography, climate and vegetation

Fieldwork was carried out in the Mongolian Altai (**Figure 12**) in the Nogoonnuur district (*sum*) lying in the northern part of the Bayan-Ölgii province (*aimag*). The altitudinal profile ranges from 1500 to more than 4000 m.asl with the Turgen Uul summit at 4029 m.asl. A north-south fault splits the landscape in half with the highland of the Altai Mountains to the west and a lowland plain to the east. The climate is strongly continental with cold, long winters (November-March) and hot, short summers (June-August). During the study period (June 2015 to July 2018), monthly temperatures averaged +18.0°C during summer (June–August) and –12.7°C during winter (December–February) with extremes ranging from +34 to −44°C (InfoClimat, 2019). Average annual rainfall is 105 mm with a maximum of precipitation occurring during summer (InfoClimat, 2019). In the winter, there is very little snowfall and most of the time no snow cover at all. Open water is rare, and consists in a few intermittent streams. The vegetation consists of alpine meadows and semi-arid steppes and is mainly composed of grasses, with a few forbs and bushes (*Caragana* sp.) or trees (*Populus laurifolia*) exclusively near rivers in lowlands and valley exits for forbs, shrubs and trees. The steppe

vegetation is dominated by plants using the C_3 photosynthetic pathway such Asteraceae, a majority of Chenopodiaceae, Poaceae, or Fabaceae (Ivanova et al., 2019; Pyankov et al., 2000). Some species using the C_4 photosynthetic pathway, such *Anabasis brevifolia, Eragrostis pilosa, Kochia prostrata*, or *Setaria veridis* have also been identified.

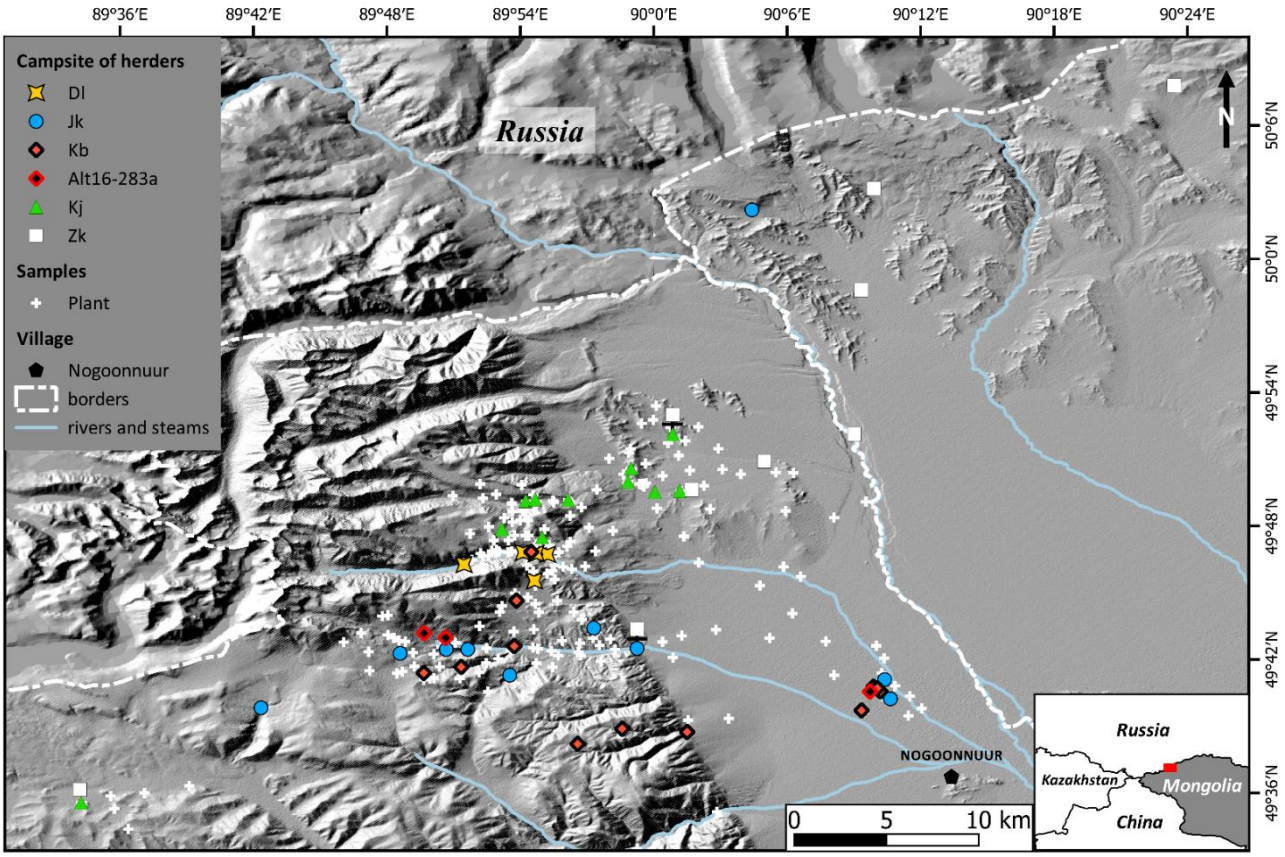

Figure 12: Map of the study area and its location in Mongolia (bottom right) with the location of the campsites of the five Kazakh-Mongolia households whose animals were tracked by GPS. The individual Alt16-283a spent most of its time with the herd of Kb herder, but during the winter 2015-2016 it used some other campsites. White crosses represent plant sampling sites (n = 246).

5.3.2 Plant materials

Plants were sampled at 246 sites distributed throughout the accessible parts of the study area (**Figure 12**), in June 2015, September 2016, November 2017 and July 2018 (**Supp. Info S5.1**). Sampling localities were chosen to represent the grazing areas of the monitored animals. Some parts of the study area could not be sampled due to difficult access or proximity to the Russian border. The average distance between neighbouring sites (calculated using the 5 nearest neighbours of each site) was 1.7 km. At each site, we collected a handful of plant material in a diameter of 2-3 meters. We collected all the plant specimens visible at these sites, and combined them before analysis. In most cases, most collected plants were grasses, but there were also

some forbs and shrubs. The majority of the material was composed of leaves but there were also stems and seeds or fruits if present. All plant material was wrapped in paper then dried in a loosely sealed envelope prior to $\delta^{13}C$ analysis.

Table 4: Information about animals equipped with GPS collars (Gb = Globalstar; Ir = Iridium) during the three study periods. * = GPS 38766 was equipped on the same individual during periods 1 & 2. ** = sampling of an animal from the same herd that did not have a GPS collar. † GPS out of service before the field mission during which the animal was sampled and the GPS collars reclaimed.

Animal &Tooth sample ID	GPS type	Species (Sex)	Start GPS	End GPS	Herder
Period 1: June 2015 – Sept. 2016					
Alt16-103	Ir	Capra (M)	17/06/2015	03/09/2016	Jk
Alt16-104	Gb	Ovis (M)	19/06/2015	07/09/2016	Jk
Alt16-156	Gb	Capra (M)	19/06/2015	05/09/2016	Jk
Alt16-258	Ir	Capra (M)	16/06/2015	11/09/2016	Kb
Alt16-285	Gb	Capra (M)	17/06/2015	12/09/2016	Kb
Alt16-283	Gb	Ovis (M)	16/06/2015	12/09/2016	Kb
Alt16-306	Ir	Ovis (M)	19/06/2015	14/09/2016	Kj
Alt16-362	Gb	Capra (M)	19/06/2015	07/10/2017 *†	Kj
Alt16-369 **	Gb	Capra (M)	19/06/2015	20/09/2016	Kj
Period 2: Sept 2016 – Nov. 2017					
2017-70	Gb	Ovis (M)	16/09/2016	17/11/2017	Dl
2017-71	Gb	Capra (M)	16/09/2016	17/11/2017	Dl
2017-146	Gb	Capra (M)	05/09/2016	03/05/2017 †	Jk
2017-98	Gb	Capra (M)	18/09/2016	09/11/2017	Kb
2017-124	Gb	Capra (M)	21/09/2016	09/11/2017	Kj
2017-130	Gb	Capra (M)	17/09/2016	29/11/2017	Zk
Period 3: Nov. 2017 – July 2018					
2018-63	Gb	Ovis (M)	17/11/2017	24/07/2018	Dl
2018-23 **	Ir	Ovis (M)	18/11/2017	20/07/2018	Kb

5.3.3 Geolocalised animal reference set

For this study, caprines and horses from the same area were monitored with GPS collars in order to compare the influence of altitude on isotopic composition of both species. Concerning caprines, between June 2015 and July 2018, 17 individuals (6 sheep and 11 goats) were equipped with a GPS collar to track the mobility of the herds of five different families of Kazakh Mongolian nomadic pastoralists (**Table 4**). GPS collars were fit on the caprines when they were around 1-1.5 years old, based on the incisor (I1) development (Schmid, 1972). Animals were equipped with Globalstar© (n = 13) or Iridium© (n = 4) GPS collars (Lotek Wireless Inc. - http://www.lotek.com/). Globalstar© and Iridium© devices were programmed to record animal position every 13 and 2 hours respectively and provided also altitude and temperature. Even if we can assume that one animal represents the entire herd (Moritz et al., 2012), we chose to monitor several animals in each herd to prevent technical failures or loss of GPS collars. Because caprines are led back to the camp every night, GPS monitoring allows us

to infer the location of the different camps and associated pastures. Interviews with the herders allowed us to establish that the animals did not receive any manufactured food complements. While adult males are only supplemented with fodder during bad years, pregnant females and very young individuals may be winter-foddered for a short period of time. To avoid any potential influence of fodder on the isotopic profiles, we only selected male individuals (**Table 4**). To allow a direct comparison between isotopic and GPS data, only teeth that grew during the GPS tracking period were selected. We sampled 20 molars from the 17 caprines (**Table 5**). Animal slaughter was operated by the herders themselves for their own consumption and was authorized by the ethics committee of the *Muséum national d'Histoire naturelle*.

Table 5: Characteristics of the geolocalised reference set used in the analyses with altitude data corresponding to the period of tooth formation. DOB = date of birth. The start and the end of formation of each tooth were calculated from the average dental development rate. [1] Time-GPS represents the percentage of the period of formation covered by GPS tracking. [2] Time-Alt represents the proportion of time, during the period of tooth formation, spent at high altitude (> 2000 m.asl). A = amplitude. * All data concerning tail hair of horses are from (Lazzerini et al., 2019).

Caprine tooth sample	Sampled tooth	Herder	Individual DOB	Start formation	End formation	$Time_{GPS}$[1]	Altitude (m)				
							Mean ± sd	Max	Min	A	Time-Alt [2]
2017-70-M3	**M_3 left**	**Dl**	**31/03/2015**	**05/02/2016**	**30/05/2017**	**66%**	**2319 ± 112**	**2895**	**1991**	**904**	**59%**
2017-71-M3	**M_3 left**	**Dl**	**31/03/2015**	**05/02/2016**	**30/05/2017**	**66%**	**2319 ± 112**	**2895**	**1991**	**904**	**59%**
2018-63B-M2	**M_2 left**	**Dl**	**31/03/2017**	**08/05/2017**	**30/04/2018**	**100%**	**2376 ± 125**	**2980**	**2100**	**880**	**100%**
Alt16-103a-M3	M_3 left	Jk	31/03/2013	05/02/2014	31/05/2015	0%	-	-	-	-	-
Alt16-104a-M3	**M_3 left**	**Jk**	**31/03/2014**	**05/02/2015**	**30/05/2016**	**77%**	**1996 ± 361**	**2973**	**1450**	**1523**	**43%**
Alt16-156a-M3	M_3 left	Jk	31/03/2013	05/02/2014	31/05/2015	0%	-	-	-	-	-
2017-146-M2	**M_2 left**	**Jk**	**31/03/2015**	**08/05/2015**	**29/04/2016**	**88%**	**2026 ± 402**	**2973**	**1450**	**1523**	**61%**
2017-146-M3	**M_3 left**	**Jk**		**05/02/2016**	**30/05/2017**	**100%**	**1934 ± 361**	**3003**	**1463**	**1540**	**31%**
Alt16-258a-M3	M_3 left	Kb	31/03/2013	05/02/2014	31/05/2015	0%	-	-	-	-	-
Alt16-283a-M3	**M_3 left**	**Kb**	**31/03/2014**	**05/02/2015**	**30/05/2016**	**77%**	**2101 ± 332**	**3132**	**1454**	**1678**	**50%**
Alt16-285a-M3	M_3 left	Kb	31/03/2013	05/02/2014	31/05/2015	0%	-	-	-	-	-
2017-98-M2	**M_2 left**	**Kb**	**31/03/2015**	**08/05/2015**	**29/04/2016**	**88%**	**2060 ± 344**	**3024**	**1437**	**1587**	**85%**
2017-98-M3	**M_3 left**	**Kb**		**05/02/2016**	**30/05/2017**	**100%**	**2119 ± 327**	**2964**	**1444**	**1520**	**57%**
2018-23A-M3	**M_3 right**	**Kb**	**31/03/2016**	**31/05/2017**	**29/06/2016**	**100%**	**2256 ± 227**	**3348**	**1455**	**1893**	**67%**
Alt16-306a-M3	**M_3 left**	**Kj**	**31/03/2014**	**05/02/2015**	**30/05/2016**	**77%**	**2059 ± 269**	**2734**	**1686**	**1048**	**33%**
Alt16-362a-M3	M_3 left	Kj	31/03/2013	05/02/2014	31/05/2015	0%	-	-	-	-	-
Alt16-369a-M3	**M_3 left**	**Kj**	**31/03/2014**	**05/02/2015**	**30/05/2016**	**77%**	**2059 ± 269**	**2734**	**1686**	**1048**	**33%**
2017-124-M2	**M_2 left**	**Kj**	**31/03/2015**	**08/05/2015**	**29/04/2016**	**88%**	**2072 ± 277**	**2734**	**1686**	**1048**	**47%**
2017-124-M3	**M_3 left**	**Kj**		**05/02/2016**	**30/05/2017**	**100%**	**2021 ± 307**	**3014**	**1690**	**132**	**22%**
2017-130-M3	**M_3 left**	**Zk**	**31/03/2015**	**05/02/2016**	**30/05/2017**	**66%**	**1645 ± 90**	**2468**	**1581**	**887**	**0.2%**
Hair sample of horses *				**Start formation**	**End formation**	**Time-GPS[1]**	**Mean ± sd**	**Max**	**Min**	**A**	**Time-Alt [2]**
Dl 1	Dl	-		05/02/2016	03/11/2017	64%	2366 ± 138	2814	1698	1116	97%
Jk 1	Jk	-		19/04/2015	16/11/2017	94%	2115 ± 476	2916	1450	1466	43%
Jk 2	Jk	-		14/02/2017	18/07/2018	44%	2580 ± 477	3216	1447	1769	81%
Kb 1	Kb	-		12/09/2014	06/11/2017	68%	2433 ± 432	3157	1205	1952	76%
Kj 1	Kj	-		22/04/2015	26/08/2016	88%	2278 ± 459	3154	1468	1686	56%
Kj 2	Kj	-		23/03/2016	06/007/2018	80%	2014 ± 356	3103	1429	1674	30%

Concerning horses, data were previously published by Lazzerini et al. (2019). To summarize, tail hair of six horses from same herders (Dl, Jk, Kb and Kj) were sequentially sampled for $\delta^{13}C$ measurements and tracked by GPS collars (Globalstar©) from June 2015 to July 2018. The period of formation of tail hairs was well time-calibrated, allowing direct comparison with altitudinal mobility data. We used the estimated $\delta^{13}C$ values of diet deriving from the measured $\delta^{13}C$ values of tail hair, for more details see Lazzerini et al. (2019).

5.3.4 Non-geolocalised horse specimens

Finally, for this study, we added 5 molars from 5 young modern horses belonging to Kazakh-Mongolian nomadic herders living in the same area. Depending of the age of the horse, the M1, M2 or M3 was sampled (**Table 6**). Two of these horses belonged to herder Kb and Kj. The horses were not slaughtered especially for the study. Some were slaughtered by the herders for their own consumption, while others were either injured by predators or accidents. The nomadic breeders, confirmed the origin of the horses but unfortunately the precise mobility of these animals could not be established through GPS collars. However, we have no reason to believe that they had a radically different occupation of the territory from the other horses in the area that were tracked by GPS (Lazzerini et al., 2019). These five horse teeth were used as a control to determine their altitudinal mobility and their occupation of high altitude pastures relative to the results obtained on individuals with known mobility.

Table 6: Characteristics of the non-geolocalised modern horses sampled for this study. DOB = date of birth. DOD = date of death Subscript and superscript indicate that the molar was taken from the lower or upper jaw, respectively.

Horse tooth sample	Herder	Sex	DOB	DOD	Estimated age (years)	Sampled tooth
2017-104 M2	Kb	F	April–May 2013	10 November 2016	2.5	M_2 right
2018-17B M3	?	M	2013–2014?	early July 2017	4	M^3 right
2018-57A M3	?	M	2003?	late February 2007	3-4	M^3 left
2018-58B M3	Kj	M	2015?	20–25 April 2018	3	M^3 right
2018-59A M1	?	F	2016?	January 2018	1.5	M_1 right

5.4 Methods

5.4.1 Estimation of tooth formation period and tooth selection

To provide a direct comparison between GPS and isotopic data, it was necessary to estimate the period of growth of the teeth sampled. Date of death was recorded for each animal. We then estimated the age at death by combining analyses of tooth eruption stages and tooth wear patterns (Grant, 1982; Jones, 2006) (**Supp. Info S5.2**). Based on interviews with herders, the season of birth extended between February and April with slight variations between years and herders. An arbitrary birth date of March 31st was chosen for all individuals. Although we are aware of the limits of this arbitrary choice, we argue that an uncertainty of about 1 month is likely to have a minor impact on subsequent comparisons given the duration of the mineralization process which is of ~4 months (Balasse, 2003; Zazzo et al., 2010). The period of formation of caprine molars was then calculated using an average value for the calendar of

caprine molar formation published in the literature (Milhaud and Nezit, 1991; Upex and Dobney, 2012; Weinreb and Sharav, 1964; Zazzo et al., 2010), with a dental crown formation that starts at 1.3 months and 10.3 months after birth for M2 and M3 respectively and ends at the age of 13 and 26 months respectively (**Table 7**). We then calculated the proportion of the tooth formation period covered by GPS tracking ($Time_{GPS}$) using the following formula:

$$Time_{GPS}(\%) = \frac{(T - \Delta d)}{T} \times 100 \quad \text{(Eq. 1)}$$

In Eq. 1, *T* is the entire time of formation of the tooth (in days) and *Δd* is the number of days within this period with no GPS record. We excluded five teeth with low $Time_{GPS}$ scores (0%), leaving us with fifteen teeth ($66\% < Time_{GPS} < 100\%$) (**Table 5**).

Table 7: Characteristics of the dental development rates (in months after birth) for molars M2 and M3 of caprines published datasets and the calculated mean data used in this study.

Start M2 (month)	End M2	Start M3	End M3	Source
2	16	14	33	Upex and Dobney (2012)
2	12	11	25	Weinreb and Sharav (1964)
0	12	8	22	Milhaud and Nezit (1991)
1	12	8	24	Zazzo et al. (2010)
1.3	**13.0**	**10.3**	**26.0**	**Mean**

5.4.2 GPS-based inference of mobility

GPS datasets were cleaned from erroneous GPS fixes. Herder mobility patterns were detected using the Lavielle's method (Lavielle, 2005, 1999), a method of segmentation of location time series. This method discriminates series of successive locations ("segments") during which movements happen at the same spatial scale but between which movements happen at different spatial scales. This allowed determining changes in animal movement, by identifying the different pastures and hence discriminating between small-scale movements (within each pasture) and large-scale movements (among pastures). Due to the nature of the landscape and after different trials (where segmentation was based on x or y coordinates), we finally based segmentation on altitude and each inferred segment was considered as a pasture, after visual validation. The Lavielle's method was implemented in the R package adehabitatHR (Calenge, 2006). Camps were identified thanks to the agglomeration of GPS points, since sheep and goats are led back to camps every night by herders to protect them from wolves.

We then used the GPS data in order to calculate, for each animal during the time of tooth and tail hair growth, their mean grazing altitude, the altitudinal range in exploited pastures, and the percentage of time spent at high altitude (above 2000 m.asl.). The limit of 2000 m was chosen because it represents the minimum altitude of alpine meadows in the mountainous western part of the study area (**Figure 12**). Below this limit, campsites and grazing animals are located on the eastern lowlands where (**Supp. Info S5.3**). The time spent above 2000 m was calculated as:

$$Time\_Alt\ (\%) = \frac{d_{2000}}{(T - \Delta d)} \times 100 \qquad \text{(Eq. 2)}$$

Where $T - \Delta d$ represent the number of days when the animal was tracked by a GPS collar and d_{2000} is the number of days spent above 2000 m.

For each herder, we compared altitudinal mobility between seasons with linear mixed models, with animal ID as a random effect (intercept), and testing for spatial and temporal auto-correlation in the GPS data (**Supp. Info S5.4**).

5.4.3 Isotopic analysis of plant material

The dried plant samples were crushed using a mixer mill. The 246 plant samples were then weighed in ultralight tin capsules and combusted in an elemental analyzer (PyroCUBE; Elementar, Hanau, Germany) coupled with an isotope ratio mass spectrometer from Isoprime Ltd (Cheadle Hulme, UK) for C stable isotope analysis at the *Laboratoire d'Ecologie des Hydrosystèmes Naturels et Anthropisés* (Lyon, France). In-house standards of sorghum flour calibrated against secondary international standards from the International Atomic Energy Agency, Vienna, Austria (IAEA-CH3, IAEA-CH6, IAEA-N1, IAEA-N2) were analyzed every twelve samples as quality control. The long-term precision (SD) for the internal laboratory standard was better than 0.3 ‰. Isotope data are presented in δ notation [δ = (Rsample/Rstandard) – 1], with R the isotope ratio ($^{13}C/^{12}C$) of the sample or international standard (V-PDB).

5.4.4 Tooth sample preparation and isotopic measures

Tooth enamel surface was cleaned by abrasion with a tungsten drill bit. Sequential sampling of modern caprine teeth was performed on the buccal side of the second and third molars, on the anterior lobe of M2 and the middle lobe of M3. The sampling spanned the width

of a lobe. For horse teeth, sequential sampling was performed on the mesial side of molars because this side has a flat surface with a narrow cementum layer and also because it should mineralize faster (Zazzo et al., 2012). For all teeth, enamel was drilled with a diamond bit, perpendicular to the tooth growth axis from the apex to the enamel root junction (ERJ). Samples were taken every 1.5-2mm through the entire thickness of the enamel layer and care was taken to avoid collecting the underlying dentine. Sample position was recorded in terms of their distance (in mm) from ERJ.

Samples weighing 3.5-7 mg were chemically treated following the procedure described in Balasse et al. (2002b). First, organic matter was removed with a solution of 2-3% NaOCl (24h, 0.1 ml solution/ mg of sample) and rinsed several times in distilled water. Then, each enamel sample was reacted with 0.1 M acetic acid (4h, 0.1 ml solution/mg of sample) to remove exogenous carbonates and rinsed in distilled water and dried in an oven at 80°C for 12h.

Purified enamel samples were weighted (600 µg approximately) and analyzed on a Kiel IV device connected to a Delta V Advantage isotope ratio mass spectrometer (IRMS) at the *Service de Spectrométrie de Masse isotopique du Muséum national d'Histoire naturelle* (SSMIM) in Paris. Samples were placed into individual vessels to react under vacuum with phosphoric acid [H_3PO_4] at 70°C and purified CO_2 in an automated cryogenic distillation system. In total, 306 enamel samples were analysed over a period comprised between October 2016 and October 2018. Analytical precision was 0.04‰ for $\delta^{13}C$ and 0.05‰ for $\delta^{18}O$ based on the repeated (n= 114) analysis of our internal laboratory carbonate standard (Marbre LM) normalized to NBS 19. Isotope data are presented in δ notation [$\delta = (R_{sample}/R_{standard}) - 1$], with *R* the isotope ratio ($^{13}C/^{12}C$ and $^{18}O/^{16}O$) of the sample, reported relative to the international standard V-PDB (Vienna PeeDee Belemnite) and expressed in per mil (‰).

5.4.5 Isotopic data treatment and statistical methods

For both C and O of caprine teeth, we compared the average isotopic values between herders using one-way ANOVAs followed by Tukey's post-hoc HSD.

We also compared $\delta^{13}C$ values of diet ($\delta^{13}C_{diet}$) in the tail hair of six horses, previously published (Lazzerini et al., 2019) and in the caprine enamel from the same herds (**Table 5**). To do so, we derived diet $\delta^{13}C$ values of caprines by applying a carbon isotope fractionation between diet and enamel of -15.4‰, determined for sheep raised on C_3 silage (Zazzo et al., 2010). The average $\delta^{13}C$ diet values between horses and caprines were then compared with a

one-way ANOVA. We then visually compared $\delta^{13}C_{diet}$ of caprines with the distribution of $\delta^{13}C$ of C_4 and C_3 plant samples in order to estimate the proportion of C4 in the diet of animals and its potential influence on altitudinal signal recorded by $\delta^{13}C$ values. For $\delta^{13}C$ values of enamel from non-geolocalised horses, we estimated the $\delta^{13}C_{diet}$ by applying a carbon isotope fractionation between diet and enamel of -13.7‰ determined for horses not raised under controlled conditions (Cerling and Harris, 1999; Tejada-Lara Julia V. et al., 2018)

The correlations between average grazing altitude (per animal) and average $\delta^{18}O$ values of caprine tooth enamel, and average $\delta^{13}C$ of diet of horse and caprine were estimated using Pearson's correlation coefficient. One-way ANCOVA was conducted to estimate the difference between horse and caprine's correlations between average grazing altitude and average $\delta^{13}C$ of diet. Pearson's correlation coefficient was also used to estimate the correlation between *Time_Alt* (Eq. 2) and the average $\delta^{13}C$ of diet of horse and caprine and $\delta^{18}O$ of caprine tooth enamel. One-way ANCOVA was also performed to estimate the difference between horse and caprine's correlations. We also used Pearson's correlation coefficient to estimate the potential influence of altitude on plant $\delta^{13}C$ values.

Finally, to assess the existence of a co-variation between $\delta^{13}C$ and $\delta^{18}O$, we used Pearson's correlation coefficient between the $\delta^{13}C$ and $\delta^{18}O$ sequences of each tooth. Then, we tested whether the frequency of altitudinal mobility was responsible for the observed variability in the patterns of co-variation of $\delta^{13}C$ and $\delta^{18}O$ sequences. To do so, we estimated the correlation between the standard deviation of mobility and Pearson's correlation coefficients between the $\delta^{13}C$ and $\delta^{18}O$ sequences.

Unless mentioned otherwise, all statistical analyses were conducted using R (version 3.4.4) with a 0.05 threshold of significance.

5.5 Results

5.5.1 The GPS record of caprines' mobility

A summary of the mobility patterns observed for sheep and goat during the period of formation are reported for each tooth in **Table 5** and the altitudinal mobility of each herder is plotted in (**Figure 13**). The herders nomadized between 9 (Dl, Kj, Zk) and 13 (Jk) times per year during the study period (June 2015 –July 2018) and used between 5 (Dl) and 12 (Kb) different campsites (**Figure 12** and more details about campsite on **Supp. Info S5.4**). The herds nomadised along an East-West (Jk, Kb and Kj) or NE-SW (Zk) gradient with an average

travelled distance per year ranging from 121 (Kj) to 291 (Zk) km. These four herders also exploited pastures situated along a wide altitudinal range (**Figure 13B-E**), from the eastern depression (around 1400-1500 m.asl) to the western mountain pastures (up to 4000 m.asl). The standard deviation (sd) of the average exploited altitude ranged from 259 (Kb) to 351 (Kj), reflecting the frequency of the altitudinal mobility of herds. On the contrary, herder Dl remained at a high altitude of 2366 ± 131 m.asl during the study period with little altitudinal variations between campsites (max 200 m – **Figure 13**) and a limited distance travelled by year of 38km (**Table 8**). Generally, for all herders, herds were significantly (*p-value* < 0.001) higher in altitude during summer than winter (**Table 8 – Supp. Data S5.4**). The lower average differences between summer and winter pastures are observed for herders Dl and Kb, with 94 m and 120 m of difference respectively.

Table 8: Characteristics of the GPS data of the five Kazakh-Mongolian nomadic pastoralists with GPS-based mobility of the study caprines. *: goat from Kb herder but not all the time with the herd during winter 2015-2016.

Herder	Dl	Jk	Kb	Kj	Zk
Start GPS	16/09/2016	19/06/2015	16/06/2015	19/06/2015	17/09/2016
End GPS	24/07/2018	17/07/2018	20/07/2018	29/07/2018	29/11/2017
N days	676	1124	1130	1136	438
N GPS data	1235	7505	7325	7357	820
Mean Altitude ± sd (m.asl)	2366 ± 131	1977 ± 334	2247 ± 268	2243 ± 351	1790 ± 274
Mean summer altitude	2425 ± 118	2259 ± 477	2349 ± 318	2501 ± 377	2124 ± 293
Mean winter altitude	2331 ± 136	1906 ± 174	2229 ± 222	2122 ± 316	1712 ± 189
N campsite	5	10	12	11	9
N nomadisation	17	40	30	28	11
N nomadisation / year	9	13	10	9	9
Average ± sd days on pasture	40 ± 23	27 ± 19	37 ± 40	40 ± 32	40 ± 48
Average distance travelled by year (km)	38	219	127	122	291

5.5.2 Plant $\delta^{13}C$ values

Plant $\delta^{13}C$ values ranged from -31.2 to -13.2‰, with an average value of -27.1 ± 2.3‰ (**Figure 14A**). A negative correlation between $\delta^{13}C$ of plants and altitude was found (Pearson's correlation: r = -0.16; r^2 = 0.02; *p-value* = 0.01 – **Supp. info S5.1**). Six samples presented $\delta^{13}C$ values specific to C4 plants (i.e. higher than -20‰). These samples were identified as *Anabasis brevifolia* (B. Oyuntsetseg, pers. comm.). They were located in the lowland pastures below 1950 m.asl (for more details see **Supp. Info S5.1**). However, the large majority of samples had low $\delta^{13}C$ (<-25 ‰) values, highlighting the high proportion of C_3 plants in the study area.

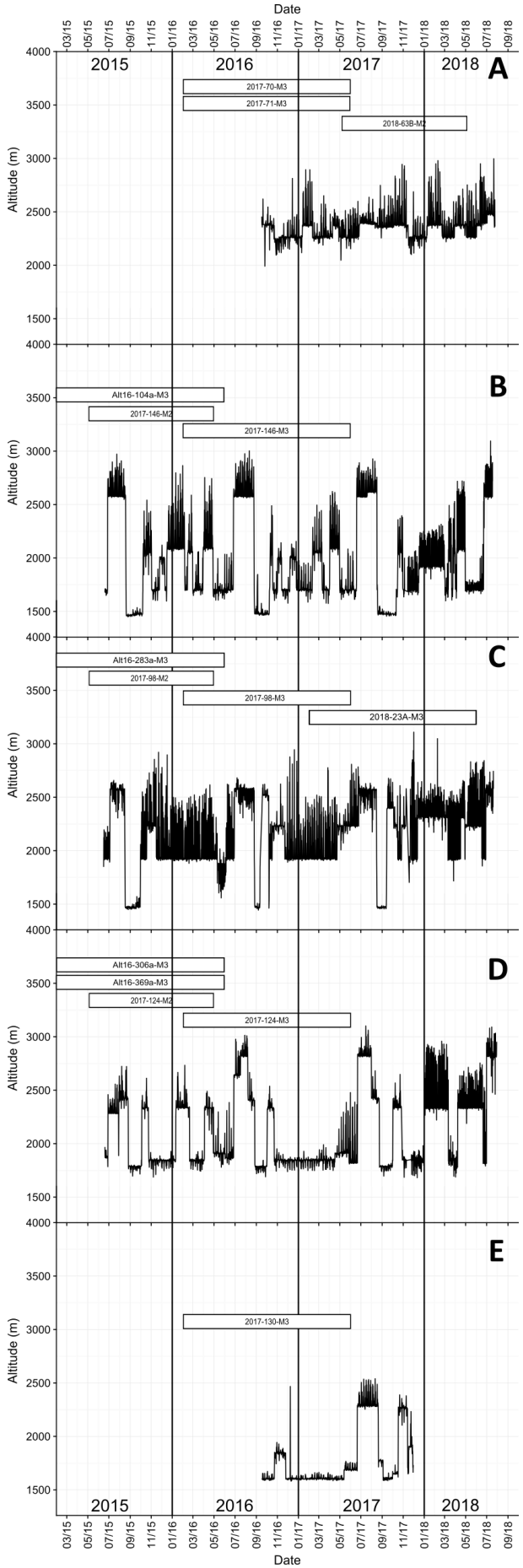

Figure 13 : Temporal altitudinal variations of GPS-monitored caprine herds from the five Kazakh-Mongolian households, based on the locations monitored by one selected GPS collar for each of the three periods. Each panel represents a different herder (**A** =Dl; **B** = Jk; **C** = Kb; **D** = Kj; **E** = Zk). The different rectangles represent the estimated growth periods of the fifteen teeth used in the study.

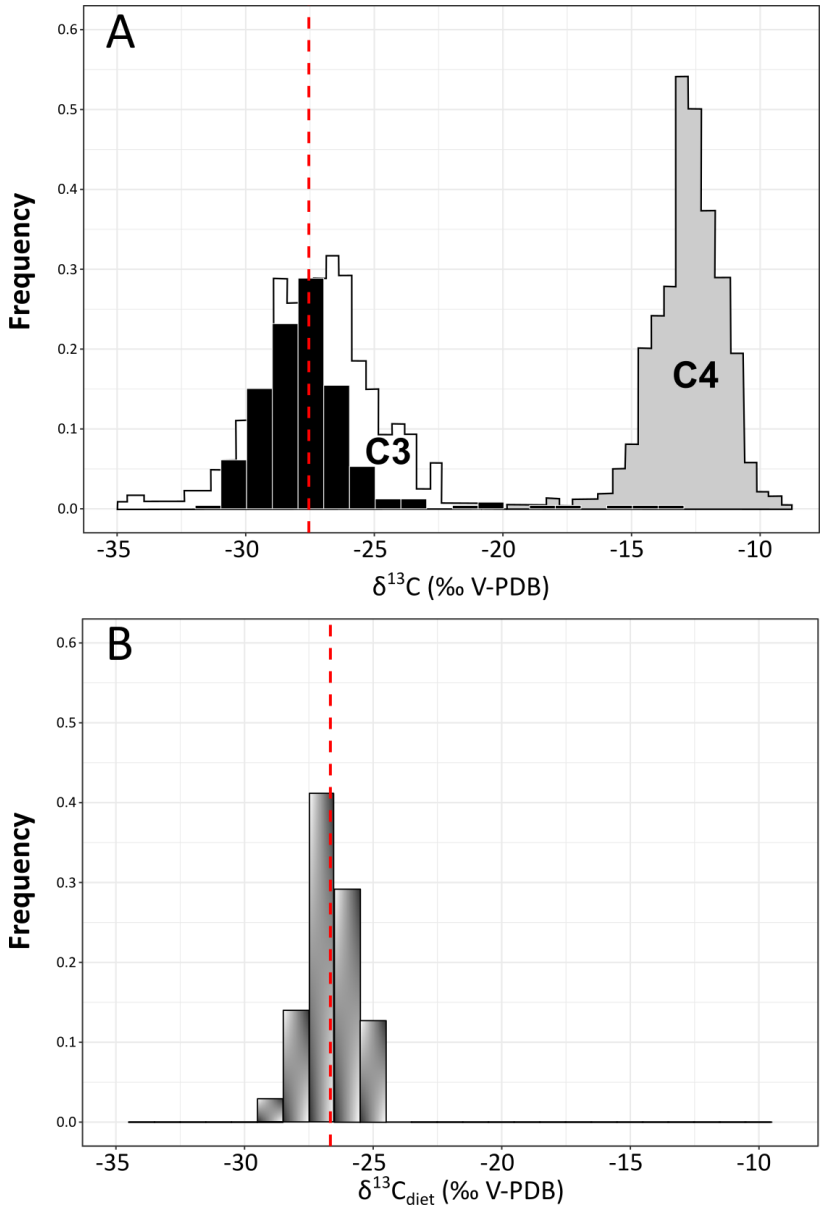

Figure 14: Histograms showing **(A)** The distribution (in black) and mean (red dashed line) of local $\delta^{13}C$ values from the 246 plant samples from the study area, on top of the $\delta^{13}C$ distribution values of global C_3 (white) and C_4 (grey) plants after O'Leary (1988). Note that because raw data of O'Leary (1988a) were not available and the original y-axis was not preserved, the C_3 and C_4 areas only show the relative frequency of $\delta^{13}C$ values of plants. **(B)** The distribution of $\delta^{13}C$ values of sheep and goat diet calculated from enamel $\delta^{13}C$ values based on a carbon isotope fractionation ratio between diet and tooth enamel bioapatite of -15.4‰ *(Zazzo et al., 2010)*. The red dashed line represents the mean $\delta^{13}C_{diet}$ value.

5.5.3 $\delta^{18}O$ values of tooth enamel

Summary results from stable isotope analyses are presented in **Table 9** and complete data are available in supplementary data (**Supp. Info S5.5**). Oxygen isotope profiles of caprines and horses followed a sinusoidal pattern with maximum values reflecting high temperature of summer and minimum values reflecting low temperatures during winter (**Figures 15 & 16**). On average, caprines had a $\delta^{18}O$ value of -7.9 ± 3.6‰, with values ranging from -14.6‰ to -0.1‰.

Intra-tooth amplitude in $\delta^{18}O$ value ranged from 9.2 to 12.2 ‰, except for 2018-63B-M2 which showed a lower amplitude of 6.5‰ because it probably not recorded a complete seasonal cycle (**Figure 15**).

Table 9: Summary statistics of the isotopic values of $\delta^{13}C$ and $\delta^{18}O$ sequences of enamel bioapatite samples. [1]: $\delta^{18}O$ values from (Lazzerini et al., 2020 – see Chapter 8). [2]: $\delta^{18}O$ values from this study. N = number of samples by tooth. Pearson's r = correlation coefficient between δ13C and $\delta^{18}O$ sequences, df = degree of freedom of the correlation, p-value = significance level.

Herder	Tooth sample	N	$\delta^{13}C$ (‰ V-PDB)				$\delta^{18}O$ (‰ V-PDB)				Pearson's r	df	*p-value*
			Mean ± sd	Max	Min	A	Mean ± sd	Max	Min	A			
Dl	2017-70-M3[1]	21	-12.14 ± 0.29	-11.6	-12.6	1.0	-7.50 ± 3.08	-3.2	-12.4	9.2	0.13	19	>0.05
	2017-71-M3[1]	20	-12.15 ± 0.33	-11.4	-12.6	1.2	-7.19 ± 3.19	-3.2	-12.4	9.2	0.33	18	>0.05
	2018-63B-M2[1]	18	-12.88 ± 0.57	-11.8	-13.7	1.9	-10.37 ± 2.14	-6.5	-13.0	6.5	0.52	16	**<0.05**
	All	**59**	**-12.37 ± 0.53**	**-11.4**	**-13.7**	**2.3**	**-8.27 ± 3.15**	**-3.2**	**-13.0**	**9.8**			
Jk	Alt16-104a-M3[1]	24	-10.70 ± 0.69	-10.0	-12.1	2.1	-7.66 ± 3.83	-1.5	-13.4	12.0	-0.91	22	**<0.001**
	2017-146-M2[2]	16	-11.60 ± 0.31	-11.2	-12.2	1.0	-7.94 ± 4.24	-1.6	-12.8	11.1	-0.37	14	>0.05
	2017-146-M3[1]	24	-11.51 ± 0.35	-11.0	-12.1	1.1	-7.69 ± 3.28	-2.3	-12.6	10.3	-0.69	22	**<0.001**
	All	**64**	**-11.23 ± 0.64**	**-10.0**	**-12.2**	**2.3**	**-7.74 ± 3.59**	**-1.5**	**-13.4**	**12.0**			
Kb	Alt16-283a-M3[1]	24	-10.87 ± 0.39	-10.2	-11.5	1.3	-8.66 ± 3.13	-3.5	-13.8	10.4	-0.78	22	**<0.001**
	2017-98-M2[2]	14	-11.47 ± 0.53	-10.8	-12.6	1.8	-10.44 ± 3.48	-3.9	-14.6	10.7	0.61	12	**<0.05**
	2017-98-M3[1]	18	-11.23 ± 0.90	-11.1	-11.8	0.7	-8.15 ± 3.35	-3.3	-13.1	9.8	0.10	16	>0.05
	2018-23A-M3[1]	21	-11.48 ± 0.41	-10.9	-12.4	1.5	-8.18 ± 4.06	-2.3	-13.3	10.9	-0.38	19	>0.05
	All	**77**	**-11.46 ± 0.39**	**-10.8**	**-12.6**	**1.8**	**-8.77 ± 3.75**	**-2.3**	**-14.6**	**12.2**			
Kj	Alt16-306a-M3[1]	24	-10.25 ± 0.57	-9.4	-11.2	1.8	-7.39 ± 3.33	-2.2	-13.2	11.0	-0.83	22	**<0.001**
	Alt16-369a-M3[1]	18	-10.86 ± 0.79	-10.1	-12.8	2.7	-6.47 ± 4.29	-0.1	-12.3	12.2	-0.74	16	**<0.001**
	2017-124-M2[2]	16	-10.93 ± 0.27	-10.4	-11.3	0.9	-7.57 ± 3.65	-1.6	-12.3	10.7	-0.39	14	>0.05
	2017-124-M3[1]	23	-10.92 ± 0.49	-10.2	-11.8	1.6	-7.77 ± 3.91	-1.1	-13.1	12.0	-0.38	21	>0.05
	All	**81**	**-10.57 ± 0.70**	**-9.4**	**-12.8**	**3.3**	**-7.38 ± 3.80**	**-0.1**	**-13.4**	**13.2**			
Zk	2017-130-M3[1]	25	-10.76 ± 0.73	-9.6	-12.3	2.6	-6.84 ± 3.57	-0.9	-11.9	11.0	-0.28	23	>0.05
Kb	2017-104 M2	30	-13..4 ± 0.4	-12.8	-14.0	1.2	-11.8 ± 1.9	-7.2	-14.7	7.5	-0.26	28	>0.05
?	2018-17B M3	20	-13.3 ± 1.6	-11.9	-16.4	4.4	-10.9 ± 3.3	-5.0	-14.5	9.5	-0.72	18	**<0.001**
?	2018-57A M3	23	-12.2 ± 1.4	-10.6	-15.0	4.4	-10.4 ± 1.7	-6.8	-13.3	6.5	-0.60	21	**<0.01**
Kj	2018-58B M3	20	-12.3 ± 0.5	-11.6	-13.0	1.4	-11.2 ± 3.1	-7.5	-16.1	8.6	-0.88	13	**<0.001**
?	2018-59A M1	16	-12.5 ± 0.7	-11.2	-13.3	2.1	-9.2 ± 2.7	-5.6	-14.4	8.8	-0.82	14	**<0.001**

On average, Dl caprines exhibited lower maximum values and higher minimum values than animals from the other herders, even if values form 2018-63B-M2 are excluded (**Table 9**). We found differences in the average $\delta^{18}O$ values of the different herds, with the lowest values found in Dl (-8.3 ± 3.2‰, n= 3) and Kb (-8.8 ± 3.7‰, n= 2)'s animals, and the highest values for Zk's animals (-6.8 ± 3.6‰, n = 1). However, these differences were not statistically significant (*p-value* > 0.05). We found no correlation between the average $\delta^{18}O$ value and average altitude (r = -0.36; r^2 = 0.13, *p-value* = 0.19) but we found a negative correlation between the intra-tooth $\delta^{18}O$ amplitude and average altitude (r = -0.62; r^2 = 0.38; *p*-value = 0.01 - **Figure 17**) and a positive correlation between the intra-tooth $\delta^{18}O$ amplitude and the standard deviation of the mean grazing altitude (r = 0.54; r^2 = 0.29; *p-value* = 0.04 –**Figure 18**).

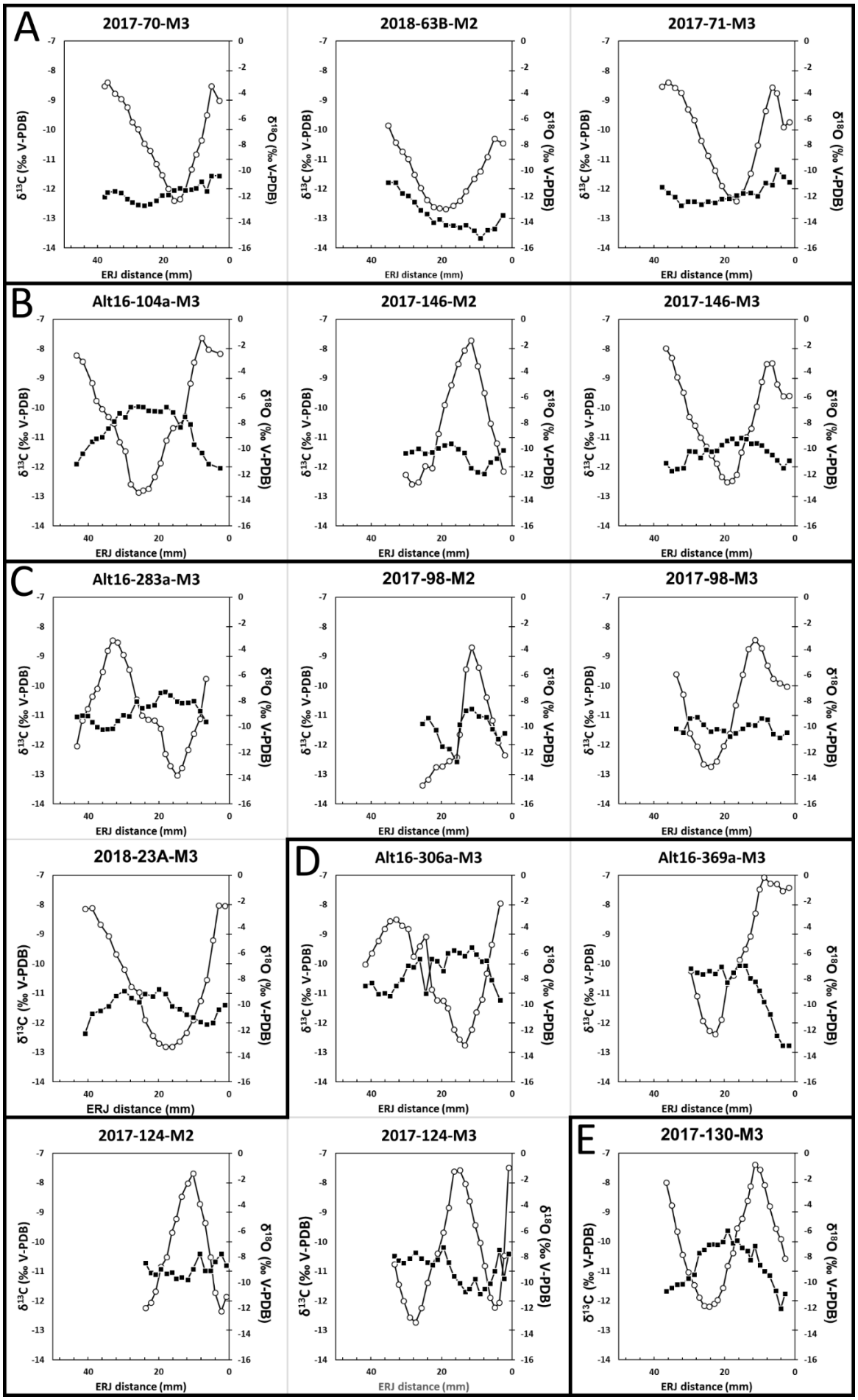
A
2017-70-M3
2018-63B-M2
2017-71-M3
B
Alt16-104a-M3
2017-146-M2
2017-146-M3
C
Alt16-283a-M3
2017-98-M2
2017-98-M3
2018-23A-M3
D
Alt16-306a-M3
Alt16-369a-M3
2017-124-M2
2017-124-M3
E
2017-130-M3
δ13C (‰ V-PDB)
δ18O (‰ V-PDB)
ERJ distance (mm)

Figure 15 (previous page): Sequential variations of $\delta^{18}O$ (white circles) and $\delta^{13}C$ (black squares) along the tooth crown from the fifteen molars of sheep and goat (M_2 and M_3) belonging to Dl (A), Jk (B), Kb (C), Kj (D) and Zk (E). Samples are located in the tooth crown using the distance from enamel-root junction (ERJ) in mm.

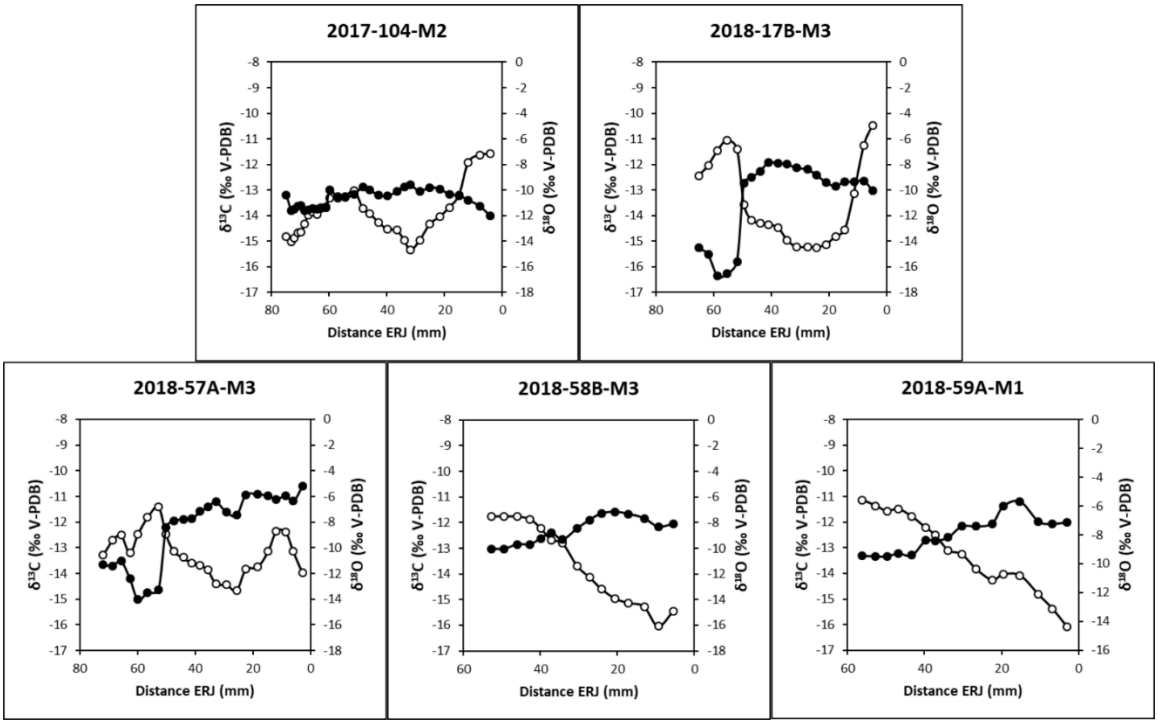

Figure 16: Oxygen ($\delta^{18}O$) and carbon ($\delta^{13}C$) isotopes values along the tooth crown of modern horse molars. ERJ is the distance between the sample and the enamel-root junction. White and black circles represent measured $\delta^{18}O$ (‰) and $\delta^{13}C$ (‰) respectively, with analytical error inside the square.

Concerning horse teeth (**Table 6**), average $\delta^{18}O$ value is at -10.8 ± 2.6‰, with values ranging from -5.0 to -16.1‰. Intra-tooth amplitude in $\delta^{18}O$ value ranged from -9.5 to -6.5 ‰. The average $\delta^{18}O$ values and intra-tooth amplitude of horse were significantly lower than those of sheep and goats (*p-value* = $7e^{-14}$ and 0.005 respectively).

5.5.4 $\delta^{13}C$ values of horses and caprines

On average, caprine enamel $\delta^{13}C$ value was -11.2 ± 0.9‰, with values ranging from -13.7‰ to -9.4‰. For each herd, the average $\delta^{13}C$ value ranged from -12.4 ± 0.5‰ (Dl) to -10.6 ± 0.7‰ (Kj) (**Table 9**). Dl caprine $\delta^{13}C$ values were significantly lower than those of all the other herders (*p-value* < 0.01). The estimated $\delta^{13}C_{diet}$ was -26.6 ± 0.9 (**Figure 19**), indicating that the caprines of the study area consumed a diet that included no or very little C_4 plants. Geolocalised horses' $\delta^{13}C_{diet}$ value was -27.5 ± 0.8‰ (Lazzerini et al., 2019), and was significantly lower (*p-value* = 0.04) than that of caprines (**Figure 19**). We found a negative correlation between the average $\delta^{13}C_{diet}$ value of caprines and the average grazing altitude

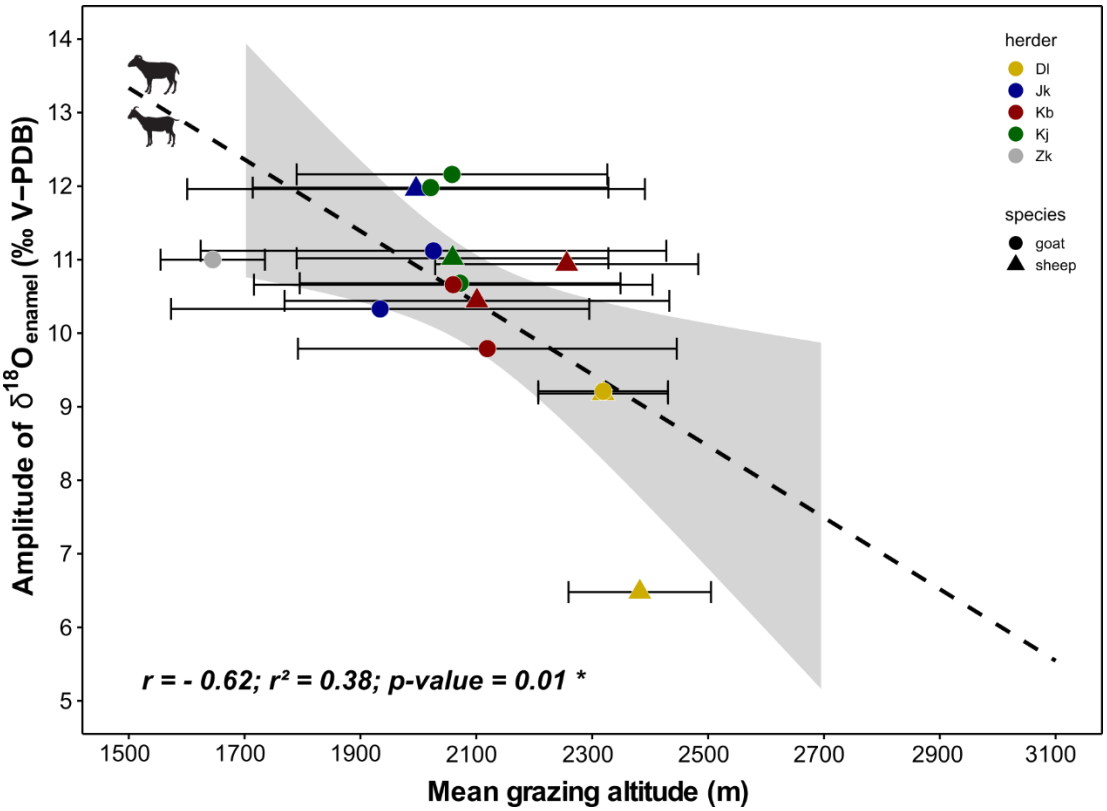

Figure 17: Intra-tooth amplitude of $\delta^{18}O$ (‰) of sheep (triangle) and goat (circle) plotted against the mean grazing altitude during tooth formation with the corresponding linear regression (dashed black line). Shaded areas are the 95% confidence interval of each linear regression. Each herder is represented with a different color. Horizontal bars indicate the standard deviation of the calculated average.

($Elev_{avrg}$ in meters) (r = -0.68; r^2 = 0.46, *p-value* = 0.006 – **Figure 19**) obtaining the following equation:

$$\delta^{13}C_{diet} = -0.002576 \times Elev_{avrg} - 21.33 \quad \text{(Eq. 3)}$$

We also found a negative correlation between the average $\delta^{13}C_{diet}$ value of geolocalised horses and the average grazing altitude (r = -0.92; r^2 = 0.85, *p-value* = 0.001 – **Figure 19**) obtaining the following equation:

$$\delta^{13}C_{diet} = -0.0014493 \times Elev_{avrg} - 24.14 \quad \text{(Eq. 4)}$$

The slopes of these two equations (3 & 4) were not significantly different ($F_{1, 19}$ = 0.89, *p-value* = 0.36), as the Y intercepts ($F_{1, 19}$ = 1.4, *p-value* = 0.25). Combining data of all livestock, we obtained the following equation between $\delta^{13}C_{diet}$ and the average grazing altitude (r = -0.76; r^2 = 0.57; *p-value* = $7e^{-5}$ – **Figure 19**):

$$\delta^{13}C_{diet} = -0.0025189 \times Elev_{avrg} - 21.52 \quad \text{(Eq. 5)}$$

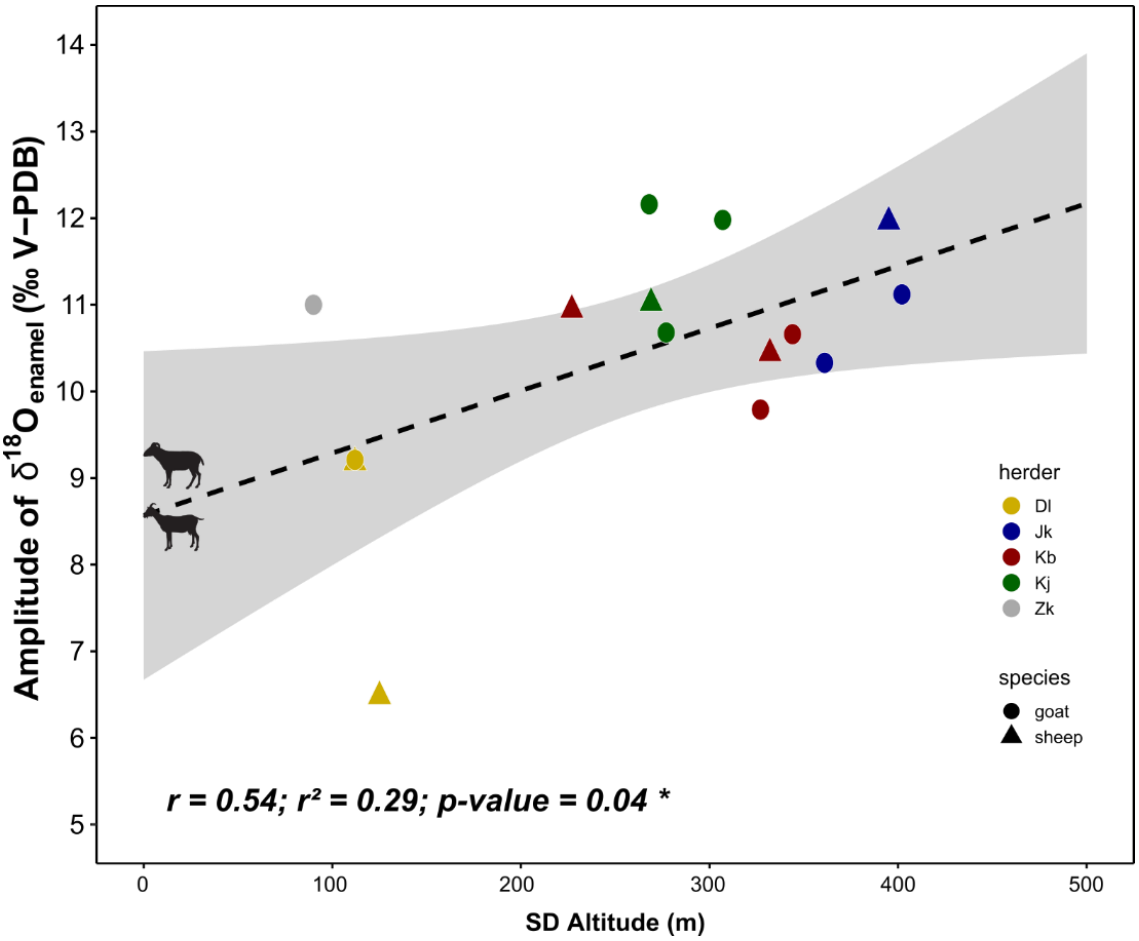

Figure 18: Intra-tooth amplitude of $\delta^{18}O$ (‰) of sheep (triangle) and goat (circle) plotted against the standard deviation of the mean grazing altitude during tooth formation with the corresponding linear regression (dashed black line). Shaded areas are the 95% confidence interval of each linear regression. Each herder is represented with a different color.

The slopes of the linear regressions between plant $\delta^{13}C$ and altitude, caprine $\delta^{13}C_{diet}$ and altitude, and horse $\delta^{13}C_{diet}$ and altitude were not significantly different (One-way ANCOVA - $F_{2, 265} = 0.14$; *p-value* = 0.87). The Y intercepts were not significantly different either ($F_{2, 265} = 0.2$; *p-value* = 0.85).

Moreover, the $\delta^{13}C_{diet}$ values of animals were negatively correlated with the percentage of time spent above 2000 m of altitude for caprines (r = -0.74; $r^2 = 0.55$, *p-value* = 0.001 – **Figure 20**) with the following equation:

$$\delta^{13}C_{diet} = -0.019783 \times Time\_Alt\ (\%) - 25.73 \qquad \text{(Eq. 6)}$$

and also for horses (r = -0.89; $r^2 = 0.80$; *p-value* = 0.02 - **Figure 20**) with the following equation:

$$\delta^{13}C_{diet} = -0.011625 \times Time\_Alt\ (\%) - 26.73 \qquad \text{(Eq. 7)}$$

The slopes of these two equations (6 & 7) were not significantly different ($F_{1, 19} = 0.80$, *p-value* = 0.38), unlike the Y intercepts ($F_{1, 19} = 5$, *p-value* = 0.03).

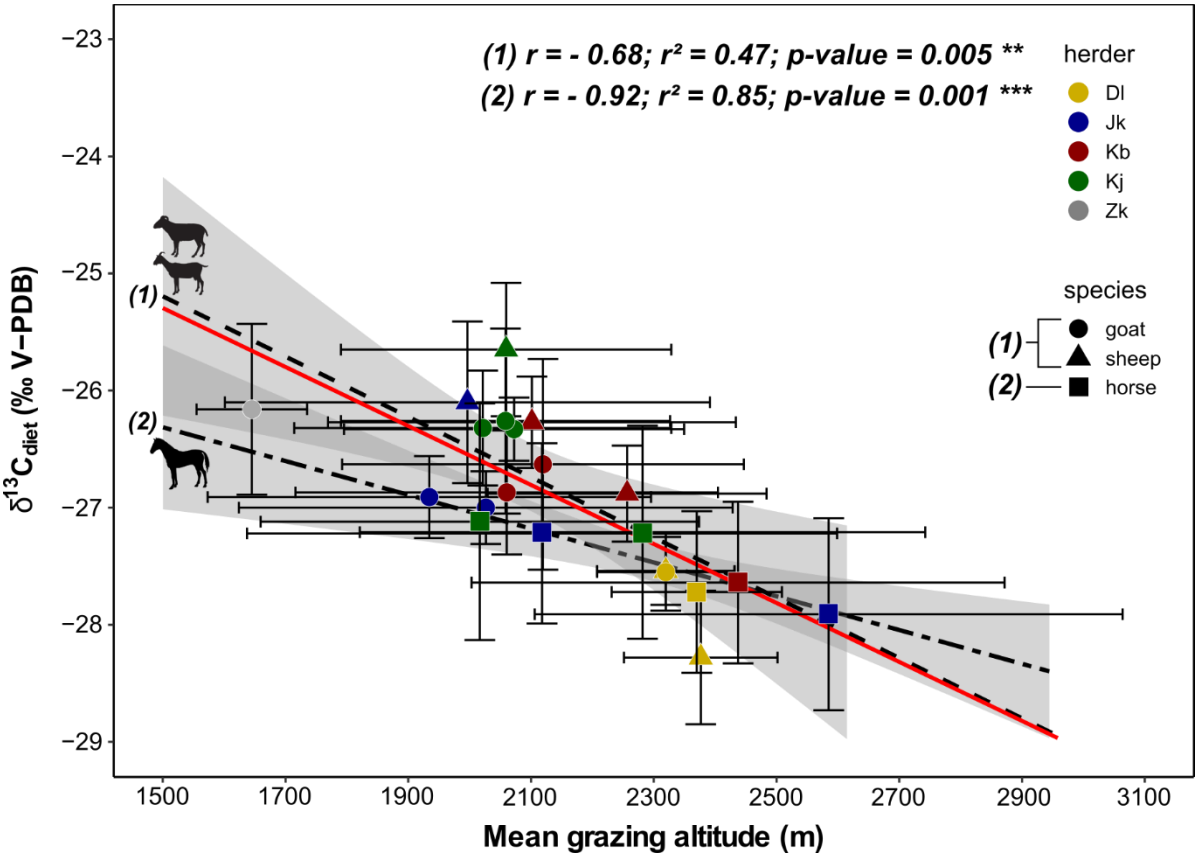

Figure 19: (1) Mean $\delta^{13}C_{diet}$ (‰) of sheep (triangle) and goat (circle) (calculated from enamel $\delta^{13}C$ values with carbon isotope fractionation of -15.4‰) plotted against the mean grazing altitude during the tooth formation with the corresponding linear regression (dashed black line). Compared with **(2)** Mean $\delta^{13}C_{diet}$ (‰) of horses (square) from the same study area (Lazzerini et al., 2019), plotted against the mean grazing altitude with the corresponding linear regression (dot dashed line). Shaded areas are the 95% confidence interval of each linear regression. Each herder is represented with a different color. Vertical and horizontal bars indicate the standard deviation of the calculated average. Red line represents the linear regression including all caprin and horse data.

Finally, on average horse enamel $\delta^{13}C$ value was –12.8 ± 1.1‰, with values ranging from -16.4 to -10.6‰ (**Table 9**). Intra-tooth amplitude in $\delta^{13}C$ value ranged from 1.2 to 4.4‰, with average amplitude of 2.7 ± 1.6‰. For these non-geolocalised horses we estimated an average $\delta^{13}C_{diet}$ of -26.5 ± 1.1, showing no significate difference (*p*-value = 0.6) with average $\delta^{13}C_{diet}$ of caprines but a significate difference (*p*-value = 0.02) with average $\delta^{13}C_{diet}$ of monitored horses. Using equations 4 we estimated a mean grazing altitude of 1584 ± 376 m, ranging from 1246 to 2012 m (**Table 10**), that is significantly lower (*p-value* = 0.03) than average grazing altitude of monitored horses (2298 ± 208 m; **Table 5**), with a mean difference of 714 m. With equation 7, we estimated an average occupation of pasture above 2000 m of

10% with a range from 0 to 28 % (**Table 10**), that is significantly lower (*p-value* = 0.002) than average occupation above 2000 m by monitored horses (64%; **Table 5**).

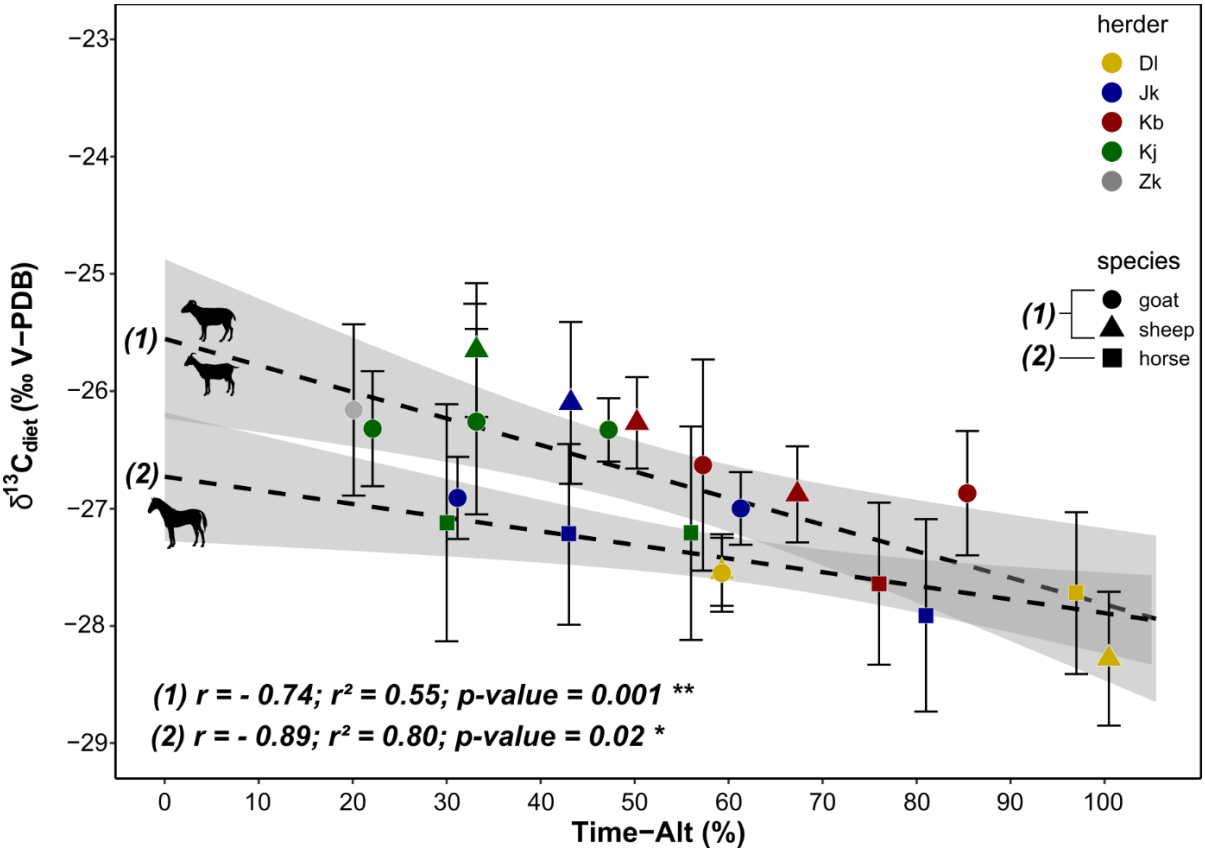

Figure 20: (1) Mean $\delta^{13}C_{diet}$ (‰) of sheep (triangles) and goats (circles) (calculated from enamel $\delta^{13}C$ values with carbon isotope fractionation of -15.4‰) plotted against the percentage of time, during tooth formation, spent grazing at high altitude (> 2000 m.asl), with the corresponding linear regression (dashed black line). Compared with **(2)** Mean $\delta^{13}C_{diet}$ (‰) of horses (square), from the same study area, plotted against the percentage of time, during tooth formation, spent grazing at high altitude (> 2000 m.asl) with the corresponding linear regression (dot dashed line). Shaded areas are the 95% confidence interval of each linear regression. Each herder is represented with a different color. Horizontal bars indicate the standard deviation of the calculated average.

Table 10: Estimated mean grazing altitude and percentage of pasture occupation above 2000 m of non-geolocalised horse based on their average $\delta^{13}C_{diet}$ estimated using the enrichment factor of 13.7 ‰ determined by Cerling and Harris (1999) or a modified one of 14.7 ‰.

Tooth sample	Herder	$\delta^{13}C_{enamel} - \delta^{13}C_{diet}$ = 13.7		δ13Cenamel - δ13Cdiet = 14.7	
		$Elev_{avrg}$ (m)	Time-Alt (%)	$Elev_{avrg}$ (m)	Time-Alt (%)
2017-104 M2	Kb	2012	28	2692	100
2018-17B M3	?	1970	23	2651	100
2018-57A M3	?	1246	0	1926	17
2018-58B M3	Kj	1287	0	1968	22
2018-59A M1	?	1405	0	2085	37

5.5.5 Co-variations between $\delta^{13}C$ and $\delta^{18}O$ values

We tested the correlations between $\delta^{13}C$ and $\delta^{18}O$ values measured in the same tooth in order to show its relation with altitudinal mobility performed by animals. Plots for all the individuals (sheep, goat and horse) are shown in **Supp. Info S5.6**. Caprines from Dl showed a weak positive correlation (r = 0.13, 0.33 and 0.53 – **Table 9**) whereas caprines from three other herders (Jk, Kj and Zk) showed negative correlations (**Table 9**). Finally, Kb's caprines exhibited both positive and negative correlations between $\delta^{13}C$ and $\delta^{18}O$ intra-tooth values (**Table 9; Figure 15**). To test the hypothesis of influence of altitudinal mobility on the co-variation between $\delta^{13}C$ and $\delta^{18}O$ values, we investigated the correlation between the Pearson's correlation coefficient and variability of altitudinal mobility. We found a negative relationship, close to the significance level (r = -0.46; r^2 = 0.37; *p-value* = 0.08) between the standard deviation of the mean grazing altitude (**Table 5**) and the Pearson's correlation coefficient between $\delta^{13}C$ and $\delta^{18}O$ values of the sheep and goat teeth (**Table 9**; **Figure 21**).

For non-monitored horses, modern horse teeth showed negative correlations between $\delta^{13}C$ and $\delta^{18}O$ intra-tooth values (r coefficient from -0.88 to -0.26) that were statistically significant (*p-value* < 0.05), except for 2017-104-M2 (**Table 6**).

5.6 Discussion

5.6.1 Influence of altitudinal mobility / residency on $\delta^{18}O$ values of livestock

We did not find any relationship between the average $\delta^{18}O$ value of caprine tooth enamel and grazing elevation. This result does not support the hypothesis that tissues of animals grazing at higher elevation should record lower $\delta^{18}O$ values than animals grazing at lower elevation (Pederzani and Britton, 2019; Poage and Chamberlain, 2001a). This lack of correlation could be explained by the fact that caprines get their water mainly from plants (Jensen, 2009) and that evapotranspiration affects their $\delta^{18}O$ value independently of altitude. Moreover, in our study area the water sources available for drinking mainly consist in streams (resulting from snow melt), which are the products of various enrichment and transport processes (e.g. Gibson et al., 2002; Barbour, 2007; Halder et al., 2015) and may not directly reflect $\delta^{18}O$ values of meteoric water, especially since the amount of rainfall is very low in this semi-arid region.

In addition, we noticed that individuals which grazed permanently at higher elevation (2017-70, 2017-71, 2018-63B) had a more restricted range in intra-tooth $\delta^{18}O$ values than individuals which grazed more frequently at lower elevation (**Figure 17**). These individuals,

which belonged to Dl herder, remained at the same altitude all year round unlike the other herders' animals. At the opposite, a large range of altitudinal residency (i.e. Jk, Kb, Kj) lead to larger intra-tooth amplitude of $\delta^{18}O$ values (**Figure 18**). This results contradicts previous studies that have stated that animal moving to avoid climatic extreme, as for vertical mobility, would lead to a reduced amplitude (Britton et al., 2009; Henton, 2012; Henton et al., 2017b; Pellegrini et al., 2008) but it is in accordance with Mashkour et al. (2005) which stated that transhumant animals should recorded larger intra-tooth $\delta^{18}O$ variability indicating the ingestion of more isotopically diverse source of water outside of the 'local' range of lowlands.

All together, our results suggest that using caprine enamel $\delta^{18}O$ values to distinguish between individuals that moved vertically a lot (i.e. Jk, Kb, Kj) and individuals that remained at the same altitude (Dl) proves challenging, in keeping with what Knockaert et al. (2018) noticed in the eastern Pyrenees. However, it would appear that a reduced amplitude indicates a more residential mobility in our case of study.

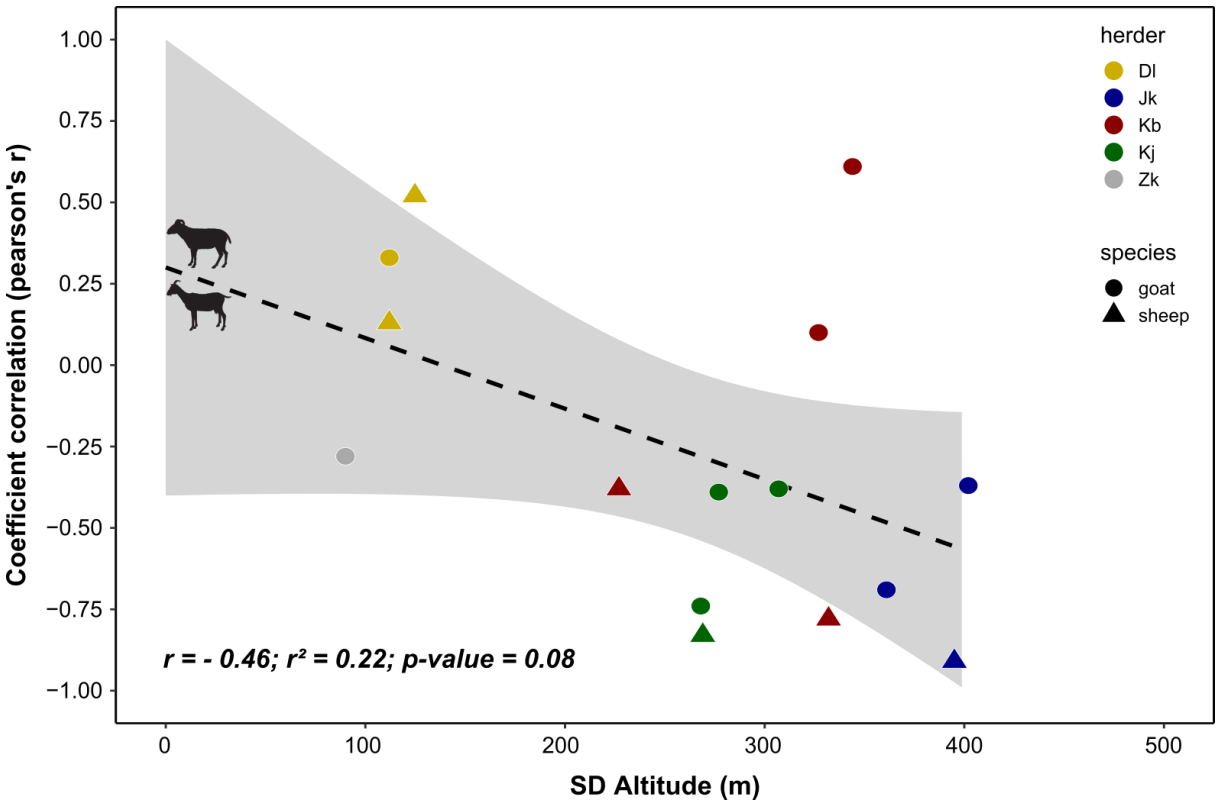

Figure 21: Correlation coefficient (Pearson's r) between $\delta^{13}C$ and $\delta^{18}O$ of enamel of sheep (triangle) and goats (circle) plotted against the standard deviation of the mean grazing altitude during tooth formation, with the corresponding linear regression (dashed black line). Shade area is the 95% confidence interval of the linear regression. Colors represent the different herders.

5.6.2 Influence of altitudinal mobility / residency on $\delta^{13}C$ values of livestock

We found a significant negative correlation between average diet $\delta^{13}C$ values and grazing altitude for caprines and horses (**Figure 19**). Because tissue $\delta^{13}C$ values derive from that of the animal's diet, it is reasonable to assume that the altitudinal effect is caused by plant $\delta^{13}C$ values (**Supp. Info S5.1**), which also exhibit this negative correlation with altitude. The negative relationship between $\delta^{13}C$ and altitude is similar to that observed in several mountainous areas like the Spanish Pyrenees (Tornero et al., 2018), central China (Liu et al., 2016), or central Mongolia (Makarewicz and Tuross, 2006). In a semi-arid environment like the Eurasian steppe, water availability is the main factor controlling plant $\delta^{13}C$ values, with more negative values associated with higher water availability (Ehleringer and Dawson, 1992; Flanagan and Farquhar, 2014; Hartman and Danin, 2010; Kohn, 2010; Liu et al., 2007; Murphy and Bowman, 2009). Thus, the decrease in enamel $\delta^{13}C$ values with altitude observed is probably caused by higher water availability at high altitude, mainly because of more abundant summer precipitation, snow melt and less evaporation (**Supp. Info S5.7**). Even if lowland pastures include a few C_4 plants, they are too rare to increase the average $\delta^{13}C$ composition of the plant community and hence sharpen this general pattern of lower $\delta^{13}C$ values with increasing altitude.

It is noteworthy that unlike what was found here, Lazzerini et al. (2019) did not find any correlation between high-resolution time series in horse tail hair $\delta^{13}C$ value and altitude. This apparent discrepancy, appearing when the same dataset is analyzed at two different scales (sequential vs. bulk), could be due to the fact that frequent (daily) changes in altitude by horses increase the noise to signal ratio and make any relationship between altitude and $\delta^{13}C$ difficult to detect in at a daily to weekly resolution.

It is also interesting to note that $\delta^{13}C_{diet}$ values of geolocalised horses were significantly lower than those of caprines, similar to what was also observed in the northern Kazakh steppe (Ventresca Miller et al., 2018). This can be interpreted as the result of different dietary preferences by the two species. Indeed, horses are more free in their mobility and prefer to feed in wetter grasslands, near streams (King, 2002; Menard et al., 2002) where vegetation is depleted in ^{13}C. On the other side, caprines can reach steep slopes in high altitude pastures to find fresh grass (Negi et al., 1993 and own field observations – **see Supp. Info S5.7**). These slope pastures are potentially dryer than valley bottoms and this may explain the higher $\delta^{13}C$ diet values of sheep and goats.

Very interestingly, our results show that average $\delta^{13}C_{diet}$ can be used to predict residency and in particularly the occupation of alpine meadows. Indeed, we found a significant negative correlation between the average $\delta^{13}C$ values of caprine and horse tooth enamel and the percentage of time spent at altitudes higher than 2000 m.asl during tissue formation (**Figure 20**). This altitudinal limit was selected to characterize the exploitation of alpine meadows of the western part of the study area (**Figure 12**). Concerning caprines, we can reasonably assume that, for the study area, average $\delta^{13}C_{diet}$ values ≤ -27‰ are indicative of preferential residency (≥ 66%) above 2000 m asl whereas average $\delta^{13}C$ values ≥ -26‰ are indicative of preferential residency (≤ 10%) below 2000 m asl. For horses (**Figure 20**), an average $\delta^{13}C$ values ≤ -27.5‰ would reflect preferential exploitation of high altitude pastures, whereas average $\delta^{13}C$ values ≥ -26.8‰ would indicate preferential exploitation of lowland pastures. However, the great variability of values $\delta^{13}C_{diet}$ in regards to the weak slope of the regressions (Eq. 3 to 7) may limit the applicability of this approach to the estimation of altitudinal occupation for modern and archaeological animals whose mobility pattern is unknown. Indeed, in the case of non-geolocalised $\delta^{13}C$ horse enamel (**Table 6**), we estimated a mean grazing elevation 700 m lower than monitored horses, with extremely low elevation (ca. 1250) impossible for the study area. There is no reason that these non-geolocalised horses performed such different altitudinal mobility patterns. This difference may be due to the 1 ‰ of difference between the $\delta^{13}C_{diet}$ of geolocalised horses and non-geolocalised horses. An estimation error of 1 ‰ would have a great impact on the estimation of high altitude exploitation due to the weak slope of these linear regressions (**Figures 19 & 20**). These misestimations of $\delta^{13}C_{diet}$ may be caused by uncertainties linked to the enrichment factor between diet and enamel of 13.7 ‰ proposed for horses by Cerling and Harris (1999). This factor is based on uncontrolled animals and is accompanied by an uncertainty of 1.9. If this enrichment factor is shifted by 1 ‰ (i.e. $\delta^{13}C_{diet}$ difference between monitored horses and non-monitored horses), we estimated a mean grazing altitude of 2264 ± 376 m, ranging from 1926 to 2692 m (**Table 10**) similar to the average grazing altitude of monitored horses (**Table 5**). Consequently, the average value of occupation of pasture above 2000 m is at 59% with a range from 17 to 100 % (**Table 10**). An enrichment factor between diet and enamel of 14.7 ‰ for horses seems reasonable as it remains within the uncertainty proposed by Cerling and Harris (1999) but also corresponds to that of zebras (*Equus burchelli*) close relatives of domestic horses (Cerling and Harris, 1999; Tejada-Lara Julia V. et al., 2018).

5.6.3 Relationship between $\delta^{13}C$, $\delta^{18}O$ and altitudinal mobility

We found that the correlation between carbon and oxygen isotope values of caprine tooth enamel (Pearson'r) was negatively correlated with the standard deviation of the animal altitudinal residency (SD-Altitude – **Figure 21**). Reasonably this relation highlighted that carbon and oxygen isotope values were negatively correlated for animals which exploited a large altitudinal range of pastures (i.e. Jk and Kj animals), whereas carbon and oxygen isotope values were positively correlated for more residential animals (i.e. Dl). This result suggests that the anti-correlation between $\delta^{13}C$ and $\delta^{18}O$ sequences can indeed be interpreted as evidence for vertical mobility, as proposed by several authors (Fisher and Valentine, 2013; Makarewicz, 2017; Makarewicz et al., 2017; Tornero et al., 2018, 2016). It is noteworthy that this relationship was found in a C_3-dominated environment and might be slightly different in a mixed C_3/C_4 environment. Moreover, this anti-covariation was also found on horse tooth enamel (**Figure 16**) which, even if not monitored, reasonably performed an altitudinal mobility. This anti-covariation can be the result of two phenomena: (i) a complete reversal of the $\delta^{18}O$ cycle with low $\delta^{18}O$ during summer (Hermes et al., 2017), or (ii) higher $\delta^{13}C$ values during winter. In our case, the first scenario is unlikely because $\delta^{18}O$ values are closely linked to the season of death of animals (Lazzerini et al., 2020 - see Chapter 8), with higher $\delta^{18}O$ values measured at the basis of the tooth crown for animals slaughtered during the warm season. Therefore, the absence or presence of covariation between $\delta^{13}C$ and $\delta^{18}O$ profiles should be due to differences in seasonal variations of $\delta^{13}C$ values between residential and mobile animals. The lower summer $\delta^{13}C$ values could be explained by the higher water-availability of alpine meadows during summer due to increase precipitation and snow melting during this period, allowing access to rich pasture for herds. The increase in $\delta^{13}C$ values during winter cannot be explained by hydric stress, as the growing season is very short and restricted to the summer period (Eisma, 2012). Alternatively, it could be explained by a diet switch. Sheep and goats of desert-steppe in Mongolia have been observed to increase the proportion of shrub and forbs in their diet during summer (Chazin et al., 2019; Wingard et al., 2011). Shrubs and forbs are relatively ^{13}C-depleted relative to grass and thus an increase in proportion in the diet would lead to lower $\delta^{13}C$ values (An and Li, 2015; Smedley et al., 1991). Forbs, as *Caragana* sp., are found only in valley bottoms and lowland areas in our study area (**Supp. Info S5.7**). However, Jk, Kb, Kj and Zk's herds did not remain at high altitude during the whole summer. They exhibited important altitudinal mobility and often stood at low altitude during spring/early summer and late summer (**Supp. Info S5.4 & S5.7**). Therefore, a seasonal preference for forbs and shrubs in the summer

vs grass in the winter could well explain the summer minimum and winter maximum measured in enamel $\delta^{13}C$ values. Moreover, mobile animal spent more times in lowlands during winter and thus consumed ^{13}C-enriched grass, which grew during summer, compared to highland pastures, increasing the $\delta^{13}C$ values. Dl animals, with a permanent residency at high altitude, had probably less access to forbs which resulted in higher $\delta^{13}C$ values during winter compared to the other animals.

5.7 Conclusion

Our study demonstrates that $\delta^{13}C$ and $\delta^{18}O$ analyses of tooth enamel and $\delta^{13}C$ of tail hair can be used to make inferences regarding animal mobility and land use in mountainous regions. We showed that average $\delta^{13}C$ values of livestock recorded mean grazing altitude and could be used to calculate the amount of time spent in alpine meadows by livestock. Vertical mobility in modern livestock from western Mongolia may also be identified through sequential sampling of $\delta^{13}C$ and $\delta^{18}O$ of sheep tooth enamel. The comparison of $\delta^{13}C$ and $\delta^{18}O$ values was very informative to reveal variation in the altitudinal pattern of animals: individuals displaying a large range of altitudinal residency also showed a negative correlation between $\delta^{13}C$ and $\delta^{18}O$ sequences, whereas individuals with a more restricted mobility displayed a positive correlation between $\delta^{13}C$ and $\delta^{18}O$ values. This pattern seems to be controlled by environmental factors, such as changes of water availability/aridity with altitude, seasonal precipitation in summer and could also be influenced by ecological factors such as the seasonal and altitudinal dependence of the relative proportion of forbs versus grasses in the diet.

It is important to note, however, that mobility patterns can be quite complex and that methodological advancements (e.g. modelling, higher sampling resolution) will be needed to more fully picture this complexity. This is important to keep in mind when interpreting mobility patterns in archaeological specimens. We also stress that directly applying our results to identify altitudinal mobility of livestock in other climatic regions may not be straightforward and will require to establish similar modern reference datasets in order to determine isotopic markers of altitudinal mobility. Finally, further investigations are needed to decipher between the influence of foddering practices (Makarewicz and Pederzani, 2017) and vertical mobility.

ACKNOWLEDGEMENTS

We are deeply indebted to all the herders who kindly participated to the study and hosted two of us (CM and AZ) during the 2017 winter and 2018 summer fieldtrips. We would like to greatly thank Pr. B. Oyuntsetseg (National University of Mongolia, Ulaanbaatar) for her help with plant identification.

Stable isotope analyses on plants were performed at the 'Isotope Ecology' platform of the Laboratory of the Ecology of Natural and Anthropised Hydrosystems (UMR 5023 LEHNA, Lyon, France). The isotopic analyses on tooth enamel were performed at the SSMIM Paris under the technical supervision of D. Fiorillo. Fieldwork was supported by the French archaeological mission in Mongolia (CNRS, MNHN, MAEDI, director SL) and by the CNRS. This research was funded by a Ph.D. grant to NL from the French National Research Agency LabEx ANR-10-LABX-0003-BCDiv, in the context of the "Investissements d'avenir" n°ANR-11-IDEX-0004-02, and by an Inalco Early Career Research Grant 2017 to CM.

SUPPLEMENTARY INFORMATION OF CHAPTER 5

All supplementary information are available here:
https://drive.google.com/open?id=1msyEEsYWScfxkmsYNH5QegvesSEo1iL5

Supplementary Info S5.1: Gathers additional information on plants

Table S5.1a: General information on plant sampling sites with the measured carbon isotope composition ($\delta^{13}C$), the period of sampling and taxa present in the sample.

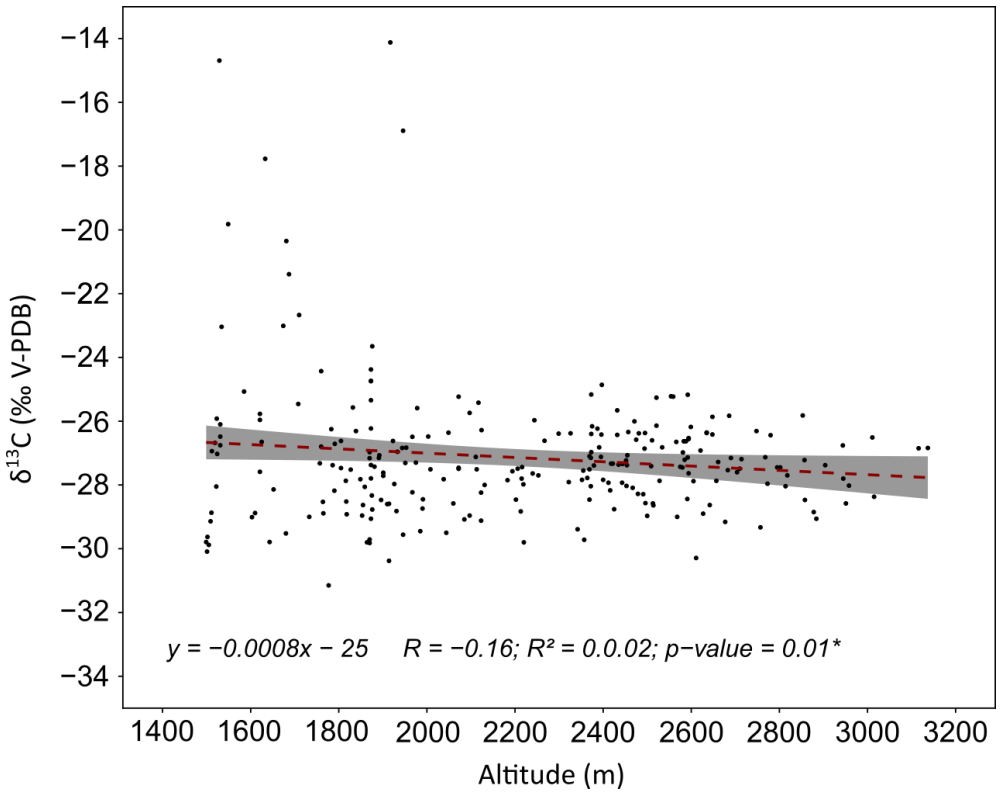

Figure 5.1a: $\delta^{13}C$ values of plant samples plotted against the altitude of the site with the corresponding linear regression (dashed red line) and the 95% confidence interval (grey shaded area). * = significance of the p-value

Supplementary Info S5.2: Age estimation of animals by tooth wear patterns -

Supplementary Info S5.3: Gathers supplementary information on geographical and calendar mobility of herds

Tables S5.3a: Summary of calendar mobility for each herder determined with the Lavielle's segmentation method.
Figures S5.3a: Localisation of camps for each herder. Maps realised with QGIS.

Supplementary Info S5.4: Statistical tests on altitudinal mobility

Tables S5.4a: Linear Mixed-Effects Models (LME) to test the influence of season on the altitude of pasture used by animals.
Tables S5.4b: One-way ANOVA with Tukey Post-hoc HSD to test the differences of altitude according to the season

Supplementary Info S5.5: Carbon and Oxygen isotopic results for each caprine and horse tooth

Supplementary Info S5.6: Plots of the Pearson's correlation between $\delta^{18}O$ and $\delta^{13}C$ values

Supplementary Info S5.7: Illustrations of the landscape and feeding behaviour of caprines

Typical lowland pasture, with few grasses and semi-arid conditions (photo taken by N. Lazzerini in September 2016).

Typical highland pasture, greener with more wet conditions (photo taken by A. Zazzo in June 2015).

Caprines grazing shrubs and forbs in the area of Moin, near Nogoonnur (photo taken by A. Zazzo in June 2015).

Exemple of steep slopes where sheep and goats can graze and not horses (photo taken by A. Zazzo in June 2015).

Chapitre 6 – Identifier une mobilité haute-fréquence via l'analyse du $^{87}Sr/^{86}Sr$ dans l'émail des dents de caprinés

Dans les deux chapitres précédents, nous avons abordé l'utilisation de la composition isotopique de l'oxygène, du carbone et de l'azote dans l'émail ou la kératine pour retracer la mobilité altitudinale des animaux domestiques. Ce chapitre propose l'étude du dernier système isotopique communément utilisé en archéologie pour inférer la mobilité des animaux, à savoir le $^{87}Sr/^{86}Sr$, généralement utilisé sous le prisme de l'origine de l'individu ('local' vs 'non-local'). Comme pour les autres systèmes isotopiques largement utilisés dans les études archéologiques, il y a un manque cruel d'études s'attachant à montrer l'applicabilité de cette méthode par l'analyse d'animaux dont l'origine et la mobilité sont connues.

L'objectif de cette étude est d'examiner l'utilisation du rapport $^{87}Sr/^{86}Sr$ selon différents niveaux d'analyses possibles. Tout d'abord montrer que les animaux enregistrent bien un signal isotopique local tout en portant une attention aux variations interindividuelles pour des animaux ayant la même mobilité. Ensuite, comparer les variations intra-dentaires de $^{87}Sr/^{86}Sr$ aux variations modélisées à partir d'une carte des distributions de $^{87}Sr/^{86}Sr$ dans l'espace géographique (isoscape) afin de tester si les variations de $^{87}Sr/^{86}Sr$ permettent de retracer le parcours de l'animal pendant la formation de la dent.

6.1 Résumé de l'étude

Les analyses isotopiques séquentielles en strontium de l'émail dentaire, ont été couramment utilisées en bioarchéologie pour étudier la mobilité et la provenance des animaux domestiques et sauvages. Bien souvent, les analyses se restreignent à la mise en évidence de la présence d'un individu 'non-local' ou ayant eu une incursion saisonnière dans une zone 'non-locale'. Plus rarement, les analyses essayent de déterminer plus précisément la zone d'origine et le parcours de l'animal en se basant sur des cartes de répartition spatiale des valeurs isotopiques en strontium biodisponible (isoscapes). Quelques rares études, sur des animaux sauvages parcourant de longues distances, ont montré que le $^{87}Sr/^{86}Sr$ avait le potentiel d'enregistrer leur mobilité (Britton et al., 2009; Glassburn et al., 2018). Cependant, la pertinence les analyses des rapports $^{87}Sr/^{86}Sr$ pour suivre une mobilité de petite échelle du bétail n'a pas encore été démontrée.

Pour évaluer la fiabilité de cette méthode, nous l'avons testée sur des caprinés domestiques actuels, vivant dans l'Altaï (Mongolie), dont la mobilité était connue grâce à leur suivi par balises GPS. Afin de limiter les biais (signal moyenné et amorti) dus à l'échantillonnage classique de l'émail par microfraisage, nous avons mesuré les variations intra-dentaires de $^{87}Sr/^{86}Sr$ par ablation laser pour pouvoir échantillonner la couche d'émail interne en partant de l'hypothèse qu'elle se minéralise plus rapidement et enregistre ainsi un signal isotopique moins atténué. En parallèle, nous avons créé un isoscape du strontium biodisponible de la région en collectant des plantes sur 156 sites d'échantillonnage et en développant un modèle géospatial d'interpolation spatiale des valeurs isotopiques échantillonnées. Les valeurs quotidiennes de $^{87}Sr/^{86}Sr$ biodisponibles ingérées par les animaux ont été extraites de l'isoscape grâce aux localisations enregistrées par les balises GPS. Ces données ont ensuite été converties en prédictions de profils intra-dent de $^{87}Sr/^{86}Sr$ à l'aide du modèle de conversion du signal isotopique alimentaire au signal isotopique du tissu de Passey et Cerling (2002) pour l'émail des dents, originellement développé pour le $\delta^{13}C$. Dans cette étude, nous faisons l'hypothèse que la cinétique d'incorporation du strontium est la même que pour le carbone dans les groupements PO_4 et CO_3 de l'hydroxyapatite. Enfin, nous avons comparé les profils modélisés aux profils mesurés.

Les moyennes de $^{87}Sr/^{86}Sr$ observées dans l'émail de tous les individus correspondent à celles établies par l'échantillonnage du strontium biodisponible. Le strontium biodisponible se caractérise par une grande variabilité et hétérogénéité facilitant la mise en évidence d'une mobilité grâce au $^{87}Sr/^{86}Sr$. Certaines dents d'un même troupeau enregistrent des valeurs moyennes et une variabilité similaire tandis que ce n'est pas le cas pour d'autres. Une raison peut être une variabilité du comportement alimentaire et de l'hétérogénéité à microéchelle du strontium biodisponible que l'isoscape n'a pas pu capter.

Les variations des profils de $^{87}Sr/^{86}Sr$ mesurés reflètent en général fidèlement les variations des profils modélisés à partir des schémas de mobilité connus des caprins, bien que pour certains individus les valeurs isotopiques absolues soient différentes des valeurs modélisées. Ceci confirme que le rapport isotopique du strontium peut être utilisé pour estimer une mobilité de fine-échelle. Ces bons résultats obtenus avec le modèle de Passey et Cerling (2002) suggèrent que le temps de résidence du Sr dans l'organisme est similaire à celui du C, contrairement à ce qui a été suggéré dans la littérature (Montgomery et al., 2010). Des études où l'alimentation est contrôlée, seront nécessaires pour confirmer cette hypothèse.

Article III: Inferring small-scale mobility of modern livestock (Altai, Mongolia) using strontium isotope ratios in tooth enamel via LA-MC-ICP-MS

Nicolas LAZZERINI, Vincent BALTER, Aurélie COULON, Théo TACCAIL, Michel LEMOINE, Charlotte MARCHINA, Noost BAYARKHUU, Sébastien LEPETZ, Antoine ZAZZO.

In preparation for submission in *PNAS*

Abstract:

Strontium isotopic analyses of sequentially formed tissues, such as tooth enamel, have been commonly used in bioarchaeology to study the provenance and mobility of domestic and wild animals. However, the ability of analyses of $^{87}Sr/^{86}Sr$ ratios to track small-scale mobility patterns of livestock has not yet been demonstrated. The reliability of the method was tested on modern livestock from Altai Mountains (Mongolia) whose mobility was known through GPS monitoring. First, we used *in situ* laser ablation to sample inner enamel layer in caprine teeth, a layer recording less attenuated isotopic signal, and measured intra-tooth $^{87}Sr/^{86}Sr$ profiles. Then, we created a bioavailable $^{87}Sr/^{86}Sr$ isoscape of the area by collecting plants at 156 sampling sites and developing a geospatial model of $^{87}Sr/^{86}Sr$ variations. Daily bioavailable $^{87}Sr/^{86}Sr$ ratios experienced by animals were extracted from the isoscape using GPS data in order to predict intra-tooth $^{87}Sr/^{86}Sr$ profiles using the tooth enamel forward model of Passey and Cerling (2002). These modelled profiles were compared to the measured intra-tooth profiles. Our results reveal that the measured $^{87}Sr/^{86}Sr$ profiles reliably reflected the known mobility patterns of caprines, except for a few individuals. Variability in diet behaviour and micro-scale heterogeneity of bioavailable strontium could be responsible for these discrepancies. Finally, the good results obtained with the forward model may suggest that, contrary to what was previously suggested, Sr residence time is similar to that of C. Controlled feeding experiments are however needed to firmly establish Sr residence time in the organism.

Keywords: pastoral mobility; GPS; mountain; sheep & goat; laser ablation; $^{87}Sr/^{86}Sr$; Mongolia

6.2 Introduction

The analysis of strontium isotope ratios ($^{87}Sr/^{86}Sr$) in tooth enamel is a common approach to studying provenance and mobility of domestic and wild mammals (Balasse et al., 2002; Bendrey et al., 2009; Bentley and Knipper, 2005; Britton et al., 2009; Copeland et al., 2016; Glassburn et al., 2018; Meiggs, 2007; Price et al., 2017; Slovak and Paytan, 2012). Indeed, $^{87}Sr/^{86}Sr$ values vary across the landscape depending on the age, chemical composition and weathering rates of the underlying geological substrate (Bentley, 2006; Koch et al., 2007). Generally, $^{87}Sr/^{86}Sr$ ratios in vegetation reflect geographical Sr variations of soil, dust and water because plants absorb Sr from these local sources through their root systems (Capo et al., 1998; Reynolds et al., 2012). Animals ingest bioavailable strontium through food and water, and incorporate it in tooth enamel without fractionation during their formation (Capo et al., 1998; Flockhart et al., 2015), substituting Sr for Ca^{2+}. $^{87}Sr/^{86}Sr$ ratios in dental enamel, hence reflect those of the environment through the dietary intake of the animal. As mammalian tooth enamel grows incrementally from the top to the base of the tooth crown and is not remodelled once fully mineralized, holding a record of individual biogeochemical history of the animal that can be documented by adopting a sequential sampling strategy along the direction of tooth growth.

The reconstruction of the geographical origin and mobility of individuals relies on the comparison between $^{87}Sr/^{86}Sr$ ratios of tooth enamel and that of the study area(s) (e.g. Bataille and Bowen, 2012; Bentley, 2006; Slovak and Paytan, 2012). Therefore, it requires (1) a precise knowledge of the distribution of bioavailable Sr across the study area (2) a good understanding of its record in the tissue of interest.

A crucial prerequisite is a clear understanding of the local bioavailable $^{87}Sr/^{86}Sr$ isotope range and its variability. To this end, isoscapes, which are predictive models of isotope variations across a landscape, have been generated using either geostatistical approaches (Bowen and Wilkinson, 2002; Copeland et al., 2016; Frei and Frei, 2011), multi-source mixing models (Bataille et al., 2012; Bataille and Bowen, 2012), machine learning (Bataille et al., 2018) or with discrete entities (Evans et al., 2009; Kootker et al., 2016; Snoeck et al., 2019). Most isoscapes have been based on direct bedrock lithology, sometimes complemented by a few environmental samples (Britton et al., 2011; Chase et al., 2018; Chazin et al., 2019; Evans et al., 2019; Gigleux et al., 2019; Makarewicz et al., 2018; Marciniak et al., 2017; Meiggs, 2007; Widga et al., 2010). They have been used successfully to provide large scale bioavailable baselines (Bataille et al., 2014; Bataille and Bowen, 2012) but have limitations. Indeed, the

$^{87}Sr/^{86}Sr$ ratio of the bioavailable strontium does not directly reflect the Sr isotopic composition of the geological substrate and significant shifts of the bioavailable strontium from the expected values can be observed and vary between different areas (Willmes et al., 2018). Different processes may cause these shifts such as preferential weathering of certain minerals, with different Sr ratios, thus lithological complex units (e.g., gravels, granites) are expected to show higher differences between bedrock and plants. Moreover, influence of atmospheric deposition (i.e. dust, precipitation, sea spray) or anthropogenic influences such as fertilizer or air pollution may also cause these shifts (Bentley, 2006; Crowley et al., 2017; Frei and Frei, 2011; Jin et al., 2011; Maurer et al., 2012; Slovak and Paytan, 2012; Widga et al., 2017). To assess regional variability, a variety of proxies can be used to constrain the baseline of bioavailable $^{87}Sr/^{86}Sr$. This includes surface/ground waters, plants, soil leachates, and faunal remains with a choice largely depending on the nature of the studied material and on the availability of samples (Bataille and Bowen, 2012; Bentley, 2006; Copeland et al., 2016; Maurer et al., 2012; Willmes et al., 2018). Measuring $^{87}Sr/^{86}Sr$ ratio in plants has been demonstrated to be a reliable method for determining local bioavailable $^{87}Sr/^{86}Sr$ (Copeland et al., 2016; Evans et al., 2009; Maurer et al., 2012; Willmes et al., 2018). Intensive field surveys are rarely conducted to create detailed Sr baseline dataset based on dense plant sampling even if baseline models are continuously being refined and improved (e.g. Bataille et al., 2018, 2014; Willmes et al., 2018).

Time-series profiles of $^{87}Sr/^{86}Sr$ ratios of ungulate tooth enamel, through sequential sampling by drilling, have been commonly used to investigate the geographical origin and seasonal mobility of domestic ungulates: the comparison of variations of $^{87}Sr/^{86}Sr$ ratios with geographical variations of $^{87}Sr/^{86}Sr$ ratios of the study area allows estimating the location of the individuals at different moments of its life (Balasse et al., 2002; Bendrey et al., 2009; Chase et al., 2018; Makarewicz et al., 2018; Meiggs et al., 2017; Towers et al., 2010) or wild ungulates (Britton et al., 2011; Copeland et al., 2016; Gigleux et al., 2019; Price et al., 2017; Widga et al., 2010). Although these studies have offered insights into important archaeological questions, the kinetics of incorporation of Sr isotopic ratio from the environment into tooth enamel during its mineralisation is still not well understood (Montgomery et al., 2010), hence limiting the precision of the estimates. This could be improved by controlled feeding experiments (Ambrose, 2002; Ayliffe et al., 2004; Podlesak et al., 2008), but it has rarely been performed on heavy elements like Sr (Anders et al., 2019; Lewis et al., 2017). Moreover, intra-tooth samples are collected by drilling enamel perpendicular to the growth axis and extending through the enamel thickness leading to time-averaging (~3-4 months in sheep and goats) and

dampening of the intra-tooth isotopic signal relative to primary isotopic variations of the environments experienced by the animal (Balasse, 2002; Blumenthal et al., 2014; Green et al., 2018b, 2018b; Passey et al., 2005; Passey and Cerling, 2002; Podlesak et al., 2008; Zazzo et al., 2012, 2010). This classic method may not be suitable to track rapid changes of pasture. Another approach have been proposed to minimize these biases by targeting the innermost enamel layer (<20 μm of thickness), at the enamel-dentine junction, where the enamel mineralizes the fastest, maturation has the least effect and intra-tooth isotopic signals are significantly less dampened (Blumenthal et al., 2019, 2014; Müller et al., 2019; Suga, 1982; Tafforeau et al., 2007; Trayler and Kohn, 2017). However, this is rarely applied because only secondary ion mass spectrometry (SIMS) could target this thin layer (Blumenthal et al., 2014) an expensive method with several constraints (i.e. small specimen size; low instrumentation availability; complicated specimen preparation). To a lesser degree, the inner enamel layer is also suitable because of its larger initial mineral content, compare to middle and outer enamel layers, and it is more easily targetable and appears to record less dampened primary isotopic environmental signal (Blumenthal et al., 2014).

It is hence needed to assess the reliability of time series profiles of $^{87}Sr/^{86}Sr$ ratios in tooth enamel combined with isoscapes of bioavaialable strontium. One possibility is to work on modern livestock with a known mobility. Rare studies with modern wild migratory animals whose breeding and wintering locations were known have shown that strontium can be a reliable proxy for detecting seasonal migration of wild herds, and that $^{87}Sr/^{86}Sr$ values from teeth match those expected in the seasonal habitat areas (Britton et al., 2009; Glassburn et al., 2018). But whereas the isotope results suggested different life histories for the herd members, information about geographical positioning at the individual level was unavailable in these studies (Britton et al., 2009; Glassburn et al., 2018).

The aim of our study was to infer the ability of Sr isotopes to detect short-term animal mobility, comparing the inferences made by high-resolution sequential $^{87}Sr/^{86}Sr$ isotope profiles and an empirically grounded strontium isoscape with the real mobility as revealed by GPS monitoring. Our study system was domestic caprines living in the Altai Mountains of Western Mongolia. We (i) used plant Sr samples to model an isoscape of the bioavailable Sr in the study area; (ii) targeted the inner enamel layer using laser ablation (LA), a microsampling method able to sampled continuous and discrete enamel zones (Blumenthal et al., 2019; Le Roux et al., 2014); (iii) compared Sr intra-tooth variations in teeth that grew while the animal was monitored by GPS tracking with predicted Sr variations at the individual location, calculated using a model

describing enamel mineralization applied on Sr isoscape values (Passey and Cerling, 2002); (iv) examined the extent of intra- and inter-individual variability between caprines from same herd in a mountainous area.

6.3 Materials

6.3.1 Climate and environment

The study area is located in the province of Bayan-Ölgii (district of Nogoonnuur) on the eastern fringes of the Altai mountain range, in its Mongolian part (**Figure 22**). Elevations range from 1500 to more than 4000 m asl. A north-south fault splits the landscapes in half with a lowland plain to the east and the Altai mountains to the west. The climate is strongly continental with long, cold winters and short, hot summers. Following Mohammat et al. (2013) and Piao et al. (2006), seasons in the area are defined as follows: winter (November-March), spring (April-May), summer (June-August) and fall (September-October). Monthly temperatures average -12.2°C during winter and +18.1°C during summer with extremes ranging from +34°C to -44°C. Temperatures vary greatly throughout the year, but also during the same day. Average annual rainfall is 131 mm with a maximum of precipitation occurring during summer (all data available at http://fr.climate.org – meteorological station based at Nogoonnuur village). Snow precipitation in winter occurs essentially at high altitude and not in lowland. The vegetation consists of semi-arid and alpine steppes, mainly composed of grass, with rare forbs and bushes near rivers in lowland and valleys. C3 plants such as Poaceae, Asteraceae and Fabaceae dominate the vegetation.

6.3.2 Caprine GPS tracking and tooth specimens

Nine caprines (four sheep and five goats) participated in the survey. The animals belonged to five different families of Kazakh-Mongolian nomadic pastoralists (named Dl, Jk, Kb, Kj and Zk). These herders had different mobility patterns in terms of altitude, distance travelled, surface area used and frequency of camp changes. This made it possible to assess the variation between individuals from different herds grazing in the same geographical area but also to assess the expected level of variation between individuals from the same herd. Caprine mobility was controlled by the herders and animals were brought back to the camp every night. Nomadisation patterns were monitored precisely thanks to GPS devices fitted on the animals. Monitoring started between June 2015 and November 2017, and was performed with Globalstar© (N=7) or Iridium© (N=1) collars (Lotek Wireless Inc. - http://www.lotek.com/)

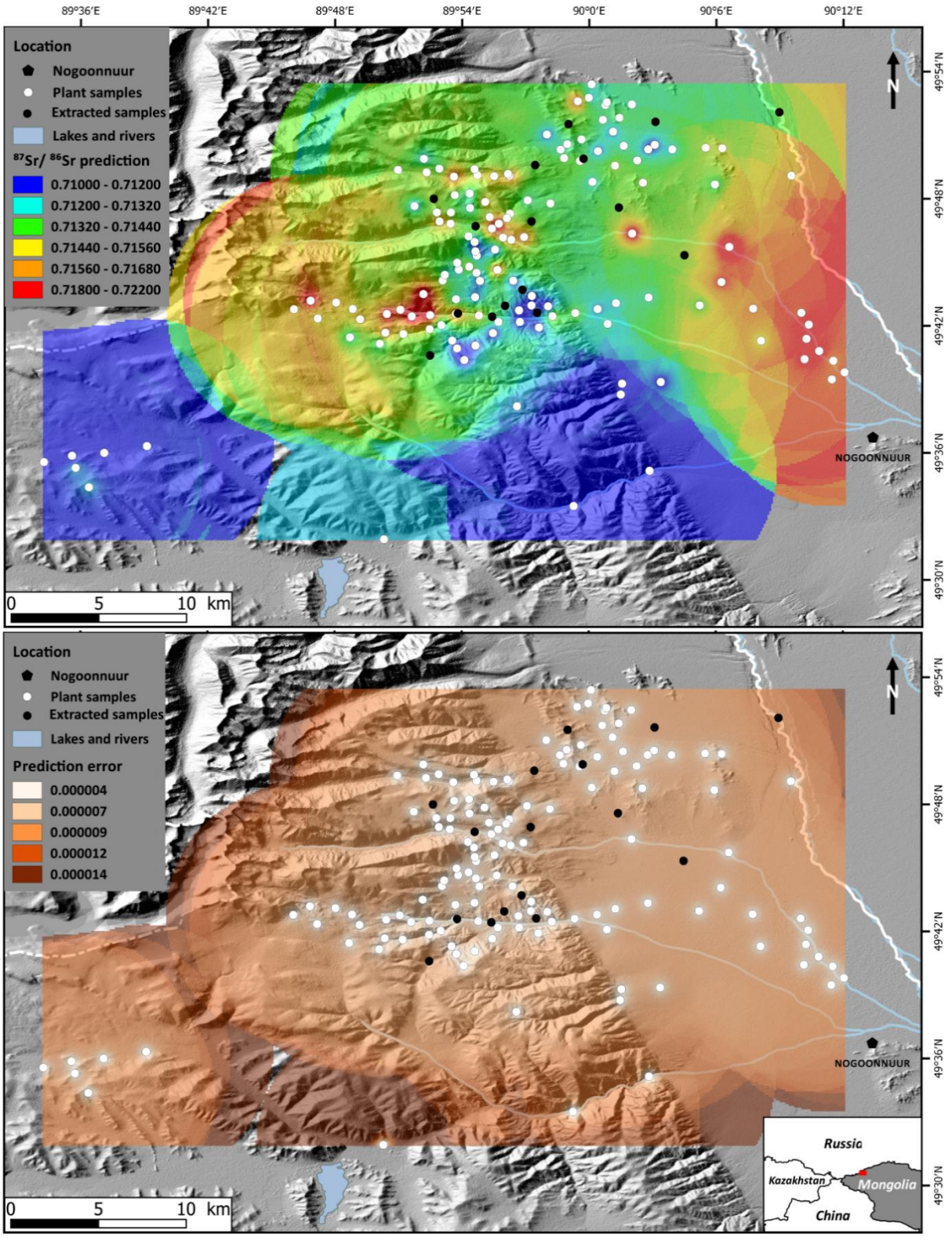

Figure 22: Bioavailable $^{87}Sr/^{86}Sr$ isoscape (top panel) and its associated predicted error (bottom panel) of the study area near the village of Nogoonnur, Western Mongolia. White circles represent bioavailable $^{87}Sr/^{86}Sr$ sampling localities used to create the model. Black dots represent the 16 randomly selected sampling locations that were extracted prior to model development and used later to test the model predictions. Colors indicate areas of lowest bioavailable $^{87}Sr/^{86}Sr$ (blue) to highest bioavailable $^{87}Sr/^{86}Sr$ (red) for the top panel and lowest predictive error (light beige) to highest predictive error (brown).

programmed to record animal position every 13 and 2 hours respectively, as well as altitude and temperature (**Table 11**). Even if one animal can represent an entire herd (Moritz et al., 2012), several animals were equipped in each herd to prevent technical failures or loss of GPS collars. Only males were sampled because females may be supplemented with fodder during winter (usually harvested in August-September), potentially overprinting the influence of mobility in enamel $^{87}Sr/^{86}Sr$ ratios.

Study animals were slaughtered on two different occasions: September 2016 (n = 4) and November 2017 (n = 4) and twelve molars were sampled for analysis (**Table 11**). Animals were in their second or third year at the time of death. In order to secure contemporaneity between GPS records and tooth enamel growth, only third molars (M3) were sampled on animals slaughtered in September 2016. For animals slaughtered in November 2017, both second (M2) and third molars were sampled. For M2 molars, we assumed that the individual mobility during the period corresponding to the growth, not monitored by GPS, was the same of the GPS-mobility of other animals of the same herd (those monitored from 2015 to 2016).

Table 11: Information about animals equipped with GPS collars (Gb = Globalstar; Ir = Iridium) and teeth sampled for $^{87}Sr/^{86}Sr$ ratios analysis. DOD = date of death. [1]Age estimated after Payne (1973) and Jones (2006). † GPS out of service before the death of the animal, we used GPS data from another collar in the same herdto complete location data until 04/11/2017.

Sample	DOD	Year of birth	Approximate age at death(months)[1]	Species	Sex	Tooth sampled	GPS type	Start GPS	End GPS	Herder
Alt16-104	05/09/2016	2014	30	*Ovis aries*	M	M_3 left	Gb	19/06/2015	07/09/2016	Jk
Alt16-283	13/09/2016	2014	30	*Ovis aries*	M	M_3 left	Gb	16/06/2015	12/09/2016	Kb
Alt16-306	14/09/2016	2014	30	*Ovis aries*	M	M_3 left	Ir	19/06/2015	14/09/2016	Kj
Alt16-369	21/09/2016	2014	30	*Capra hircus*	M	M_3 left	Gb	19/06/2015	20/09/2016	Kj
2017-71	17/11/2017	2015	32	*Capra hircus*	M	M_2 & M_3 left	Gb	16/09/2016	17/11/2017	Dl
2017-98	20/11/2017	2015	32	*Capra hircus*	M	M_2 & M_3 left	Gb	18/09/2016	09/11/2017	Kb
2017-124	24/11/2017	2015	32	*Ovis aries*	M	M_2 & M_3 left	Gb	21/09/2016	09/11/2017	Kj
2017-146	23/11/2017	2015	32	*Capra hircus*	M	M_2 & M_3 left	Gb	05/09/2016	03/05/2017 †	Jk

6.3.3 Plant sampling to model bioavailable strontium isoscape

In order to build the isoscape of the bioavailable Sr we sampled plants at 156 sites distributed throughout the study area in September 2016 and November 2017 (**Figure 22; Supp. Info Table S6.1**). Sampling localities were selected to cover as much as possible the grazing areas of the animals based on their GPS records, complemented by sites located between grazing areas (**Supp. Info Figure S6.1**). The average distance between neighbouring sites was 2.5 km, and ranged between 0.2 km and 17.2 km. However, some parts of the study area were difficult to reach due to escarpment, proximity to the Russian border to the north. Each sample represented a mix of plant species present within a circle of ca. 2-3 m in diameter.

The assemblage was usually dominated by grasses, but also included some forbs and shrubs (see **Supp. Info Table S6.1**). In most cases, most collected plant items were plant leaves, but stems, seeds and fruits were also collected if present. All plant material was dried then placed in a loosely sealed envelope.

6.4 Methods

6.4.1 GPS-based inference of mobility

GPS data were cleaned by removing GPS fixes for which the location was obviously erroneous. Herder mobility patterns were detected using the Lavielle's method (Lavielle, 2005, 1999) implemented in the R package adehabitatHR (Calenge, 2006). This method allows the segmentation of location time series by discriminating series of successive locations ("segments") during which movements happen at the same spatial scale but between which movements happen at different spatial scales. In our case, this allowed discriminating between small-scale (within each pasture) and large-scale movements (between successive pastures). Due to the nature of the landscape and after different trials (where segmentation was based on x or y coordinates), segmentation was based on altitude and each inferred segment was considered as a pasture, after visual validation. Because caprines are brought back to the camp overnight, camps were easily identified thanks to a high concentration of GPS points.

6.4.2 Plant $^{87}Sr/^{86}Sr$ ratio analysis: dissolution method ICP-MS

Before Sr extraction, plant sample material was crushed using a mixer mill and then placed in a porcelain crucible with a lid. Plant samples were then reduced to ashes in a muffle furnace with temperatures ramped to level off at 300 °C and then increased to 850 °C in 2 hours and held at that temperature for 10h.

Strontium isotope analyses were performed at the *Ecole Normale Supérieure* in Lyon (ENSL). For each ashed plant sample, 5 mg were digested in 1 ml of 15N HNO_3 and 1 ml of 30% H2O2 in a closed Teflon beaker placed during 8 hours on a hotplate set at 120 °C. Then beakers were opened and samples were re-dissolved with 500 µL of 3N HNO_3 during 1 hour after evaporation. The Sr content of the sample was separated using a column filled with a volume of Sr-specific resin (Sr-Spec Eichrom®). Following several washes with MilliQ® water and the conditioning of the resin with 2N HNO_3, samples were loaded into the columns and washed repeatedly with 2N HNO3. Finally, Sr was eluted with MilliQ® water. The whole procedure of Sr extraction was conducted in a clean lab with a Sr blank typically lower than

0.002 ppb. The separated Sr fraction for each plant sample was dried down under fume hood at 120°C during one night, dissolved in 1 mL of 0.05N HNO3 and diluted to 200 ppb Sr concentrations for isotope analysis using a Nu instruments NuPlasma 1700 HR MC-ICP-MS (Nu Instruments Ltd.). Analyses were referenced to bracketing analyses of NIST SRM 987, using a $^{87}Sr/^{86}Sr$ reference value of 0.71026 ± 0.00009 (2 standard deviation -2SD) (Lugli et al., 2017) to ensure instrument calibration. Repeated analyses of the NIST SRM 987 yielded a $^{87}Sr/^{86}Sr$ ratio of 0.71024 ± 0.00005 (2SD). All strontium isotope data were corrected for isobaric ^{87}Rb interference using the measured signal for ^{85}Rb and the natural $^{85}Rb/^{87}Rb$ ratio. The measured isotope ratios were normalized for mass fractionation using the naturally invariant value for $^{88}Sr/^{86}Sr$ of 8.37521 (Lugli et al., 2017) and the exponential fractionation law.

We calculated the Pearson's correlation coefficient between geographic variables (i.e. altitude, longitude, latitude) and $^{87}Sr/^{86}Sr$ values of plant samples. All statistical analyses were conducted using R (version 3.4.4) with a threshold of significance at *p-value* < 0.05.

6.4.3 Geospatial modelling of the strontium isoscape

A kriging method was used to create the strontium isoscape. Kriging is a geostatistical interpolation method based on a variogram, a statistical model of spatial autocorrelation between pairs of sampled points (here, the 156 plant $^{87}Sr/^{86}Sr$ ratios) (Saby et al., 2006). The variogram model was used to interpolate (predict) the value of the modelled variable ($^{87}Sr/^{86}Sr$ ratio) in between sample sites. We used ordinary kriging to estimate patterns of $^{87}Sr/^{86}Sr$ variation.

The Sr isoscape was built using 90 % (N = 140) of the original sample, the remaining 10 % (N = 16) being saved to test model predictions (see below). First, the variogram model was fitted with the functions *variogram* (cutoff = 0.1) and *fit.variogram* implemented in the R package gstat (Pebesma, 2004). The predictive model of bioavailable $^{87}Sr/^{86}Sr$ across our study area was then built with the kriging function in ArcGIS 10.0 (ESRI), using the parameters of the variogram model (cell size = 1.4 10^{-3} °; see **Supp. Info Table S6.2a**). The isoscape reliability was tested by calculating the difference between the field values of the validation dataset and the values predicted in the isoscape.

6.4.4 Enamel $^{87}Sr/^{86}Sr$ ratio analysis: laser ablation method ICP-MS

Caprine teeth were washed in distilled water mounted in polyester resin (GBS - BROT LAB) to expose the whole dental structure, sliced longitudinally with a diamond disc, and polished (Abrading with silicon carbide powder 13 and 5 µ – F500 and F1000 Escil®).

$^{87}Sr/^{86}Sr$ was measured *in situ* by a laser-ablation multi-collector inductively coupled plasma mass spectrometer (LA-MC-ICP-MS). Sr data were acquired with Nu 500 HR MC-ICP-MS (Nu Instruments Ltd.), coupled to a 193 nm laser ablation system - Photon Machines Excite®) at the *Ecole Normale Supérieure* in Lyon (ENSL). The inner enamel layer was ablated using 85 µm diameter ablation spots, a laser scan speed of 60 $\mu m.s^{-1}$, 100% laser intensity and 10-Hz frequency (**Supp Info Table S6.3** summarizes the operating parameter used for the LA-MC-ICP-MS measurements). LA profiles were realized mainly on the buccal side of the tooth but some were done on the lingual side.

Teeth were analysed in two or three consecutive runs depending on tooth total length. For each laser ablation sequence, calibration of the LA-MC-ICP-MS was achieved by analyzing NIST SRM 1400 (bone ash). Sample aerosol was carried to the ICP-MS using a mixture of He and N_2. Masses 88, 87, 86, 85, 84 and 83 were measured on Faraday cups. The isobaric interference of ^{87}Rb was corrected using the ^{85}Rb. Krypton interferences at masses 84 and 86 were corrected using ^{83}Kr. Measurements of NIST SRM 1400 gave an average $^{87}Sr/^{86}Sr$ value of 0.71384 ± 0.000214, in good agreement with the published values for this material (Weber et al., 2018). A single correction was applied for each tooth based on the average NIST SRM 1400 values measured between the different transects. Finally, a centered moving average on 35 individual measurements (~2 mm length) was used to smooth variability of the final profiles.

6.4.5 Intra-tooth modelling of $^{87}Sr/^{86}Sr$ ratios based on bioavailable signal

The isoscape was used to calculate for each herd its predicted daily bioavailable $^{87}Sr/^{86}Sr$ values, based on the GPS locations of one of its monitored animals. Indeed, as expected the GPS locations of the different animals belonging to the same herd were very close (< 80 meters, data not shown), so for simplicity we selected one GPS collar in each herd to predict intra-tooth Sr variations based on animal locations). To do this, we extracted, for each GPS data covered by the isoscape, the $^{87}Sr/^{86}Sr$ values from the raster using the function *extract* (method = "simple") of the package raster (Hijmans, 2018). For the animals equipped with a Globalstar© collar, we kept all the GPS datapoints (including the night data) due to the lower recording

density. We then estimated daily predicted bioavailable $^{87}Sr/^{86}Sr$ values for each animal during the entire survey period, as the average of the different bioavailable $^{87}Sr/^{86}Sr$ values predicted within the same day.

The predicted daily bioavailable $^{87}Sr/^{86}Sr$ values were then used to model intra-tooth $^{87}Sr/^{86}Sr$ values and compare them with the actual intra-tooth $^{87}Sr/^{86}Sr$ values measured by LA-MC-ICP-MS. Modelled intra-tooth $^{87}Sr/^{86}Sr$ values were calculated using the forward model of Passey and Cerling (2002). Originally, this forward model was developed for continuously-growing teeth but it has also been used to describe time averaging in teeth with definite growth, such as ungulate teeth (Blumenthal et al., 2014; Trayler and Kohn, 2017; Zazzo et al., 2012, 2010, 2005). This model was initially designed for $\delta^{18}O$ and $\delta^{13}C$ (Blumenthal et al., 2014; Passey and Cerling, 2002; Trayler and Kohn, 2017; Zazzo et al., 2012, 2010, 2005). In this study, we assumed that the kinetics of Sr incorporation is the same as for O and C in PO_4 and CO_3 groups of hydroxyapatite. The main model parameters include the initial mineral content during enamel deposition (f_i), the length of maturation (l_m) (corresponding to the length along the tooth over which maturation stage of the amelogenesis occurs). The model for signal attenuation during enamel formation can be expressed as follows:

$$\delta_{ei} = (f_i * \delta_{mi}) + (1 - f_i) * \frac{\sum_{n=i+1}^{i+1+l_m} \delta_{m_n}}{l_m} \quad \text{(Eq. 8)}$$

Eq. (8) implies that the isotope value of fully mineralized enamel at position i (δ_{ei}) reflects a contribution from the appositional layer (with δ_{mi} the initial isotope value; in our case, the environmental $^{87}Sr/^{86}Sr$ value) and a time-integrated contribution of average isotope values of the input signal over the length l_m.

We fixed a length of maturation of 4 months (~ 120 days) as proposed by Zazzo et al. (2010) and we set f_i to 0.25, based on previous estimates of the mineral content of developing tooth enamel (Blumenthal et al., 2014; Passey and Cerling, 2002). We kept l_m constant for any stage of the crown, hence assuming a constant growth rate for tooth enamel.

6.4.6 Time calibration of measured intra-tooth $^{87}Sr/^{86}Sr$ profiles

To be able to compare predicted $^{87}Sr/^{86}Sr$ values of tooth to measured intra-tooth $^{87}Sr/^{86}Sr$ profiles, it was necessary to associate the position in the tooth with calendrical approximation. To do this, it is necessary to know the date of birth of the animal, as well as the

dental development rate and the growth rate of its molars. However, none of these parameters are known with certainty.

First, we based our time calibration on three assumptions. (i) A common birth date for all individuals was determined based on interviews with herders. The birth period of caprines is strongly controlled for by the herders and an arbitrarly birth date of March 31st for all individuals, corresponding to the peak of the birth season, was chosen. (ii) Then, we calculated an average caprine dental development rate for M2 (1.3-10.3 month) and M3 (13-26 months) based on the literature (Milhaud and Nezit, 1991; Upex and Dobney, 2012; Weinreb and Sharav, 1964; Zazzo et al., 2010) (**Supp. Info Table S6.4a**). (iii) Finally, we calculated a constant growth rate by dividing the tooth length by the duration of tooth formation.

In a second time, for a possible improvement of the procedure, we have varied the three parameters of the first time-calibration by trial/error. (i) It would be reasonable to allow some variation for birth dates. Indeed, even if herders try to control the births of their livestock as much as possible, births would rather be spread out over a longer period, from February to April, mostly, with a peak at the end of March. (ii) Moreover, tooth crown development is variable between breeds and between individuals. In caprines, tooth crown development starts at ~0-2 months old and ends at 12 months old (Milhaud and Nezit, 1991; Upex and Dobney, 2012; Zazzo et al., 2010) or 16 months old for M_2 (Weinreb and Sharav, 1964). For M_3s, there is a more variable dental development timing according to individuals and breed, with the formation beginning around 10-12 months old and completing between 20 and 30 months old (Milhaud and Nezit, 1991; Upex and Dobney, 2012; Weinreb and Sharav, 1964; Zazzo et al., 2010) We tested, by trial/error different dental development rates within limits proposed in the literature. (**Supp. Info Table S6.4a**). (iii) Finally, time calibration can be improved by taking into account the fact that M3 tooth grow rate may decrease exponentially (Zazzo et al., 2012), i.e. that each sample does not represent the same amount of time (i.e. 6-7 days in the upper crown and nearly a month in the lower crown). According to this model, it is possible to convert measured distances along the tooth into time (t_d) for any point at a distance *d* from the enamel-root junction using the following equation:

$$t_d = t_0 + {}^{1}/_{\lambda} \ln(\frac{L_{max}}{d}) \quad \text{(Eq. 9)}$$

Where λ is the rate constant of the growth (λ = ln(2) / $t_{1/2}$), $t_{1/2}$ is the time taken for the tooth to grow to half of its maximum length (L_{max}) and t_0 is the time at which the tooth begins to grow. Thus, t0 depends on the birth date and the start of formation of the M3. We set $t_{1/2}$ to

141 days (Zazzo et al., 2012). Given the model characteristics, the last 2-3 millimetres give dates tending well beyond the date of the individual's death. We hence omitted those dates.

The last step consisted in testing the correlation between the measured and modelled $^{87}Sr/^{86}Sr$ time series in order to estimate the reliability of measured data. We compared variations of both $^{87}Sr/^{86}Sr$ time series by calculating the first derivatives of each time series to estimate the slope of the variation. Then the first derivative was smoothed on 30 days. Finally, each first derivatives of measured and modelled $^{87}Sr/^{86}Sr$ time series were compared using Pearson's correlation coefficient between their first derivatives. A positive correlation coefficient is expected if measured intra-tooth $^{87}Sr/^{86}Sr$ variations are similar to modelled intra-tooth $^{87}Sr/^{86}Sr$ variations signifying that tooth enamel recorded bioavailable $^{87}Sr/^{86}Sr$ values ingested by the animal. Unless mentioned otherwise, all statistical analyses were conducted using R (version 3.4.4) with a threshold of significance at *p-value* < 0.05.

6.5 Results

6.5.1 Mobility patterns of caprines inferred by GPS monitoring

Lavielle's segmentation of GPS data indicates that caprines of the five different herders had different mobility patterns (**Table 12; Figure 23**). All animals but one (the one of Dl – 2017-71) displayed more or less an East-West mobility (**Figures S6.5 and Table S6.5**), and exploited both the eastern depression (1451 – 1684 m asl) and the western mountain pastures (2540 - 3102m asl). On the contrary, animals of Dl remained at a high altitude of 2364 ± 130 m asl (**Table 12**) during the study period and had a very limited mobility per year (30 km) compared to the mean distance travelled by the other herders (161 ± 98 km). As expected the GPS locations of the different animals belonging to the same herd were very close (c.a. < 80 meters, data not shown) indicating that individuals from a same pasture exploitation, thus allowing to compare $^{87}Sr/^{86}Sr$ ratios of tooth of non-monitored animal (e.g. 2017-146-M2) with $^{87}Sr/^{86}Sr$ ratios of tooth of monitored animal (e.g. Alt16-104-M3).

6.5.2 Bioavailable $^{87}Sr/^{86}Sr$ and geospatial modelling of strontium isoscape

Strontium isotope ratios of plants from the 156 sampling sites of the study area ranged between 0.71007 and 0.72340. The average $^{87}Sr/^{86}Sr$ ratio of the study area was 0.71456 ± 0.0054 (2SD). There was no relationship between bioavailable $^{87}Sr/^{86}Sr$ and geographic variables (i.e. latitude, longitude and altitude – **Figure S6.1**).

The semivariogram for the kriging revealed that the $^{87}Sr/^{86}Sr$ values were isotropic. There was a small mean error ($-2.5E^{-05}$) between predicted and measured $^{87}Sr/^{86}Sr$ values, indicating unbiased prediction errors. The root mean-square error was also low (0.0005) and not different from the standard error of the estimate (0.0005), indicating a robust assessment of variability in the model predictions. This was confirmed by the small absolute difference between the $^{87}Sr/^{86}Sr$ values of the subset of plant samples (N = 16) removed from the original dataset to build the isoscape and model predictions at their locations (mean = 0.00022, range = -0.0022 to 0.0031). All model parameters and detailed characteristics and results are provided in **Supp. Info S6.2**.

The $^{87}Sr/^{86}Sr$ values predicted by the strontium isoscape ranged from 0.71007 to 0.72251, with a mean value of 0.71417 (2SD = ± 0.004) (**Figures 22 & 24**). There was a spatial heterogeneity in $^{87}Sr/^{86}Sr$ values. The southern part of the study area was dominated by low $^{87}Sr/^{86}Sr$ values, while the highest $^{87}Sr/^{86}Sr$ values were found in the eastern and western parts of the study area.

Table 12: Characteristics of the GPS data from caprines equipped with GPS collars belonging to the five herders with GPS-based mobility for each herder. N = number. SD = standard deviation. One-way ANOVA with Tukey's post-hoc HSD was used to compare the means of altitude between herds. *** = the average altitude of the herds is significantly different from that of all other herds. Detailed mobility patterns with camps are provided in Figures S6.6 (supplementary data).

Herder id		Dl	Jk	Kb	Kj
Start GPS		16/09/2016	19/06/2015	16/06/2015	19/06/2015
End GPS		17/11/2017	04/11/2017	09/11/2017	09/11/2017
N days		427	869	877	874
N GPS data		1239	1599	1608	1606
Altitude (m.asl)	mean ± SD	2364 ± 130***	1980 ± 420***	2127 ± 339***	2076 ± 338***
	max	3002	3005	2946	3102
	min	1990	1451	1453	1684
N camps		5	8	10	11
N nomadisation		9	31	21	23
N nomadisation/year		7.7	13.0	8.7	9.6
Distance travelled (km)		35	513	327	318
Distance travelled/year (km)		30	216	136	133
N days on pasture	mean ± SD	50 ± 27	28 ± 17	40 ± 44	39 ± 33
	max	90	59	178	175
	min	18	4	9	20

P < 0.1 = .
P < 0.05 = *
P < 0.01 = **
P < 0.001 = ***

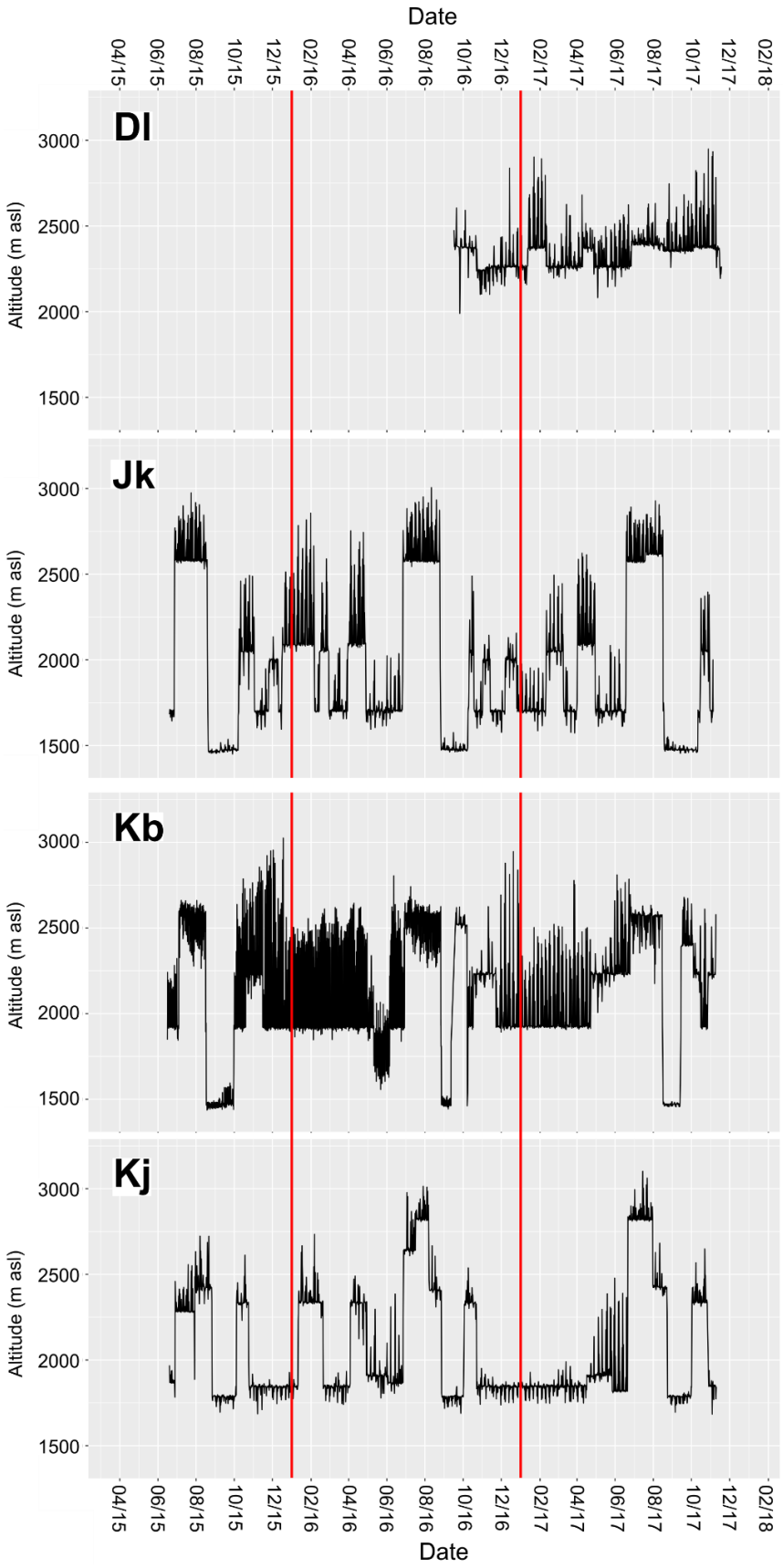

Figure 23: Temporal altitudinal variation of GPS monitored caprines. Each panel represents a different herder (Dl to Kj). Dl shows a lower variability of altitudinal mobility than the other herders Vertical red lines represent the change of year (2015/2016/2017).

6.5.3 Strontium isotope variations in tooth enamel

The results of the $^{87}Sr/^{86}Sr$ analysis of caprine enamel are reported in **Table S6.6**. On average, the enamel $^{87}Sr/^{86}Sr$ value was 0.71414 ± 0.00210 (2SD) (**Table 13**), falling within the range of bioavailable strontium predicted by the isoscape (**Figure 24**). The average $^{87}Sr/^{86}Sr$ ratio, however, differed between individuals, and ranged from 0.71200 ± 0.00087 (2SD; 2017-98-M3) to 0.71602 ± 0.0099 (2SD; Alt16-369-M3). There were significant differences in $^{87}Sr/^{86}Sr$ means and median (Kruskal Wallis, $p < 2.2e^{-16}$) and in variance (Bartlett, $p < 2.2e^{-16}$) between herds. On average the Kb's animal teeth (n =3) had the lowest mean values, at 0.71344 ± 0.00311(2SD), with the individual 2017-98 (M2 and M3) showing the lowest mean individual values, at 0.71261 ± 0.00172(2SD). On average the Kj's animal teeth (n =4) had the highest mean values, at 0.71465 ± 0.00226 (2SD), with Alt16-269-M3 showing the highest mean individual values, at 0.71602 ± 0.001988 (2SD).

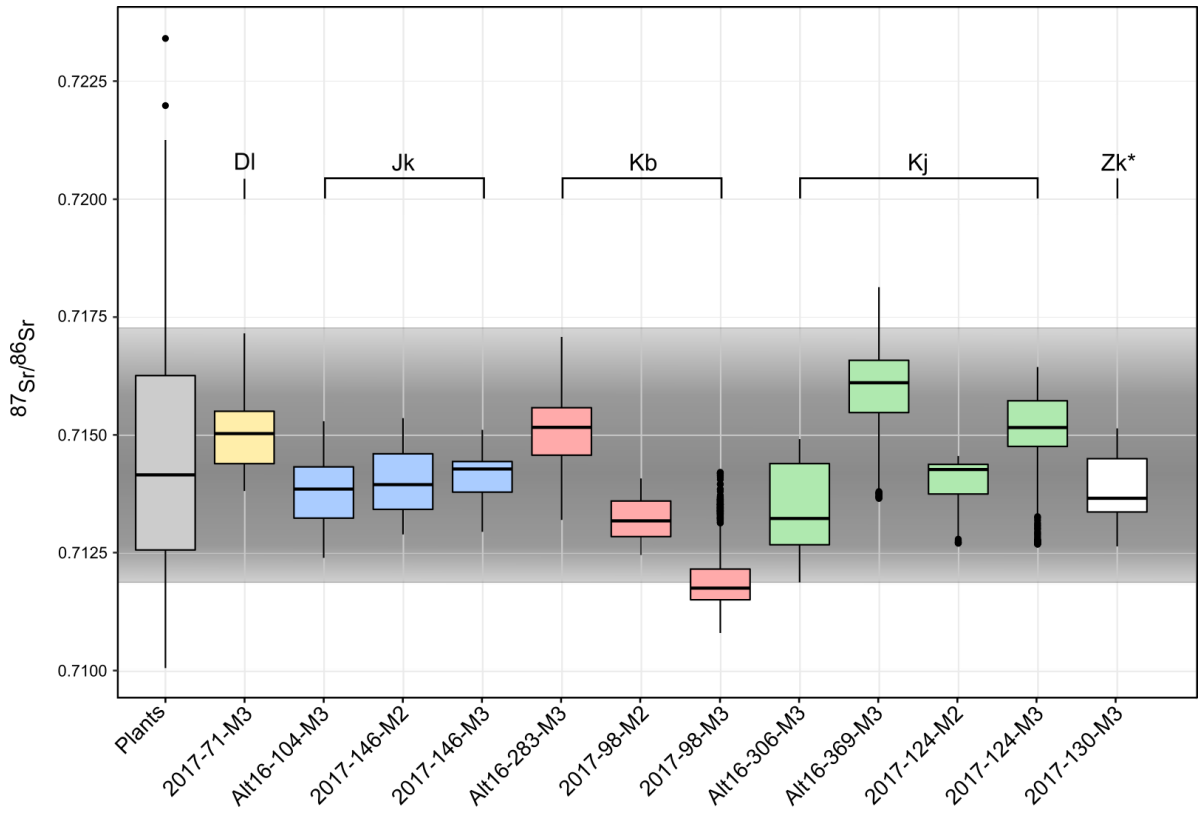

Figure 24: Sr isotope ratios of modern caprine teeth from western Mongolia with a horizontal bracket for each animal belonging to one herder (Jk, Kb, Dl, Kj, Zk). Bio-available Sr isotope ratios (Plants - grey boxplot) are reported for comparison. The grey shade represents the mean ± 1 SD of plant $^{87}Sr/^{86}Sr$.

Intra-individual variation in Sr isotope ratios was 0.00142 on average and varied from 0.00087 (2017-98-M2) to 0.00198 (2016-369-M3) (**Table 13; Figure 24**). Large inter-individual differences within the same herd were observed, ranging from 0.00226 (Kj) to

0.00311 (Kb), whereas animals from Jk herd exhibited an inter-individual difference of 0.00033.

Some teeth, belonging to individuals of the same herd, grew during a similar period of time (2017-146-M2 & Alt16-104-M3 for Jk; 2017-98-M2 & Alt16-283-M3 for Kb; 2017-124-M2 & Alt16-306-M3 & Alt16-369-M3 for Kj) and thus these individuals had the same mobility. Both teeth from herder Jk (Alt16-104-M3 & 2017-146-M2) recorded close average $^{87}Sr/^{86}Sr$ values (0.71400 and 0.71381; *p-value* = 0.07) and a similar range of values. However, both teeth from herder Kb (Alt16-283-M3 & 2017-98-M2) recorded significantly different means (**Table 13**; *p-value* < 2.2e-16) and a higher amplitude for Alt16-283-M3 (0.0039) than 2017-98-M2 (0.0016). Similarly, Kj's three teeth (Alt16-306-M3, Alt16-369-M3 & 2017-124-M2) exhibited significantly different means (**Table 13**; *p-value* < 2.2e-16) and different ranges of values (0.00030; 0.0045 and 0.0018 respectively).

Table 13: Summary results of measured intra-tooth $^{87}Sr/^{86}Sr$ values, for a moving average on 35 individual measurements (top panel) and modelled intra-tooth $^{87}Sr/^{86}Sr$ values (bottom panel).

Tooth	Herder	Moving average of $^{87}Sr/^{86}Sr$ ratio					
		Mean	2SD	Max	Min	Amplitude	N
Alt16-104-M3	Jk	0.71381	0.00145	0.71530	0.71240	0.00289	664
Alt16-283-M3	Kb	0.71509	0.00164	0.71708	0.71321	0.00388	670
Alt16-306-M3	Kj	0.71346	0.00183	0.71492	0.71189	0.00303	686
Alt16-369-M3	KJ	0.71602	0.00198	0.71814	0.71366	0.00447	515
2017-71-M3	Dl	0.71499	0.00139	0.71716	0.71382	0.00334	644
2017-98-M2	Kb	0.71322	0.00087	0.71409	0.71246	0.00162	429
2017-98-M3	Kb	0.71200	0.00158	0.71422	0.71081	0.00340	630
2017-124-M2	Kj	0.71406	0.00094	0.71456	0.71271	0.00185	365
2017-124-M3	Kj	0.71507	0.00185	0.71656	0.71269	0.00375	547
2017-146-M2	Jk	0.71400	0.00132	0.71536	0.71290	0.00246	620
2017-146-M3	Jk	0.71414	0.00093	0.71511	0.71296	0.00216	494
Modelled							
	Dl	0.71450	0.00185	0.71657	0.71298	0.00359	562
	Jk	0.71496	0.00176	0.71670	0.71281	0.00389	902
	Kb	0.71531	0.00198	0.71740	0.71304	0.00437	984
	Kj	0.71446	0.00079	0.71521	0.71367	0.00153	995

6.5.4 Modelled vs measured intra-tooth $^{87}Sr/^{86}Sr$ ratios

The model predicted similar average $^{87}Sr/^{86}Sr$ ratios for all herders, ranging from 0.71446 ± 0.00079 (2SD) (herder Kj) to 0.71531 ± 0.00198 (2SD) (herder Kb), with amplitude ranging from 0.00153 (herder Kj) to 0.00437 (herder Kb) (**Table 13; Figure 25**). Average intra-tooth variation by herder varied from 0.00274 (herder Kb) to 0.00328 (herder Kj). With the

exception of Kj caprines, the range in measured intra-tooth variations was usually lower than that of modelled values (**Table 13; Figure 25**). Moreover, the average in measured $^{87}Sr/^{86}Sr$ ratios was usually closed to the average $^{87}Sr/^{86}Sr$ ratios of modelled values, with the exception of the individual 2017-98 (Kb) exhibiting much lower average measured values and Alt16-369 (Kj) showing higher values.

When applying a constant growth rate with average calendar dental development and a common birth date (1st approach – see 3.6) the temporal variations of measured intra-tooth $^{87}Sr/^{86}Sr$ ratios showed some similarities with those modelled (**Supp. Info Fig. S6.7a**). For five teeth (2017-98-M2 and all teeth from Kj) the Pearson's correlation between the first derivative of modelled and measured $^{87}Sr/^{86}Sr$ ratios was positive but significant for only two teeth (Alt16-369-M3 and 2017-124-M3 - **Table 14**). For the six others teeth, the Pearson's correlation coefficient was significantly negative (**Table 14**). For these teeth, similar variations can be observed but with a certain time-lag that can vary depending of the tooth, from minus 2 months (Alt16-104-M3 and 2017-146-M3) to plus 2 months (2017-146-M2 and Alt16-283-M3). While for 2017-71-M3, the offset is negative or positive depending on the part of the enamel having mineralized first or last.

Table 14: Correlations between the first derivatives of modelled and measured intra-tooth $^{87}Sr/^{86}Sr$ values in the case of average dental development rates, common birth date and constant growth rate: correlation coefficient (Pearson's R), significance level (p-value: < 0.05 = *; < 0.01 = **; < 0.001 = ***) and degree of freedom (df). Positive correlations are in bold.

Tooth	Herder	R	R^2	p-value	df
2017-71-M3	Dl	-0.23	0.05	***	205
Alt16-104-M3	Jk	-0.27	0.07	***	304
2017-146-M2	JK	-0.03	1e-03	0.49	416
2017-146-M3	Jk	-0.27	0.07	***	273
Alt16-283-M3	Kb	-0.21	0.05	***	305
2017-98-M2	**Kb**	**0.11**	**0.01**	**0.06**	**274**
2017-98-M3	Kb	-0.32	0.11	***	418
Alt16-306-M3	**Kj**	**0.1**	**1e-03**	**0.08**	**302**
Alt16-369-M3	**Kj**	**0.23**	**0.05**	*******	**298**
2017-124-M2	**Kj**	**0.08**	**0.01**	**0.18**	**2668**
2017-124-M3	**Kj**	**0.36**	**0.13**	*******	**414**

Table 15: Modified characteristics for the calendar development rate of tooth and birth date of caprines for the time calibration of intra-tooth $^{87}Sr/^{86}Sr$ values, with a constant (CST) growth rate for M2 and a growth rate decreasing exponentially (1/EXP) for M3. * (in months).

Tooth	Herder	Growth rate	Individual's birth	Start formation *	End formation *
2017-71-M3	Dl	1/EXP	31/03/2015	12.2	29
Alt16-104-M3	Jk	1/EXP	31/03/2014	12	30
2017-146-M2	JK	CST	15/04/2015	2.4	13
2017-146-M3	Jk	1/EXP	15/04/2015	11.1	28
Alt16-283-M3	Kb	1/EXP	31/03/2014	13.5	29
2017-98-M2	Kb	CST	31/03/2015	2	14
2017-98-M3	Kb	1/EXP	31/03/2015	11	29
Alt16-306-M3	Kj	1/EXP	31/03/2014	11	28
Alt16-369-M3	Kj	1/EXP	30/04/2014	14	29
2017-124-M2	Kj	CST	31/03/2015	1	14
2017-124-M3	Kj	1/EXP	31/03/2015	11	28

However, when applying the second method of time calibration with decreasing exponentially growth rate for M3, variable dental development rates and birth date, described in **Table 15**, the temporal variations measured intra-tooth $^{87}Sr/^{86}Sr$ ratios are more in line with those modelled (**Figure 25**). The Pearson's correlations between the first derivatives of modelled and measured $^{87}Sr/^{86}Sr$ variations are better and became significantly positive for nine out of the eleven teeth (**Table 16**). The temporal variations measured intra-tooth $^{87}Sr/^{86}Sr$ ratios showed some similarities with those modelled. The time-lags previously observed are absent. However, some parts of teeth exhibited clear different variations than modelled intra-tooth $^{87}Sr/^{86}Sr$, as the last part of Alt16-104-M3 (**Figure 25B**) and 2017-98-M3 (**Figure 25C**) or the rapid and important variations observed in Alt16-369-M3 and 2017-124-M3 (**Figure 25D**).

Table 16: Correlations between the first derivatives of modelled and measured intra-tooth $^{87}Sr/^{86}Sr$ values in the case of variable dental development rates, variable birth date, constant growth rate for M2 and decreasing exponentially growth rate for M3 (Table 15): correlation coefficient (Pearson's R), significance level (p-value: < 0.05 = *; < 0.01 = **; < 0.001 = ***) and degree of freedom (df). Positive correlations are in bold.

Tooth	Herder	R	R^2	p-value	df
2017-71-M3	Dl	0.56	0.32	***	194
Alt16-104-M3	Jk	0.15	0.02	**	347
2017-146-M2	Jk	0.56	0.31	***	278
2017-146-M3	Jk	0.29	0.08	***	351
Alt16-283-M3	Kb	0.37	0.14	***	347
2017-98-M2	Kb	0.12	0.01	0.06	274
2017-98-M3	Kb	0.40	0.16	***	356
Alt16-306-M3	Kj	0.46	0.21	***	282
Alt16-369-M3	Kj	0.01	2e-04	0.8	307
2017-124-M2	Kj	0.44	0.20	***	296
2017-124-M3	Kj	0.52	0.27	***	414

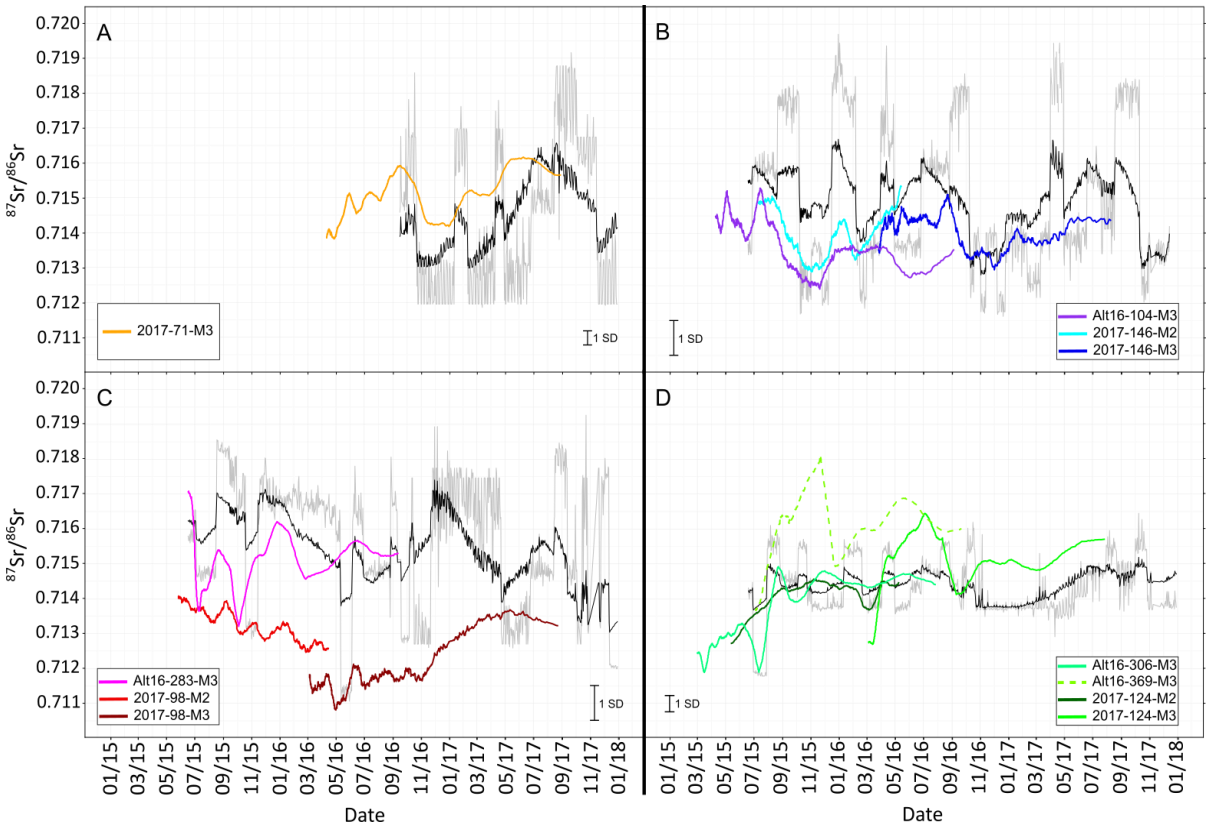

Figure 25: Comparison between the variation of $^{87}Sr/^{86}Sr$ values of pastures (grey line), the modelling of intra-tooth variations predicted by the forward model (thick black line) and the measured intra-tooth variations of $^{87}Sr/^{86}Sr$ running mean (coloured full line) for animals belonging to (**A**) Dl, (**B**) Jk, (**C**) Kb and (**D**) Kj. The time calibration of measured intra-tooth profiles was done using modified characteristics of dental development rates, birth date and growth rate (Table 15). The black error bars at the bottom of each panel represent the mean standard deviation for all intra-tooth running means of the corresponding panel.

6.6 Discussion

6.6.1 Accuracy of LA-MC-ICP-MS measurements

The main disadvantage of using LA-MC-ICP-MS when measuring $^{87}Sr/^{86}Sr$ ratios in teeth is that it provides lower precision and accuracy than solution methods (Horstwood et al., 2008; Vroon et al., 2008). The precision of LA-MC-ICP-MS values on teeth are at the third or fourth decimal place. While, the precision of TIMS (a solution method) measurements of $^{87}Sr/^{86}Sr$ ratios in tooth enamel are typically at the sixth decimal place, and those of solution MC-ICP-MS values are at least at the fifth decimal place. LA-MC-ICP-MS accuracy may be too low for geographic areas with a very narrow range of bioavailable Sr isotope ratios. In our case, the average value on NIST SRM 1400 is of 0.71384 ± 0.000214, with a precision on the fourth decimal. Most importantly, the variability of bioavailable $^{87}Sr/^{86}Sr$ ratios, at ± 0.0054 (2SD) determined from plants (**Figures 22 and 24**) is broad enough compared to the precision

of our measurements, that $^{87}Sr/^{86}Sr$ ratios in teeth obtained by LA-MC-ICP-MS can be used to track the mobility of individuals in this study area.

6.6.2 Bioavailable strontium isoscape

The study area exhibited a large range in bioavailable strontium isotope ratios, going from 0.71007 to 0.72340 (amplitude = 0.01333) (**Figures 22 & 24**). This variability is 5 times higher than in Köşk Höyük (Central Turkey, 0.0025 - Meiggs et al., 2017) and 25 times higher than in Oldupai Gorge, (Tanzania, 0.00052 - Tucker et al., 2020), two areas of similar size (roughly 40 x 20 Km). A comparable large variability was only found in larger areas, such as the southern coast of South Africa (0.7092 – 0.7254; Copeland et al., 2016), or Ireland to a lesser degree (0.7067 – 0.7164; Snoeck et al., 2019). Such a high variability is expected for a mountaineous area like Altai. Indeed, in geologically and/or structurally complex regions, with patchy bedrock geology, Sr isotope ratios are expected to be more variable (Crowley et al., 2017; Hoppe et al., 1999). Clastic sediments, common in this type of areas, can vary significantly in their $^{87}Sr/^{86}Sr$ ratios depending on their source region and weathering. Only the high sampling density, comparatively to other studies (e.g. Copeland et al., 2016; Meiggs et al., 2017) allowed us to catch this variability. This heterogeneity, coupled with the geographical structuration of the $^{87}Sr/^{86}Sr$ ratios, offers the possibility to decipher between different geographical origins and mobility practices within a small area. The Southern part of the study area is characterized by lower $^{87}Sr/^{86}Sr$ ratios than the rest of the area. Higher values characterized the major part of southeast lowlands. We can observe that samples from the northernmost river of the sampled area showed higher $^{87}Sr/^{86}Sr$ values than the surrounding steppe, probably because of the transport of sediments from rocks upstream with high $^{87}Sr/^{86}Sr$ values.

6.6.3 Implications of intra and inter-individual variability of $^{87}Sr/^{86}Sr$ ratio for the distinction between local and non-local individuals

The average of Sr isotope ratios of all local caprine teeth (0.71414 ± 0.002 - 2SD) was consistent with the average bioavailable $^{87}Sr/^{86}Sr$ value of the study area based on plant analysis (0.71456 ± 0.005 – 2SD) (**Figure 24**).

Several publications have suggested a cut-off value of ± 0.001, based on $^{87}Sr/^{86}Sr$ ratios of faunal remains to distinguish between 'local' and 'non-local' individuals (Grupe et al., 1999; Schweissing and Grupe, 2003; Söllner et al., 2016). In other words, if the $^{87}Sr/^{86}Sr$ ratio lies

outside the cut-off range, it can be considered as 'non-local'. This cut-off value was proposed for the Bavarian region characterized by a relatively homogeneous signature (from 0.709 to 0.7135) and may not be suited to more geologically heterogeneous landscapes. Söllner et al. (2016) proposed to use three standard deviations of the average $^{87}Sr/^{86}Sr$ ratio of the fauna. In our case, this would lead to a cut-off value of ± 0.003 with a 'local' range from 0.71114 to 0.71714, including all individuals average $^{87}Sr/^{86}Sr$ values but highest of Alt16-369-M3 or lowest values of 2017-98-M3 are outside of this 'local' range. This determination of cut-off range restricting by a factor of 3 the variability observed in the plants (± 0.008 – 3SD) that could lead to misinterpretation of the origin of a potential individual pasturing only on southern part or eastern part of the study area. Consequently, a cut-off value of ±3SD of the average faunal values do not fully described the variability of the bioavailable strontium, at least for this study area.

A study on modern pigs born and raised in identical conditions with same food, showed an inter-individual variability of 0.00186 in tooth (Anders et al., 2019). It should be noted that the diet was not controlled in this study and that isotopic compositions may have varied over time. However, the inter-individual variability observed by the authors remains interesting as a point of comparison, especially since few studies exist. In our study, animals from herder Jk (Alt16-104-M3 and 2017-146-M2), born and raised under the exact same conditions (same age and same mobility pattern) displayed a difference of 0.0004. However, for Kb with Alt16-283-M3 and 2017-98-M2, the difference in intra-individual variability was 0.00225, with distinct average values ($\Delta = 0.00187$). The pattern with Kj's animals is more complex. Three teeth grew during the same period (Alt16-306-M3; Alt16-369-M3; 2017-124-M2). There was a great difference in intra-tooth variability ($\Delta = 0.00263$) between Alt16-369-M3 and 2017-124-M2 (**Figure 24**) with high difference between average $^{87}Sr/^{86}Sr$ ratio ($\Delta = 0.00196$). Consequently, these differences observed in intra-tooth of individuals from same herds could suggest that they did not have the same mobility pattern and one have moved more than the other during the time of tooth formation, but this is not supported by the GPS data. It can be stated that criteria used in archaeological studies would lead to misinterpretation of our data for both intra and inter-individual variability. This high difference in variability between both individuals with the same history of life is surprising.

A difference in microscale feeding behaviour, between sheep and goat for example, could be a possible explanation for this difference in the intra-individual variability. In some areas, especially in lowlands, shrubs and grasses are available for caprines. Root depth and

microhabitat can affect the strontium isotope composition of plants. Snoeck et al. (2019) observed a difference between grasses, shrubs and trees being as high as 0.0052 at some sites, and larger in clastic sedimentary formations. Finally, drinking behaviour may also have an influence on strontium isotope variability, with rivers which may have different $^{87}Sr/^{86}Sr$ values than the rest of the landscape (Crowley et al., 2017).

6.6.4 Modelled vs measured intra-tooth $^{87}Sr/^{86}Sr$ ratio

For the majority of teeth, there is a positive correlation between the modelled and measured variations of $^{87}Sr/^{86}Sr$ values. These positive correlations (**Table 16**) show that the measured intra-tooth $^{87}Sr/^{86}Sr$ variations are strongly concordant with the modelled $^{87}Sr/^{86}Sr$ variations based on animal locations (**Figure 25**), and thus can be used as a proxy to track the mobility of domestic and wild animals – provided there is sufficient spatial heterogeneity in bioavailable strontium. Despite a good concordance in the range and variation of modelled vs measured $^{87}Sr/^{86}Sr$ ratios of each tooth, some of the isotope profiles (i.e. 2017-98-M2 &M3; Alt16-369-M3; 2017-124-M3) did not match the predictions of the model in terms of absolute $^{87}Sr/^{86}Sr$ values and/or variability. It is important to note that several assumptions had to be done to predict intra-tooth $^{87}Sr/^{86}Sr$ values. First, the Sr isotope values used as input data in the forward model are only an approximation of the dietary value actually ingested by the caprines. This could partly explain the difference observed between modelled and measured values. Indeed, Crowley et al. (2017) showed that mammal skeletal tissues are most accurately predicted when they live in region at low Sr complexities, which it is not our case. In this case, even if the density of plant sampling was high compared to other studies, the complexity of the study area in terms of $^{87}Sr/^{86}Sr$ geographical distribution could explain the offset observed between predicted and measured tooth profiles (e.g. Copeland et al., 2016; Meiggs et al., 2017). Moreover, the difference between modelled and measured data could reflect the way mammals integrate spatial information through grazing and a certain local heterogeneity of areas that is not captured by the isoscape model. Indeed, the isoscape was not specifically built on what animals ate. In some areas such as valley bottoms or eastern lowlands, shrubs and grasses are available for caprines. Differences in root depths could lead to differences in $^{87}Sr/^{86}Sr$ ratio, especially in clastic sedimentary environments, as mountain ranges (Snoeck et al., 2019) and explained partially differences between modelled and measured $^{87}Sr/^{86}Sr$ ratios.

Moreover, temporal fluctuations in $^{87}Sr/^{86}Sr$ could influence the modelled $^{87}Sr/^{86}Sr$ ratios. Indeed, variations in temperature, precipitation, run-off sources, weathering or dust can

temporally influence the bioavailable Sr pool (Brennan et al., 2015; Douglas et al., 2013, 2002; Feranec et al., 2007; Price et al., 2002; Reynolds et al., 2012; Rose and Fullagar, 2005). Potential temporal fluctuations could not be considered by the isoscape and our sampling method. However, described seasonal fluctuations in $^{87}Sr/^{86}Sr$ in literature occurred in more humid region (i.e Canada, Alaska) than western Mongolia. It seems unlikely that snow melting and increase in precipitation during spring and summer changed dramatically $^{87}Sr/^{86}Sr$ ratios of some pasture areas and lead to great difference between predicted and measured data.

Finally, the good agreement between measured and modelled intra-tooth profiles (**Figure 25**) suggests that the environmental-based model (Passey and Cerling, 2002) used to predict intra-tooth $^{87}Sr/^{86}Sr$ variations is adapted for strontium too. Indeed, this model was initially developed for C and O isotope systems, in which elements are incorporated over a period of ~ 3-4 months (Passey and Cerling, 2002; Podlesak et al., 2008; Zazzo et al., 2012, 2010, 2005). This suggests that $^{87}Sr/^{86}Sr$ profiles may be synchronous with those of $\delta^{13}C$ and $\delta^{18}O$. This is in contradiction with Montgomery et al. (2010) who suggested that $^{87}Sr/^{86}Sr$ profiles may not be synchronous with those of $\delta^{18}O$ and $\delta^{13}C$, because strontium is incorporated over a period in excess of 12 months and it may be not possible to recover strontium variations with a high time resolution. However, it must be specified that Montgomery et al. (2010) sampled only the outer enamel and this layer records more dampened and time-average primary isotopic environmental signal than inner enamel. Possibly, the kinetics of incorporation of Sr isotopic ratio could be different between these layers. But, in view of the variations observed in intra-tooth profiles, compared to the spatial heterogeneity in $^{87}Sr/^{86}Sr$ values of our study area, the residence time for strontium does not seem to be as high as proposed. However, the potential impact of long-term residence time of strontium in body pools and the extended incorporation of strontium in enamel on the time resolution and time calibration of strontium isotope values in tooth enamel remains understudied. This issue can only be fully addressed via controlled feeding experiments on captive animals.

6.7 Conclusion

This study demonstrates that strontium isotope time series of tooth enamel can be used to track small-scale animal mobility. Based on the results of this pilot study, we can offer some initial conclusions. The average $^{87}Sr/^{86}Sr$ ratios of all the individuals matched that of the local baseline characterized by a high degree of heterogeneity. While teeth from the same herd showed similar average $^{87}Sr/^{86}Sr$ values and variability, it was not the case for others, possibly

due to variability in diet behaviour and micro-scale heterogeneity of bioavailable strontium. Generally, intra-tooth measured profiles fell well within the predicted range of intra-tooth values, obtained by the forward model developed for C and O isotope systems. Moreover, temporal variations of measured intra-tooth profiles are well correlated with those of modelled intra-tooth profiles when modifying reasonably dental development rates, growth rate of molars and birth date of caprine. However, for some teeth the synchronicity of measured and modelled $^{87}Sr/^{86}Sr$ profiles has not been achieved. Mountains are complex regions making it difficult to predict accurately bioavailable strontium, even at a small-scale, and clastic sediments may produce important $^{87}Sr/^{86}Sr$ variability that are difficult to map. Although controlled feeding studies are needed to firmly establish the residence time of Sr in the organism, the good results obtained with the model of Passey and Cerling (2002) may suggest that residence time of Sr is similar to that of C.

For archaeological applications, results should be treated with an appropriate degree of caution depending of the resolution of the sampling method and the variability of bioavailable strontium of the study region. We argue that intra-tooth profiles based on few sequential samples are not suitable to track mobility in complex strontium regions as mountains but can still be used to study the origin of individuals as "local" vs "non-local" based on average values. Moreover, precise interpretation of $^{87}Sr/^{86}Sr$ profiles in term of mobility can be challenging. Indeed, it is possible to have the same type of profile with very different mobilities within the same region, due to the combination of the complexity of the geology, the multiplicity of possible route types, and the duration of the mineralization process.

Additional sampling coupled with knowledge of the local geology and improved geostatistical framework to incorporate existing geospatial covariates would further improve the accuracy and resolution of our bioavailable isoscape model and would improve predicted intra-tooth profiles. In addition, a future step would be to try to infer probable mobility pattern of these animals only from intra-tooth $^{87}Sr/^{86}Sr$ profiles.

ACKNOWLEDGEMENTS

We would like A. Lamboux (UMR 5276 LGLTPE, ENSL, UCBL, Lyon) for her help in preparation of plant and tooth samples before their analysis. The isotope analysis were performed at the *Ecole Normale Supérieure* in Lyon (UMR 5276, LGLTPE, ENSL) under the technical supervision of P. Telouk. Fieldwork was supported by the French archaeological mission in Mongolia (CNRS, MNHN, MAEDI, director SL) and by the CNRS. This research

was funded by a Ph.D. grant to NL from the French National Research Agency LabEx ANR-10-LABX-0003-BCDiv, in the context of the "Investissements d'avenir" n°ANR-11-IDEX-0004-02, and by an Inalco Early Career Research Grant 2017 to CM.

SUPPLEMENTARY INFORMATION CHAPTER 6

All supplementary information are available here:
https://drive.google.com/drive/folders/1ky3WkXs7KFv2tFrmv_yIJub1CNUqi4EH?usp=sharing

Supplementary Info S6.1: Gathers additional information on plants

Table S6.1a: General information on plant sampling sites with the measured $^{87}Sr/^{86}Sr$ and associated standard error (SE) and taxa present in the sample.

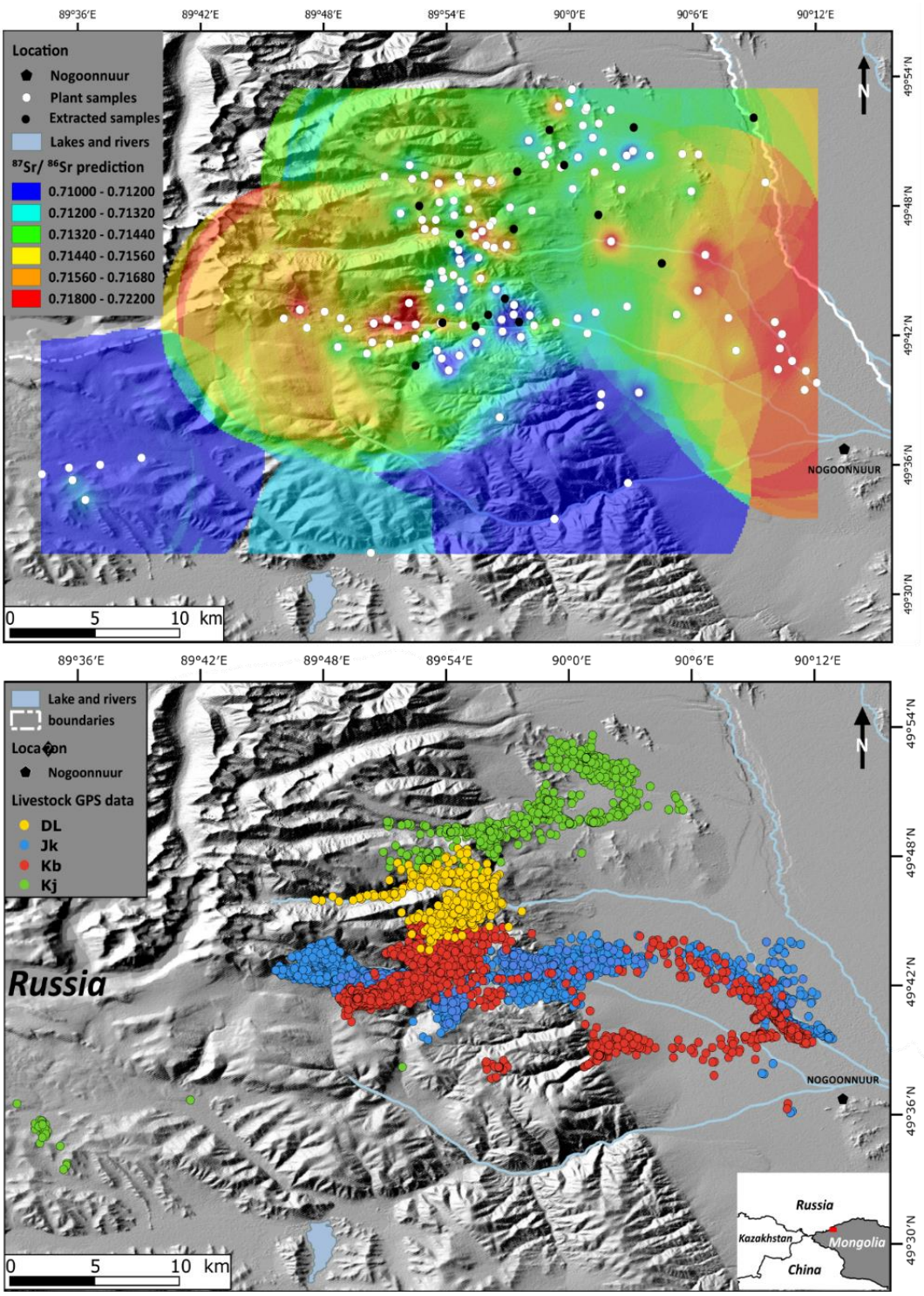

Figure S6.1a: Plant samples locations (top panel) compared to GPS data of livestock (bottom panel)

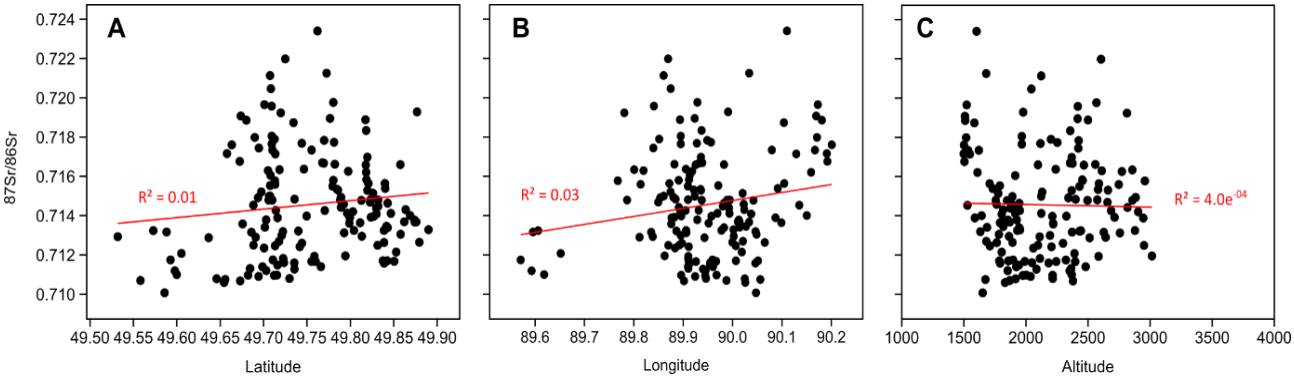

Figure S6.1b: Bioavailable $^{87}Sr/^{86}Sr$ values from the modern sampling localities plotted relative to (A) latitude, (B) longitude and (C) altitude.

Supplementary Info S6.2: Gathers additional information on kriging

Table S6.2a: Parameters of the geospatial modelling with characteristics and accuracy of kriging model.

Model Parameters	
Kriging Type	Ordinary
Semivariogram	Exponential
Major range	0.019338
Partial sill	0.000007219
Nugget	0
Lag Size	0.01
output cell size	1.43235.10-3
search radius	fixed
distance	0.1
Kriging results	
Number of Samples	140
Mean error	-2.51E-05
Root mean square error (RMSE)	0.0005
Mean absolute percentage error (MAPE)	0.387251
Residual standard error	0.0005
standard deviation Predicted values	0.0026
standard deviation of error	0.0005
Results of the reliability assessment of the kriging model	
Number of Samples	16
Mean error	0.00022
Residual standard error	0.0008
Standard deviation of error	0.0016
Root mean square error (RMSE)	0.0149
max error	0.0031
min error	-0.0022

Table S6.2b: Details of the geospatial model of bioavailable strontium

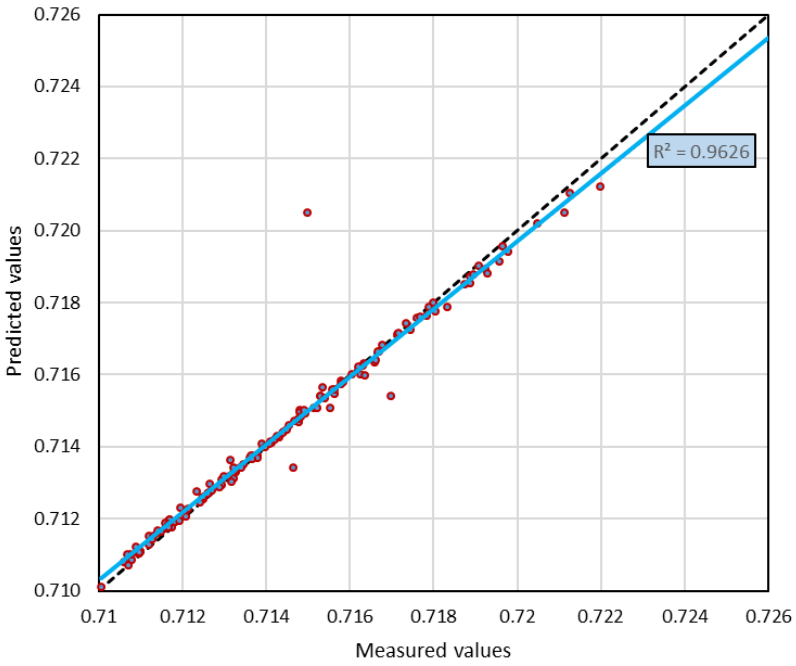

Figure S6.2a: Scatter plot showing predicted values (Y-axis) versus measured values (X-axis) of bioavailable strontium isoscape. The black line is the 1:1 regression line whereas the blue line is the fitted regression line, showing overprediction of small values and underprediction of larger values.

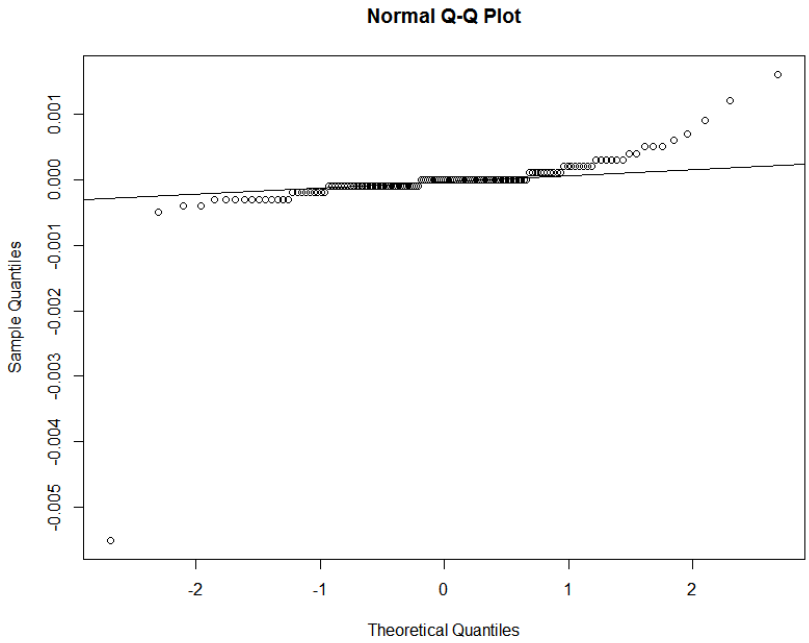

Figure S6.2b: QQ plot showing on the Y-axis quantiles of the error between the predicted and measured data values and normal values on the X-axis subdivided by their corresponding quantiles. The grey line represents a normal distribution.

Supplementary Info S6.3: Parameters and operating conditions for Sr isotope determination by laser ablation MC-ICPMS.

Parameters	Values
Laser ablation 193 nm Excite	
Wavelength	193 nm
He flow rate	0.7 L/min
Ablation	
Spot size	85 µm
Frequency	10 Hz
Fluence	15.18 J/cm²
Sampling scheme	Line (dynamic)
Line translation rate	60 µm/s
sample Line length	~ 18 mm
standard line length	3 mm
MC-ICPMS Nu 500 HR	
Argon cool gas flow rate	14 L/min
Auxillary gas glow	1.4 L/min
Sample gas flow	0.7 L/min
Plasma power	1350
Resolution	
Data collection	
Gas background	30 s
Sample	~ 300 s
Integration	2 s

Supplementary Info S6.5: Characteristics of the dental development rates (in months after birth) for molars M2 and M3 of caprines published datasets and the calculated mean data used in this study.

Start M2 (month)	End M2	Start M3	End M3	Source
2	16	14	33	Upex and Dobney (2012)
2	12	11	25	Weinreb and Sharav (1964)
0	12	8	22	Milhaud and Nezit (1991)
1	12	8	24	Zazzo et al. (2010)
1.3	**13.0**	**10.3**	**26.0**	**Mean**

Supplementary Info S6.6: Gathers supplementary information on geographical and calendar mobility of herds

Tables S6.6: Summary of calendar mobility for each herder determined with the Lavielle's segmentation method.

Figures S6.6: Localisation of camps for each herder. Maps designed with QGIS.

Supplementary Info S6.7: $^{87}Sr/^{86}Sr$ results for each caprine tooth measured by LA-MC-ICP-MS

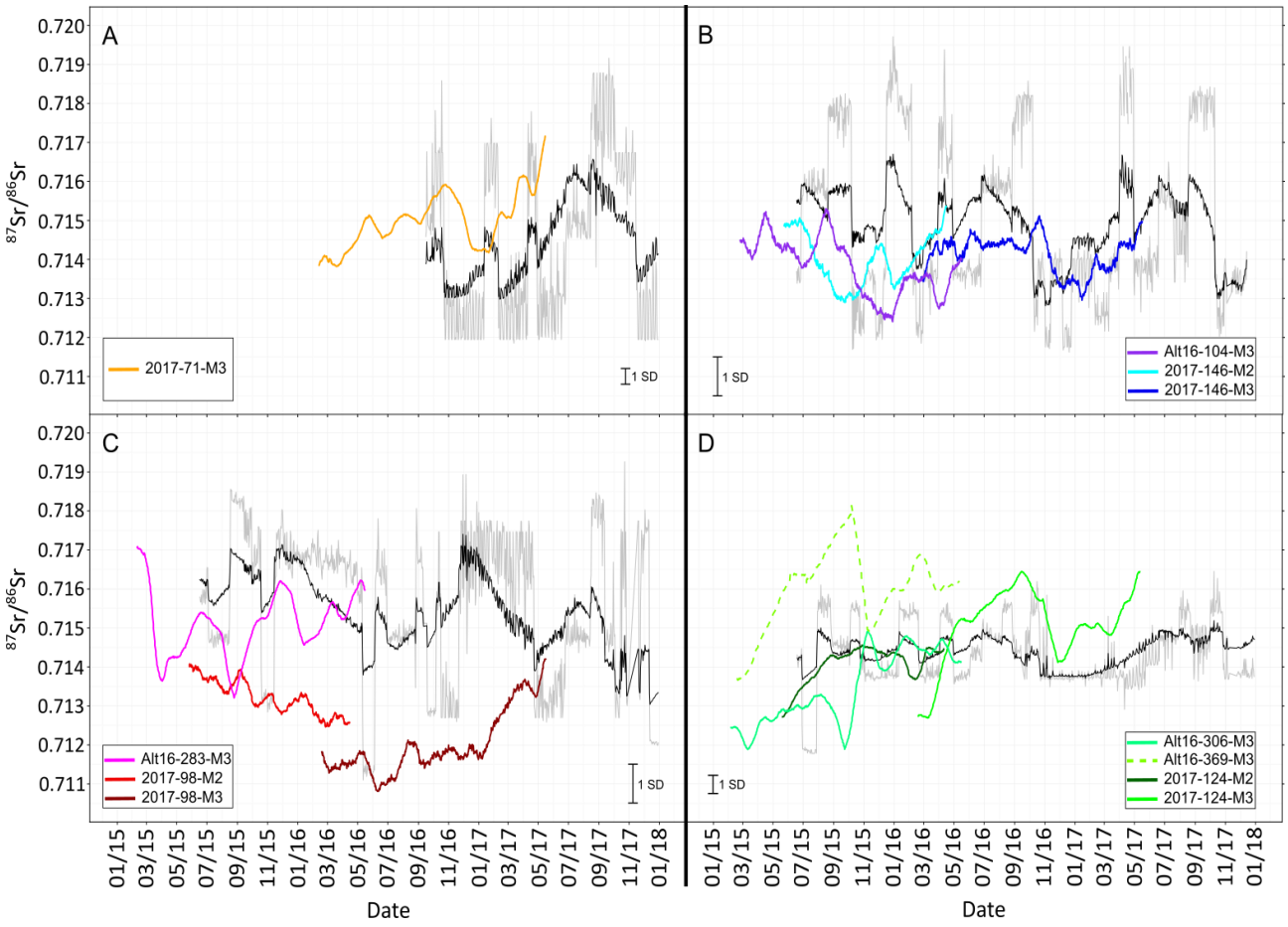

Figure S6.7: Comparison between the variations of bioavailable $^{87}Sr/^{86}Sr$ values at the animal locations (grey line), the modelling of intra-tooth variations by the forward model (thick black line) and the measured intra-tooth variations of $^{87}Sr/^{86}Sr$ running mean (coloured full line) for animals belonging to (A) Dl, (B) Jk, (C) Kb and (D) Kj. The time calibration of measured intra-tooth profiles was done using average dental development rates, common birth date and constant growth rate. The black error bars at the bottom of each panel represent the mean standard deviation for all intra-tooth running means of the corresponding panel.

Supplementary Info S6.8: Plots of the Pearson's correlation between the first derivative of measured and modelled intra-tooth $^{87}Sr/^{86}Sr$ values for each tooth in the case of variable dental development rates, birth date and growth rate decreasing exponentially for M3.

Chapitre 7 – Origine et mobilité des chevaux de l'âge du Bronze et de la période Türk du site de Burgast (Altaï, Mongolie) par une approche multi-isotopique (C, O, Sr).

Dans les chapitres précédents, nous avons vu que la combinaison du $\delta^{13}C$ et $\delta^{18}O$ de l'émail dentaire permet de mettre en évidence une mobilité altitudinale. De plus, le $\delta^{13}C$ des tissus biologiques permet d'affiner l'exploitation des pâtures d'altitude car la valeur moyenne est liée à l'altitude moyenne de pâturage ainsi qu'au pourcentage d'occupation des pâtures alpines. En revanche les valeurs de $\delta^{18}O$ semblent peu utiles pour distinguer des stratégies d'occupation altitudinale des pâtures. Enfin, l'influence de la mobilité sur les variations de $^{87}Sr/^{86}Sr$ enregistrées dans l'émail est probante, permettant d'interpréter les variations de $^{87}Sr/^{86}Sr$ en termes de mobilité.

Ce chapitre propose l'étude de l'origine et de la mobilité de chevaux de l'âge du Bronze (début du 1er millénaire av. n.e.) et de la période Türk (fin du 1er millénaire ap. n.e.) retrouvés en contexte funéraire sur le site de Burgast en Mongolie occidentale. L'objectif est d'appliquer les méthodes, abordées dans les chapitres précédents, aux molaires des chevaux afin d'estimer l'origine géographique et de préciser les modalités d'exploitation du territoire (et notamment des pâtures alpines) via une analyse isotopique combinée ($\delta^{13}C$, $\delta^{18}O$, $^{87}Sr/^{86}Sr$).

7.1 Résumé de l'étude

Les témoignages archéologiques attestent de l'impact économique et culturel important du cheval sur le mode de vie nomade des sociétés ancienne et cela depuis l'âge du Bronze. Son utilisation comme moyen de transport et comme animal d'élevage ont permis d'accroitre l'interaction entre les communautés pastorales mobiles. Cette évolution et intensification de son usage et de la mobilité des communautés s'est accompagnée de profonds changements dans l'expression des pratiques rituelles avec notamment la présence des chevaux, partie intégrante, des cérémonies et monuments funéraires de la fin de l'âge du Bronze. Cependant, les pratiques d'élevage et de mobilité durant la vie de l'animal, voire l'origine géographique de l'animal (qui peut provenir d'un échange, de vol ou être un cadeau) sont assez difficiles à approcher dans ce type de contexte, limitant le nombre d'études apportant des éléments de réponses à ces questions.

Ici, l'analyse séquentielle de la composition isotopique du strontium, de l'oxygène et du carbone de l'émail des dents a été utilisée pour estimer la mobilité des chevaux déposés dans un khirgisuur de la fin de l'âge du Bronze et dans une tombe de la période Türk du site de Burgast (province de Bayan-Ölgii, Mongolie occidentale).

Les valeurs de $^{87}Sr/^{86}Sr$ obtenues à partir de l'émail des dents des chevaux de l'âge du Bronze sont homogènes suggérant une origine commune. Le cheval Türk a des valeurs légèrement plus basses que les chevaux de l'âge du Bronze. Dans tous les cas, les chevaux des deux périodes ont des valeurs de $^{87}Sr/^{86}Sr$ compatibles avec celles retrouvées au sein de l'isoscape de la région d'étude, et particulièrement avec les valeurs basses du strontium biodisponible au sud de l'isoscape. Toutefois, rien ne permet d'exclure une origine géographique en dehors de la zone cartographiée car d'autres valeurs compatibles peuvent être trouvées proche de la zone d'étude, voir au delà. L'anticovariation entre les valeurs de $\delta^{18}O$ et le $\delta^{13}C$, ainsi que les valeurs de $\delta^{13}C$ seules vont dans le sens d'une mobilité altitudinale et d'une exploitation de pâturages d'altitude (aussi importantes que celles des chevaux actuels). Ces résultats suggèrent que, malgré certaines différences, l'incorporation des stratégies de pâturage impliquant une mobilité verticale dans la gestion du bétail remonte au moins à la fin de l'âge du Bronze. De plus, les chevaux de cette époque présentent des variations intra-dentaires $^{87}Sr/^{86}Sr$ similaires, composées de fréquentes augmentations et diminutions de $^{87}Sr/^{86}Sr$. Ce patron suggère un schéma de mobilité commun et une appartenance probable à un même troupeau. On peut donc penser que seule une petite communauté, voire une seule unité familiale est intervenue lors des rites funéraires sur ce khirgisuur. Ces résultats viennent compléter ceux d'une autre étude menée sur de plus grands khirgisuurs de Mongolie Centrale. Il faut préciser que cette étude n'a analysé qu'un faible pourcentage des restes de chevaux associés à chaque structure. Notre étude est la première a proposé l'analyse de la majorité des chevaux en laint avec une même structure. Toutefois, cette étude sur des khirgisuurs de Mongolie Centrale concluait, sur la base d'analyses isotopiques en strontium, à des origines diverses des chevaux et à l'intervention d'une communauté plus grande et venant d'un plus large territoire.

Enfin, les valeurs de $^{87}Sr/^{86}Sr$ du cheval Türk sont moins variables et seule une augmentation faible progressive est observée. L'analyse des valeurs de $\delta^{18}O$ et le $\delta^{13}C$ va dans le sens d'une mobilité altitudinale. Ceci peut impliquer une mobilité moins fréquente. La dent était en cours de croissance et n'a enregistré qu'une courte période de la vie de l'animal. Un seul mouvement d'une zone vers une autre, avec des valeurs en strontium biodisponible

proches, est envisageable. Les harnais trouvés dans la tombe suggèrent qu'il s'agissait d'un cheval de monte, limitant ainsi sa mobilité à la proximité des campements, contrairement aux chevaux restant avec le troupeau qui sont libres de leurs mouvements. Mais une réflexion doit encore être menée pour envisager l'ensemble des explications possibles.

Article IV: Isotopic evidence of local origin and mountain exploitation in the Altai Mountain of ritual horses (Mongolia) during the Bronze Age and Turkic period.

Nicolas LAZZERINI, Antoine ZAZZO, Vincent BALTER, Aurélie COULON, Théo TACCAIL, Michel LEMOINE, Charlotte MARCHINA, Noost BAYARKHUU, Tsagan TURBAT, Sébastien LEPETZ

In preparation for submission in *Journal of Anthropological Archaeology*.

Abstract:

Archaeological evidence attests to the important economic and cultural impact of the horse on the nomadic lifestyle of ancient societies since the Bronze Age. Its use as transport and livestock animal has increased the interaction between mobile pastoral communities. The evolution and intensification of its use and the mobility of communities has been accompanied by profound changes in the expression of ritual practices, including the integral part of horses in late Bronze Age ceremonies and funeral monuments. However, little is known on the geographical origin of the horses deposited in these monuments and on the landscape used by LBA pastoralists. Here, strontium, oxygen and carbon isotopic analyses of dental enamel were used to estimate the mobility patterns of horses deposited in a Late Bronze Age khirgisuur and a tomb from Turkic Period from the site of Burgast (Bayan-Ulgii province, western Mongolia). The isotope time series obtained from tooth enamel reveals that horses from both periods were possibly all native from the local area and exploited high elevation pastures during summer. These results suggest that despite some possible differences pasturing strategies involving vertical mobility into livestock management goes back to the LBA at least. Moreover, LBA horses exhibited similar intra-tooth $^{87}Sr/^{86}Sr$ variations that may suggest a common mobility pattern and a probable membership to common household suggesting that only a small community was involved in the funeral rites of this khirgisuur. Finally, the lower variability in the $^{87}Sr/^{86}Sr$ ratios of the Turkic horse may imply a less frequent mobility. This pattern could be due to the fact that it was a riding horse, as indicated by the harnesses found in the tomb, restricting its mobility linked to the mobility of campsites between two isotopic areas.

Keywords: mobility; pastoralism; Mongolia; Bronze Age; Turkic; oxygen; strontium; carbon; isotopes; laser ablation

7.2 Introduction

The horse, as a domestic animal, had a strong impact on the construction of cultures and the organisation of ancient societies of the eastern steppes of Eurasia (Anthony, 2007; de Barros Damgaard et al., 2018; Gaunitz et al., 2018; Outram et al., 2009). It has been a source of meat, dairy products, leather, and hair, but above all, it has allowed people to move faster and to transport goods and people more efficiently. In Mongolia, horses were used for riding or pulling carts from the end of the 2nd millennium BCE on (Taylor, 2017). Although the details of these modalities still need to be clarified, it is argued that the emergence of horse riding and chariotry may have encouraged the adoption of nomadic pastoralism. Indeed, horses would have been an essential component of nomadic lifestyles as movements between pastures is a key element of the subsistence strategy of pastoral systems. In contemporary and historic nomadic pastoral systems, distances and seasonal mobility can vary considerably across the Eurasian steppes, from a few kilometres to over a thousand (Ferret, 2014; Finke, 2004; Houle, 2017). In mountain regions such as Altai, vertical mobility also plays a major role in survival strategy (Finke, 2004).

The importance of horses is clearly visible in the numerous archaeological remains. During the Late Bronze Age (ca. 1200-700 BC), a period of time corresponding to an intensification of horse use in ceremonies, impressive ritual and mortuary complexes called khirgisuurs and deer stones (KDS), are found abundantly in central and northern Mongolia but also found on the foothills of Altai (Allard and Erdenebaatar, 2005; Honeychurch, 2015b; Houle, 2016; Taylor et al., 2017; Wright, 2007). They are composed of a central stone burial chamber covered by a massive stone mound. A quadrangular or circular fence of aligned stones surrounds this central mound. Most of the time, khirgisuurs are also associated with peripheral structures constituted of small stone mounds and circles (Allard and Erdenebaatar, 2005). The stone circles often contain burnt bones of domesticated animals in their centre. Under the stone mounds is placed one (sometimes two) horse's head (positioned to face east) together with elements from the neck and hooves of the animal (Allard and Erdenebaatar, 2005; Broderick et al., 2014, 2016; Fitzhugh, 2009; Lepetz et al., 2019; Zazzo et al., 2019). These deposits can be quite small and include less than ten horse heads, but they can also reach the hundreds, over a potentially long period of edification (Lepetz et al., 2019; Zazzo et al., 2019), raising the question of the origin and mobility of horses, with potential distant origins for some of the horses through gift, trade or exchange because of its social importance (Makarewicz et al., 2018; Taylor et al., 2017).

However, this question also arises for all ancient human communities in Mongolia, since the practice of depositing horse bones in burials can be observed in the Iron Age (e.g. Lepetz and Decanter, 2013), the Xiongnu period (e.g. Brosseder, 2009; Wright et al., 2009) or the Turkic period (e.g. Konstantinov et al., 2018) for example, even if the remains are of different natures (parts of animals or whole animals). Thus, with strong nuances linked to each culture, trying to define the origin and pastures exploitation of horses allows first of all questions linked to the economic and political organization of these different peoples but also to the cultural practices.

Despite the numerous recent researches, which have focused on the Eurasian steppes' societies, identifying the origin and the mobility, as well as their occupation of the territory, of domesticated horses associated with these monuments remains a considerable challenge due to the ephemeral nature of nomadic occupation (Cribb, 2004).

Strontium isotope ratios ($^{87}Sr/^{86}Sr$) are commonly used to study animal movements and origin through geospatial differences in the distribution of local bioavailable strontium (Balasse et al., 2002; Britton et al., 2011; Copeland et al., 2016; Gron et al., 2016; Makarewicz et al., 2018; Meiggs, 2007; Meiggs et al., 2017; Price et al., 2017). The $^{87}Sr/^{86}Sr$ of bioavailable strontium varies depending on age, chemical composition and weathering rate of the underlying bedrock and is also influenced by wind, glacial or alluvial deposits to local soils (Bentley, 2006; Slovak and Paytan, 2012). Through dietary ingesta, including water, strontium is incorporated into tooth enamel during amelogenesis with no fractionation between environmental $^{87}Sr/^{86}Sr$ values and skeletal tissue values (Capo et al., 1998; Flockhart et al., 2015), allowing a direct comparison between them.

In addition, approaches that utilize oxygen isotope analysis ($\delta^{18}O$) of tooth enamel to determine movement take advantage of the geospatial distribution of $\delta^{18}O$ in meteoric waters (Bendrey et al., 2017; Britton et al., 2009; Dufour et al., 2014; Knockaert et al., 2018). $\delta^{18}O$ in meteoric waters is influenced by temperature, humidity, rainfall amount, altitude and continentality (see review of Pederzani and Britton, 2019). The $\delta^{18}O$ measured in herbivore tooth enamel reflects body water, which is sourced from atmospheric oxygen, oxygen from food and imbibed water (Bryant and Froelich, 1995; Green et al., 2018b; Longinelli, 1984; Luz et al., 1984; Podlesak et al., 2008). Modern equids are water-dependent grazers (Bahloul et al., 2001; Crowell-Davis et al., 1985; King, 2002; Ogutu et al., 2010) and tooth enamel $\delta^{18}O$ values reflect meteoric water, the primary drinking water source (Bryant et al., 1994; Hoppe et al.,

2005, 2004). $\delta^{18}O$ values from modern horse enamel collected along a latitudinal transect showed the latitudinal variation in $\delta^{18}O$ precipitation (Bell et al., 2006; Stacy, 2009).

Carbon isotopic composition ($\delta^{13}C$), reflecting the $\delta^{13}C$ value of ingested plants, can be used to determine the use of alpine meadows in mountainous region. The dominant factor influencing $\delta^{13}C$ values is the photosynthetic pathway used for fixing C: plants using the C_3 pathway have an average $\delta^{13}C$ value of -26‰, those using the C_4 pathway exhibit an average $\delta^{13}C$ value of -12‰ (Kohn, 2010; O'Leary, 1988). The ecological differences between C_3 and C_4 plants trigger an increase in the relative proportion of C_3 vs C_4 plants with altitude and thus a decrease of plant communities $\delta^{13}C$ values (Cavagnaro, 1988; Li et al., 2009; Tieszen et al., 1979). In C_3 - dominated environments, the range of isotopic variations is more restricted. However, several studies have documented a relationship between $\delta^{13}C$ values of C_3 plants and altitude. Depending of local environmental conditions (i.e. drought stress) or metabolism of plant (i.e. stomatal conductance), increasing (Körner et al., 1988; Li et al., 2006, 2009, 2007; Liu et al., 2016; Morecroft and Woodward, 1990) or decreasing (Liu et al., 2016; van de Water et al., 2002) $\delta^{13}C$ values with altitude can be observed. A such pattern can be recorded in the $\delta^{13}C$ values of livestock tissues (Männel et al., 2007; Samec et al., 2017) (**see Chapter 4**).

Because tooth enamel is not remodelled once fully mineralized, it records the biochemical life history over the time of tooth development. Sequential sampling along the growth axis of hypsodont (high-crowned) tooth enamel provides a chronological record changes of dietary preferences, climatic conditions and mobility (Balasse, 2003; Pederzani and Britton, 2019; Zazzo et al., 2002). Thus, isotopic composition of bioapatite records temporal variations, spanning the period of enamel formation and maturation and preserving behavioral and environmental information on seasonal time scales (Balasse, 2002; Green et al., 2018a; Passey and Cerling, 2002; Towers et al., 2011; Zazzo et al., 2010). The combination of O and C isotopes in sequentially sampled tooth enamel was recently proposed to determine altitudinal mobility of livestock (Makarewicz et al., 2017; Tornero et al., 2018). Generally, a co-variation of both $\delta^{18}O$ and $\delta^{13}C$ intra-tooth variations is expected for stationary herbivores in temperate and semi-arid environments (Balasse et al., 2009, 2002; Fraser et al., 2008), with high values during hot seasons and lower values during cold seasons. However, an anti-covariation between $\delta^{18}O$ and $\delta^{13}C$ intra-tooth variations has been observed in different cases (e.g. Fisher and Valentine, 2013; Makarewicz et al., 2017; Makarewicz and Pederzani, 2017; Tornero et al., 2018, 2016) (**see Chapter 4**). This anti-covariation has been interpreted as reflecting the

altitudinal mobility of sheep and goats towards highlands pasture in summer and midland/lowland pastures in winter.

Only a few studies applied stable isotope analysis to ancient horse remains from Mongolia. One study in the Khanuy Valley, north-central Mongolia, explored the origin of ceremonially furnished horses found in peripheral stone mounds using C, O and Sr and proposed that Bronze Age horses from khirgisuurs came from geographically distant locations (Makarewicz et al., 2018). For Khanuy Valley, Stacy (2009) compared $\delta^{18}O$ and $\delta^{13}C$ of Bronze Age horses from Central Mongolia to modern Mongolian horses to investigate climate changes. Thus, precautions must be taken when comparing isotopic values over time due to probable past shifts in climate systems (Pollard et al., 2011). It must be highlighted that these studies on Khanuy Valley have not been extensive on all horses of the same khirgisuur but they focused on 1 or 2 individuals per structure. Furthermore, these studies concern central Mongolia, a region rich in grassland and without high mountains. Unfortunately, the regional variability of these practices in other climatically different areas such as the Gobi Desert in the south or the Altai Mountains in the west is poorly known. For Altai mountains, Bendrey et al. (2017) investigated the 'local' or 'non-local' origin of Iron Age horses from tomb of two sites (Baga Turgen Gol and Tsengel Khairkhan) using the latitudinal stratification of $\delta^{18}O$ values of meteoric waters (Pederzani and Britton, 2019). To our knowledge, there are no diachronic studies encompassing horses from older times with horses from more recent times from a same archaeological site in order to study the temporal evolution of breeding and mobility practices related to these horses found in a funerary context.

Here, we bring new data from western Mongolia, a region dominated by the Altai Mountains. This would complete a limited corpus concerning the mobility and origin of funerary domesticated animals in this region and particularly the use, and its origin, of high elevation pasture. In 2016, excavations at the site of Burgast (Bayan-Ulgii province) yielded the remains of several horses deposited around a khirgisuur together with a complete horse buried next to a woman body, and dating from the Turkic period. We propose (i) to explore their origin and whether horses from khirgisuurs were supplied by pastoralist communities local to the monument or by more distant social communities, and (ii) in the case of 'local' horses, to investigate their mobility patterns and especially the potential practices of altitudinal mobility through use of alpine meadows. We do so through sequential analysis of $^{87}Sr/^{86}Sr$, $\delta^{18}O$ and $\delta^{13}C$ isotope analyses of enamel teeth. Moreover, isotopic data from modern plants and

livestock (Lazzerini et al., n.d. – **see Chapter 5 and 6**) were also used in order to constrain the local isotopic baseline.

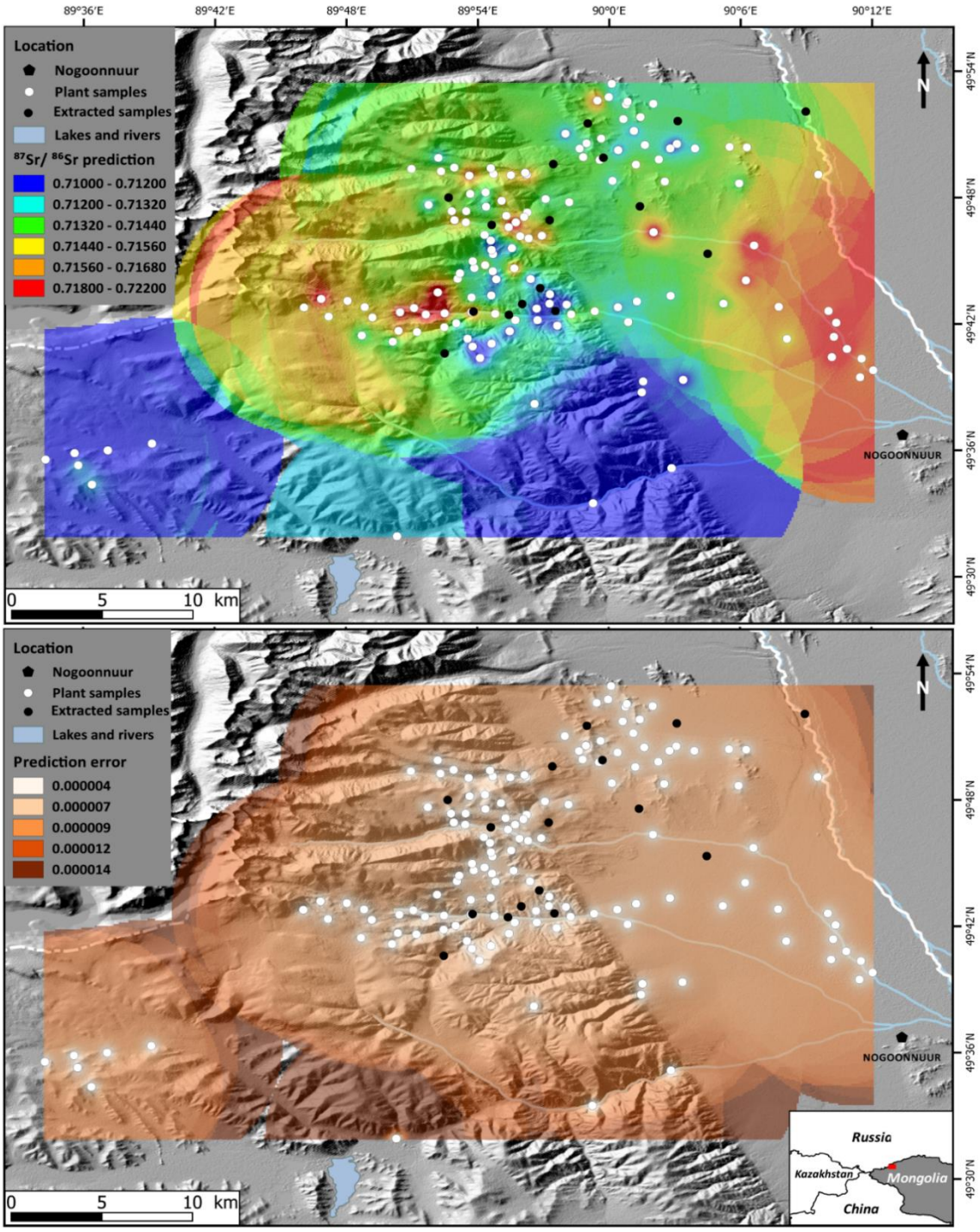

Figure 26: Bioavailable $^{87}Sr/^{86}Sr$ isoscape (top panel) and its associated predicted error (bottom panel) of the study area near the village of Nogoonnur, Western Mongolia and encompassing the study site of Burgast (white star) (Lazzerini et al., n.d. –see Chapter 6). White circles represent bioavailable $^{87}Sr/^{86}Sr$ sampling localities used to create the model. Black dots represent the 16 randomly selected sampling locations that were extracted prior to model development and used later to test the model predictions. Colors indicate areas of lowest bioavailable $^{87}Sr/^{86}Sr$ (blue) to highest bioavailable $^{87}Sr/^{86}Sr$ (red) for the top panel and lowest predictive error (light beige) to highest predictive error (brown) (from Lazzerini et al., n.d. – see Chapter 6).

7.3 Materials

7.3.1 The archaeological site of Burgast and the horse specimens

The site of Burgast is located in the Aimag of Bayan-Ulgii (Sum of Nogoonnuur), about 100 km north-east from Ulgii as the crow flies, about 15 km from the border with the Republic of Tuva and about 20 km south of the Republic of Altai (**Figure 26**). This area is located on the eastern fringes of the Altai mountain range, in its Mongolian part. Bordered to the south by a river and to the north by a rocky massif, the site has the shape of a triangular terrace of ca. 20 ha, at an altitude of 1900 m. Archaeological remains from several periods (Late Bronze Age, Hun Sarmate, Türk) are scattered along the terrace, and these were excavated in 2015 and 2016 by the French-Mongolian Joint Archaeological Expedition. Among the different structures, a khirgisuur and an intersecting Turkic tomb, excavated in 2016, are the purpose of this article (**Figure 27**).

7.3.1.1 The khirgisuur and the Bronze Age horses

This Late Bronze Age khirgisuur has a "classical" structure for this type of funerary monument found in Mongolia. It is composed of a 15.5 × 14 m central stone mound (ST 60 – **Figure 27**) containing the remains of a human body oriented west-east. Excavation of the stones revealed the existence of a casing made of large rocks. No grave good was found in association with the deceased. A quadrangular fence (20 × 18 m) formed by an alignment of stones and having small mounds at the corners surrounds this central mound. As with most khirgisuurs, it is associated with external structures in the form of mounds and stone circles. On the western side of the rectangular area, there are four stone circles aligned over a length of 14 m (ST 68 to 71). These stone circles did not reveal any remains, although these structures generally yield burnt bones and teeth of caprines (Broderick et al., 2014, 2016; Lepetz et al., 2019). On the eastern side, there are seven mounds (ST 61 to 67) yielding horse remains of at least 8 individuals, mainly represented by their skulls or mandibles and sometimes accompanied by connected cervical vertebrae and terminal phalanges. The horse remains are fairly well preserved, but bone displacements, breakage and missing parts seem to indicate that taphonomic disturbances (possibly by burrowing animals) have occurred, although it is not always possible to precisely define their extent. Two males and one female have been identified. Individual ages range from 1 to 18–20 years old.

Five out of the eight horses (ST 61; ST 63; ST 65A & B; ST 66) were included in the study. The other ones (ST 62; 64 and 67) were too old at death, making their heavily worn teeth difficult to sample without damaging the enamel (**Table 17**).

Table 17: Characteristics of the Bronze Age samples analysed in this study. Subscript and superscript indicate that the molar was taken from the lower or upper jaw, respectively. Teeth are classed as complete when root development has begun. The ^{14}C dates were provided by A. Zazzo. More information on dating methodology is available in Zazzo et al (2019).

Sample	Species	Sex	Estimated age (years)	^{14}C date ± error (1σ)	Target #	Calibrated date (BCE)		Sampled tooth	State of tooth
						from	to		
ST 61 M1	*Equus caballus*	?	1	2814 ± 28	ECHo 1507	−1052	−898	M_1 right	Incomplete
ST 61 M2								M_2 right	Incomplete
ST 63 M2	*Equus caballus*	?	?	2838 ± 27	ECHo 1509	−1085	−918	M_2 left	Complete
ST 63 M3	*Equus caballus*							M_3 left	Complete
ST 65A M2	*Equus caballus*	?	?	2874 ± 26	ECHo 1511	−1126	−941	M^2 right	Complete
ST 65A M3	*Equus caballus*							M^3 right	Complete
ST 65B M2	*Equus caballus*	M	?	2846 ± 28	ECHo 1512	−11110	−921	M_2 left	Complete
ST 65B M3	*Equus caballus*							M_3 left	Complete
ST 66 M2	*Equus caballus*	M	~ 5	2887 ± 25	ECHo 1513	−1190	−979	M^2 right	Complete
ST 66 M3	*Equus caballus*							M^3 right	Incomplete
ST 72 M2	*Equus caballus*	?	~2.5	1235 ± 25	ECHo 1515	688	877	M^2 right	Incomplete
ST 72 P4	*Equus caballus*							P^4 right	Incomplete

7.3.1.2 The horse from the Turkic period

The structure 72 (ST 72 – **Figure 27**) intersecting the quadrangular fence of the khirgisuur (ST 60) on its northern side, is the individual grave of a 20-30 years old adult female aged, associated with the remains of a horse, placed on his belly with the lower limbs folded under him and head oriented to the south. These remains were dated from the 7-8th century AD (**Table 17**). The human and horse remains were not found in the same pit but in two separate excavations, separated by a large block of stone. Several pieces of ornaments (pearl necklaces, bronze rings) and offerings (bark bowl, caudal vertebra of sheep) accompany the subject. The horse is accompanied by four iron objects: a bit located near the mandible on the left side, a small loop located near the head and two stirrups on both sides of the spine. The stage of dental eruption indicates that this animal was approximately 2.5 year old at death (Cornevin and Lesbre, 1894).

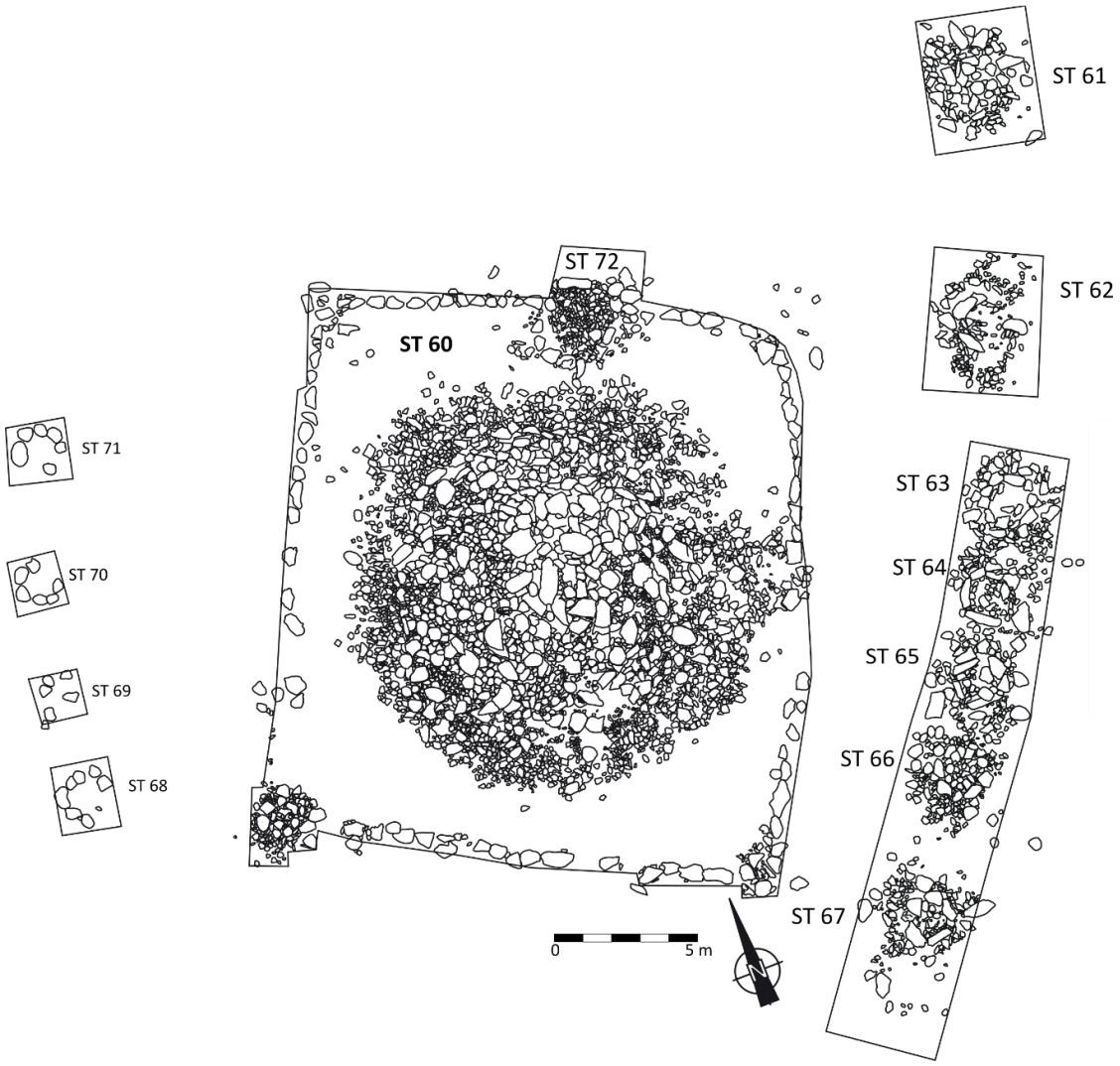

Figure 27: General view of the Burgast khirigsuur with the central stonemound (ST 60) in the quadrangular stone enclosure and its peripheral structures that provided horse remains (ST 61 to ST 67). On the north side of ST 60, there is the Turkic tomb intersecting the stone enclosure (ST 72) (figure by S. Lepetz).

7.3.2 The 'local' isotopic baseline

In order to determine origin and mobility of archaeological horses, we need to provide an assessment of local geographical $\delta^{18}O$, $\delta^{13}C$ and $^{87}Sr/^{86}Sr$ variation, supposing minors' changes in plants communities, geological bedrocks, precipitation and temperatures.

Lazzerini et al. (n.d. – **see Chapter 6**) already produced a bioavailable strontium isoscape for this area that was based on modern plant samples, displaying a range of $^{87}Sr/^{86}Sr$ values from 0.71007 to 0.72340 with a mean of 0.71456 (2SD = 0.0053 - **Figure 26**) and on modern caprines$^{87}Sr/^{86}Sr$ values. This high variability represents the Sr complexity of mountain range. The different grazing areas are completely free of modern agricultural fertilizers that

have been known to alter local strontium isotope composition (Frei and Frei, 2011; Maurer et al., 2012; Thomsen and Andreasen, 2019). Thus, modern plants and livestock provide a good estimate of bioavailable strontium of the area around the site of Burgast. Unfortunately, the area north of Burgast could not be sampled as intensively due to the proximity with the Russian border (**Figure 26**). Moreover, oxygen and carbon isotopic composition of archaeological horses were compared to modern horses' isotopic composition (**Table 18; Figure 28**) that were previously analysed by Lazzerini et al. (n.d. – **see Chapter 5**). In this study, we added measurements of $^{87}Sr/^{86}Sr$ for one modern horse's tooth (2017-104-M2).

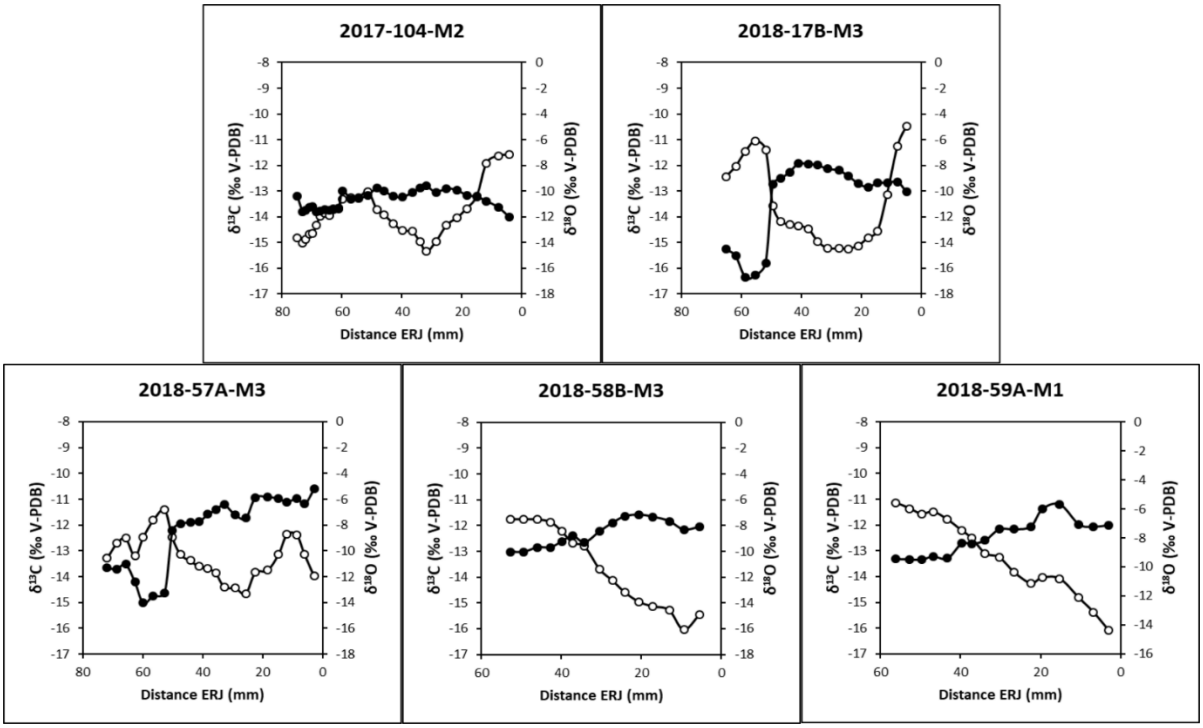

Figure 28: Oxygen ($\delta^{18}O$) and carbon ($\delta^{13}C$) isotopes values along the tooth crown of modern horse molars. ERJ is the distance between the sample and the enamel-root junction. White and black circles represent measured $\delta^{18}O$ (‰) and $\delta^{13}C$ (‰) respectively, with analytical error inside the square (from Lazzerini et al., n.d. – see Chapter 5).

7.4 Methods

7.4.1 Carbon and oxygen isotopic analysis

Horse teeth surfaces were cleaned by mechanical abrasion with tungsten drill bits to remove the cement. Sequential sampling of modern and archaeological teeth was performed on the mesial side of the first (M1), second (M2) or third (M3) mandibular or maxilla molars, depending on preservation and age of individuals. The mesial side was chosen for practical convenience (this side has a flat surface with a narrow cementum layer) and also because it

should mineralize faster (Zazzo et al., 2012). The sampling spans the width of the mesial side. Enamel was drilled with a diamond bit, perpendicular to the tooth growth axis from the top of the crown to the enamel root junction (ERJ). Samples were taken every 1.5-2mm through the entire thickness of the enamel layer and care was taken to avoid collecting the underlying dentine. Sample position was recorded in terms of their distance (in mm) from ERJ. Powdered enamel thus recovered (~ 6-7mg) samples were chemically treated following the procedure described in Balasse et al. (2002). First, organic matter was removed with a solution of 2-3% NaOCl (24h, 0.1 ml solution/ mg of sample) and rinsed several times in distilled water. Then, each enamel sample reacted with 0.1 M acetic acid (4h, 0.1 ml solution/mg of sample) to remove exogenous carbonates and rinsed in distilled water and dried in an oven at 80°C for 12h. The same protocol was applied to modern and archaeological samples to avoid biases due to pre-treatment-induced changes in the $\delta^{18}O$ values of enamel (M. Balasse et al., 2012; Koch et al., 1997).

Purified enamel samples were weighted (600 µg approximately) and analyzed on a Kiel IV device connected to a Delta V Advantage isotope ratio mass spectrometer (IRMS) at the *Service de Spectrométrie de Masse isotopique du Muséum national d'Histoire naturelle* (SSMIM) in Paris. Samples were placed into individual vessels to react under vacuum with phosphoric acid [H_3PO_4] at 70°C and purified CO_2 in an automated cryogenic distillation system. Analytical precision was 0.04‰ for $\delta^{18}O$ and 0.02‰ for $\delta^{13}C$ based on the repeated (n= 30) analysis of our internal laboratory carbonate standard (Marbre LM) normalized to NBS 19. Isotope data are presented in δ notation [$\delta = (R_{sample}/R_{standard}) - 1$], with R the isotope ratio ($^{18}O/^{16}O$ and $^{13}C/^{12}C$) of the sample, reported relative to the international standard V-PDB (Vienna PeeDee Belemnite) and expressed in per mil (‰).

The average $\delta^{18}O$ and $\delta^{13}C$ values between individuals and time periods were compared using the One-way ANOVA statistical test coupled with Tukey's post-hoc test using R software version 3.4.4 with a significance threshold at p-value < 0.05.

7.4.2 Enamel $^{87}Sr/^{86}Sr$ ratio analysis: LA-MC-ICP-MS

Sr isotope profiles were performed on the second molar (M2) of one modern horse (individual 2017-104) and 6 archaeological horses using LA-MC-ICP-MS (Laser Ablation - Multiple Collector - Inductively Coupled Plasma - Mass Spectrometry). One third molar (M3), of individual ST 63, were analysed. Following $\delta^{18}O$ and $\delta^{13}C$ analysis, the teeth were washed in distilled water and then were sliced longitudinally with a diamond disc, mounted in polyester

resin (GBS - BROT LAB) to expose the whole dental structure and polished (Abrading with silicon carbide powder 13 and 5 µ – F500 and F1000 Escil®).

We targeted the inner enamel layer, because this zone is highly mineralized early in the mineralization process which limits the attenuation of the isotopic signal (Balasse, 2003; Blumenthal et al., 2014; Tafforeau et al., 2007; Zazzo et al., 2005). LA profiles were performed mainly on the lingual side for practical reason, to avoid the pits caused by $\delta^{18}O$ and $\delta^{13}C$ analysis. $^{87}Sr/^{86}Sr$ was measured *in situ* by a laser-ablation multi-collector inductively coupled plasma mass spectrometer (LA-MC-ICP-MS). Sr data were acquired with Nu 500 HR MC-ICP-MS (Nu Instruments Ltd.), coupled to a 193 nm laser ablation system - Photon Machines Excite®) at the *Ecole Normale Supérieure* in Lyon (ENSL). The inner enamel layer was ablated using 85 µm diameter ablation spots, a laser scan speed of 60 $\mu m.s^{-1}$, 100% laser intensity and 10-Hz frequency (**Supp. Info S7.1** summarizes the operating parameter used for the LA-MC-ICP-MS measurements).

Teeth were analysed in two or three consecutive runs depending on tooth total length. For each laser ablation sequence, calibration of the LA-MC-ICP-MS was achieved by analyzing NIST SRM 1400 (bone ash). Sample aerosol was carried to the ICP-MS using a mixture of He and N_2. Masses 88, 87, 86, 85, 84 and 83 were measured on Faraday cups. The isobaric interference of ^{87}Rb was corrected using the ^{85}Rb. Krypton interferences at masses 84 and 86 were corrected using ^{83}Kr. Measurements of NIST SRM 1400 gave an average $^{87}Sr/^{86}Sr$ value of 0.71384 ± 0.000214, in good agreement with the published values for this material (Weber et al., 2018). A single correction was applied for each tooth based on the average NIST SRM 1400 values measured between the different transects. Finally, a centered moving average on 35 individual measurements (~2 mm length) was used to smooth variability of the final profiles.

7.4.3 Estimation of highland occupation and altitudinal mobility

We estimated the average grazing elevation of the ancient horse using the equation proposed by Lazzerini et al. (n.d. – **see Chapter 5**) who found a significant negative correlation between average $\delta^{13}C$ of diet ($\delta^{13}C_{diet}$) and the mean grazing altitude ($Elev_{avrg}$ *(m)*; Eq. 1):

$$\delta^{13}C_{diet} = -0.0014493 \times Elev_{avrg} - 24.14 \quad \text{(Eq. 10)}$$

Moreover, we estimated the percentage of time spent above 2000 m (i.e. representing the minimum altitude of alpine meadows in the mountainous western part of the study area – **Figure 26**). Using the equation proposed by Lazzerini et al. (n.d. - **see Chapter 5**) who found

a significant negative correlation between average $\delta^{13}C$ of diet ($\delta^{13}C_{diet}$) and the time spent at high elevation (Time_Alt; Eq. 2):

$$\delta^{13}C_{diet} = -0.011625 \times Time\_Alt\ (\%) - 26.73 \qquad \text{(Eq. 11)}$$

In order to apply it to ancient material, it is necessary to correct the isotope values by -2‰ (Dombrosky, 2019; Graven et al., 2017) to take into account the Suess effect (Suess, 1955). The $\delta^{13}C_{diet}$ value were calculated using $\delta^{13}C$ enamel and a isotope fractionation of 14.7‰ modified from (Cerling and Harris, 1999), as proposed by Lazzerini et al (*n.d.* – **see Chapter 5**).

Finally, to investigate the potential existence of altitudinal mobility by horses, we calculated the Pearson's correlation coefficient between $\delta^{13}C$ and $\delta^{18}O$ values of a same tooth to estimate the potential altitudinal mobility of archaeological horses. We hypothesize that anti-covariation in the between carbon and oxygen isotopic values indicates an altitudinal mobility performed by horses with exploitation of lowlands and highlands (Lazzerini et al., n.d. - **see Chapter 5**; Makarewicz et al., 2017; Tornero et al., 2018).

7.5 Results

7.5.1 Oxygen isotopes

Summary oxygen and carbon isotopic results obtained for all horses are reported in **Table 18** and complete data are available in supplementary data (**Supp. Info S7.2**). Oxygen isotope profiles followed a sinusoidal pattern with maximum and minimum values reflecting hot seasons and cold seasons respectively (**Figures 28 & 29**). The LBA horses had an average $\delta^{18}O$ value of -12.8 ± 2.4‰, with values ranging from -17.9 to -5.7‰. Their intra-tooth amplitude in $\delta^{18}O$ value are significantly lower (*p-value* = 0.001) than that of the modern horses (-10.8 ± 2.6‰ - **Table 18**), and ranged from 3.5 to 6.9 ‰ (**Table 18**). The Turkic horse exhibited an average $\delta^{18}O$ value of -11.2 ± 1.2‰, with values ranging from -14.6 to -8.8 ‰ with amplitude of 2.2 ‰ and 5.7 ‰ recorded in the P4 and M2, respectively.

The average $\delta^{18}O$ values are significantly different between the modern and the LBA horses (*p-value* < 2.2e-16) but not between the modern and the Turkic horse (*p-value* = 0.58). Average $\delta^{18}O$ values are significantly different between the LBA and the Turkic horse (*p-value* = 2.0e-04) (**Figure 30**).

This significantly lower average $\delta^{18}O$ values recorded by LBA horses are caused by a significant difference in intra-tooth maximum values (*p-value* = 0.009). On average, intra-tooth maxima were higher in modern horse than in BA horse (-6.4 ± 1.1‰ vs 10.1 ± 2.3‰). They were also more variable, ranging from -7.5 to -5.0 ‰ in modern horse and from -13.1 to -5.7‰ in LBA horses (**Table 18**; **Figure 30**). On the contrary, there was no significant difference in minimum $\delta^{18}O$ values between LBA and modern horses (*p-value* = 0.86). The average minimum $\delta^{18}O$ values are -14.6 ± 1.0‰ and -15.2 ± 2.3‰ for modern and LBA horses respectively (**Figure 30**).

Table 18: Summary statistics of the oxygen and carbon isotopic analyses of enamel bioapatite samples. A = Amplitude; N = number of samples by tooth. $\delta^{13}C$ (‰ V-PDB) of archaeological horses have been shifted of -2‰ ("Suess effect"). Pearson's r = correlation coefficient between $\delta^{13}C$ and $\delta^{18}O$ sequences with the associated degree of freedom of the correlation (df) and the significance level (p-value). $Elev._{avrg}$ (m) = the estimated mean grazing altitude calculated from the average $\delta^{13}C$ value based on Eq. (1). Time-Alt (%) = the estimated percent of time spent in high elevation pastures (> 2000 m). * = isotopic values from modern horses (Lazzerini et al., n.d. –see Chapter 5).

Sample	$\delta^{18}O$ (‰ V-PDB)					$\delta^{13}C$ (‰ V-PDB)						Pearson's r	df	*p-value*	$Elev_{avrg}$	*Time-Alt (%)*
	Mean	SD	Min	Max	A	Mean	SD	Min	Max	A	N					
ST 61 M1	-11.7	2.0	-13.7	-6.8	6.9	-12.9	0.4	-14.0	-12.4	1.6	19	0.16	17	0.52	2382	74
ST 61 M2	7.0	1.0	-9.2	-5.7	3.5	-15.0	0.3	-15.4	-14.7	0.7	14	-0.32	12	0.27	3796	100
ST 63 M2	-15.7	1.9	-17.9	-13.1	4.8	-13.0	1.9	-13.2	-12.8	0.4	10	0.38	8	0.27	2478	86
ST 63 M3	-13.5	1.6	-15.7	-10.3	5.5	-12.8	1.6	-13.3	-10.7	2.6	20	0.07	18	0.75	2313	66
ST 65A M2	-13.9	1.3	-15.5	-11.5	4.1	-12.4	1.3	-12.8	-11.6	1.1	15	-0.66	13	0.008	2002	27
ST 65A M3	-13.5	1.4	-15.5	-11.4	4.1	-12.4	1.4	-13.0	-11.9	1.1	19	0.06	17	0.80	2057	34
ST 65B M2	-14.5	1.4	-16.1	-11.9	4.2	-12.5	1.4	-13.6	-11.8	1.7	32	-0.37	33	0.04	2078	36
ST 65B M3	-12.5	1.7	-16.0	-10.6	5.4	-12.7	1.7	-13.0	-12.2.	0.8	28	-0.29	26	0.13	2223	54
ST 66 M2	-13.0	1.9	-15.9	-10.1	5.8	-12.4	1.9	-12.9	-11.4	1.5	32	-0.09	30	0.63	2037	31
ST 66 M3	-12.9	1.5	-16.1	-10.2	5.9	-12.2	1.5	-12.8	-11.6	1.2	36	-0.16	34	0.35	1926	17
ST 72 M2	-11.4	1.4	-14.6	-8.8	5.7	-13.2	1.4	-13.7	-12.5	1.2	30	-0.23	28	0.22	2575	98
ST 72 P4	-11.0	0.7	-12.0	-9.8	2.2	-13.1	0.7	-13.3	-12.7	0.6	16	0.17	14	0.53	2533	93
2017-104-M2 *	-11.8	1.9	-14.7	-7.2	7.5	-13..4	0.4	-14.0	-12.8	1.2	30	-0.26	28	0.17	2692	100
2018-17B-M3 *	-10.9	3.3	-14.5	-5.0	9.5	-13.3	1.6	-16.4	-11.9	4.4	20	-0.72	18	3e-04	2651	100
2018-57A-M3 *	-10.4	1.7	-13.3	-6.8	6.5	-12.2	1.4	-15.0	-10.6	4.4	23	-0.60	21	0.002	1926	17
2018-58B-M3 *	-11.2	3.1	-16.1	-7.5	8.6	-12.3	0.5	-13.0	-11.6	1.4	20	-0.88	13	2e-05	1968	22
2018-59A-M1 *	-9.2	2.7	-14.4	-5.6	8.8	-12.5	0.7	-13.3	-11.2	2.1	16	-0.82	14	8e05	2085	37

7.5.2 Carbon isotopes

The LBA horses had an average $\delta^{13}C$ value, corrected from 'Suess effect', of –12.7 ± 0.7‰, with values ranging from -15.4 to -10.7‰. These horses showed an intra-tooth $\delta^{13}C$ amplitude ranging from 0.4 to 2.6‰, with average amplitude of 1.3 ± 0.6‰ (**Table 18**). The Turkic horse had an average $\delta^{13}C$ value of -13.2 ± 1.2‰, with values ranging from -13.7 to -12.5 ‰ with amplitude of 0.6 ‰ and 1.2 ‰ recorded in the P4 and M2 molars respectively.

We calculated an average $\delta^{13}C_{diet}$ value of -27.5 ± 1.1‰, -27.4 ± 0.7‰ and -27.9 ± 0.3‰ for modern, LBA, and Turkic horses respectively, indicating that the horses consumed a diet including no or very little C_4 plants. There was no statistical difference between the $\delta^{13}C$ values of modern and

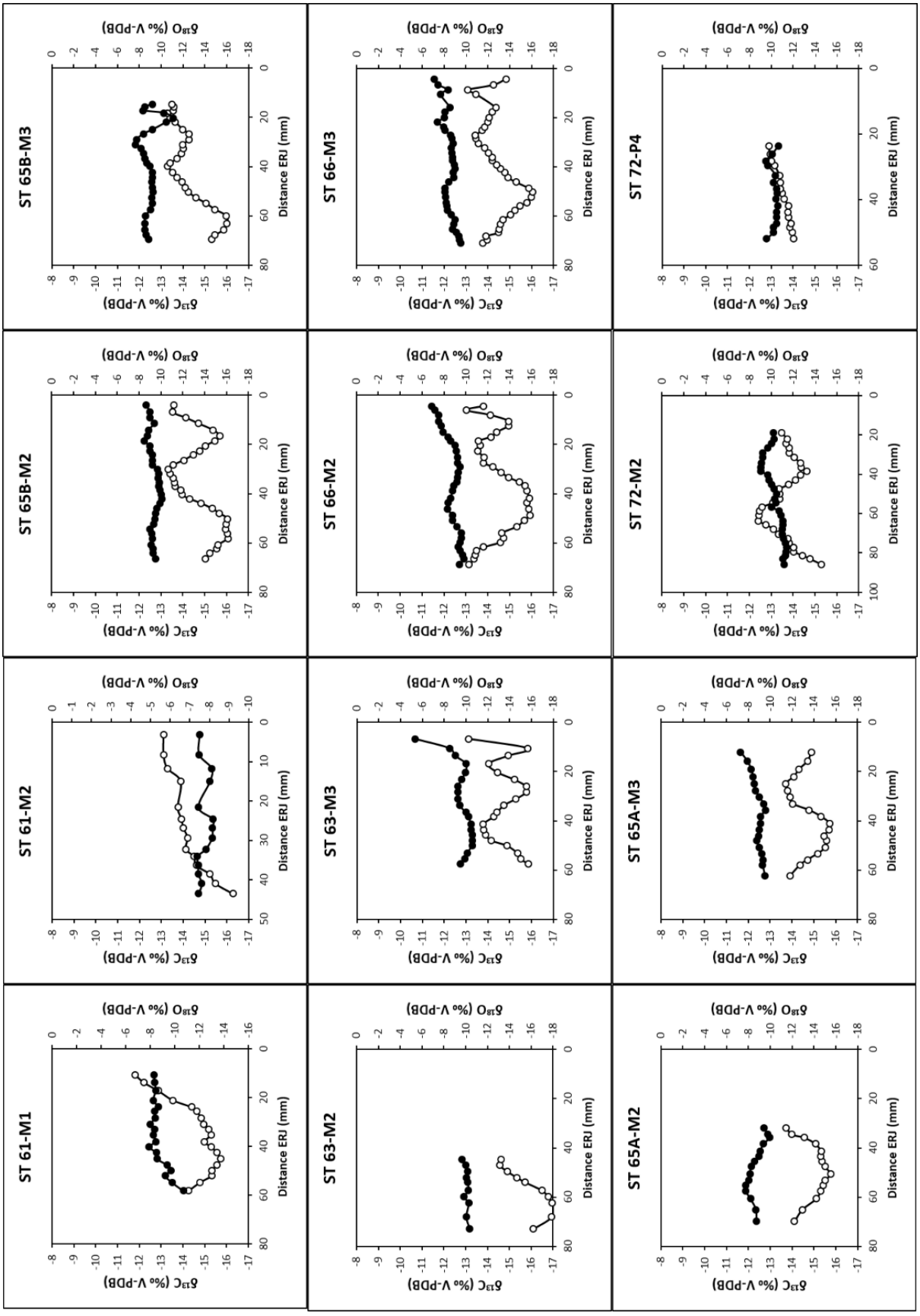

Figure 29: Oxygen ($\delta^{18}O$) and carbon ($\delta^{13}C$) isotopes values along the tooth crown of archaeological horse molars. ERJ is the distance between the sample and the enamel-root junction. White and black circles represent measured $\delta^{18}O$ (‰) and $\delta^{13}C$ (‰) respectively, with analytical error inside the square.

LBA horses (*p-value* = 0.4). The intra-tooth amplitude of modern horse was significantly higher than that of the LBA horses (*p-value* = 0.046), (**Figure 30**). This is due to two individuals 2017-17B and 2017-57A which exhibited high intra-tooth variations of 4.4‰ with a rapid isotope shift occurring in the upper part of the crown (**Table 18; Figure 30**).

Based on the equations (8) and (9), we estimated an average grazing altitude of 2329 ± 376 m for the LBA horses, ranging from 1926 to 3796 m (**Table 18**) and an altitudinal occupation of 68 ± 68%, ranging from 17% to 100%. For the Turkic horse, we estimated an average grazing altitude of 2575 and 2533 m based on the M2 and the P4, respectively, with a time spent at high elevation superior to 90% (**Table 18**).

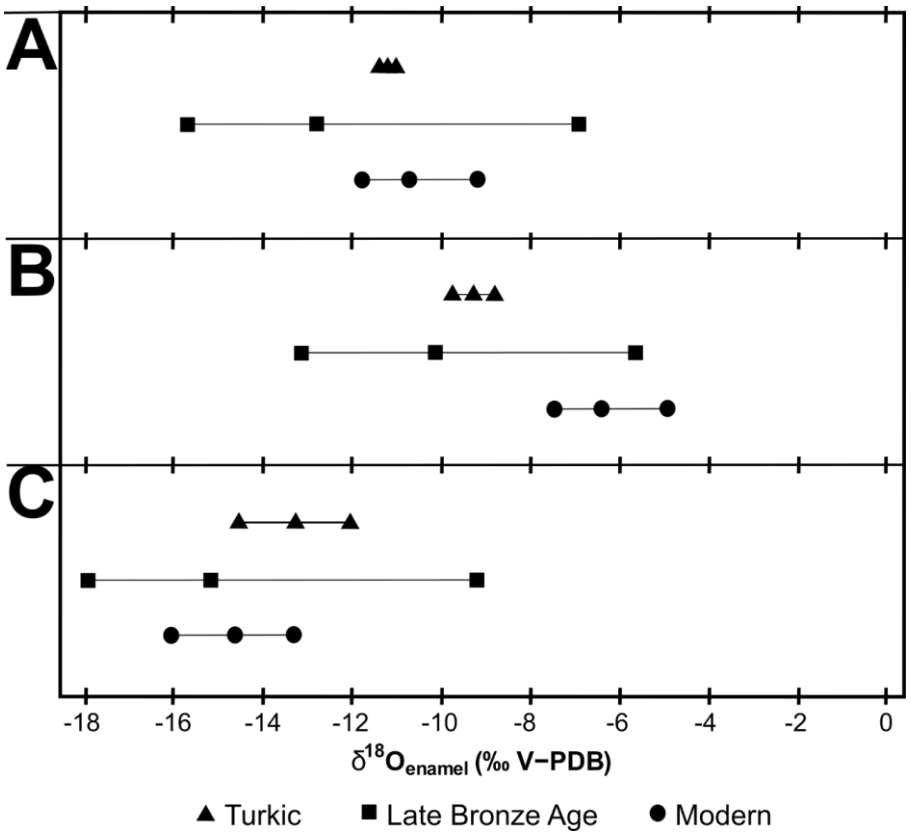

Figure 30: Comparison of (A) means, (B) maxima and (C) minima $\delta^{18}O$ (‰ V-PDB) of modern, BZA and Turkic teeth.

7.5.3 Correlation between $\delta^{18}O$ and $\delta^{13}C$ variations

We tested the correlations between $\delta^{13}C$ and $\delta^{18}O$ values measured in the same tooth. Plots for all the individuals are shown in (**Supp. Info S7.3**). Isotope values were negatively correlated in the modern horse teeth (r coefficient from -0.88 to -0.26). These correlations were statistically significant (*p-value* < 0.05), except for 2017-104-M2 (**Table 18**). LBA horse teeth exhibited more variable Pearson's correlation coefficients, ranging from -0.66 to +0.38, and

few were statistically significant (**Table 18**). Finally, the two Turkic horse teeth showed a correlation coefficient of +0.17 and -0.23, which were not statistically significant.

7.5.4 Strontium isotopes

Strontium isotopic data from archaeological and modern horses are presented in **Table 19**, **Figures 31 & 32**. Complete LA-MC-ICP-MS results are available in **Supp. Info. S7.4**.

The $^{87}Sr/^{86}Sr$ ratio of the modern individual was 0.71271 ± 0.001 (2 SD) on average and ranged between 0.71177 and 0.71488 (amplitude = 0.00310), within the range of the bioavailable strontium defined for the study area (**Figure 31**). The $^{87}Sr/^{86}Sr$ profile was relatively flat, except toward the tooth base where a large and rapid variation of ca. 0.003 was observed (**Figure 32**).

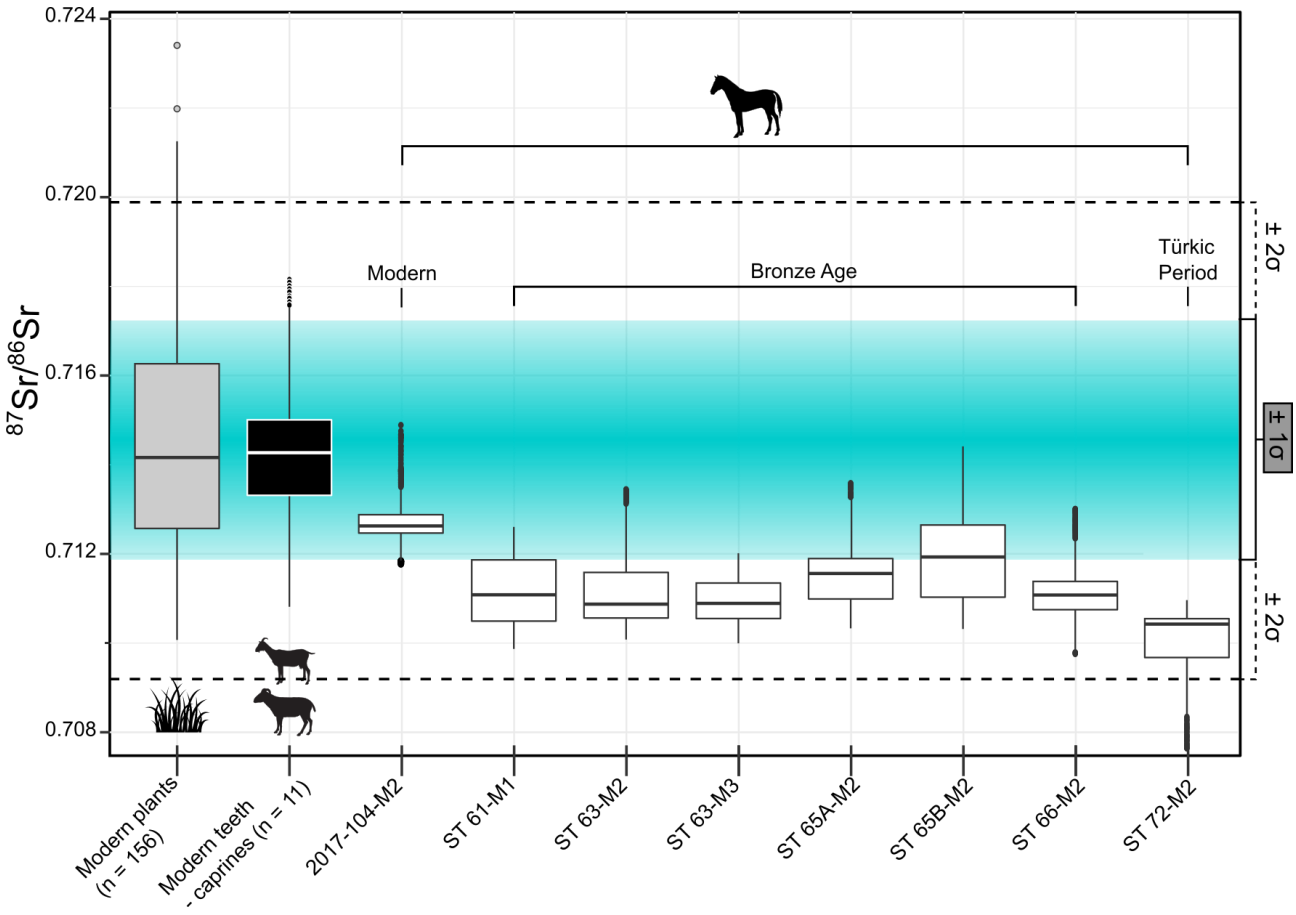

Figure 31: Sr isotope ratios of modern and archaeological horses (white boxes) and modern caprines (black box), compared to the bioavailable Sr isotope ratios (grey box), estimated from plants from Burgast, western Mongolia. The blue shade represents the mean ± SD of plant $^{87}Sr/^{86}Sr$ and hence illustrates the local range of Sr isotope ratios.

The average $^{87}Sr/^{86}Sr$ ratios of the LBA horse was comprised between 0.71097 ± 0.001 (2 SD) to 0.71188 ± 0.002 (2 SD), significantly lower than for the modern horse (*p-value* < 2e-^{16}). Most of individuals showed lower values than the defined average local bioavailable strontium baseline ± 1σ (**Figure 31**). The $^{87}Sr/^{86}Sr$ ratio of the five LBA horses had similar intra-tooth amplitude, ranging from 0.00273 to 0.00409. LBA horses exhibited different intra-tooth patterns than modern horses with a general stable trend interspersed with more frequent and closer variations along the tooth crown (**Figure 32**). Generally, these variations showed similar increasing and decreasing values (ca. 0.002), sometimes more. Even with these variations, the average $^{87}Sr/^{86}Sr$ ratio trend along the tooth remained stable, except for ST 65B which exhibited a general decreasing trend.

The Turkic horse, had $^{87}Sr/^{86}Sr$ ratios ranging from 0.70765 and 0.71096, exhibiting values lower than the 'local' bioavailable strontium, but average value is within the local baseline ± 2σ (**Figure 31**). Average value for Turkic horse is significantly lower than for the modern horse and LBA horses (*p-value* < 2e-^{16}) The intra-tooth profiles showed a slow and constant increase along the tooth crown from the apex to the base of the crown, except a successive rapid decrease and increase at the apex of the tooth crown (**Figure 32**).

Table 19: Summary results of measured intra-tooth $^{87}Sr/^{86}Sr$ values, for a moving average on 35 individual measurements.

Sample	Moving average of $^{87}Sr/^{86}Sr$						
	Mean	**2SD**	**Min**	**Max**	**A**	**Median**	**N**
ST 61 M1	0.71116	0.00152	0.70987	0.71260	0.00273	0.71108	798
ST 63 M2	0.71114	0.00166	0.71008	0.71344	0.00336	0.71087	1110
ST 63 M3	0.71097	0.00101	0.71000	0.71201	0.00202	0.71089	1235
ST 65A M2	0.71152	0.00129	0.71033	0.71358	0.00325	0.71156	962
ST 65B M2	0.71188	0.00197	0.71032	0.71440	0.00409	0.71193	1143
ST 66 M2	0.71112	0.00134	0.70976	0.71300	0.00324	0.71108	1031
ST 72 M2	0.71271	0.00067	0.70765	0.71096	0.00331	0.71043	1023
2017-104-M2	0.71271	0.00100	0.71177	0.71488	0.00310	0.71262	1374

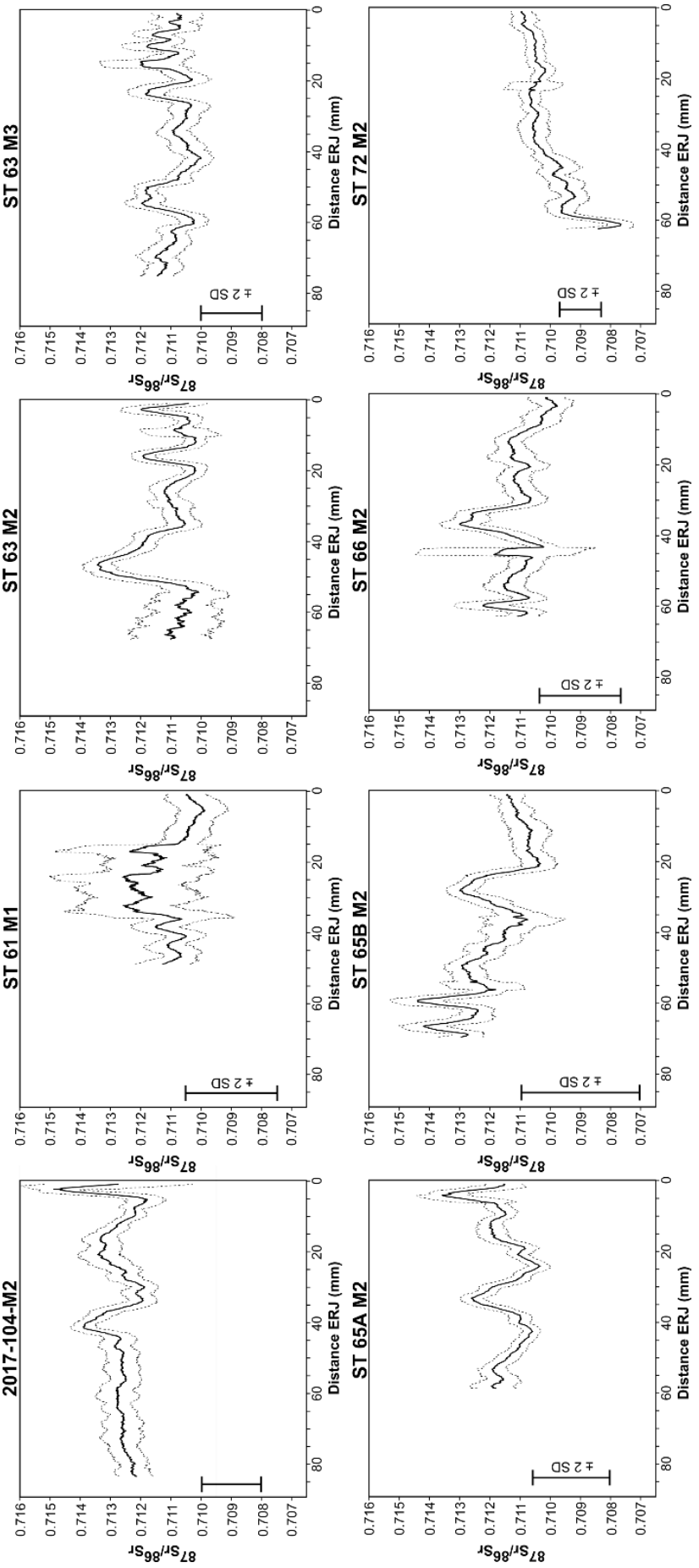

Figure 32: Strontium isotope values along the tooth crown of modern (2017-104-M2) and archaeological horse molars. ERJ is the distance between the sample and the enamel-root junction. The thick black line light grey shading indicates a 35-point running average of the $^{87}Sr/^{86}Sr$ datapoints. Dashed lines represents the ± 1σ.

7.6 Discussion

7.6.1 Deciphering the geographical origin of the horses

We observed a significant difference between the $\delta^{18}O$ values of modern and ancient horses (*p-value* < 0.05), with significantly lower $\delta^{18}O$ values for archaeological specimens. The archaeological horses recorded lower maxima and lower amplitude than the modern horses (**Figure 30**). Moreover, amplitude of modern horses are higher than those recorded in the teeth of other horses in Mongolia (Bendrey et al., 2017; Blumenthal et al., 2019; Stacy, 2009). The sinusoidal variations in the oxygen isotopic time series of sampled teeth reflect seasonal changes in the $\delta^{18}O$ of ingested water, with high $\delta^{18}O$ values reflecting summer season and low $\delta^{18}O$ values reflecting winter season.

Since there is a direct relationship between the isotopic composition of horse enamel and that of drinking water, which is linked to environmental parameters, these lower values of $\delta^{18}O$ are caused by lower temperatures, higher amounts of precipitation, or an ^{18}O enrichment of open water or plants due to evaporation, which is less important especially during the summer period (Dansgaard, 1964; Pederzani and Britton, 2019; Rozanski et al., 1993). Thus, the lower values could be explained by a more northern origin, from upper region of central Asia, due to the latitudinal variation of $\delta^{18}O$ values of meteoric waters (Pederzani and Britton, 2019), as proposed by Bendrey et al. (2017) for two Iron Age horses buried in the Mongolian Altai. However, we cannot exclude the possibility that climate change may have had an influence on $\delta^{18}O$ environmental values. Based on geomorphological and sedimental analysis of glacier, dendrochronology and palynological approaches, the Bronze Age was described as being colder and wetter with larger glaciers (Agatova et al., 2014, 2012; Unkelbach et al., 2018). A generally colder and wetter climate during this periods could explain the lower average value and amplitudes for horses. This is supported by other data from North-Central Mongolia, where Bronze Age horses recorded also lower $\delta^{18}O$ values than modern horses from the same area (Stacy, 2009). For the more recent Turkic Period there is no consensus, and some authors suggest an increase in temperatures (Agatova et al., 2014), while others propose that the climate remained cold and humid (Nazarov et al., 2012; Unkelbach et al., 2018). Consequently, the parsimonious interpretation of the $\delta^{18}O$ values did not allow us to infer the origin of the horses found in Burgast.

The average $^{87}Sr/^{86}Sr$ ratios of the archaeological horses are lower than the average value of the modern plants and livestock from the same area but still within 2 SD (**Figure 31**).

It is important to bear in mind that proximity to the Russian border prevented us from sampling further north and west of Burgast, limiting our knowledge of the bioavailable strontium of the area. In addition, the plant samples showed a great $^{87}Sr/^{86}Sr$ ratio variability (**Figure 26**). Such a high variability is expected for a mountainous area like Altai. Indeed, in geologically and/or structurally complex regions, with patchy bedrock geology, Sr isotope ratios are expected to be more variable (Crowley et al., 2017; Hoppe et al., 1999). When compared to isotope value of modern caprines and horses, archaeological recorded lower $^{87}Sr/^{86}Sr$ ratios than modern livestock on average, they still remain within the variability recorded by the plant samples (**Figures 26 & 31**) and do not necessarily indicate a 'non-local' origin. Actually, these horses $^{87}Sr/^{86}Sr$ values are similar to the values measured in the southern part of the study area and could therefore originate from there (**Figure 26**).

On the basis to the evidence to hand, oxygen and strontium isotopic values suggest that archaeological horses from LBA and Turkic period are from the area and probably from southern part. The probable local origin of Late Bronze Age horses is to be compared with the recent results onLate Bronze Age horses from khirgisuurs located in the Khanuy Valley, Central-North Mongolia (Makarewicz et al., 2018). The authors suggested that the horses came from diverse geographically distant locales, through trading, gift or exchange, indicating social networks active over great regional scale, between communities. It should be noted that most of these horses were associated with larger khirgisuurs, than the one of Burgast, with numerous stone mounds (thus horse skulls) ranging from a few dozens to several hundred (Allard and Erdenebaatar, 2005; Lepetz et al., 2019; Makarewicz et al., 2018). For example, two analysed horses from the larger khirgisuur (KYR-1 with 1700 stone mounds) showed $^{87}Sr/^{86}Sr$ ratios superior and inferior to the local baseline. These large khirgisuur were constructed quickly (Zazzo et al., 2019) and thus have drawn on an area luch larger than local communities, suggestion social network active over great distances (Houle, 2017). Regarding our data, the local origin of all horses from a common monument may suggest a single and local community, *a priori* linked with the small size of this khirgisuur.

7.6.2 Landscape use since the Bronze Age

The general opposite trends in intra-tooth carbon and oxygen isotope profiles identified in archaeological horse teeth (**Table 18; Supp. Info S7.3**) could be related to the same patterns observed in modern livestock modern horse and caprine teeth from the same area showing negative correlation between intra-tooth $\delta^{18}O$ and $\delta^{13}C$variations (Lazzerini et al., n.d. – **see**

Chapter 5). Lazzerini et al. (n.d. – **see Chapter 5**) have observed that the comparison of $\delta^{13}C$ and $\delta^{18}O$ values informed on variation in the altitudinal pattern of animals. Individuals displaying a large range of altitudinal residency showed a negative correlation between $\delta^{13}C$ and $\delta^{18}O$ sequences, whereas individuals with a more restricted mobility displayed a positive correlation between $\delta^{13}C$ and $\delta^{18}O$ values. In addition, the inversed pattern between $\delta^{18}O$ and $\delta^{13}C$ intra-tooth sequences has been also identified in caprines from Pyrenees exhibiting a vertical transhumance from lowland areas occupied in the winter to higher altitude meadows during the summer (Tornero et al., 2018). Modern domesticated horses and caprines from Burgast area exploit alpine meadows of the Altai mountains (Finke, 2004; Lazzerini et al., 2019; Lazzerini et al., n.d. - **see Chapter 5**). This altitudinal mobility is characterized by frequent movements between lowland and highlands pastures with generally higher mean grazing altitude during summer than during winter. Consequently, the negative Pearson's correlation (**Table 18**) observed in teeth from the modern horses, is in good agreement with the mobility pattern already documented for livestock in the same area. The low summer $\delta^{13}C$ values seen in most LBA horses indicate these animals grazed in high elevation pastures mainly due the higher humidity of these pasture caused to the higher influence of summer precipitations, snow melting and less evapotranspiration at this altitude. Moreover, the absence of significant difference between mean $\delta^{13}C$ values of modern and horse suggest a potential exploitation of the same ecological areas and particularly high altitude pastures with an mean grazing altitude for BA horses around 2300 m (**Table 19**) similar to the one of modern horses in Altai (Lazzerini et al., 2019). Concerning, the Turkic horse, ST 72, the M2 recorded an inversed pattern between its $\delta^{18}O$ and $\delta^{13}C$ sequences, but not the P4 (**Table 18; Figure 29**). The P4 was still growing when sampled preventing the record of a complete seasonal cycle and possibly the record of anti-correlation for the P4. Combined oxygen and carbon isotopic composition indicated that horses from the Late Bronze Age and Turkic period performed altitudinal mobility between highland and lowland pastures. Moreover, $\delta^{13}C$ values indicated a mean grazing altitude comparable to extant horses around 2300 m (**Table 18**) at this period.

The intra-tooth variations in strontium ratios of the ancient horses reflected their mobility between different geological bedrock areas (**Figure 32**). Unfortunately, identifying which areas were exploited specifically, by the modern horse, is difficult because its mobility pattern remains unknown. Therefore, accurate determination of the mobility of LBA and Turkic horses with respect to their strontium intra-tooth variations is unlikely. However, similarities in the pattern of strontium intra-tooth variation recorded by all LBA horses could be pointed out.

Indeed, all teeth exhibited frequent increase and decrease of $^{87}Sr/^{86}Sr$ ratio around an average values (**Figure 32**). The variations of $^{87}Sr/^{86}Sr$ can be observed in caprine teeth from the same and are closely linked to their mobility between pastures (et al, n.d. – **see Chapter 6**). Molars M2 and M3 of horses mineralizes in ~2 - 2.5 years (Hoppe et al., 2004). Thus, in the case of complete teeth (i.e. ST 63; ST 65A; ST 65B and ST 66 – **Figure 32**), we can link these frequent changes of $^{87}Sr/^{86}Sr$ ratios to frequent changes of pastures and suggest that these horses had probably a more complex mobility, comparable to today's horses, than a single summer vertical move and a lowland occupation during winter. Moreover, comparable intra-tooth patterns between LBA horses could suggest a similar pattern of mobility for these five horses between the same pastures. To go further, it is conceivable that a similar mobility could be a sign that the horses belong to the same herd and probably belong to a same household. This supports that the funeral practices associated with this small monument are only the result of a small community but it would suggest that potentially only one household related to the deceased were involved in the monument and probably over a short period.

Finally, the Turkic horse recorded a different intra-tooth $^{87}Sr/^{86}Sr$ variation with a stable increasing trend of values and only rapid variations at the start of the tooth formation (**Figure 32**). Its altitudinal mobility may have taken place between isotopically similar low and high elevation pastures, indicating a different exploitation of alpine meadows than LBA horses. Moreover, the absence of frequent intra-tooth important increase and decrease of $^{87}Sr/^{86}Sr$ values may suggest less frequent mobility over the period of the tooth formation compared to LBA horses. Moreover, the tooth was not fully mineralized and thus record a shorter period of time. The progressive increasing trend of values could be the result of one mobility between two isotopically different areas. This reduced mobility pattern could be related to the iron objects (a bit; small loop; two stirrups) found with the horses, suggesting a status of riding horse. Such a horse could potentially be more restricted in its mobility, staying close to the camp and moving only with its rider compared to herds of horses that could graze freely and thus moved more frequently. However, today, almost all the horses in the herd are riding horses (Marchina, 2016). There is a rotation to maintain a consistent level of familiarity with all the individuals in a herd. There is no reason to think that this could not have been the case in the past. Thus, a reflection still needs to be carried out to consider all possible explanations for this particular trend in strontium values in the horse Türk.

7.7 Conclusion

This study presents a new contribution to understand the movements of domesticated horses in the Altai Mountains and ritual practices of the populations related to the deposition of these horse remains associated with the funeral structures. The strontium isotopic data presented here suggest a common local origin for the five horses from the Late Bronze Age khirgisuur of Burgast and the one from the Turkic period. The average $^{87}Sr/^{86}Sr$ low values, comparing to modern livestock, suggest on exploitation of pasture, within the modern local baseline, from southern area. However, improving and extending the isoscape of bioavailable strontium of the study area, and Mongolia in general, would be necessary to more precisely assess the origin of these horses. Oxygen and carbon isotopic data presented here suggested an exploitation of alpine meadows by horses with the presence of seasonal altitudinal mobility since the Late Bronze Age and over Turkic period, similar to present day horses in Altai. Finally, the common origin of horses from one single LBA monument and similarities in intra-tooth strontium variation suggest that animals deposited in small khigisuurs may have belonged to a single household representing small-scale community from a local area related to the deceased of the Burgast's khirgisuur. Further DNA analysis may be useful to investigate kinship relationships of horses to support their membership to a common herd.

Acknowledgements

We are deeply indebted to all the herders who kindly participated to the study, providing the modern horse reference set, and to Bayarkhuu Noost (Institute of History and Archaeology, Mongolian Academy of Sciences, Mongolia) for the logistics and assistance during fieldwork. The isotopic analyses were performed at the Service de Spectrométrie de Masse Isotopique of the Muséum national d'Histoire naturelle of Paris (SSMIM) under the technical supervision of Denis Fiorillo. Fieldwork was supported by the French archaeological mission in Mongolia (CNRS, MNHN, MAEDI, director SL) and by the CNRS. This research was funded by a Ph.D. grant to NL from the French National Research Agency LabEx ANR-10-LABX-0003-BCDiv, in the context of the "Investissements d'avenir" n°ANR-11-IDEX-0004-02, and by an Inalco Early Career Research Grant 2017 to CM.

SUPPLEMENTARY INFORMATION CHAPTER 7

All supplementary information are available here:
https://drive.google.com/drive/folders/1hYCcbg_KaOxNDHQ8IzTb5HM2WABO2_Qd?usp=sharing

Supplementary Info S7.1: Parameters and operating conditions for Sr isotope determination by laser ablation MC-ICPMS.

Parameters	Values
Laser ablation 193 nm Excite	
Wavelength	193 nm
He flow rate	0.7 L/min
Ablation	
Spot size	85 µm
Frequency	10 Hz
Fluence	15.18 J/cm²
Sampling scheme	Line (dynamic)
Line translation rate	60 µm/s
sample Line length	~ 18 mm
standard line length	3 mm
MC-ICPMS Nu 500 HR	
Argon cool gas flow rate	14 L/min
Auxillary gas glow	1.4 L/min
Sample gas flow	0.7 L/min
Plasma power	1350
Resolution	
Data collection	
Gas background	30 s
Sample	~ 300 s
Integration	2 s

Supplementary Info S7.2: Complete data of oxygen and carbon isotopic analysis of tooth enamel from archaeological horses from Burgast. $\delta^{13}C$ was also corrected from the suess effect.

Supplementary Info S7.3: Plots of the Pearson's correlation between $\delta^{18}O$ and $\delta^{13}C$ values within intra-tooth sequential series for all individuals from Bronze Age and Turkic period.

Supplementary Info S7.4: $^{87}Sr/^{86}Sr$ results for each horse tooth measured by LA-MC-ICP-MS

PARTIE III – DETERMINER LA SAISON D'ABATTAGE

Chapitre 8 – Mise en place d'un référentiel moderne pour estimer la saison d'abattage par l'analyse du $\delta^{18}O$ de l'émail dentaire

Dans cette troisème partie de la thèse, nous abordons la détermination de la période d'abattage grâce à l'outil isotopique. Cette question est un paramètre crucial pour comprendre les pratiques d'élevage, de chasse, les stratégies d'occupation du territoire et les pratiques rituelles parfois liées à un calendrier saisonnier ou lithurgique.

En s'appuyant sur un référentiel moderne composé d'animaux dont la date de mort est précisément connue, ce premier chapitre de cette 3ème partie a comme objectif de montrer que les valeurs de $\delta^{18}O$ mesurées dans les dents des caprinés, reflétant les variations saisonnières de température, peuvent permettre de déterminer la période de mort de l'animal.

8.1 Résumé de l'étude

Pour évaluer la date de mort des animaux trouvés dans les sites archéologiques, trois méthodes, basées sur l'étude des dents, sont généralement utilisées. La première, qui couple les dates d'éruption et d'usure dentaire, ne permet qu'une approche indirecte puisqu'elle nécessite de connaitre, ou d'évaluer, la date de naissance de l'animal. La deuxième approche, qui utilise la cémentochronologie, a une précision variable limitée le plus souvent à une estimation large, de l'ordre de la demi-année ou au mieux de la saison. La dernière méthode, très approximative, s'appuie sur la micro-usure dentaire et dépend de la connaissance de la saisonnalité de croissance des plantes et du type de plantes consommées. Pour tenter de surmonter les limites des méthodes classiques, nous proposons de déterminer la date de mort des caprinés à l'aide de l'analyse séquentielle du rapport en isotopes stables de l'oxygène de l'émail dentaire dont les variations dans l'environnement sont contrôlées saisonnièrement. La méthode isotopique a déjà été appliquée à des cas d'étude archéologique, mais limitée à une estimation large de l'ordre de la saison.

Nous avons construit un ensemble de référence composé de molaires en développement (i.e. enregistrant le dernier signal environnemental) provenant de quatorze moutons et chèvres modernes de Mongolie occidentale et centrale, dont la date de mort est connue. Les dents ont été échantillonnées séquentiellement et les séquences de $\delta^{18}O$ obtenues ont été modélisées. La méthode consiste à utiliser une fonction cosinus afin de positionner précisément la dernière

valeur de $\delta^{18}O$ (δf), au bas de la couronne dentaire, dans le cycle annuel représenté par 360°. Nous posons l'hypothèse que dans un cycle annuel 0° (= 360°) représente le milieu de l'hiver, là où la valeur de $\delta^{18}O$ est minimale, et 180°, le milieu de l'été là où la valeur de $\delta^{18}O$ est maximale.

Nous avons constaté que les valeurs de δf sont significativement corrélées avec la date de mort ($R^2 = 0,88$), ce qui permet d'utiliser cette régression pour estimer la date de mort avec une précision d'environ ±25 jours (1σ). Cette incertitude est indépendante de la saison de mort (i.e. cémentochronologie) ou de l'âge de l'animal (i.e. l'usure dentaire et les stades d'éruption).

Cette méthode a été appliquée pour déterminer la date de mort de chèvres trouvées dans deux tombes de la nécropole Xiongnu d'Egiin Gol, en Mongolie. Il s'agit d'une zone climatique très similaire à celle dont le référentiel moderne est issu. Nous avons déterminé une date d'abattage de fin juillet pour une tombe et de fin septembre pour une autre, ce qui suggère que la mise en terre a eu lieu pendant la saison chaude. Lorsque l'on combine la date de mort de ces animaux avec leur âge à leur mort, évalué à l'aide des stades d'éruption et d'usure dentaire, il est possible de déterminer la période de naissance des caprins. Nous avons estimé une naissance des caprins ayant lieu principalement en avril. Ainsi le $\delta^{18}O$ de dents de caprinés en cours de croissance permet d'estimer la période de mort et indirectement la période des naissances.

Il reste des limites méthodologiques à cette approche : (i) cette relation ne doit pas être appliquée directement à d'autres échantillons provenant de zones climatiques différentes, particulièrement où les précipitations peuvent perturber le cycle saisonnier enregistré par le $\delta^{18}O$ de l'émail ; (ii) Par ailleurs, des pratiques pastorales, comme la distribution d'eau de puits, peuvent perturber le cycle saisonnier car la composition isotopique de ces eaux ne varie que très peu ; (iii) Enfin, il est nécessaire de préciser que cette méthode est complémentaire des autres, car elle ne ne s'applique qu'à des jeunes bêtes dont la croissance des dents n'est pas terminée.

Article V: Date of death of domestic caprines assessed by oxygen isotopic analysis of developing molars: implications for deciphering the calendar of pastoral activities in prehistory

Nicolas LAZZERINI, Antoine ZAZZO, Aurélie COULON, Charlotte MARCHINA, Tsagan TURBAT, Sébastien LEPETZ

Manuscript submitted (accepted with minor revisions) in *Journal of Archaeological Science*.

Abstract:

The assessment of the date of death (DOD) of animals found in archaeological sites provides insights into the exploitation of their environment by ancient mobile and sedentary populations. In an attempt to overcome the limitations of the classical methods we propose to determine the DOD of domestic caprines using sequential oxygen isotope analysis of developing tooth enamel. We built a reference set composed of developing molars from fourteen modern sheep and goats from Western and Central Mongolia, with known DOD. The teeth were sequentially sampled and $\delta^{18}O$ sequences were modelled using a cosine function in order to position the lowermost $\delta^{18}O$ value (δ_f) within the annual cycle. We found that δ_f values are strongly linearly correlated with the DOD ($R^2 = 0.88$), allowing the use of this regression to estimate the DOD with a precision of about ±25 d (1σ). This method was applied to determine the DOD of caprines found in two graves from the Xiongnu necropolis of Egiin Gol, Mongolia. We determined a slaughter date of late July and late September for the two graves, respectively, suggesting that burial occurred during the warm season. By combining this information with age at death assessed using tooth eruption stages and tooth wear patterns we were also able to determine that caprine births occurred mostly in April and was strongly controlled within this seasonal window by the herders much like in Mongolia today.

Keywords: Sequential $\delta^{18}O$ analyses; modelling, Mongolia; Egiin Gol; Seasonality of birth; funerary practices; Xiongnu

8.2 Introduction

The timing of slaughter of domestic or wild animals is a key parameter to understand interactions between humans and their environment in the past. Indeed, the moment when an animal is slaughtered relates to husbandry, hunting and settlement strategies, i.e. when and why the archaeological sites were used by humans (e.g. Carter, 2001; Helmer et al., 2005; Hesse, 1982; Lubinski, 2001; Nývltová Fišáková, 2013). Animals also play a role in various ritual practices and in this context, seasonality of slaughter can also highlight the existence of a sacrificial calendar (e.g. Crubézy et al., 1996; Henton et al., 2014; Lepetz and Decanter, 2013).

Three different approaches have been developed to determine the date of death (DOD) of animals found in archaeological sites. All of these approaches are based on the analysis of teeth, the most resistant and often the best preserved skeletal remains in archaeological contexts (Kohn and Cerling, 2002; Newesely, 1989; Smith and Tafforeau, 2008; Trautz, 1967). The first approach is based on the analysis of known sequences of tooth eruption (e.g. Hoppe et al., 2004; Noddle, 1974; Silver, 1963) and tooth wear (e.g. Ervynck, 2005; Grant, 1982; Greenfield and Arnold, 2008; Payne, 1973; Zeder, 2006). This method, which requires prior knowledge of the timing of tooth growth, can provide a precise estimation of the animal age at death (Greenfield and Arnold, 2008) but the accuracy cannot be less than two month and decreases with the age of the animals (Jones, 2006). However, this method only indirectly informs on the date of slaughter as it requires an *a priori* estimate of the date of birth (e.g. Lepetz and Decanter, 2013; Rodríguez-Hidalgo et al., 2016). The second approach is based on cementochronology, i.e. the interpretation of the cyclic patterns of growth of tooth cement, characterized by the alternation of distinct broad/translucent (summer) and narrow/opaque (winter) layers (i.e. Burke and Castanet, 1995; Crubézy et al., 1996; Gourichon and Parmigiani, 2016; Greenfield et al., 2015; Landon, 2014; Li et al., 2017; Pike-Tay, 1995). The relative percentage of length of the last cement layer in proportion to the maximum expected length enables to determine the time of year when the animal died. The precision of cementochronology varies depending on the time of year, from 1-3 months during winter up to 6 months during summer (Burke and Castanet, 1995; Nývltová Fišáková, 2013; Schmaus et al., 2019). But most of the time, the estimation of the date of death remains qualitative, i.e., allowing to distinguish between cold and warm seasons (i.e. Burke and Castanet, 1995; Greenfield et al., 2015; Li et al., 2017; Schmaus et al., 2019). Moreover,the precision of this approach relies on the good preservation of the cement but also on the absence of apatite crystallites that can introduce a bias in the determination of the date of death (Stutz, 2002). Inter- and intra-individual variability in cementogenesis can

also hamper the determination of the date of death (Burke and Castanet, 1995). Other factors such as age (Naji et al., 2016) and geographical variability (Grue and Jensen, 1976) can also bias the results. The third approach is based on tooth microwear analysis, i.e., the analysis of the microscopic features produced by food on the occlusal surface of teeth. Due to a high turnover rate, dental microwear reflects the diet of the last days or weeks of an animal ("the last super effect") (Grine, 1986; Henton et al., 2017a; Mainland et al., 2016; Mainland, 1998; Rivals et al., 2015; Rivals and Deniaux, 2005; Rodríguez-Hidalgo et al., 2016; Solounias and Semprebon, 2002). Tooth microwear can hence potentially record the season of death, assuming that seasonally available food resources can be distinguished by specific microwear signals (Henton et al., 2017a). This method, which requires large assemblages (*N* individuals > 10) has been used to distinguish between single or multiple mortality events in fossil assemblages (Rivals et al., 2015, 2009; Rodríguez-Hidalgo et al., 2016). The temporal precision of this method has not been assessed in detail, but depends on several parameters including knowledge of the seasonality of plant growth and the type of plants consumed, and also the subjectivity of the observer recording the marks (Teaford, 2007). This rapid review of the available methods illustrates their current limits in terms of temporal precision. There is therefore a need to develop a method which is both precise and does not depend on *a priori* assumptions (i.e. period of birth, dietary inputs, etc.).

Stable isotope analysis of serial tooth enamel samples is a suitable alternative to investigate the season of death of ancient high-crowned mammals. This method relies on the fact that in terrestrial mammals, the stable oxygen isotope ratios ($\delta^{18}O$) of tooth enamel bioapatite are linked to the $\delta^{18}O$ of drinking water and plant water ingested (Kohn, 1996; Longinelli, 1984; Luz and Kolodny, 1985; Pederzani and Britton, 2019). $\delta^{18}O$ in precipitation and plants water reflect local temperature at high and middle latitudes, with higher $\delta^{18}O$ values in the summer and lower $\delta^{18}O$ values in the winter (Dansgaard, 1964; Fricke and O'Neil, 1999; Rozanski et al., 1993). Seasonal variations in $\delta^{18}O$ values of environmental water are then recorded in the $\delta^{18}O$ of enamel bioapatite during tooth growth (Bernard et al., 2009; Fricke and O'Neil, 1996; Koch et al., 1989; van Dam and Reichart, 2009). Thus, sequential sampling of bioapatite allows the reconstruction of detailed records of seasonal variations in diet and climate during the time period of tooth formation. This method has been used on ever-growing teeth, like tusks, to determine the season of death of proboscideans (El Adli et al., 2017; Fisher et al., 2003a; Fisher and Fox, 2007; Koch et al., 1989; Stuart-Williams and Schwarcz, 1997). In order to extend it to ungulate teeth with definite growing periods, the method requires to select young

animals for which the mineralization process was still on-going at the time of death. There are a couple of studies where $\delta^{18}O$ analysis of immature ungulate teeth have been performed in order to determine the nature (catastrophic or attritional) of archaeological assemblages (Julien et al., 2015; Knipper et al., 2008). However, quantitative determination of the date of death (DOD) using the isotopic approach requires a reference set with animals whose DOD is known with precision. Indeed, tooth mineralization takes several months before completion and as a result of this process, the isotopic signal of fully mineralized enamel is shifted and dampened compared to the input (environmental) signal (Passey and Cerling, 2002; Balasse, 2003, 2002; Zazzo et al., 2005). Although the impact of the mineralization process on the isotopic value should be smaller on developing tooth enamel than on mature enamel, this remains to be tested and quantified.

Our aim is to establish a proof-of-concept for DOD determination using $\delta^{18}O$ analysis of developing ungulate teeth. To this end, we built a reference set composed of developing molars from modern caprines from Western and Central Mongolia, with known DOD. We then applied the method to the caprine material from the archaeological site of Egiin Gol (Xiongnu culture, 4th c. B.C. - 2nd c. A.D), in order to illustrate the potential of our approach to document the calendar of pastoral activities of ancient communities of Mongolia.

8.3 Materials

8.3.1 Modern reference set

The modern reference set comes from two different locations in Mongolia. The first location is situated in the district (sum) of Nogoonnuur, north of the province (aimag) of Bayan-Ölgii in the most western part of the country and the second location is situated 40km north of the city of Tsetserleg in the district of Ikhtamir, center of the Arkhangai province (**Figure 33**). These two regions are characterized by a strong continental climate with long and cold winters and short, hot summers. Average annual rainfall is 131 mm and 303 mm for the Nogoonnuur and Ikhtamir districts respectively, with a maximum of precipitation occurring during summer (http://fr.climate.org). Due to strong continental climate, the seasons are defined as follows: spring (April and May), summer (June–August), autumn (September and October), and winter (November–March) following Mohammat et al., (2013) and Piao et al. (2006).

We sampled developing molars from fourteen modern domestic sheep (*Ovis aries*, n=9) and goats (*Capra hircus*, n=5) in their second or third year (**Table 20**). The animals were sourced

from different families of nomadic pastoralists with different mobility patterns in terms of distance, frequency and surface used by the herds. Information about pastoral practices was documented through interviews conducted yearly with the herders. Season of birth ranges from January to May with a main lambing period between March and April. Because livestock is grazing on pasture and drinking water from local streams and plant water, their teeth should be a good recorder of seasonal variations in $\delta^{18}O$ values of environmental water. Study animals were slaughtered on five different occasions: July 2013 (n= 2), June 2015 (n= 2), September 2016 (n= 4), November 2017 (n= 4) and late June-July 2018 (n= 2 - **Table 20**). The mandibles were collected immediately after slaughter and were defleshed and cleaned by boiling. Then, developing teeth were extracted from the mandibular bone with a cut-off wheel. We selected the second molar from two sheep and the third molar from seven sheep and five goats.

Figure 33: Map of Mongolia showing the origin of the modern (Nogoonnuur and Ikhtamir) and archaeological (Egiin Gol) samples.

8.3.2 Archaeological samples

Mongolia has been occupied by populations whose funeral practices, lifestyles, agro-pastoral activities and economic circuits are the subject of numerous research (e.g. (Honeychurch, 2010; Kovalev and Erdenebaatar, 2009; Kradin, 2011; Lepetz et al., 2019; Taylor, 2017; Wright and Makarewicz, 2015; Zazzo et al., 2019). Among them, the Xiongnu (4^{th} c. B.C. - 2^{nd} c. A.D) were a confederation of nomadic or semi-nomadic herders who had lived in the Eastern steppes of present-day Mongolia, southern Siberia, northern China and Xinjiang. Many necropolis of this period have been excavated and one of them, Egiin Gol

(Northern Mongolia), has been studied in detail (e.g. Crubézy et al., 1996; Giscard (ed.) et al., 2013; Wright et al., 2009). The necropolis, which contains hundreds of tombs, is located in the Peri-Baïkal region in the north of Mongolia (49° 26'N. 103° 30'E. – **Figure 33**) in the province of Bulgan and the district of Khutag-Öndör. The tombs are bounded on their surface by piles of stones. They are mostly north-south oriented with a wooden chest placed on their northern side above the head and containing various offerings (e.g. ceramics, culinary sticks, part of the spine –lumbar, vertebra, sacrum, caudal - of bovids, horses and caprines). Animal remains including skulls and mandibles from horse, cattle, sheep and goat were also found in a niche situated behind this wooden chest. Two tombs (T77 and T60b) were selected for this study. In the offering chest of T77, a complete goat cut into 8 or 9 pieces of meat and elements of the lower legs of a cattle were found. The niche of T60b was the richest of the site. It delivered the remains belonging to 3 horses, 5 oxen, 18 goats (many of them very young) and 3 sheep. Interestingly, all hyoid bones were present, attesting that the flesh was still attached to the skull and that the animals were deposited rapidly following slaughter (Lepetz and Decanter, 2013). Stratigraphic data indicate that the deposits were made in a single operation, probably contemporaneous to the individual's death. The third mandibular molars from T77 (n= 1) and T60b (n= 2) goats were not fully mineralized and selected for stable isotope analysis (**Table 21**).

Table 20: Characteristics of the modern reference set used in the analyses. DOD = date of death.

Sample	DOD	Year of birth	Approximate age at death(months)[1]	Species	Origin	Sex	Tooth sampled
P2015-112 M3	18/06/2015	2013	28	*Ovis aries*	Nogoonnuur	?	M_3
P2015-147 M3	23/06/2015	2013	28	*Capra hircus*	Nogoonnuur	?	M_3
2018-23A M3	29/06/2018	2017	16	*Ovis aries*	Nogoonnuur	M	M_3 right
2018-63B M2	24/07/2018	2016	28	*Ovis aries*	Nogoonnuur	M	M_2 left
P330-M2	29/07/2013	2012	16	*Ovis aries*	Ikhtamir	?	M_2 right
P331-M3	29/07/2013	2011	29	*Ovis aries*	Ikhtamir	?	M_3 left
Alt16-104a M3	05/09/2016	2014	30	*Ovis aries*	Nogoonnuur	M	M_3 left
Alt16-283a M3	13/09/2016	2014	30	*Ovis aries*	Nogoonnuur	M	M_3 left
Alt16-306a M3	14/09/2016	2014	30	*Ovis aries*	Nogoonnuur	M	M_3 left
Alt16-369a M3	21/09/2016	2014	30	*Capra hircus*	Nogoonnuur	M	M_3 left
2017-70 M3	17/11/2017	2015	32	*Ovis aries*	Nogoonnuur	M	M_3 left
2017-71 M3	17/11/2017	2015	32	*Capra hircus*	Nogoonnuur	M	M_3 left
2017-98 M3	20/11/2017	2015	32	*Capra hircus*	Nogoonnuur	M	M_3 left
2017-146 M3	23/11/2017	2015	32	*Capra hircus*	Nogoonnuur	M	M_3 left

[1] this estimate was calculated based on an assumed date of birth in March according to herders

T**able 21:** Summary statistics of the isotopic values of enamel bioapatite samples. N = number of samples by tooth.

Sample	N	$\delta^{18}O$ (‰ V-PDB)			
		Mean ± SD	Max	Min	Amplitude
P330-M2	19	-8.97 ± 6.0	-0.71	-16.83	16.12
P331-M3	15	-9.21 ± 4.9	-0.85	-15.21	14.36
P2015-112 M3	22	-8.65 ± 4.1	-2.37	-13.87	11.50
P2015-147 M3	21	-7.56 ± 4.0	-0.38	-12.35	11.97
Alt16-104a M3	24	-7.66 ± 3.8	-1.45	-13.42	11.97
Alt16-283a M3	24	-8.66 ± 3.1	-3.35	-13.79	10.44
Alt16-306a M3	24	-7.39 ± 3.3	-2.15	-13.17	11.02
Alt16-369a M3	18	-5.79 ± 4.4	-0.14	-12.3	12.16
2017-70 M3	20	-7.64 ± 3.1	-3.18	-12.36	9.18
2017-71 M3	20	-7.19 ± 3.2	-3.18	-12.39	9.21
2017-98 M3	17	-8.22 ± 3.4	-3.31	-13.11	9.8
2017-146 M3	24	-7.69 ± 3.3	-2.26	-12.59	10.33
2018-23A M3	19	-8.77 ± 3.8	-2.33	-13.27	10.94
2018-63B M2	18	-10.374 ± 2.1	-6.53	-13.00	6.47
T60b-P80 M3 †	17	-7.41 ± 3.4	-1.50	-11.67	10.17
T60b-P82 M3 †	19	-7.13 ± 3.4	-1.84	-12.05	10.21
T77-P90 M3 †	22	-8.04 ± 2.7	-4.44	-11.84	7.41

† = archaeological samples

8.4 Methods

8.4.1 Tooth enamel sampling and isotope analysis

Teeth surfaces were cleaned by abrasion with tungsten drill bits to remove the cement. Sequential sampling of modern and archaeological teeth was performed on the buccal side of the second and third molars, on the anterior lobe of M2 and the middle lobe of M3. The sampling spans the width of a lobe. Enamel was drilled with a diamond bit, perpendicular to the tooth growth axis from the apex to the enamel root junction (ERJ). Samples were taken every 1.5-2mm through the entire thickness of the enamel layer and care was taken to avoid collecting the underlying dentine. Sample position was recorded in terms of their distance (in mm) from the ERJ, when the tooth was in final development stage (maturation phase), or from the base of the tooth crown when the tooth was still growing in length at the time of death.

Samples weighing 3.5-7 mg were chemically treated following the procedure described in Balasse et al. (2002b). First, organic matter was removed with a solution of 2-3% NaOCl (24h, 0.1 ml solution/ mg of sample) and rinsed several times in distilled water. Then, each enamel sample was reacted with 0.1 M acetic acid (4h, 0.1 ml solution/mg of sample) to remove

exogenous carbonates, rinsed in distilled water and dried in an oven at 80°C for 12h. The same protocol was applied to modern and archaeological samples to avoid biases due to pre-treatment-induced changes in the $\delta^{18}O$ values of enamel (M. Balasse et al., 2012; Koch et al., 1997).

Purified enamel samples were weighted (600 µg approximately) and analyzed on a Kiel IV device connected to a Delta V Advantage isotope ratio mass spectrometer (IRMS) at the *Service de Spectrométrie de Masse isotopique du Muséum national d'Histoire naturelle* (SSMIM) in Paris. Samples were placed into individual vessels to react under vacuum with phosphoric acid [H_3PO_4] at 70°C and purified CO_2 in an automated cryogenic distillation system. Analytical precision was 0.04‰ based on the repeated (n= 160) analysis of our internal laboratory carbonate standard (Marbre LM) normalized to NBS 19. Isotope data are presented in δ notation [$\delta = (R_{sample}/R_{standard}) - 1$], with *R* the isotope ratio ($^{18}O/^{16}O$) of the sample, reported relative to the international standard V-PDB (Vienna PeeDee Belemnite) and expressed in per mil (‰).

8.4.2 Modelling sequential $\delta^{18}O$ series and inferences of the slaughter date

We tested the differences in isotopic values among individuals and sites using Kruskal-Wallis tests for modern and archaeological individuals separately.

Oxygen isotope sequences, recording the seasonal cycle of temperature, usually follow a sinusoidal pattern. For each individual animal we modelled the oxygen isotope sequences using an equation derived from a cosine function proposed by Balasse et al., (2012):

$$\delta^{18}O_m = Ae^{\left(\frac{x-x_b}{x_A}\right)} \cos\left(2\pi \frac{x - x_0}{X + b_x}\right) + M + px \quad \text{(Eq. 12)}$$

where $\delta^{18}O_m$ is the modelled $\delta^{18}O$ value and *x* is the distance of the sample to the ERJ. The four following parameters are keys to describing the individual $\delta^{18}O$ sequences: *X* is the period (in mm) of the cycle and corresponds to the length of tooth crown potentially formed over a year, *A* is the amplitude of the isotopic signal [= (max-min)/2] (in ‰), *M* is the mean, x_0 is the position of the highest $\delta^{18}O$ values in the tooth crown. The last four parameters have less influence: *p* is the slope (in ‰.mm^{-1}) of the mean - when the sequence measured spans over a year, the mean M might change from year to year (change in the mean annual ambient temperature, for example). x_A and x_B (in mm) model the attenuation of the amplitude A and *b* is the gradation of the period (no unit). Values were fixed to 0 for *p* and x_B and to 10^6 for x_A (Balasse et al., 2012).

Parameter *b* was also introduced in the model because it helps to describe the attenuation of the growth rate from the apex to the neck of the crown on the third molar. We used it also for the second molar, even if it has less influence, in order to compare the models based on these two types of teeth. For each sample, parameter estimation was performed using an iterative method, performed in Microsoft Excel, based on the method of minimization of the least squares (for more information on method estimation, including the comparison of three alternative versions of the model, **see Supp. Info S8.1**).

Because the cycles in the sinusoidal modelled sequence (SMS) have a period of one year, there is a simple and direct proportional relationship between the position *P* of a sample on the SMS and the date d (in days) to which it corresponds, such as:

$$d = P(°) \times \frac{365.25}{360} \quad \text{(Eq. 13)}$$

P is the position (in degrees) in the annual cycle, with *P*=0° for the lowest $\delta^{18}O$ value of each sequence, and *d* is the number of days elapsed since *P*=0°. We propose that *P*=0° corresponds to Mongolia mid-winter (January15th) and that *P*=180° corresponds to Mongolia mid-summer (July 17th - **see Supp. Info S8.2**). To directly get estimates of the number of days since the 1st day of a calendar year (i.e. January 1st), Eq. 13 can be modified as follows:

$$d = P(°) \times \frac{365.25}{360} + 15 \quad \text{(Eq. 14)}$$

where the number 15 corresponds to the number of days between Jan. 1st and Jan. 15th. DOD can then be calculated by applying Eq. 14 to the position (in °) of the $\delta^{18}O$ values at the ERJ (δ_f). To precisely calculate the position (P_f) of δ_f in the annual cycle, we used one of the following two equations, depending on whether the end of the modeled SMS was in increasing (Eq. 15) or in decreasing phase (Eq. 16):

$$P_f\ (°) = \left(\frac{\delta_f - \delta_{min}}{2A}\right) \times 180 \quad \text{(Eq. 15)}$$

$$P_f\ (°) = \left(\frac{\delta_0 - \delta_f}{2A}\right) \times 180 + 180 \quad \text{(Eq. 16)}$$

where δ_0 is the highest $\delta^{18}O$ value in the SMS and δ_{min} is the lowest $\delta^{18}O$ value.

We tested the accuracy of our approach by comparing the known and calculated DOD through a linear regression between the two sets of dates. We calculated the standard error of the estimated DOD of our samples as follows:

$$\sigma = \sqrt{\frac{(DOD_c - DOD_k)^2}{N - 2}} \qquad \text{(Eq. 17)}$$

where σ is the standard error of the estimate, DOD_c is the estimated DOD, DOD_k is the known DOD and N the number of samples.

8.4.3 Age estimation of the archaeological goats

The age of the archaeological goats from T77 and T60b was estimated by combining the analysis of tooth eruption stages and tooth wear patterns (Grant, 1982; Jones, 2006). Because inter-individual variations in tooth wear and tooth eruption patterns can impact age-at-death estimation, the uncertainty of the age estimate is two months for individuals <6 months-old and increases with the age of the animal (Greenfield and Arnold, 2008; Jones, 2006).

Unless mentioned otherwise, all statistical analyses were performed in Past version 3.24.

8.5 Results and Discussion

8.5.1 Inter- and intra-individual variability in the $\delta^{18}O$ sequences of the modern reference set

The results of the stable isotope analysis are presented in **Supp. Info Tables S8.3**. The average $\delta^{18}O$ value of all samples was -8.1 ± 1.1‰ (1σ), with a maximum value of -5.8‰ and a minimum value of -10.4‰ per individual, on average. The lowest and highest $\delta^{18}O$ values were -16.8‰ to -0.1‰, respectively. Intra-individual variability was 11.1 ± 2.3‰ on average, with a maximum of 16.1‰ and a minimum of 6.5‰. Maximum values ranged between -6.5‰ and -0.1‰ and minimum values ranged between -16.8‰ and -12.3‰ (**Table 21**). The large amplitude of seasonal $\delta^{18}O$ variations of modern teeth was representative of the marked continental climate with little annual precipitations (~131 mm), typical of Mongolia. The oxygen isotopic values from the two , Nogoonnuur (n = 253) and Ikhtamir (n = 33), were not statistically different (One-way ANOVA - *p-value* = 0.27), with mean values of -7.4 ± 8.6‰ and -9.1 ± 5.5‰ respectively.

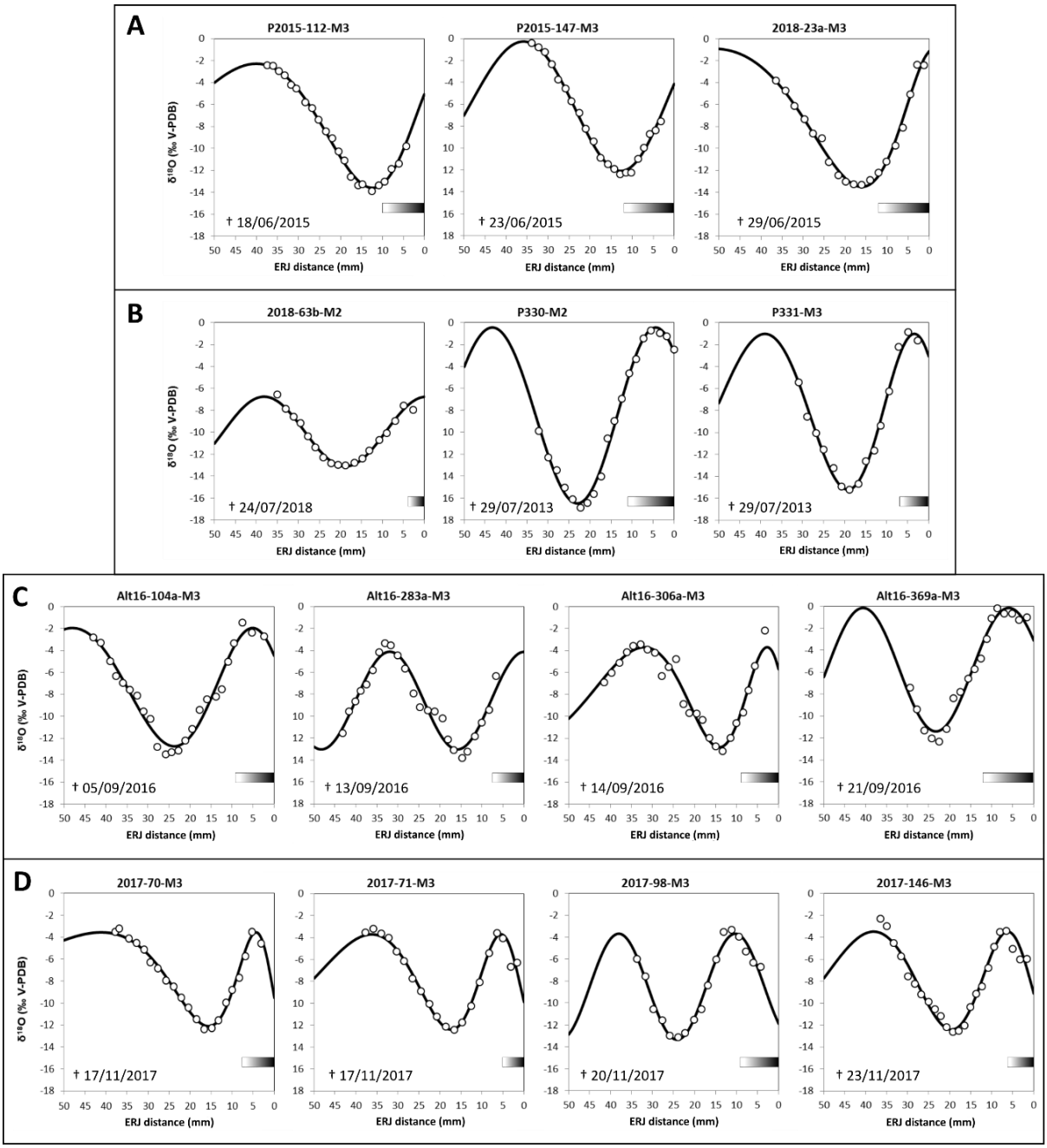

Figure 34: Variations of oxygen isotope values along the tooth crown of the modern sheep and goat molars. The position of the sample is expressed by the distance between the sample and the enamel-root junction (ERJ). The circles represent the measured data, and the black line is the best sinusoidal model that fits the data. Each panel represents a different slaughter period: late June (A), late July (B), September (C) and November (D). The sample in grey was not included in the modelling. The grey shaded areas indicate the extent of immature enamel along the tooth crown.

For each individual, $\delta^{18}O$ sequences showed large intra-tooth variation, following a sinusoidal pattern (**Figure 34**). The position of the last $\delta^{18}O$ values within the sinusoidal curve of each tooth (δ_f) differed depending on the slaughtering periods. Indeed, sinusoidal patterns were in an increasing phase for the three individuals slaughtered in late June (**Figure 34A**). They were in a plateau for individuals slaughtered between late July (**Figure 34B**) and

September (**Figure 34C**). Finally, they were in advanced decreasing phase for animals slaughtered in November (**Figure 34D**). Nevertheless, we noticed similarities in the isotope profiles of some animals that were slaughtered more than a few weeks apart (e.g. P330 vs Alt16-104a; Alt16-306a vs 2017-70).

8.5.2 Accuracy of the modelled DOD

Parameters selected for the models of best fit are presented in **Table 22**. For each tooth, Pearson's correlation coefficient of the model was larger than or equal to 0.97 (**Table 22**). There was at least one minimum for each sequential series and most sequences showed one maximum and one minimum along the tooth crown. We chose the minimum value corresponding to the winter immediately preceding the animal slaughter and observed in all specimens, as the starting point (=0°) of the annual cycle.

Calculated DOD range from 137.7 to 352.6 d (from January 1st) whereas known DOD range from 169 to 327 d (**Table 22**). The absolute difference between modelled and known DOD is 18.6 ± 14.7 d on average, and range from 3.9 to 59.4 d. There is no statistical difference between sheep and goat (One-way ANOVA- *p-value* = 0.68), with mean values of 17.4 ± 16.6 d and 20.9 ± 11.8 d respectively. There was a strong linear relationship between modelled (**Table 22**) and the known DOD (**Figure 35**):

$$y = 1.07(\pm 0.11)x - 23.90\ (\pm 29) \qquad R^2 = 0.88 \quad p = 6.46e^{-07}\ *** \qquad \text{(Eq.18)}$$

Differences in the known DOD of individual slaughtered a few days from each other explainse only a small part of the variability measured in the *P* of δ_f of individuals slaughtered a few days from each other. As a result, standard deviation in the known DOD of these individuals, slaughtered in different period, ranged from 3 to 7 d, while standard deviation in the calculated DOD ranged from 15 to 29 d (**Table 22**). This additional variability could come from differences in physiology, such as body water balance, or differences in the rate of mineralization as tooth growth proceeds. To assess the possible influence of the mineralisation stage, we measured the length of immature enamel and the length of apposition on the developing molars (**Supp. Info Table S8.4**). Indeed, the appositional layer (*La*) marks the first layer of enamel deposited during the secretion stage (Suga, 1982; Zazzo et al., 2012). When the tooth approaches its maximal length and the growth rate decreases, the length of this newly accreted enamel layer decreases. This appositional layer records the isotopic signal closest to the animal's death, so the longer this zone is, the closer we should be from the known DOD.

Table 22: Individual modelling characteristics for the date of death (DOD) estimation based on sequential sampling of $\delta^{18}O$ variations in teeth. A (amplitude), M (mean), x_0 (delay), X (period) and b (gradation) are parameters of the cyclical models of $\delta^{18}O$ sequences and Pearson's correlation coefficient measure their fit. P of δ_f is the position on the annual cycle (in °) of the last $\delta^{18}O$ values at the neck of the tooth crown. The last two columns are reminders of the calculated and known DOD in days from Janurary 1st.

Sample	*A* (‰)	*M* (‰)	x_0 (mm)	*X* (mm)	*b* (s.u.)	Pearson's corr. coeff. R	δ_f (‰)	*P* of δ_f (in °)	Calculated DOD	Known DOD	Period of death	Mean ± SD Calculated DOD per period	Mean ± SD Known DOD per period
P2015-112 M3	5.66	-7.96	40.0	47.93	0.60	0.998	-5.1	135.6	152.6	169			
P2015-147 M3	5.93	-6.17	35.82	44.45	0.15	0.997	-4.1	121.0	137.7	174	Late June	162 ± 29	174 ± 6
2018-23a M3	6.30	-7.19	-1.08	26.0	0.51	0.993	-1.1	176.9	194.5	180			
2018-63b M2	3.18	-9.92	-0.51	38.66	0	0.990	-6.8	179.7	197.3	205			
P330-M2	8.02	-8.26	4.39	35.39	0.09	0.997	-2.7	205.7	223.7	210	Late July	215 ± 15	208 ± 3
P331-M3	7.09	-7.90	3.45	27.77	0.2	0.994	-3.1	206.0	224	210			
Alt16-104a M3	5.41	-7.34	5.12	31.81	0.23	0.983	-4.5	222.2	240.4	247			
Alt16-283a M3	4.44	-8.58	-0.08	31.72	0.01	0.968	-4.1	180	197.6	257			
Alt16-306a M3	4.57	-8.27	2.75	17.65	0.36	0.973	-5.7	219.7	237.9	258	September	230 ± 22	257 ± 7
Alt16-369a M3	5.64	-5.77	5.96	34.71	0	0.986	-3.1	227.5	245.8	265			
2017-70 M3	4.27	-7.85	4.35	13.83	0.56	0.993	-9.53	305.4	324.9	321			
2017-71 M3	4.34	-8.06	5.49	17.19	0.38	0.987	-9.89	307.9	327.4	321			
2017-98 M3	4.83	-8.50	10.33	27.70	0	0.987	-11.89	332.8	352.6	324	November	329 ± 17	323 ± 3
2017-146 M3	4.46	-7.96	6.22	21.29	0.28	0.979	-9.1	293.7	313	327			
T60b-P80 M3 †	4.94	--6.62	6.00	30.62	0.05	0.997	-5.07	239.9	258.4				
T60b-P82 M3 †	5.08	-6.61	3.16	14.62	0.61	0.993	-5.5	251.0	269.6				
T77-P90 M3 †	3.83	-8.13	26.68	23.88	0.18	0.974	-4.89	192.9	210.7				

† = archaeological samples

However, we found no relationship between *La* length and the absolute difference between the modelled and the known DOD (*p value > 0.5*). Alternatively, variability in modelled DOD could come from inter-individual differences in the $\delta^{18}O$ value of the input signal with differences in the relative proportion of sources of ingested water (e.g. snow, plant water, drinking water, well water) across a year, leading to differences in the δ_f values and variation of the seasonal amplitude from one year to the next. Unfortunately, these parameters were not controlled for in our study.

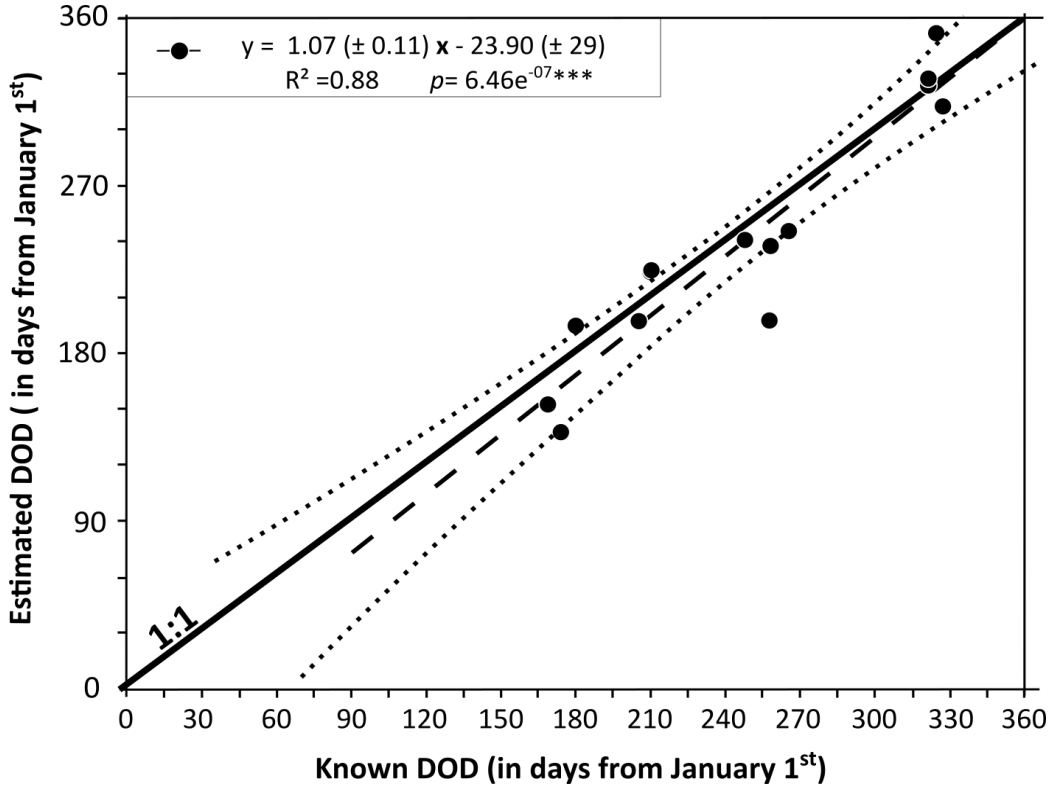

Figure 35: Calculated date of death (DOD) plotted against the known DOD (black circles). The corresponding linear regression line (ordinary least square regression; dashed line) is drawn along with associated 95% confidence bands (dotted lines). The linear regression is compared with the expected slope 1:1 of perfect match between calculated DOD and known DOD (thick black line).

Overall, the standard error of the calculated DOD in our modern reference set was less than a month ($1\sigma = \pm 25$ d). This uncertainty is time-independent, unlike other methods which precision remains qualitative and can vary depending on the time of the year (i.e. cementochronology - Burke and Castanet, 1995; Nývltová Fišáková, 2013; Schmaus et al., 2019) or the age of the animal (i.e. tooth wear and eruption stages - Greenfield and Arnold, 2008; Jones, 2006). Moreover, the main advantage of the isotopic approach is that it does not rely on any assumption such as the type of food resources (unlike the tooth microwear method) or the date of birth of the animal (unlike tooth wear and eruption stages method).

8.5.3 Archaeological application

8.5.3.1 Estimation of the date of death

Tooth enamel $\delta^{18}O$ values from the three archaeological specimens ranged from -1.5 to -12.1 ‰ (mean -7.5 ± 0.5‰) (**Table 21**). Intra-individual variability ranged from 7.4 to 10.2 ‰. For each specimen, maximum values ranged from -4.4‰ to -1.5 ‰ and minimum values ranged from -12.1‰ to -11.7‰ (**Table 21**). Complete results are presented in **supplementary information table S8.3** There were no significant differences among the three archaeological individuals (One-way ANOVA; *p-value* = 0.5), and between modern and archaeological individuals (One-way ANOVA, *p-value* = 0.9).

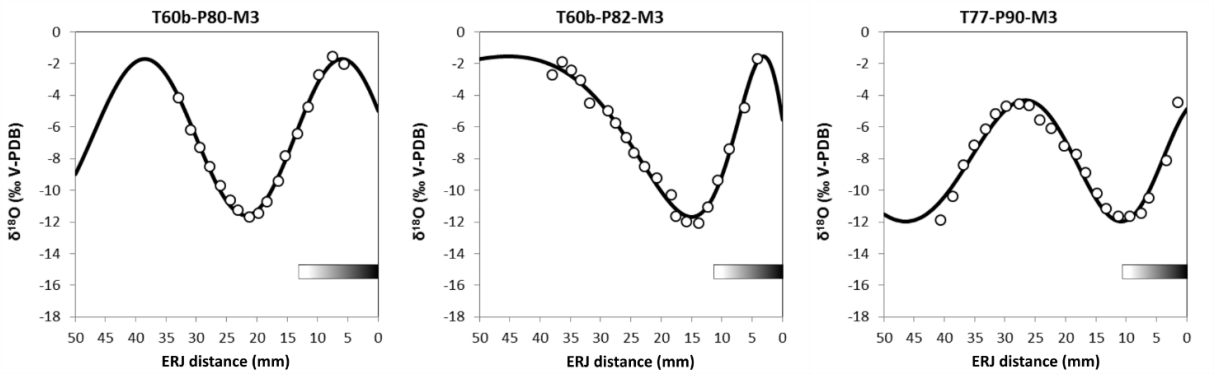

Figure 36: Variations of oxygen isotope values along the tooth crown of the archaeological goat molars from Egiin Gol. The position of the sample is expressed by the distance between the sample and the enamel-root junction (ERJ). The circles represent the measured data, and the black line is the best sinusoidal model that fits the data. The grey shaded areas indicate the extent of immature enamel along the tooth crown.

Parameters selected for the models of best fit of the sequential $\delta^{18}O$ sequences of archaeological specimens (**Figure 36**) are presented in **Table 22**. The positions *P* of δ_f values on the annual cycle were 239.9°, 251.0° and 192.9° for T60b-P80, T60b-P82, T77-P90, respectively. Calculated DOD were September 15th and September 26th for the two individuals in T60b and July 29th for the individual in T77 (**Figure 37**). Given the uncertainty of our method (±29 d), calculated DOD for the two individuals from Tomb 60b were not significantly different and indicated that the individuals were buried in autumn, slightly later than the individual from Tomb 77, which was buried in summer.

Among nomadic peoples, death can occur at a time of year when the human group is far from the family burial place (when there is one). Therefore, there may be a delay between the death of an individual and its burial. Being able to precisely determine the period of the year

during which the bodies were placed in the ground is therefore of great importance to document the mobility of these populations and their funerary practices. Previous attempts at determining burial periods at Egiin Gol were based on cementochronology (Crubézy et al., 1996) on the animal remains of another tomb (EF 1 – sep. 15) and the tooth eruption and wear stages (Lepetz and Decanter, 2013) for T60b. and it suggested that animal slaughtering occurred during the warm season. Our results are in good agreement with this interpretation. The proposed date for T60b corresponds to a time when temperatures are already decreasing but where the soil is not frozen yet and can be easily dug (Dashtseren et al., 2014; Nandintsetseg and Shinoda, 2011), in accordance with what is generally assumed. In addition, our preliminary results suggest that the funerals of the individual at T77 and T60b did not take place at the same time of the year. More work is required to extend these preliminary results to the entire necropolis

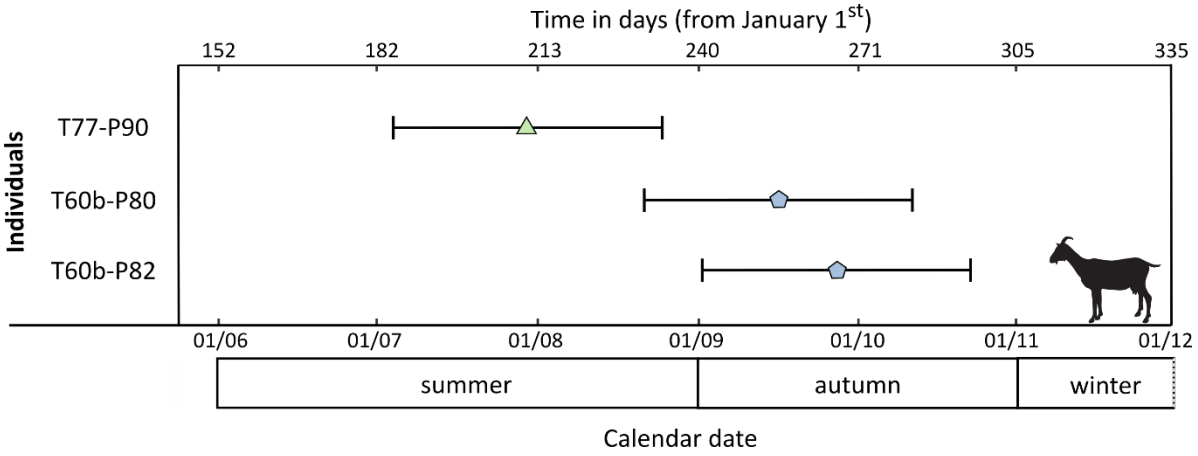

Figure 37: Calculated DOD (in days from January 1st – and in calendar date) and associated standard error (± 1σ) for the three archaeological samples of tomb T77 (green triangle) and tomb T60b (blue pentagon) at Egiin Gol.

8.5.3.2 Seasonality of birth

Because all the individuals from T60b and T77 were deposited fresh, one can assume that they were buried immediately following slaughter. Thus, we can use the DOD estimate to reconstruct the seasonality of birth of the caprines deposited in these grave. We base our reconstruction on individuals found in tomb T60b because it was one of the richest of the site and delivered the remains of 21 caprines. Tooth wear and eruption stages provided an estimated age of 18 and 20-24 months-old, for the individuals P80 and P82, respectively. The proposed age for ten other young goats varies between 4±1 and 11±2 months-old on average (**Supp. Info S8.5 & 8.6)** for eruption and wear stages and age-at-death determination).

To precisely reconstruct the seasonality of birth we only used the youngest (< 18 months-old) goats from this tomb (N = 11) for which the error associated with the estimation

of their age is the lowest (**Figure 38**). Assuming a slaughter date on September 20th, the lambing season would extend from November to May with a lambing peak in April (**Figure 38**). This is consistent with the data collected from modern herders which indicates that parturition takes place from February to May with a peak between late March and mid-April. Today, Mongolian herders tend to favour relatively early births among sheep and goats so as to give them time to grow strong enough by the end of autumn (Legrand, 2011 - p. 219).

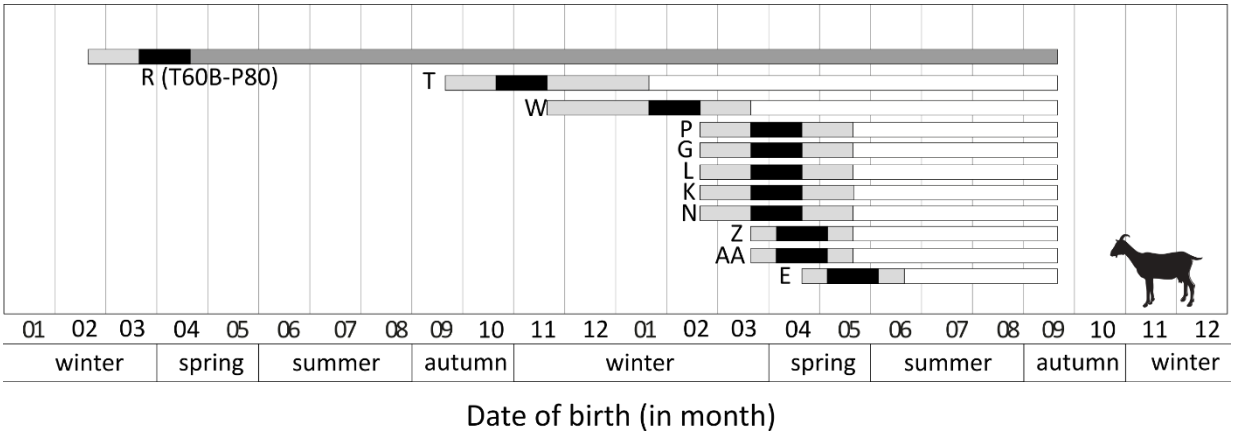

Figure 38: Date of birth (black boxes), with associated uncertainty (light grey) of the youngest archaeological goats from tomb 60b of the Egyin Gol necropolis based on the estimation of age-at-death by eruption and wear stages (**Supp. Info S8.4 & 8.5**) and using the DOD estimated by the $\delta^{18}O$ sequences of individuals R (T60b-P80 – in dark grey) and X (T60b-P82 – not shown) (**see Figure 37**).

8.5.4 Physiological, ecological and environmental limits of the method

Although promising, there are several limitations to the use of the isotope method of determination of the DOD. Because this method requires individuals with developing teeth, the first obvious limit is the age of animal itself. Animals should not be too old because the enamel would have already stopped growing at the time of death, but they should not be too young either because enamel needs to record at least one full isotopic cycle. The first molar of caprines appear as a poor prospect due to its rapid growth (~ 6-9 months) (Weinreb and Sharav, 1964; Zazzo et al., 2010) and wear (Hillson, 2005). The second and third molars are better candidates (Upex and Dobney, 2012, fig. 2) and can be used to determine the DOD of animals between 9 months-old and 2-3 years old. The method can be applied to other domestic species with high-crowned teeth such as horse or cattle. However, due to a longer duration of enamel mineralisation for large ungulates such as the horse (Bendrey et al., 2015; Hoppe et al., 2004), it will be necessary to build reference sets for the species of interest before applying the method to ancient remains.

Animal drinking behaviours can also affect the $\delta^{18}O$ sequences recorded in their teeth. The main source of water is one of these factors. Non-obligate drinkers like sheep and goat obtain their water preferentially from the plants they eat. Plant water $\delta^{18}O$ values are strongly affected by evaporation, leading to large seasonal variations in tooth enamel $\delta^{18}O$ values of caprines. On the contrary, obligate drinkers obtain their water preferentially from lakes or rivers, which are commonly more isotopically stable through time. As a result, the seasonal variations recorded in tooth enamel are dampened (Darling et al., 2003; Halder et al., 2015; West et al., 2014), making DOD determination more hazardous. Pastoral practices, such as distribution of water from a well digging, can also strongly reduce the $\delta^{18}O$ amplitude recorded along the tooth crown, as suggested in various archaeological context by Dufour et al. (2014); Goepfert et al. (2013); Henton et al. (2014), and limit the application of $\delta^{18}O$ sequences for the determination of death period.

Environmental factors can also limit the application of this method. The approach proposed here is well suited to mid- and high-latitude sites where temperature is the main factor driving oxygen isotope variations of precipitation (Dansgaard, 1964; Pederzani and Britton, 2019; Rozanski et al., 1993). It is probably not well suited to low latitude regions and areas characterized by monsoon activity, where air temperature remains essentially constant and precipitation $\delta^{18}O$ values are primarily controlled by humidity (Dansgaard, 1964). Precipitation and/or humidity increase causes $\delta^{18}O$ of meteoric water to decrease (Dansgaard, 1964; Higgins and MacFadden, 2004; Rozanski et al., 1993; Straight et al., 2004). Thus, a decrease in tooth enamel $\delta^{18}O$ values can potentially occur during the hottest months in locations where humidity maximum occurs during summer.

Finally, it is important to consider the potential impact of diagenesis when working on immature enamel. Immature enamel is not well mineralized and is more prone to isotope-exchange with environmental carbonate, much like bone (Zazzo et al. 2004). We anticipate that a difference in the rate of isotopic exchange between mature and immature enamel will result in an isotopic discontinuity that should be easily detected. We did not observe any discontinuity along the isotopic curves between the mature and immature part of tooth enamel in the ancient teeth analysed here. So at least in our case (for fairly recent material found in grave contexts) there was no visible effect of diagenesis. For older / less well preserved material, an alternative would be to select the phosphate group instead, which is less prone to isotopic exchange than the carbonate group (Iacumin et al., 1996; Lee-Thorp, 2008; Zazzo et al., 2004).

8.6 Conclusion

In this study, we propose a method to determine the DOD of caprines based on $\delta^{18}O$ analysis of developing tooth enamel. We show that this date can be estimated with an error of ± 1 month (1σ) and applied the method to determine the DOD of three goats found in two tombs from the Xiongnu cemetery of Egiin Gol, Mongolia. This allowed us to reconstruct the date of birth of the individual animals placed in the tomb based on their estimated age-at-death. Although the proposed method has shown its potential, it would be desirable to enlarge the dataset, in particular with animals slaughtered in winter and spring in order to improve its accuracy. The method proposed here is restricted to young animals and may not be valid in different environmental contexts. With these limitations in mind, our method provides clues to explore animal management strategies in ancient pastoral societies and more broadly, to reconstruct the exploitation of their environment by past mobile or sedentary societies. As such, it provides a complementary approach of classical methods (cementogenesis, tooth microwear pattern or tooth wear and eruption sequence) for DOD studies that does not rely on any assumption regarding the type of food resources ingested or the date of birth of the animal.

Acknowledgements

We are deeply indebted to all the herders who kindly participated to the study and to N. Bayarkhuu (Institute of History and Archaeology, Mongolian Academy of Sciences, Mongolia) for the logistics and assistance during fieldwork. We would like to thank D. Vettese (UMR 7194 HNHP, MNHN, Paris) for her help in sampling and analyzing archaeological samples from Egiin Gol. M. Balasse (UMR 7209 AASPE, MNHN, Paris) for her help with the modeling of the $\delta^{18}O$ sequences, and the two anonymous reviewers for their constructive comments. The isotopic analyses were performed at the SSMIM Paris under the technical supervision of D. Fiorillo. Fieldwork was supported by the French archaeological mission in Mongolia (CNRS, MNHN, MAEDI, director SL) and by the CNRS. This research was funded by a Ph.D. grant to NL from the French National Research Agency LabEx ANR-10-LABX-0003-BCDiv, in the context of the "Investissements d'avenir" n°ANR-11-IDEX-0004-02, and by an Inalco Early Career Research Grant 2017 to CM.

SUPPLEMENTARY INFORMATION CHAPTER 8

All supplementary information are available here:
https://drive.google.com/drive/folders/1a3nMq3Lpl4heviPlUNFNf4zcOGeUdKkP?usp=sharing

Supplementary Info S8.1: Modeling of the sinusoidal patterns of oxygen isotope sequences of the modern and archaeological data sets.

The model used in this study was developed by (M. Balasse et al., 2012) to investigate the seasonality of birth by analysing the oxygen isotope composition of the enamel of M2 teeth of sheep. We applied the same model to our dataset, as described in Eq. 12:

$$\delta^{18}O_m = Ae^{\left(\frac{x-x_B}{x_A}\right)} \cos\left(2\pi \frac{x-x_0}{X+bx}\right) + M + px$$

where $\delta^{18}O_m$ is the modelled $\delta^{18}O$ value and x is the distance of the sample to the ERJ. The four following parameters are keys to describing the individual $\delta^{18}O$ sequences: X is the period (in mm) of the cycle and corresponds to the length of tooth crown potentially formed over a year, A is the amplitude of the isotopic signal [= (max-min)/2] (in ‰), M is the mean, x_0 is the position of the highest $\delta^{18}O$ values in the tooth crown. The last four parameters have less influence: p is the slope (in ‰.mm^{-1}) of the mean - when the sequence measured spans over a year, the mean M might change from year to year (change in the mean annual ambient temperature, for example). x_A and x_B (in mm) model the attenuation of the amplitude A and b is the gradation of the period (no unit).

For each sample, parameter estimation was performed using an iterative method based on the method of minimization of the least squares to find the best fit of the model to the measured data. We used Microsoft Excel software to perform the calculation.

We compared the performance of three alternative ways of estimating model parameters:

We first applied the model allowing the parameters X, A, x_0 and M to vary, and fixed p, b and x_B to 0 and x_A to 10^6 (= the four-parameter model as described by Balasse et al. (2012).

We also tried a five-parameter model, in which, on top of X, A, x_0 and M, b was also allowed to vary, so that the model includes a description of the attenuation of the growth rate from the apex to the neck of the crown on third molars. Indeed, we mainly analysed M3 tooth, that grow during a longer period than other teeth, often over one periodic cycle and can have variations of tooth growth rate with time. To apply the same method to all samples, parameter b was also allowed to vary for both samples of the M2 tooth (2018-63b & P330).

Third, we also tested the eight-parameter model, in which all parameters (X, A, x_0, M, p, x_A, x_B and b) were allowed to vary.

We used the three versions of model estimation to estimate animal date of death (DOD), as detailed in the main text: we used the models to calculate the position P_f of the last $\delta^{18}O$ values (δ_f) on the annual cycle using the equations 4 or 5 (see main text) and estimated DOD using equation 3.

The four-parameter model provided estimated DOD that were slightly correlated with the known DOD (Supp. Info. Fig. S8.1A – R^2 =0.50) and were associated with a large standard error of ± 61 d (1σ). Moreover, the slope of the linear regression was very different from the expected slope 1:1 of perfect match between estimated and known DOD.

The five-parameter model provided a stronger relationship between estimated and known DOD (Supp. Info. Fig. S8.1B - R^2 = 0.88 + see main text), suggesting that parameter *b* is important in order to reliably estimate DOD. Moreover, the slope of the linear regression was congruent to the expected slope 1:1 of perfect match between estimated and known DOD.

With the eight-parameter model, x_A always remained very high (10^6) and x_B very low (from 10^{-9} to 10^{-5}) and thus they had a small influence on the modelled sequences, suggesting that no attenuation of the isotopic signal towards the neck of the tooth is detected on our data set. The slope *p* varied between -0.3 and 0.9‰ mm^{-1}. Such slopes were considered unsuitable to describe the data set because of unrealistic modelled sequences. It may be useful to describe inter-annual variations in longer sequences spanning over more than one periodic cycle. The eight-parameter model provided a strong linear relationship between estimated and known DOD (R^2 = 0.71 – see Supp. Info. Fig. S8.1C), with a high standard error of the estimate of ± 67 d (1σ). The slope of the linear regression was different from the expected slope 1:1 of perfect match between estimated DOD and known DOD.

Based on those results, we used the five-parameter model in the rest of our analyses.

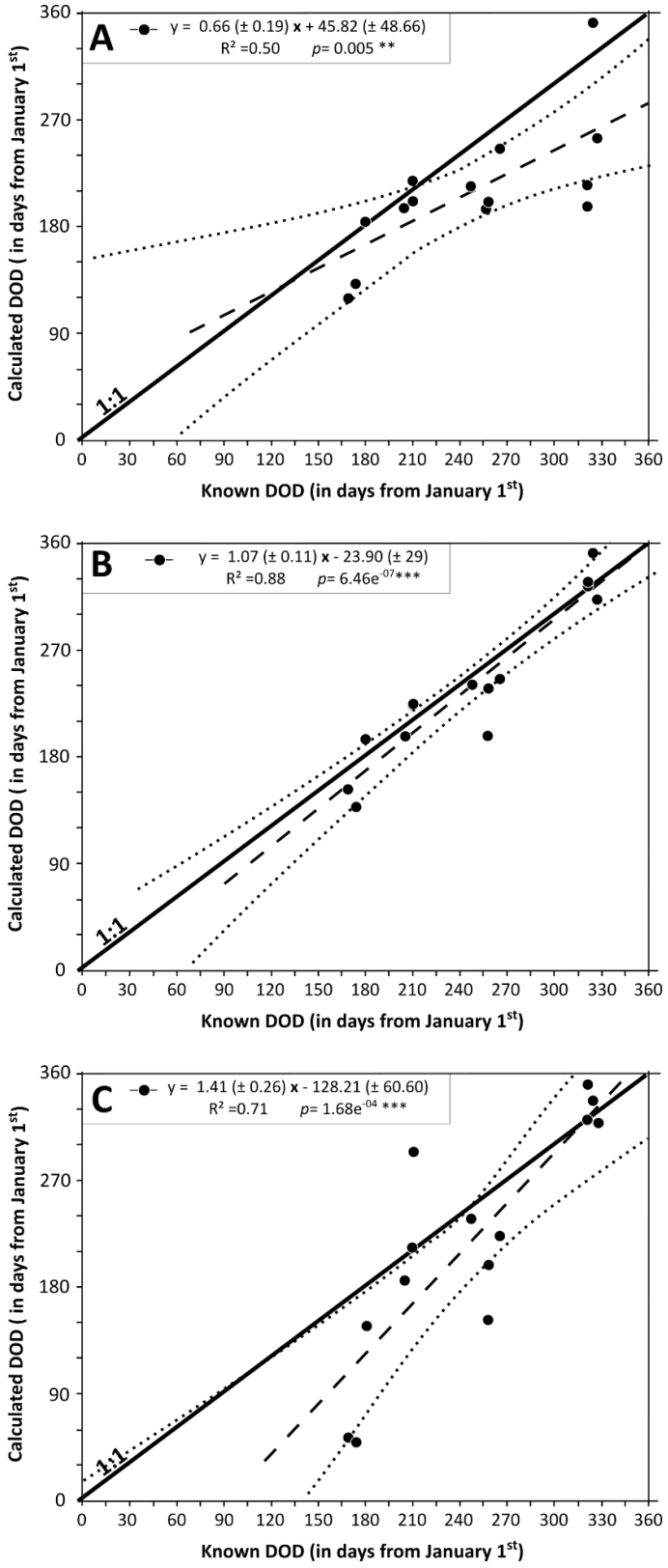

Figure S8.1: Calculated DOD plotted against known DOD (black circles) when DOD estimation was based on **A)** the four-parameter model (X, A, M and x_0), **B**) the five-parameter model (X, A, M, x_0 and b), **C**) the eight-parameter model. (X, A, M, x_0, p, b, x_A and x_B). For each data set the corresponding linear regression line (ordinary least square regression; dashed line) is drawn along with associated 95% confidence bands (dotted lines). For comparison, the thick black line represents the expected slope 1:1 of perfect match between estimated and known DOD.

Supplementary Info S8.2: Daily temperature variations at Nogoonnur from January 1st, 2014 to December 31st, 2018 (https://www.infoclimat.fr). Vertical blue and red dashed lines indicate mid-winter (January 15th) and mid-summer (July 17th) respectively, and correspond to the position 0° and 180° in the annual cycle. This graph shows that assumed mid-winter and mid-summer closely correspond to the minimum and maximum recorded temperatures. Therefore, we can reasonably assume a good correspondence with minimum and maximum environmental oxygen isotope values.

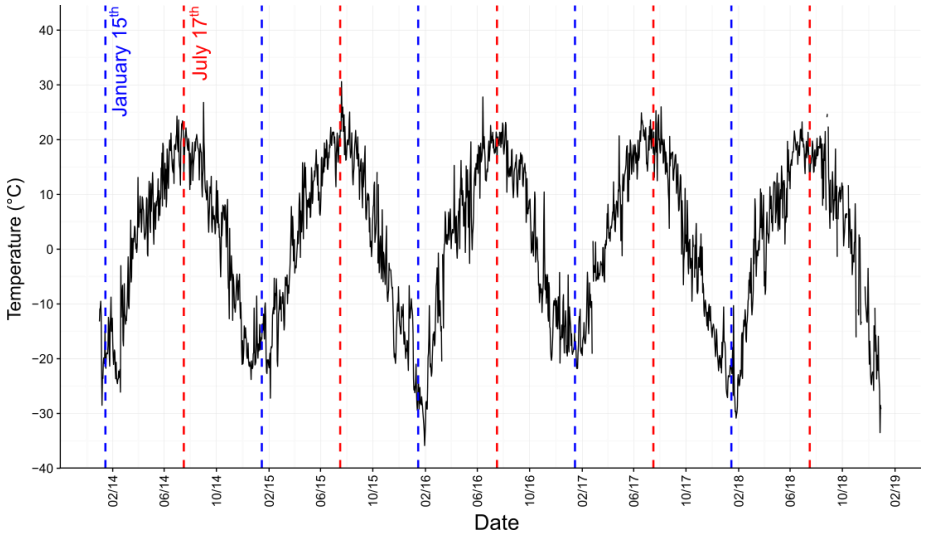

Supplementary Info S8.3: Results from stable isotope analysis of enamel bioapatite from the sheep and goat molars

Supplementary Info S8.4: Information about immature enamel of the modern and archaeological samples. ***La*** = the length of apposition is the distance along the tooth from where a new appositional layer contacts the enamel-dentine junction and where that layer contacts the outer enamel surface. ***Lm*** = the length of maturation is the length of the tooth that is not fully mineralized. **?** = the neck of the crown was partially broken preventing the measurement of *La*. **ABS** = absolute difference between calculated DOD and Known DOD.

Sample	*La* (mm)	*Lm* (mm)	total length of immature enamel	ABS(calculated DOD-known DOD)
P2015-112-M3	2.5	10.1	12.6	3.6
P2015-147-M3	4.9	8.9	13.8	16.3
2018-23A-M3	3.8	8.7	12.5	34.5
2018-63B-M2	?	3.9	3.9	12.3
P330-M2	?	11.6	11.6	33.7
P331-M3	?	6.5	6.5	34
Alt16-104a-M3	3.7	5	8.7	13.4
Alt16-283a-M3	1.4	5.1	6.5	39.4
Alt16-306a-M3	0.9	7.6	8.5	0.2
Alt16-369a-M3	3.7	7.4	11.1	0.8
2017-70-M3	1.4	6.4	7.8	36.2
2017-71-M3	0.4	4.8	5.2	26.4
2017-98-M3	1.4	7.6	9.0	48.6
2017-146-M3	0.9	4.8	5.7	6.0
T60B-P80 †	4.6	7.8	12.4	-
T60B-P82 †	3.7	7.6	11.3	-
T77-P90 †	2.1	8.6	10.7	-

† archaeological samples

Supplementary Info S8.5:

Results from wear stages (Grant, 1982) from the teeth of goat from the tomb 60B and 77 of the necropolis of Egiyn Gol. Individuals R and X were analysed for their oxygen isotope composition to determine their slaughtering period.

	tooth	d4	M1	M2	M3
Tomb 60b - goat	individual	piercing	-	-	-
	E	d	a	-	-
	AA	f	a	-	-
	Z	g	a	-	-
	G	f	b	-	-
	L	f	b	-	-
	K	f	b	-	-
	N	f	b	-	-
	P	g	b	-	-
	W	e	c	-	-
	T	h	d	½ out	-
	R (T60B-P80)	g	g	e	piercing
	X (T60B-P82)	g	g	d	b
	S	-	h	h	d
	U	-	j	h	b
	Y	-	m	h	g
	M	-	k	m	h
	Q	-	l	m	k
Tomb 77	T77-P90	g	g/h	g	d

Supplementary Info S8.6:

Results for the age-at-death determination of goats from tomb 60B of Egyin Gol. Letters represent the different individuals (see Supp Info S8.4).

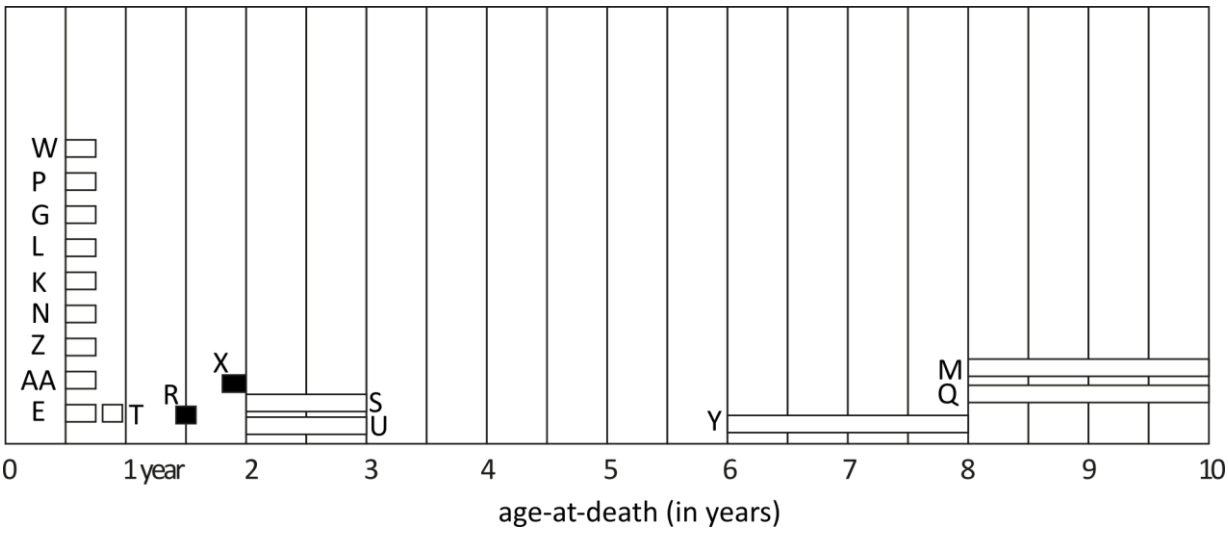

Chapitre 9 – Estimation de la période de mort des chevaux de l'âge du Bronze retrouvés en contexte funéraire et rituel

Ce chapitre est consacré à la détermination de la saison d'abattage de plusieurs chevaux de l'Âge du Bronze (khirgisuur) mis au jour dans un contexte funéraire et rituel à Burgast (Atltaï mongole). L'objectif était d'appréhender le calendrier rituel, lié à cette structure funéraire, par l'estimation de la saison de mort des chevaux associés. Nous nous sommes inspirés pour cela de l'approche développée dans le chapitre précédent à partir des caprinés et qui utilise l'analyse isotopique du $\delta^{18}O$ de l'émail de leurs molaires. Néanmoins, les relations déterminées au chapitre précédent ne pouvaient pas être appliquées directement en raison de la durée du processus de minéralisation de l'émail qui est beaucoup plus longue chez les chevaux que chez les caprinés et complique la modélisation des courbes avec la fonction cosinus utilisée dans le chapitre 6.

Par conséquent, l'interprétation des courbes isotopiques en terme de période de mort ne s'est faite que qualitativement et aucune estimation numérique de la période de mort n'a été avancée. Pour améliorer l'estimation de la saison de mort, nous avons comparé les profils de $\delta^{18}O$ des chevaux de l'âge du Bronze aux profils réalisés sur des dents en cours de croissance de chevaux modernes.

9.1 Résumé de l'étude

Depuis son introduction dans les steppes orientales de l'Eurasie, le cheval a eu un fort impact sur la construction des cultures et l'organisation des sociétés anciennes en permettant aux gens de se déplacer plus rapidement et plus efficacement. L'évolution de cette mobilité s'est accompagnée de profonds changements dans l'expression des pratiques rituelles, et le cheval est très présent dans les monuments funéraires (i.e. khirgissuur, pierre à cerfs) de la fin de l'âge du Bronze. Des recherches récentes ont permis de progresser sur la question de la nature et des pratiques liées aux dépôts de restes de chevaux dans et autour des tombes, de nombreux points restent à éclaircir et notamment les intérrogations liées à la mise en place (qu'elle période de l'année ?) et la régularité des visites (saisonnalité ?) de ces monuments funéraires. Définir la saison d'abattage des chevaux peut permettre d'affinier notre perception des pratiques rituelles.

Ce travail propose d'utiliser les variations saisonnières des isotopes de l'oxygène ($\delta^{18}O$) enregistrées par les molaires en développement pour estimer la saison d'abattage des chevaux. L'analyse d'un ensemble de référence moderne composé de cinq chevaux de la région de Burgast (province de Bayan-Ölgii, Mongolie occidentale) montre qu'il est possible d'estimer la période de la mort avec une résolution de l'ordre de la saison. L'analyse isotopique de deux chevaux juvéniles déposés autour d'un khirgisuur de l'âge du bronze a ensuite permis d'établir que la saison de la mort était centrée dans les deux cas sur la saison hivernale. L'étude géochimique et zooarchéologique conjointe révèle que le premier cheval est mort en début d'hiver (novembre) et a été déposé peu après sa mort (i.e. dépôt frais – crâne et mandibule en connection anatomique), tandis que le second cheval est mort à la fin de l'hiver (février) et n'a été déposé que plusieurs mois après sa mort.

Deux calendriers sont donc concernés : un calendrier technique, qui favorise un abattage hivernal, et un calendrier rituel, qui est lié aux funérailles et à la commémoration. Ces résultats montrent l'importance de cette approche pour l'étude des pratiques rituelles à l'âge du bronze, et ils suggèrent que des scénarios plus complexes doivent être envisagés que ceux impliquant un sacrifice de plusieurs chevaux au moment et à l'endroit des funérailles. Toutefois, cette application illustre une limite de cette méthode isotopique liée à l'âge des animaux. En effet, seuls deux chevaux parmi les 8 retrouvés autour du khirgisuur étaient suffisament jeunes au moment de leur mort pour pouvoir être analysés isotopiquement.

Article VI: Season of death of domestic horses deposited in a ritual complex from Bronze Age Mongolia: Insights from oxygen isotope time-series in tooth enamel

Nicolas LAZZERINI, Antoine ZAZZO, Aurélie COULON, Noost BAYARKHUU, Vincent BERNARD, Mathilde CERVEL, Denis FIORILLO, Dominique JOLY, Charlotte MARCHINA, Tsagan TURBAT, Sébastien LEPETZ

Manuscript submitted in *Journal of Archaeological Science: Reports*

Abstract:

Since its introduction in the eastern steppes of Eurasia, the horse has had a strong impact on the construction of cultures and the organisation of ancient societies by enabling people to move faster and transport goods and people more efficiently. The evolution of this mobility was accompanied by profound changes in the expression of ritual practices, and horses are very present in funerary monuments of the Late Bronze Age. While recent research has made progress on the question of the frequency of these horse deposits, little is known yet about the season in which the animals were slaughtered and the time of year when the funerary and ritual sites were visited. This work proposes to use oxygen isotope variations ($\delta^{18}O$) recorded by developing molars of horses to estimate their season of slaughter. The analysis of a modern reference set consisting of five horses from the Burgast region (Bayan-Ölgii province, western Mongolia) shows that it is possible to date the time of death with a resolution of the order of the season. Isotopic analysis of two juvenile horses deposited around a Bronze Age khirgisuur then made it possible to establish that the season of death centred on the winter season for these two individuals. The geochemical and zooarchaeological study reveals that the first horse died in early winter (November) and was deposited shortly after death, while the second horse died during late winter (February) and was deposited several months after death. Two calendars are therefore involved: a technical calendar, which favours a winter slaughter, and a ritual calendar, which is linked to funerals and commemoration. These results show the importance of this approach for the study of ritual practices in the Bronze Age, and they suggest that more complex scenarios need to be considered than those involving a multiple-horse sacrifice at the time and place of the funeral.

Keywords: khirgisuur; geochemistry; nomadism; funerary practices; archaeozoology; Altai

9.2 Introduction

Since its introduction into the eastern steppes of Eurasia as a domestic animal, the horse has had a strong impact on the construction of cultures and the organisation of ancient societies (Anthony, 2007; de Barros Damgaard et al., 2018; Gaunitz et al., 2018; Outram et al., 2009). It has been a source of meat, dairy products, leather, and hair, but above all, it has allowed people to move faster and to transport goods and people more efficiently. In Mongolia, horses were used for riding or pulling carts from the end of the 2nd millennium BCE on (Taylor, 2017). Although the details of these modalities still need to be clarified, it is argued that the emergence of horse riding and chariotry may have encouraged the adoption of nomadic pastoralism. The evolution of this mobility was accompanied by profound changes in the expression of ritual practices. The final Bronze Age witnessed the appearance of the khirgisuurs and deer stones and (KDS) culture, characterised by its funerary complexes. The KDS complexes are abundant in central Mongolia but can also be found as far away from there as the foothills of the Altai. They are characterised by stone monuments (tombs or deer stones) and are usually surrounded by circular or rectangular enclosures, which are, in turn, surrounded by stone circles and stone mounds (Allard and Erdenebaatar, 2005; Fitzhugh, 2009; Lepetz et al., 2019; Wright, 2007). The stone circles often contain charred bones of domestic animals, most often caprines. The stone mounds cover horse skulls, which are sometimes associated with neck and hoof components (Allard and Erdenebaatar, 2005; Broderick et al., 2014, 2016; Fitzhugh, 2009; Zazzo et al., 2019). These deposits can include hundreds of heads, and in some cases more than a thousand. The size of the monuments is probably a function of the social importance of the deceased or the size of the community attached to that person. This importance is perceptible through the height and diameter of the central mound, the quality and number of the deer stones, the size of the enclosure, and, above all, the number of mounds and circles, and thus the quantity of animals involved in the ceremonies. While the gestures leading to these accumulations have been interpreted as marks of homage to ancestors, whether real or mythical, as well as to deities (Fitzhugh, 2009; Lepetz et al., 2019), the arrangement of the heads around the grave and the direction toward which they are oriented evoke the image of horses pulling the khirgisuur, and thus echo the Altai rock art representations of a cart used to transport the deceased (Jacobson-Tepfer, 2012; Lepetz et al., 2019).

Recent advances in research have improved our knowledge on the frequency of these deposits. At the scale of the structure, radiocarbon dating of the horse remains indicates that the deposits were not made simultaneously and may have taken place spread over several decades

in the case of large khirgisuurs (Zazzo et al., 2019). At the scale of the deposit, the remains of horses do not appear to come from animals that were all killed on site and immediately covered with stones. Indeed, while some of the horse parts were deposited fresh, shortly after slaughter, other parts were probably deposited at least several months later (Lepetz et al., 2019). This possible disconnection between the date of slaughter and the date of deposition also raises the question of the season of site frequentation and the ritual calendar, which remains totally unknown today. It is not known, for example, whether these visits were carried out throughout the year or whether they were confined to a particular time of the year.

Oxygen isotope analysis ($\delta^{18}O$) of tooth enamel can be used to address the question of the season of death of animals (El Adli et al., 2017; Fisher et al., 2003; Julien et al., 2015; Knipper et al., 2008; Koch et al., 1989; Lazzerini et al., *minor revisions*). During its growth, tooth enamel records the isotopic composition of ingested water (drinking water and plant water), which is itself under environmental control. In middle and high latitudes, there is seasonal variation in the $\delta^{18}O$ value of meteoric water, with high values during the warm season and low values during the cold season. Sequential sampling along the growth axis of tooth enamel provides a chronological record of climatic conditions (Balasse, 2003; Fricke et al., 1998; Pederzani and Britton, 2019; Zazzo et al., 2002). If the teeth were still developing at the time of death, stable isotope analysis can be used to determine the date of death. In Mongolia, this approach allowed researchers to estimate that caprines deposited in two tombs in the Xiongnu necropolis of Egiin Gol were slaughtered during the warm season (Lazzerini et al., *minor revisions* - see Chapter 8).

In 2016, excavations at the site of Burgast (Bayan-Ölgii province, western Mongolia) yielded remains of several horses belonging to a khirgisuur. Two of these horses had teeth that would still have been growing at the time of death, providing an opportunity to determine their slaughter season. Applying this approach, however, requires establishing a reference set constituted of animals slaughtered on a known date. This reference set must be built using the species of interest, because the timing and duration of tooth mineralisation varies from one species to another (Kohn, 1996; 2004; Kohn et al., 1996; Balasse, 2002; Kohn and Cerling, 2002; Passey and Cerling, 2002; Zazzo et al., 2005, 2010, 2012). For this reason, we built a reference set with molars from modern juvenile horses with a known date of death that had lived in the same area. Comparing the results of the isotope analysis and the archaeozoological observations lays the foundation from which to discuss the season of site visits and the ritual calendar during the Bronze Age.

9.3 Materials

9.3.1 The archaeological site of Burgast and the Bronze Age horses

The site of Burgast is located in the province of Bayan-Ölgii (Nogoonnuur district), about 100 km north-east from Ulgii as the crow flies, about 15 km from the border with the Republic of Tuva and about 20 km south of the Republic of Altai (**Figure 39**). This area is located on the eastern fringes of the Altai mountain range, in its Mongolian part. Bordered to the south by a river and to the north by a rocky massif, the site has the shape of a triangular terrace of ca. 20 ha, at an altitude of 1900 m. Archaeological remains from several periods (Late Bronze Age, Hun Sarmate, Türk) are scattered along the terrace, and these were excavated in 2015 and 2016 by the French-Mongolian Joint Archaeological Expedition. Among the different structures, a khirgisuur was excavated in 2016, and it is the subject of this article (**Figure 40**).

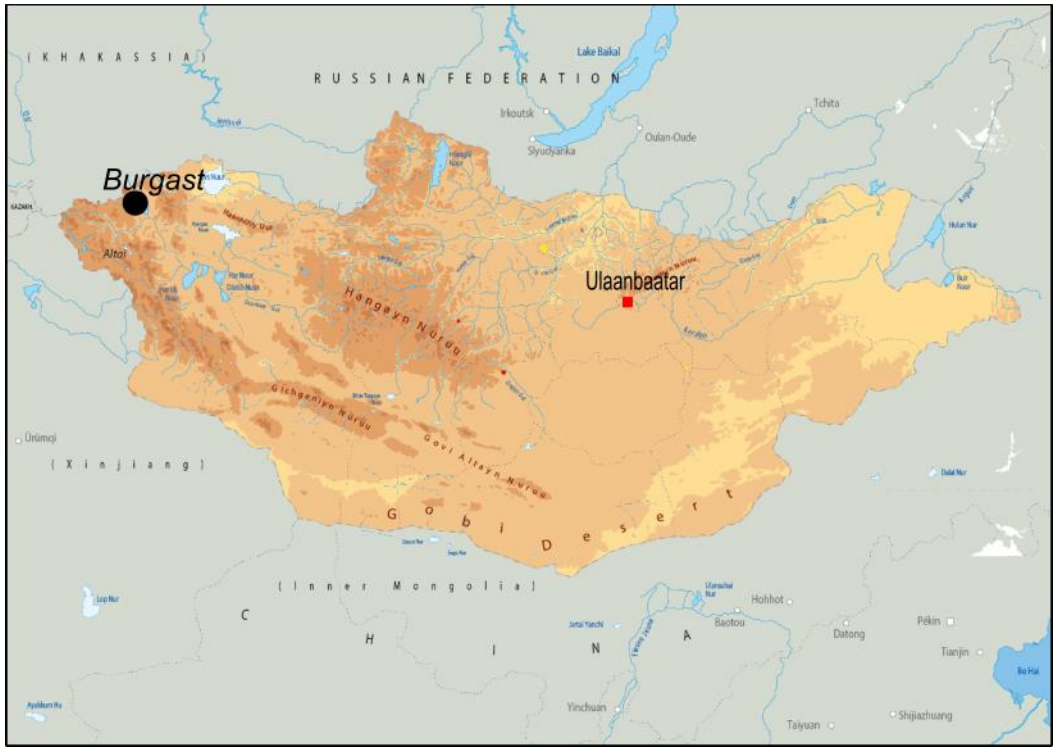

Figure 39: Map of Mongolia showing the location of the study site.

This Late Bronze Age khirgisuur is composed of a 15.5 × 14 m central mound (ST 60) made up of large blocks. This mound is inscribed in a rectangular area of 20 × 18 m covered with stones laid on the ancient ground and presenting small mounds at the four corners. The central mound contains the remains of a human body (oriented west–east) in dorsal decubitus position. Excavation of the stones revealed the existence of a casing made of large rocks. No grave good is associated with the deceased. To the west, the complex is flanked by four stone

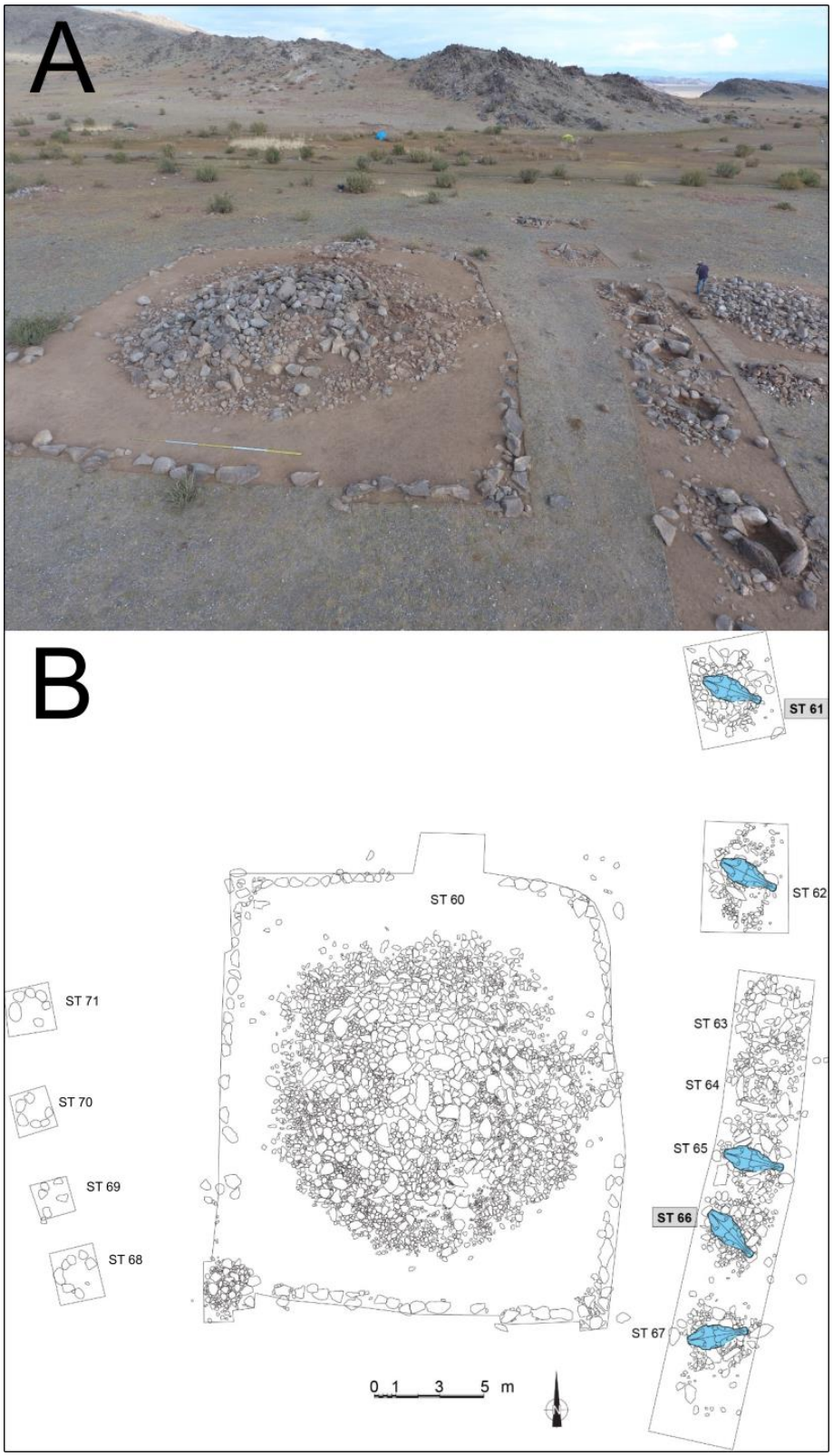

Figure 40: (A) view and (B) plan of khirgisuur ST 60 and its peripheral structures, including the four stone circles (ST 68-71) and seven stone mounds (ST 62-67), located west and east of the central mound, respectively, some of which contained the remains of horses. The stone mounds that contained the individuals analysed in this study are highlighted in grey. Photograph: S. Lepetz.

circles, aligned over a length of 14 metres (ST 68 to 71). Their diameter varies from 1.6 to 2 m. Although stone circles generally yield burnt bones and teeth of caprines (Broderick et al., 2014, 2016; Lepetz et al., 2019), these four were empty. To the east, and aligned over a length of 30 m, are seven mounds (ST 61 to 67) of 1.7 to 2 m in diameter, each delimiting a central space of about 1.3 to 1.5 m and each yielding horse remains (**Figure 40B**). The horse remains are fairly well preserved, but bone displacements, breakage and missing parts seem to indicate that taphonomic disturbances (possibly by burrowing animals) have occurred, although it is not always possible to precisely define their extent. The remains comprise elements of heads (skull or mandibles), sometimes accompanied by connected cervical vertebrae and terminal phalanges. The heads are oriented towards the south-east (between 80° and 135°). Two males and one female have been identified. Individual ages range from 1 to 18–20 years old.

Two of the seven mounds (ST 61 and ST 66) contained juvenile individuals that were radiocarbon dated to the very end of the second millennium BCE (**Table 23**). The remains of structure ST 61 are in the form of a head (skull and mandible) associated with two terminal phalanges and five cervical vertebrae (C2 to C6). The head was placed upside down and rested on its frontal and nasal bones. The stage of dental eruption indicates that this animal was approximately 1 year old at death (Cornevin and Lesbre, 1894). There is an overlap in the formation calendar of M1 and M2 (**Figure 41**). Because the M1 and M2 of the right mandible were in the process of mineralisation, and because the lower part of M1 was broken, both teeth were selected for analysis in order to be able to obtain as much information as possible. Structure ST 66 yielded the skull (i.e., without mandible) of a young male. The skull had been deposited on its right side. No vertebrae or phalange were present. The stage of dental eruption and wear of the incisors (very little wear on the third incisor), allows us to estimate that the animal was about 5 years old at death. The M3 was still in the process of mineralisation and was therefore sampled.

Table 23: Characteristics of the Bronze Age samples analysed in this study. Subscript and superscript indicate that the molar was taken from the lower or upper jaw, respectively.

Sample	Species	Sex	Estimated age (years)	^{14}C date ± error (1σ)	Target #	Calibrated date (BCE)		Sampled tooth
						from	to	
ST 61 M1 ST 61 M2	*Equus caballus*	?	1	2814 ± 28	ECHo 1507	−1052	−898	M_1 right M_2 right
ST 66 M3	*Equus caballus*	M	~ 5	2887 ± 25	ECHo 1513	−1190	−979	M^3 right

9.3.2 The modern horses

The reference dataset consists of five young individuals whose teeth were still growing at the time of death (**Figure 42**). These animals come from different herds belonging to Kazakh-Mongolian nomadic herders living around the site of Burgast (**Table 24**). The horses were not slaughtered specifically for the study, but either succumbed to injuries caused by accidents or predators, or were slaughtered by the herders themselves for consumption. We were not on site when the horses died, and the date of death was provided to us by the herders with a precision equal to or better than 1 month. The date of death of the sampled animals covers the entire calendar year, from the beginning (2018-59a, January) to the end of the year (2017-104b, end of November), providing the opportunity to observe the seasonal recording of the isotopic oxygen composition of the tooth enamel during its formation. Due to the age of the animal at death, which differs between individuals, we had to sample M1 (n = 1), M2 (n = 2) or M3 (n = 2). Field constraints and the availability of skeletal remains meant that we had to sample either the upper (n = 3) or lower (n = 2) molar.

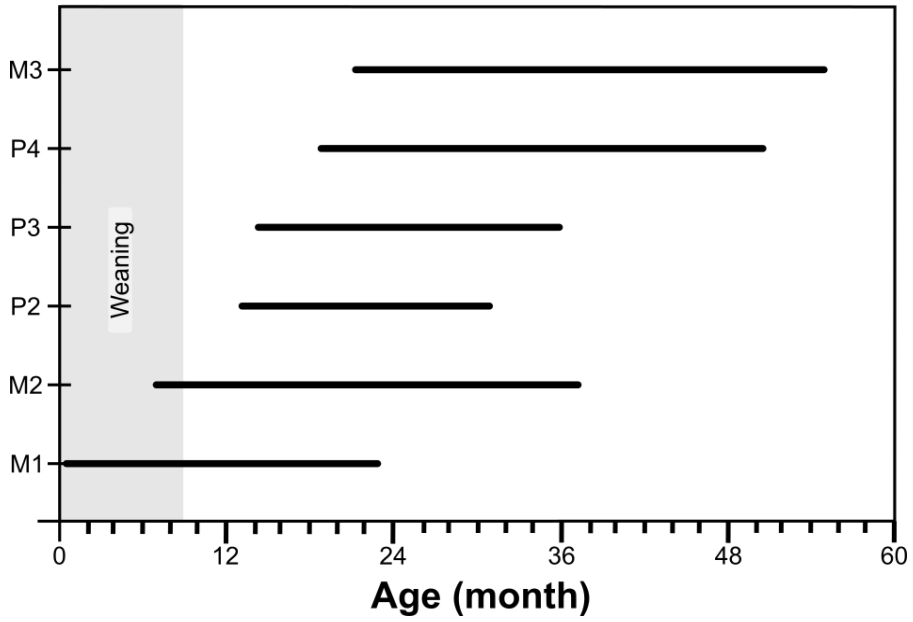

Figure 41: Calendar of horse tooth mineralisation, modified after Hoppe et al. (2004). P2-P4 (premolars) and M1-M3 (molars) refer to tooth from either the upper or the lower jaw.

Table 24: Characteristics of the modern reference set analysed in this study. Subscript and superscript indicate that the molar was taken from the lower or upper jaw, respectively.

Sample	Species	Sex	Birth	Death	Season	Sampled tooth
2017-104 M2	*Equus caballus*	F	April–May 2013	10 November 2016	winter	M_2 right
2018-17B M3	*Equus caballus*	M	2013–2014?	early July 2017	summer	M^3 right
2018-57A M3	*Equus caballus*	M	2003?	late February 2007	winter	M^3 left
2018-58B M3	*Equus caballus*	M	2015?	20–25 April 2018	spring	M^3 right
2018-59A M1	*Equus caballus*	F	2016?	January 2018	winter	M_1 right

9.4 Methods

Tooth sampling was carried out on the mesial side, both for practical convenience (this side has a flat surface with a narrow cementum layer) and also because it should mineralize faster (Zazzo et al., 2012). The outer surface of the tooth was first cleaned with a tungsten burr to remove the cementum. Tooth enamel was then removed by abrasion with a diamond burr. Each sample consists of a horizontal sample of about 1 mm, spanning the entire thickness of the enamel layer and parallel to the growth axis of the tooth. The enamel powder thus recovered (~6–7 mg) was chemically treated following the procedure described in Balasse et al. (2002b). The organic matter was removed with a NaOCl solution (2–3%, 0.1 ml solution/mg enamel, for 24 hours). The samples were then rinsed several times with distilled water. Each sample was then reacted with 0.1 M acetic acid (0.1 ml solution/mg enamel, for 4h) to remove exogenous carbonates, rinsed with distilled water and oven dried at 80°C for 12h.

The purified enamel samples were weighed (~ 600 µg) and analysed using a Kiel IV automatic device coupled to a Delta V Advantage Isotope Mass Spectrometer (IRMS) at the Service de Spectrométrie de Masse Isotopique of the Muséum national d'Histoire naturelle (SSMIM) in Paris. The accuracy of the data was checked by repeated analysis of the laboratory's internal carbonate standard (LM Marble) standardised against the international standard NBS 19. The analytical accuracy, estimated by the repeated analysis (n = 80) of LM Marble, was 0.04‰, and the correction applied to bioapatite samples ranged from +0.16‰ to +0.25‰. The isotopic data are presented in δ notation [$\delta = (R_{sample}/R_{standard}) - 1$], with R being the isotopic ratio ($^{18}O/^{16}O$) of the sample to that of the international standard in V-PDB (Vienna PeeDee Belemnite) and expressed in per thousand (‰). The average $\delta^{18}O$ values between individuals and time periods were compared using the One-way ANOVA statistical test coupled with Tukey's post-hoc test using R software version 3.4.4 with a significance threshold at p-value < 0.05.

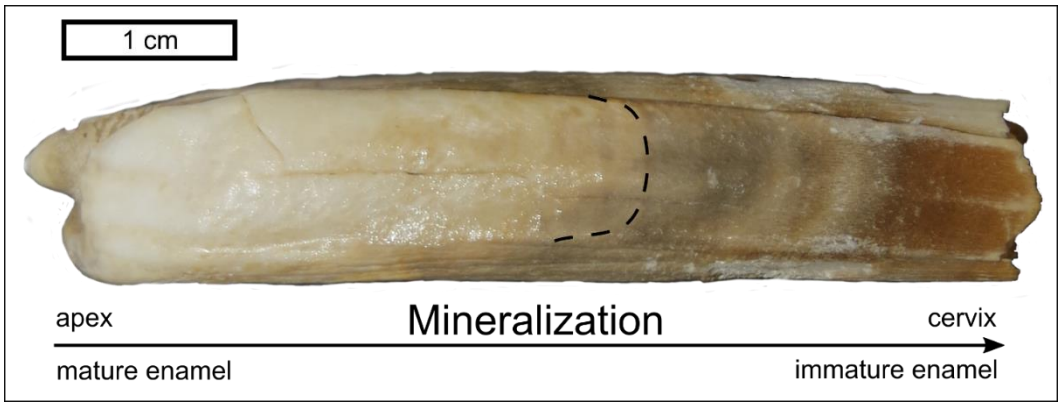

Figure 42: First molar from individual 2018-59a (view from the mesial side). The tooth was still growing at the time of death, and immature enamel (brown in colour) is clearly visible in the lower part of the tooth. The dotted black line indicates the limit between mature and immature enamel. Photograph: N. Lazzerini.

Table 25: Stable isotope analysis of enamel bioapatite ($\delta^{18}O$‰ V-PDB) from the molars (M1, M2, and M3) of the modern horses. Subscript and superscript indicate that the molar was taken from the lower or upper jaw, respectively. Sample position is indicated as the distance from the base of the tooth crown.

2017-104b M_2		**2018-17b M^3**		**2018-57a M^3**		**2018-58b M^3**		**2018-59a M_1**	
† November		† July		† February		† April		† January	
distance (mm)	$\delta^{18}O$ (‰)	distance (mm)	$\delta^{18}O$ (‰)	distance (mm)	$\delta^{18}O$ (‰)	distance (mm)	$\delta^{18}O$ (‰)	distance (mm)	$\delta^{18}O$ (‰)
74.8	−13.7	65.2	−8.9	71.9	−10.6	67.6		56.2	−5.6
73.1	−14.1	61.8	−8.1	68.7	−9.4	64.6		52.7	−6.0
72.2	−13.8	58.6	−6.9	65.7	−9.0	61.7		49.8	−6.4
71.0	−13.4	55.3	−6.1	62.7	−10.4	58.8		46.9	−6.2
69.8	−13.3	51.9	−6.8	59.9	−8.9	55.4		43.3	−6.7
68.5	−12.6	49.5	−11.2	56.5	−7.6	52.7		39.8	−7.5
67.3	−11.9	46.8	−12.4	52.8	−6.8	49.4	−7.5	37.2	−8.0
65.6	−11.7	43.9	−12.6	50.2	−9.0	46.1	−7.5	33.9	−9.1
64.2	−11.9	41.0	−12.7	47.4	−10.3	42.7	−7.5	30.4	−9.3
62.8	−11.4	37.6	−13.0	44.2	−10.8	39.9	−7.7	26.6	−10.4
61.1	−11.3	34.5	−13.9	41.4	−11.2	37.2	−8.5	22.5	−11.1
59.8	−10.6	31.3	−14.5	38.5	−11.3	34.2	−9.3	19.6	−10.7
57.0	−10.5	27.5	−14.5	35.7	−11.7	30.4	−9.6	15.2	−10.8
54.4	−10.5	24.3	−14.5	32.9	−12.8	27.1	−11.4	10.5	−12.1
51.3	−10.0	21.0	−14.3	29.2	−12.9	24.1	−12.3	6.8	−13.1
48.3	−11.4	17.7	−13.6	25.7	−13.3	20.6	−13.2	2.9	−14.4
45.9	−11.9	14.5	−13.1	22.5	−11.8	17.1	−13.9		
42.8	−12.5	11.4	−10.3	18.5	−11.5	13.0	−14.2		
39.7	−13.1	7.8	−6.5	14.8	−10.3	9.4	−14.5		
36.5	−13.1	4.9	−4.9	11.9	−8.7	5.4	−16.1		
34.0	−14.0			8.7	−8.8				
31.8	−14.7			6.1	−10.3				
28.6	−13.9			2.9	−11.9				
25.1	−12.7								
21.7	−12.1								
18.4	−11.4								
15.0	−10.4								
11.8	−7.9								
7.9	−7.3								
4.2	−7.2								

9.5 Results

The isotopic values of the 173 modern and archaeological samples are presented in **Tables 25 and 26**. Summary statistics are presented in **Table 27**.

9.5.1 The modern horses

The average $\delta^{18}O$ value of the modern individuals is −10.7 ± 1.0‰ (1σ). The $\delta^{18}O$ values range from −16.1 to −5.0‰, with an average maximum of −6.4 ± 1.1‰ and minimum of −14.6 ± 1.0‰. The average amplitude is 8.2 ± 1.9‰, and the amplitude varies from 6.5 to 9.5‰ (**Table 27**). With the exception of two individuals (2017-104-M2 and 2018-59A-M1, $p < 0.05$), the samples from the modern horses are not statistically different from each other ($p > 0.05$). For each individual, the intra-tooth isotope variations follow a sinusoidal signal (**Figure 43**). The minimum values correspond to the portion of mineralized enamel during mid-winter (temperature minimum), while the maximum values correspond to the portion of mineralized enamel during mid-summer (temperature maximum). The values recorded at the base of the crown during mineralisation correspond to the environmental conditions prevailing during the last weeks or months of the animal's life (**Figure 43**). The last values recorded by the two individuals who died in January and February plot along a decreasing curve, but have not quite reached the winter minimum yet. It is not possible to visually distinguish between these two individuals (**Figure 43**). The individual that died at the end of April (2018-58B) has recorded the winter minimum and is a little more advanced in the seasonal cycle. The last values recorded by the individual who died in early July (2018-17B) plot along a strongly rising curve and are nearing the summer maximum. Finally, the last values recorded by the M2 of the individual who died in November 2016 (2017-104) has already recorded the summer maximum and reached a plateau.

9.5.2 The Bronze Age horses

The average $\delta^{18}O$ value of Bronze Age horse tooth enamel is −11.3 ± 2.8‰ (1σ). The isotopic composition of the enamel samples ranges from −16.1 to −5.7‰ (**Table 27**), with an average maximum value of −7.6 ± 2.3‰ and an average minimum value of −13.0 ± 3.5‰. The seasonal isotopic amplitude recorded by tooth enamel is 8.0‰ for individual ST 61 and 5.9‰ for individual ST 66. The isotope profile of the lower part of the M1 overlaps with that of the M2 (**Figure 44**). The last values recorded by the two teeth of the ST 61 individual are placed along an ascending curve to reach a plateau around −6‰. The M3 of individual ST 66 is much

more advanced in its formation and recorded a full seasonal signal. The lower part of the tooth records a decrease in $\delta^{18}O$ values but has not reached a plateau yet.

Table 26: Stable isotopes analysis of enamel bioapatite ($\delta^{18}O$‰ V-PDB) from the molars (M1, M2, and M3) of the Bronze Age horses. Subscript and superscript indicate that the molar was taken from the lower or upper jaw, respectively. Sample position is indicated as the distance from the base of the tooth crown.

ST61 M_1		**ST 61 M_2**		**ST66 M^3**	
distance (mm)	$\delta^{18}O$ (‰)	distance (mm)	$\delta^{18}O$ (‰)	distance (mm)	$\delta^{18}O$ (‰)
13.9	−11.1	3.7	−9.2	71.0	−11.5
17.3	−12.0	6.2	−8.3	69.6	−12.0
20.1	−13.0	8.6	−8.0	68.2	−11.8
22.1	−13.0	10.8	−7.3	66.8	−13.0
24.4	−13.4	13.1	−7.2	65.3	−13.0
27.0	−13.7	15.0	−6.8	63.4	−13.1
29.5	−13.5	17.8	−6.9	61.5	−13.4
31.9	−13.0	20.4	−6.7	59.6	−14.1
34.0	−12.4	22.7	−6.6	57.8	−14.5
36.8	−13.0	25.7	−6.4	55.9	−14.9
39.1	−12.8	32.2	−6.5	54.7	−15.6
41.2	−12.4	35.5	−5.9	52.4	−16.0
43.7	−12.1	39.0	−5.7	50.3	−16.1
46.5	−11.8	44.1	−5.7	48.6	−15.7
48.2	−11.4			46.2	−14.6
51.0	−9.9			44.3	−13.8
54.9	−8.7			42.2	−13.5
58.3	−7.5			40.9	−13.1
61.3	−6.8			39.2	−12.8
				37.5	−12.4
				36.1	−12.4
				34.5	−12.1
				32.5	−11.7
				30.6	−11.1
				28.6	−10.9
				27.3	−10.9
				25.2	−11.5
				23.8	−11.7
				21.8	−12.0
				20.0	−12.1
				17.8	−12.4
				16.0	−12.7
				10.5	−10.9
				8.8	−10.2
				6.8	−12.5
				4.3	−13.7

Table 27: Summary statistics of the oxygen isotopic values ($\delta^{18}O$) of tooth enamel in the modern and Bronze Age (†) horses. Subscript and superscript indicate that the molar was taken from the lower or upper jaw, respectively. N = number of samples per tooth. SD = standard deviation.

Samples	N	$\delta^{18}O$ (‰ V-PDB)			
		Mean ± SD	Max.	Min.	Amplitude
2017-104b-M_2	25	−11.8 ± 1.9	−7.2	−14.7	7.5
2018-17b-M^3	20	−10.9 ± 3.3	−5.0	−14.5	9.5
2018-57a-M^3	23	−10.4 ± 1.7	−6.8	−13.3	6.5
2018-58b-M^3	16	−11.2 ± 3.1	−7.5	−16.1	8.7
2018-59a-M_1	16	−9.2 ± 2.7	−5.6	−14.4	8.8
ST 61 M_1 †	19	−11.7 ± 2.0	−6.8	−13.7	6.9
ST 61 M_2 †	14	−6.9 ± 1.0	−5.7	−9.2	3.5
ST 66 M^3 †	36	−12.9 ± 1.5	−10.2	−16.1	5.9

9.6 Discussion

9.6.1 The oxygen isotope record of the season of death of the modern horses

Our results indicate that the isotopic value of the last mineralized tooth enamel samples is clearly related to the date of death of the modern horses. The terminal isotope values of the animals that died in late winter are close to the minima, whereas a plateau is reached in the lower part of the tooth of the animal that died in spring. The individual who died in summer approaches a maximum value, and a plateau is reached in the animal that died in early winter. These results differ slightly from those obtained on modern caprine molars from Mongolia (Lazzerini et al., *minor revisions* - see Chapter 8). Indeed, it can be noted that for animals slaughtered at the same time of year, the patterns of variation in $\delta^{18}O$ are more advanced in caprines than in horses. For example, the values for caprines slaughtered in July have already reached a plateau of high values, while the values for the horse which died at the same period are still rising. Similarly, the terminal values of $\delta^{18}O$ of caprines slaughtered in November follow a decreasing curve, while those of the horse slaughtered at the same period have not yet started to decrease. This probably corresponds to the fact that horses' tooth development spreads over a longer period of time and that enamel mineralisation lasts longer in horses than in caprines (Bendrey et al., 2015; Hoppe et al., 2004). These findings emphasize the importance of building a reference set based on the species of interest.

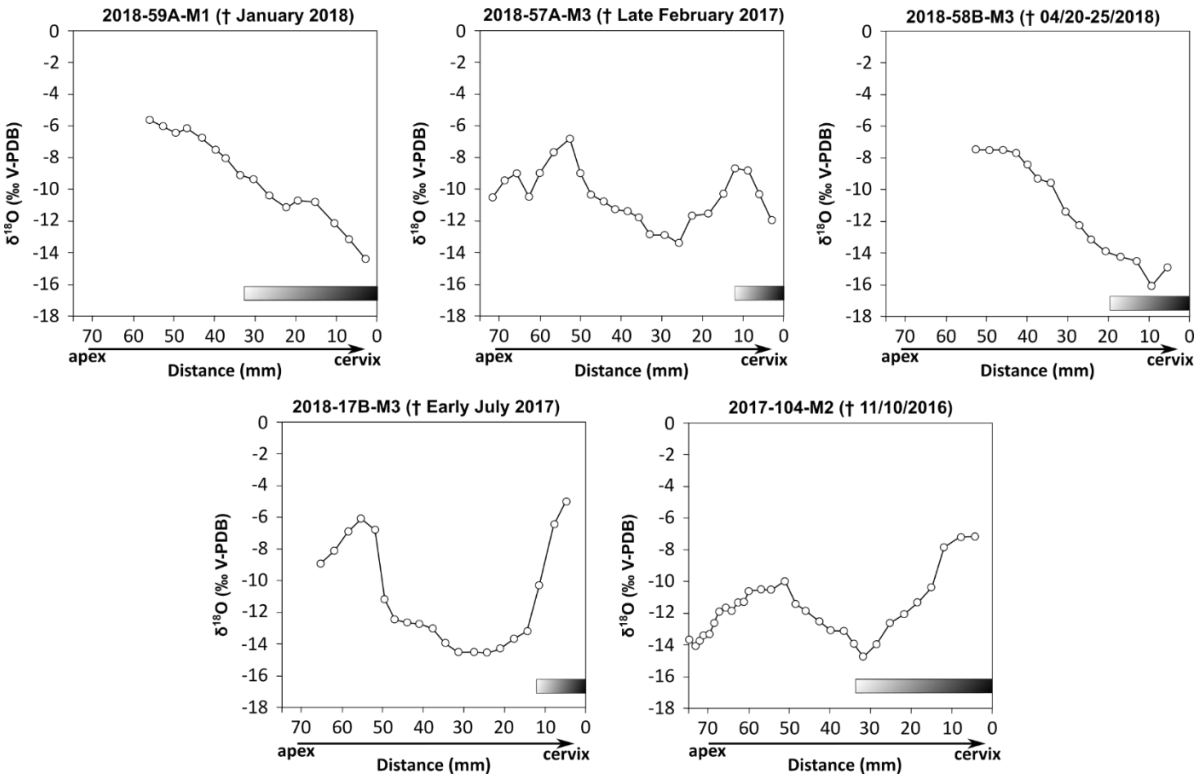

Figure 43: Oxygen isotope ($\delta^{18}O$ ‰) variations recorded along the tooth enamel of the molars from the five modern horses. The position of the sample is expressed as the distance between the sample and the base of the tooth crown, with the oldest enamel on the left and the youngest enamel on the right. The white circles represent the measured data. The period of death of the animal is indicated after the sample label. The results are presented according to the season of death, from January (top left) to November (bottom right). The grey shaded area represents the immature enamel zone.

Our results also suggest that the temporal resolution provided by the modern reference set seems variable. Indeed, there is little difference between the terminal isotope values recorded by the individual that died in July (2018-17B) and the one that died four months later, in early November (2017-104) (**Figure 43**). Conversely, it is easy to distinguish between two individuals that died 2–3 months apart in spring (2018-58B) and summer (2018-17B). In addition, some inter-individual variability seems to exist. The tooth belonging to the individual that died in January (2018-59A) seems slightly ahead of the tooth from the one that died at the end of February (2018-57A). This variable resolution can be explained by the fact that we are comparing different molars (M1 vs. M3) that do not have the same growth rate. M3 grows more slowly than M1 and M2, and this could lower the temporal resolution of the isotope signal recording in this tooth (Bendrey et al., 2015; Hoppe et al., 2004). In addition, this dataset is made up of teeth that are not all at the same stage of growth: some have almost completed their growth, while others are less advanced. However, the growth rate of horse molars decreases exponentially: 1 cm of enamel taken near the apex corresponds to a growth time period twice as short as a 1 cm taken near the enamel–dentin junction (Bendrey et al., 2015). Not all portions

of enamel are equivalent, and therefore not all enamel samples taken incorporate the same amount of time. It can therefore be assumed that the isotope signal of the M1 of individual 2018-59A-M1 is better resolved chronologically than that of the M3 of individual 2018-57A-M3, which grew more slowly. This may explain the fact that the seasonal cycle recorded in the tooth of the animal that died in January appears to be at the same point as, or even slightly ahead of, the one that died at the end of February (**Figure 43**). Therefore, we recommend favouring teeth that form first (M1 and M2), and whose crown has not finished growing in length, for estimating the period of death, as they will provide a better temporal resolution. Although preliminary, the reference dataset presented here is consistent and therefore allows us to distinguish between different seasons of death in ancient horses.

9.6.2 Season of death of the Bronze Age horses

Two developing teeth (M1 and M2) were analysed for the individual from ST 61 (**Figure 44**). While the terminal values of the two teeth follow an ascending curve, those of M1 have not yet reached a plateau, unlike those of M2. This difference can be explained by the fact that it was not possible to sample the last 10 mm of M1 because the tooth was broken. On the other hand, due to the exponential decrease in the growth rate of horse teeth, it is possible that the temporal resolution was better for M2 which, unlike M1, had not yet completed its growth in length. For these two reasons, we believe that the slaughter date is better approximated by the isotope profile recorded in M2. This profile is very similar to that observed on the modern horse that died in early November (sample 2017-104). In the case of the ST66 horse, the tooth sampled (M3) had almost completed its growth in length and recorded a decrease in isotope values, but had not reached a plateau. This profile is very similar to that observed on the M3 of individual 2018-57A, which died in late February, and therefore suggests that death occurred in mid- to late winter. It is interesting to note the presence of a hypoplasia located 11–15 mm from the base of the dental crown of this individual (**Figure 44**). Such an anomaly in enamel mineralisation is potentially caused by ecological or climatic factors, such as water or dietary stress, but may also be due to stress related to infections or injuries (Dobney et al., 2004; Upex and Dobney, 2012). This cessation of growth influences the isotope record, which rapidly shifts from a phase of decreasing values of $\delta^{18}O$ to a phase of increasing values. It can be seen that this enamel growth defect occurred at the same time as the $\delta^{18}O$ values were decreasing, and therefore corresponds to the winter period. It is reasonable to assume that the harsh climatic conditions reigning in winter were somehow at the origin of this hypoplasia.

Our results therefore indicate that the two Late Bronze Age horses died at two different periods during the cold season: in early winter (November) for one (ST 61) and during the second half of winter (late February) for the other (ST 66). Today, horses are slaughtered at the beginning of the winter season (November to December), to be consumed until spring. The winter temperatures make it possible to preserve the large amount of meat for at least four months. In addition, this animal is considered by the Mongols to be a "warm muzzle" (*khaluun khoshuutai*, in Mongolian), meaning that the energy characteristics of its meat adapt well to the cold season (Marchina et al., 2017). It would be unwise to transpose directly the cultural justifications put forward by modern herders to the Bronze Age. But we can reasonably assume that the pragmatic reasons for meat preservation may had led to the slaughter of horses being organised according to the same seasonal calendar. Although based on a reduced corpus that would benefit from being expanded, the Burgast dataset attests for the first time to the practice of winter slaughter of horses in the Bronze Age.

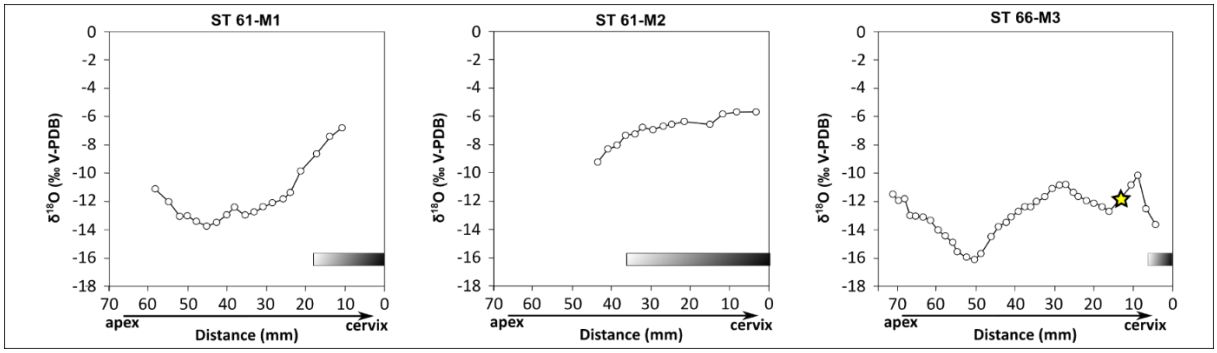

Figure 44: Oxygen isotope ($\delta^{18}O$ ‰) variations recorded along the tooth enamel of the molars from the two Bronze Age horses. The position of the sample is expressed as the distance between the sample and the base of the tooth crown, with the oldest enamel on the left and the youngest enamel on the right. The white circles represent the measured data. The grey shaded area represents the immature enamel zone. The yellow star indicates the position of the hypoplasia.

The data highlight another important fact: these two horses were not killed during a single ceremony. It is therefore necessary to abandon the idea that is implicit in discussions in the literature that the horses deposited in khirgisuurs were all sacrificed on the day of the funeral of the deceased person. This conclusion had already been proposed on the basis of radiometric arguments for large khirgisuurs comprising several hundred individuals (Zazzo et al., 2019). It therefore seems that this conclusion can be extended to smaller monuments. However, the data do not suggest that the individuals were deposited at two different time periods. ST 61 yielded the remains of a skull and associated mandibles in anatomical connection with part of the animal's neck and together with parts of its feet, suggesting that the bones were deposited fresh.

This therefore suggests that these elements were placed under the mound shortly after the animal's death. In contrast, ST 66 yielded a single skull, with no mandible and no other bones. This can be interpreted as the deposition of dry skeletal parts, indicating that the slaughter and deposition were not necessarily synchronous (Lepetz et al., 2019). At the large khirgisuur (B10) of Tsatsiin Ereg (central Mongolia) the presence of isolated skeletal elements under the mounds, including skulls without mandibles, and the association of skulls and mandibles belonging to different individuals, indicate that in some cases the remains must have come from horses killed several months before deposition (Lepetz et al., 2019). It is unclear whether this delay is related to a practical reason that would have prevented immediate deposition (which would be the case, for example, if the animal had been slaughtered several days' travel away from the khirgisuur) or whether there was a ritualistic desire to expose the skeletonised head, similar to the practices observed today among modern herders (Marchina et al., 2017). The slaughter itself may have been sacrificial or purely domestic. It is also possible that some individuals died naturally. At Burgast, based on the archaeozoological and isotopic data, two scenarios are possible. One could argue for a synchronous deposit (at the time of the funeral, for example, but not necessarily) of animals slaughtered at different time periods, which could include horses consumed during the previous year. But one could also argue for successive deposits of fresh and non-fresh animals.

9.7 Conclusion

Sequential oxygen isotopic analysis of developing molars allows researchers to distinguish between different periods of death for horse remains in an archaeological context. The establishment of a modern reference has allowed us to obtain a temporal resolution of the order of the season and thus to propose a date of death centred on the winter season for two Bronze Age horses deposited in a khirgisuur in western Mongolia. In order to improve the accuracy of the dates of death reconstructed by this approach, it would be desirable to expand the modern reference set and include a larger number of animals of known date of death to better document the impact of tooth type, advance in the mineralisation process, or rate of tooth growth. Our preliminary results are already enriching our understanding of ritual practices in the Bronze Age. Our results indicate that archaeologists need to take into account more complex scenarios than one involving the sacrifice, at the site, of multiple horses on the day of the funeral. In practice, the location of slaughter cannot be determined. These slaughtering events may have been conceived solely in a domestic setting, and therefore related to the practical necessities of acquiring and preserving the meat. Therefore, it is important to keep in mind that

both a technical calendar (governing the slaughter of horses, with a focus on winter) and a ritual calendar (governing the deposition of animal remains) are involved.

Acknowledgments

We are deeply indebted to all the herders who kindly participated to the study and all the French and Mongol excavators of the 2016 fieldwork at Burgast. Fieldwork was supported by the French archaeological mission in Mongolia (CNRS, MNHN, MAEDI, director SL) and by the CNRS. We thank S. Needs for English editing. This research was funded by a Ph.D. grant to NL from the French National Research Agency LabEx ANR-10-LABX-0003-BCDiv, in the context of the "Investissements d'avenir", grant number ANR-11-IDEX-0004-02, and by an Inalco Early Career Research Grant 2017 to CM.

Credit roles:

Conceptualisation (AZ, AC, SL); Data curation (NL, SL, CM, BN, VB, DJ, MC, NB, TT, AZ); Formal analysis (NL, DF); Funding acquisition (AC, SL, AZ); Investigation (NL, AC, SL, AZ); Methodology (NL, AZ); Project administration (AZ); Resources (NL, SL, CM, NB, TT, AZ); Software (NL, AC); Supervision (AZ, AC, SL); Validation (NL, AZ, DF); Visualisation (NL, SL); Roles/Writing - original draft (NL, AC, SL, AZ); Writing - review & editing (CM, MC, TT).

PARTIE IV - CONCLUSION GÉNÉRALE

En s'appuyant sur des traits de vie connus (mobilité, date d'abattage) d'animaux domestiques actuels, ce travail de thèse avait pour objectif de compléter un référentiel moderne trop rare concernant l'utilisation de l'outil isotopique dans le cadre de l'étude des pratiques d'élevage. Pour la première fois, du bétail d'éleveurs nomades a été suivi sur une longue durée (3 ans) par balises GPS en couplage avec des analyses isotopiques des tissus biologiques (crins et dents). Cela a permis d'estimer le potentiel de l'échantillonnage séquentiel et des analyses multi-isotopiques des tissus biologiques pour reconstruire la mobilité saisonnière et la date d'abattage des animaux modernes. Le but était de fournir un cadre de référence fiable pour appliquer ces méthodes aux registres archéologiques.

Les données séquentielles et bulks des tissus biologiques ont été interprétés en fonction des paramètres environnementaux, comportementaux, géographiques et climatiques connus pour ces animaux modernes, permettant une évaluation des méthodes d'analyses isotopiques utilisées. Plusieurs individus de plusieurs espèces d'ongulés domestiques (mouton, chèvre, cheval) appartenant aux troupeaux de 5 éleveurs différents, caractérisés par des parcours de mobilité différents, ont été suivis et analysés isotopiquements. Cela a permis d'estimer les différences et les ressemblances entre et au sein des troupeaux. Les résultats sur ces animaux modernes ont permis d'identifier des marqueurs de la mobilité et de la date d'abattage mais également de montrer les limites de certains de ces traceurs.

Cette recherche a aussi pris le temps de proposer une application d'exploration des schémas de mobilité et d'occupation du territoire ainsi que de la saisonnalité d'abattage des chevaux archéologiques retrouvés en contexte funéraire sur le site de Burgast (âge du Bronze et période Türk), situé dans la même zone que les troupeaux modernes étudiés. Les méthodes utilisées et les interprétations des analyses sur les animaux domestiques modernes ont été transposées à ces restes archéologiques et ont permis d'alimenter les hypothèses concernant la mobilité et les pratiques d'élevage durant ces périodes, encore peu étudiées, en Mongolie. Nous avons pu identifier une mobilité altitudinale et une occupation importante des pâtures d'altitude dès l'âge du Bronze, et proposer que les chevaux avaient été tués en hiver comme c'est le cas aujourd'hui.

En reprenant les différents objectifs (Chapter 3), les principaux résultats de cette recherche sont résumés ci-dessous :

- Les variations temporelles du $\delta^{13}C$ et du $\delta^{15}N$ enregistrées par les crins de cheval ne permettent pas de retracer finement la mobilité altitudinale des chevaux. Tous les crins

ont enregistré des tendances similaires, malgré des mobilités différentes, mettant en avant une influence principale de la saisonnalité et des préférences alimentaires.

- En revanche les valeurs moyennes du $\delta^{13}C$ du régime alimentaire, calculées à partir des crins ou des dents, sont bien corrélées avec l'altitude et permettent d'estimer une altitude moyenne de pâturage et un taux d'occupation des pâtures de haute altitude, que ce soit pour les caprinés ou les chevaux.
- Une incohérence apparaît lorsque le même ensemble de données ($\delta^{13}C$ des crins) est analysé à deux échelles différentes (séquentielle et globale). Ceci pourrait être dû au fait que les changements quotidiens d'altitude des chevaux augmentent le rapport bruit/signal et rendent tout relation entre altitude et $\delta^{13}C$ difficile à détecter dans une résolution quotidienne et hebdomaire.
- Les valeurs moyennes du $\delta^{18}O$ de l'émail ne sont pas liées à l'altitude moyenne de pâturage des animaux.
- En revanche, l'amplitude des variations saisonnières du $\delta^{18}O$ enregistrée par l'émail d'animaux ayant une forte mobilité altitudinale est plus importante que celle des animaux ayant une faible mobilité altitudinale, causait par une plus grande diversité isotopique des sources d'eau ingérée.
- La corrélation entre les valeurs de $\delta^{18}O$ et $\delta^{13}C$ des dents dépend de la fréquence de la mobilité altitudinale. Des animaux ayant une mobilité altitudinale très fréquente et prononcée ont des valeurs de $\delta^{18}O$ et $\delta^{13}C$ qui sont anticorrélées, même dans un environnement dominé par des plantes en C_3.
- Comme attendu les valeurs moyennes de $^{87}Sr/^{86}Sr$ des différents animaux modernes se situent dans la gamme des variations de l'environnement local. Cependant, une valeur seuil de ±3SD des valeurs moyennes de la faune, couramment utilisée en archéologie, ne décrit pas complètement la variabilité du strontium biodisponible, du moins pour cette zone d'étude.
- Des animaux de même mobilité montrent des variabilités du $^{87}Sr/^{86}Sr$ similaires pour un troupeau. En revanche pour deux autres troupeaux, les individus ayant eu des histoires de vie très similaires ont des valeurs moyennes $^{87}Sr/^{86}Sr$ différentes, au-delà d'une variabilité inter-individuelle calculée précédemment chez des animaux d'élevage intensif. Le comportement alimentaire à micro-échelle ainsi que les formations clastiques de zones montagneuses sont des hypothèses pour expliquer cette forte différence surprenante entre des individus ayant eu la même histoire de vie.

- L'analyse séquentielle par ablation laser de l'émail des ongulés herbivores, dont la mobilité est connue, a montré que le $^{87}Sr/^{86}Sr$ enregistre en général fidèlement les différents changements de pâturage avec une bonne résolution temporelle bien que pour certains individus les valeurs isotopiques absolues soient différentes des valeurs modélisées. Toutefois, on observe une forte corrélation entre les variations isotopiques mesurées et les variations isotopiques modélisées confortant le résultat que les changements de pâture peuvent être retracer pour les variations en strontium.
- Le temps de résidence du strontium semble similaire à celui du carbone, rendant leurs variations potentiellement synchrones et donc comparables.
- La période de mort des caprinés modernes peut être déterminée quantitativement, avec une erreur associée de ± 25 jours, à partir de la modélisation des séquences du cycle saisonnier enregistré par le $\delta^{18}O$ de l'émail immature.
- Pour les chevaux modernes, la détermination de la période de mort reste visuelle à cause d'un enregistrement du cycle saisonnier, qui est très amorti et moyenné et ne permet pas d'utiliser la modélisation mise au point sur les caprinés.
- Les valeurs $^{87}Sr/^{86}Sr$ des dents des chevaux archéologiques du site de Burgast concordent avec une probable origine locale. Les valeurs plus basses de $^{87}Sr/^{86}Sr$ des chevaux archéologiques suggèrent qu'ils n'exploitaientt pas exactement la même zone géographique que les individus modernes étudiés.
- Tous les chevaux de l'âge du Bronze du site de Burgast montrent des variations de $^{87}Sr/^{86}Sr$ très proches, suggérant une mobilité commune, avec l'appartenance à un même troupeau d'une même communauté. Le cheval Türk a enregistré une variabilité plus faible du $^{87}Sr/^{86}Sr$ avec une tendance à l'augmentation progressive des valeurs $^{87}Sr/^{86}Sr$ de pouvant être lié à sa qualité de cheval de monte, qui peut le restreindre dans sa mobilité quotidienne, mais une réflexion doit encore être menée pour envisager l'ensemble des explications possibles.
- Les analyses séquentielles du $\delta^{18}O$ et $\delta^{13}C$ mettent en évidence une mobilité altitudinale et une exploitation importante des pâtures d'altitude déjà présente à l'âge du Bronze à Burgast.
- Pour les jeunes chevaux du site archéologique de Burgast, une période d'abattage en début et fin d'hiver a été déterminée. Le couplage des analyses isotopiques aux données zooarchéologiques suggère un calendrier de subsistance favorisant un abattage hivernal et un calendrier rituel lié aux funérailles avec le dépôt de restes non frais.

Bien que les échantillons modernes aient fourni une base robuste pour l'interprétation des données archéologiques, plusieurs limites subsistent. Malgré un grand nombre de données ait été généré pour ces approches multi-isotopiques, le nombre d'individus appartenant à un même troupeau est assez réduit, limitant l'évaluation de la variabilité pour des animaux ayant eu une histoire de vie similaire. Un nombre plus important d'individus, avec des dents dont la formation est contemporaine du suivi GPS ou des animaux abattus à des périodes de l'année non couvertes pour le référentiel moderne pour déterminer la saison d'abattage (voir chapitre 8), permettrait de mieux soutenir les conclusions tirées. Cette limite est particulièrement forte pour les chevaux, dont le référentiel ne contient pas de juvéniles ayant été suivis par des balises GPS. De plus, les différents troupeaux que nous avons équipés avec les colliers GPS ont eu des parcours de mobilité assez complexes avec de nombreux et fréquents changements de pâtures. L'utilisation de troupeaux à mobilités saisonnières plus simples (avec moins de déplacements) aurait facilité la compréhension de l'intégration du signal isotopique dans les tissus biologiques. Nous avons pu collecter des données d'animaux ayant une mobilité altitudinale et géographique assez restreinte (éleveur Dl), mais malgré tout, cela ne correspond pas à un groupe contrôle robuste qui aurait dû être composé d'animaux sédentaires. Les contraintes du terrain étant ce qu'elles sont, il faut toutefois noter qu'il n'est cependant pas sûr que ce genre d'individus puisse être trouvé dans la région d'étude. En complément, l'échantillonnage effectué pour cartographier l'environnement isotopique reste à améliorer. L'effort réalisé pour le strontium biodisponible est important et plutôt robuste même si certaines zones n'ont pas pu être échantillonnées avec la même intensité en raison notamment de l'accessibilité réduite en zone de montagne, ou de la proximité avec la frontière russe. Un échantillonnage saisonnier et spécifique des plantes plus complet aurait amélioré notre compréhension des variations temporelles des compositions isotopiques en C et N des plantes. De plus, les limites concernant nos interprétations sur les variations des valeurs de $\delta^{18}O$ des dents de caprinés auraient pu être réduites par un échantillonnage saisonnier et altitudinal des différentes sources d'eau disponibles pour les animaux afin d'avoir un meilleur cadre de référence pour interpréter les données isotopiques de l'émail. Cependant, de telles cartographies isotopiques sont assez difficiles à réaliser en particulier sur des terrains aussi éloignés et difficiles d'accès et dépassaient le cadre de ce projet (en termes de calendrier et de financement).

Le cas d'étude sur du matériel archéologique a démontré le potentiel de ces méthodes pour la paléomobilité et la paléosaisonnalité des pratiques d'élevage et l'intérêt qu'il y a à poursuivre leur utilisation pour d'autres sites, d'autres régions. Cependant, l'extrême usure des

dents des chevaux âgés a limité le nombre d'individus analysés. Idéalement, l'ajout des restes de caprinés dans notre matériel aurait été un plus pour caractériser les pratiques d'élevage passées. En effet, d'après les références actuelles la gestion des troupeaux de caprinés et de chevaux peut être différente. De plus, l'unique spécimen de l'époque Türk limite les conclusions que nous pouvons apporter pour les pratiques d'élevage pour cette époque.

En dépit des quelques limites évoquées plus haut, ce projet de recherche a permis pour la première fois de mettre en relation des analyses isotopiques séquentielles de $\delta^{13}C$, $\delta^{15}N$, $\delta^{18}O$ et $^{87}Sr/^{86}Sr$ sur des tissus biologiques d'animaux domestiques actuels avec leur mobilité et leur date de mort précisément déterminées. Couplée a un échantillonnage intense de l'environnement isotopique, cela a permis de produire un cadre de référence pour les études archéologiques pour des environnements comparables afin d'explorer la mobilité et les pratiques d'élevage des sociétés pastorales passées.

Plusieurs pistes sont à explorer pour donner suite à ces travaux de thèse. Tout d'abord, il est nécessaire pour améliorer notre compréhension des variations temporelles du $^{87}Sr/^{86}Sr$ enregistré par les tissus biologiques de connaître plus précisément le temps de résidence du Sr dans l'organisme. Pour cela, il conviendrait de concevoir des expériences au cours desquelles différentes ressources alimentaires distinctes isotopiquement sont proposées aux animaux en séquence. Actuellement, il est relativement difficile d'établir des origines géographiques/géologiques exactes ainsi qu'un parcours spécifique précis des animaux à partir de leurs restes archéologiques. Une prochaine étape serait de mettre en place une méthode d'assignation qui permettrait de calculer la localisation la plus probable d'origine d'un échantillon à partir de sa valeur de $^{87}Sr/^{86}Sr$ et de l'isoscape de la zone d'étude. Cette approche permettrait de retracer le parcours d'un individu à partir des variations séquentielles des isotopes de Sr dans l'émail de ses dents. Cette méthode pourrait être mise au point sur des individus modernes, aux parcours connus, puis être appliquée sur les dents archéologiques pour inférer une probabilité des zones géographiques successivement occupées.

La transposition de ces méthodes à un autre terrain d'étude était prévue au début du travail de thèse. Il aurait consisté à comparer les enregistrements isotopiques de l'Altaï avec ceux d'une autre zone géographique, à caractéristique environnementale et aux prastiques pastorales différentes. En Mongolie centrale, par exemple, il s'agit de steppes vallonnées et les éleveurs nomadisent moins fréquemment (3-4 fois par an). L'idée était de voir si des traceurs comme le $\delta^{13}C$, $\delta^{15}N$, $\delta^{18}O$ et $^{87}Sr/^{86}Sr$ pouvaient permettre de suivre la mobilité des animaux

dans une zone plus restreinte et homogène topographiquement, et probablement isotopiquement. L'analyse des cornes des caprinés était aussi un autre élément qui n'a pas pu être abordé faute de temps, alors que cela était prévu. Les cornes sont des tissus kératinisés, au même titre que les crins, qui peuvent se conserver en contexte archéologique. Elles permettraient d'enregistrer des séries temporelles isotopiques sur de plus longues périodes de temps que les poils. Potentiellement, nous aurions un enregistrement complet de la naissance à la mort de l'animal. De plus, contrairement aux poils, il est beaucoup plus facile de collecter assez de matériel pour les analyses isotopiques, en particulier pour les analyses du $^{87}Sr/^{86}Sr$. Enfin, une dernière piste serait d'étudier l'influence du fourrage sur les compositions isotopiques des tissus biologiques des animaux modernes afin de pouvoir convenablement l'identifier en contexte archéologique. En effet, le signal de l'affouragement proposé dans la littérature se confond avec celui de la mobilité altitudinale par l'enregistrement d'une anticovariation entre les valeurs de $\delta^{13}C$ et $\delta^{18}O$. La mise en place d'un référentiel moderne est nécessaire avec un cadre pendant lequel les éleveurs récolteraient le fourrage localement, où la composition isotopique du fourrage serait contrôlée, et que l'on suivrait précisément les quantités et l'organisation et le calendrier de distribution. Les études de cas modernes restent nécessaires et permettent de parvenir à une compréhension plus approfondie et plus largement applicable des isotopes stables dans les tissus des animaux. De progrès importants peuvent être réalisés en poursuivant et en élargissant le travail expérimental sur des sociétés pastorales modernes dans d'autres environnements que la Mongolie.

Brièvement, des perspectives concernant l'application archéologique peuvent être envisagées afin d'étoffer les conclusions. L'utilisation de la cémentochronologie pour étudier la saison d'abattage des vieux individus serait intéressante afin d'avoir une vision d'ensemble pour le khirgisuur. De plus, des analyses ADN seraient envisageables afin d'estimer la nature des relations de parenté des chevaux associés au khirgisuur pour tester l'hypothèse proposée ici d'une appartenance commune à un même troupeau. L'étude d'un grand nombre de chevaux associés à de plus grands khirgisuurs serait intéressante afin d'évaluer la variabilité des origines et préciser la taille des communautés ayant participé à l'érection de tels monuments et aux rites funéraires les entourant.

Cette étude a avant tout montré à quel point la mise en place de référentiels contrôlés était absolument nécessaire avant d'envisager des applications archéologiques aux analyses isotopiques. La quantité de variables de type environnementales ou anthropiques est telle qu'il n'est pas simple de proposer des interprétations de type historique aux variations des signatures

géochimiques relevées sur les animaux élevés par les communautés du passé. Mais elle a aussi malgré tout, montré tout l'intérêt de ce type d'analyses pour tester certaines hypothèses et faire ainsi parler les restes archéologiques.

RÉFÉRENCES

Abu-Saad, K., Weitzman, S., Abu-Rabiah, Y., Abu-Shareb, H., Fraser, D., 2001. Rapid lifestyle, diet and health changes among urban Bedouin Arabs of southern Israel. Age 30, 44.

Agatova, A.R., Nazarov, A.N., Nepop, R.K., Rodnight, H., 2012. Holocene glacier fluctuations and climate changes in the southeastern part of the Russian Altai (South Siberia) based on a radiocarbon chronology. Quat. Sci. Rev. 43, 74–93. https://doi.org/10.1016/j.quascirev.2012.04.012

Agatova, A.R., Nepop, R.K., Slyusarenko, I.Yu., Myglan, V.S., Nazarov, A.N., Barinov, V.V., 2014. Glacier dynamics, palaeohydrological changes and seismicity in southeastern Altai (Russia) and their influence on human occupation during the last 3000 years. Quat. Int., Human dimensions of palaeoenvironmental change: Geomorphic processes and geoarchaeology 324, 6–19. https://doi.org/10.1016/j.quaint.2013.07.018

Agirre-García, J., Edeso-Fito, J.M., Lopetegi-Galarraga, A., Moraza-Barea, A., Ruiz-Alonso, M., Pérez-Díaz, S., Fernández-Crespo, T., Goikoetxea, I., Martínez de Pancorbo, M.A., Palencia, L., Baeta, M., Núñez, C., Cardoso, S., Mujika-Alustiza, J.A., 2018. Seasonal shepherds' settlements in mountain areas from Neolithic to present: Aralar – Gipuzkoa (Basque country, Spain). Quat. Int., Casting a glance over the mountain – multi-proxy approaches to the understanding of vertical mobility 484, 44–59. https://doi.org/10.1016/j.quaint.2017.03.061

Allard, F., Erdenebaatar, D., 2005. Khirigsuurs, ritual and mobility in the Bronze Age of Mongolia. Antiquity 79, 547–563. https://doi.org/10.1017/S0003598X00114498

Ambach, W., Dansgaard, W., Eisner, H., Møller, J., 1968. The altitude effect on the isotopic composition of precipitation and glacier ice in the Alps. Tellus 20, 595–600. https://doi.org/10.3402/tellusa.v20i4.10040

Ambrose, S.H., 2002. Controlled diet and climate experiments on nitrogen isotope ratios of rats, in: Biogeochemical Approaches to Paleodietary Analysis. Springer, pp. 243–259.

Ambrose, S.H., 1991. Effects of diet, climate and physiology on nitrogen isotope abundances in terrestrial foodwebs. J. Archaeol. Sci. 18, 293–317. https://doi.org/10.1016/0305-4403(91)90067-Y

Amundson, R., Austin, A.T., Schuur, E. a. G., Yoo, K., Matzek, V., Kendall, C., Uebersax, A., Brenner, D., Baisden, W.T., 2003. Global patterns of the isotopic composition of soil and plant nitrogen. Glob. Biogeochem. Cycles 17, 1031. https://doi.org/10.1029/2002GB001903

An, H., Li, G., 2015. Effects of grazing on carbon and nitrogen in plants and soils in a semiarid desert grassland, China. J. Arid Land 7, 341–349. https://doi.org/10.1007/s40333-014-0049-x

Anders, D., Osmanovic, A., Vohberger, M., 2019. Intra- and inter-individual variability of stable strontium isotope ratios in hard and soft body tissues of pigs. Rapid Commun. Mass Spectrom. 33, 281–290. https://doi.org/10.1002/rcm.8350

Anthony, D.W., 2007. The Horse, The Wheel, and Language: How Bronze-Age Riders from the Eurasian Steppes Shaped the World. Princeton University Press, Princeton.

Arbuckle, B.S., Hammer, E.L., 2018. The Rise of Pastoralism in the Ancient Near East. J. Archaeol. Res. https://doi.org/10.1007/s10814-018-9124-8

Arnold, E.R., Greenfield, H.J., 2017. 12. A Zooarchaeological Perspective on the Origins of Vertical Transhumant Pastoralism and the Colonization of Marginal Habitats in Temperate Southeastern Europe. Colon. Migr. Marg. Areas Zooarchaeological Approach 96.

Arnold, E.R., Greenfield, H.J., Creaser, R.A., 2013. Domestic cattle mobility in early farming villages in southern Africa: harvest profiles and strontium ($^{87}Sr/^{86}Sr$) isotope analyses from Early Iron Age sites in the lower Thukela River Valley of South Africa. Archaeol. Anthropol. Sci. 5, 129–144. https://doi.org/10.1007/s12520-013-0121-z

Auerswald, K., Rossmann, A., Schäufele, R., Schwertl, M., Monahan, F.J., Schnyder, 2011. Does natural weathering change the stable isotope composition (^{2}H, ^{13}C, ^{15}N, ^{18}O and ^{34}S) of cattle hair? Rapid Commun. Mass Spectrom. 25, 3741–3748. https://doi.org/10.1002/rcm.5284

Ayliffe, L.K., Cerling, T.E., Robinson, T., West, A.G., Sponheimer, M., Passey, B.H., Hammer, J., Roeder, B., Dearing, M.D., Ehleringer, J.R., 2004. Turnover of carbon isotopes in tail hair and breath CO_2 of horses fed an isotopically varied diet. Oecologia 139, 11–22.

Badeck, F.-W., Tcherkez, G., Nogués, S., Piel, C., Ghashghaie, J., 2005. Post-photosynthetic fractionation of stable carbon isotopes between plant organs—a widespread phenomenon. Rapid Commun. Mass Spectrom. 19, 1381–1391. https://doi.org/10.1002/rcm.1912

Bahloul, K., Pereladova, O.B., Soldatova, N., Fisenko, G., Sidorenko, E., Sempéré, A.J., 2001. Social organization and dispersion of introduced kulans (Equus hemionus kulan) and Przewalski horses (Equus przewalski) in the Bukhara Reserve, Uzbekistan. J. Arid Environ. 47, 309–323. https://doi.org/10.1006/jare.2000.0714

Balasse, M., 2003. Potential biases in sampling design and interpretation of intra-tooth isotope analysis. Int. J. Osteoarchaeol. 13, 3–10. https://doi.org/10.1002/oa.656

Balasse, M., 2002. Reconstructing dietary and environmental history from enamel isotopic analysis: time resolution of intra-tooth sequential sampling. Int. J. Osteoarchaeol. 12, 155–165. https://doi.org/10.1002/oa.601

Balasse, M., Ambrose, S.H., 2005. Mobilité altitudinale des pasteurs néolithiques dans la vallée du Rift (Kenya): premiers indices de l'analyse du $\delta^{13}C$ de l'émail dentaire du cheptel domestique. Anthropozoologica 40, 147–166.

Balasse, M., Ambrose, S.H., Smith, A.B., Price, T.D., 2002. The Seasonal Mobility Model for Prehistoric Herders in the South-western Cape of South Africa Assessed by Isotopic Analysis of Sheep Tooth Enamel. J. Archaeol. Sci. 29, 917–932. https://doi.org/10.1006/jasc.2001.0787

Balasse, M., Bocherens, H., Mariotti, A., Ambrose, S.H., 2001. Detection of Dietary Changes by Intra-tooth Carbon and Nitrogen Isotopic Analysis: An Experimental Study of Dentine Collagen of Cattle (Bos taurus). J. Archaeol. Sci. 28, 235–245. https://doi.org/10.1006/jasc.1999.0535

Balasse, Marie, Boury, L., Ughetto-Monfrin, J., Tresset, A., 2012. Stable isotope insights ($\delta^{18}O$, $\delta^{13}C$) into cattle and sheep husbandry at Bercy (Paris, France, 4th millennium BC): birth seasonality and winter leaf foddering. Environ. Archaeol. 17, 29–44.

Balasse, M., Mainland, I., Richards, M.P., 2009. Stable isotope evidence for seasonal consumption of marine seaweed by modern and archaeological sheep in the Orkney archipelago (Scotland). Environ. Archaeol. 14, 1–14. https://doi.org/10.1179/174963109X400637

Balasse, M., Obein, G., Ughetto-Monfrin, J., Mainland, I., 2012. Investigating Seasonality and Season of Birth in Past Herds: A Reference Set of Sheep Enamel Stable Oxygen Isotope Ratios. Archaeometry 54, 349–368. https://doi.org/10.1111/j.1475-4754.2011.00624.x

Balasse, M., Tresset, A., 2002. Early Weaning of Neolithic Domestic Cattle (Bercy, France) Revealed by Intra-tooth Variation in Nitrogen Isotope Ratios. J. Archaeol. Sci. 29, 853–859. https://doi.org/10.1006/jasc.2001.0725

Balasse, M., Tresset, A., Bălăşescu, A., Blaise, E., Tornero, C., Gandois, H., Fiorillo, D., Nyerges, É.Á., Frémondeau, D., Banffy, E., Ivanova, M., 2017. Animal Board Invited Review: Sheep birth distribution in past herds: a review for prehistoric Europe (6th to 3rd millennia BC). animal 1–8. https://doi.org/10.1017/S1751731117001045

Balasse, M., Tresset, A., Obein, G., Fiorillo, D., Gandois, H., 2019. Seaweed-eating sheep and the adaptation of husbandry in Neolithic Orkney: new insights from Skara Brae. Antiquity 93, 919–932. https://doi.org/10.15184/aqy.2019.95

Barbosa, I.C., Kley, M., Schäufele, R., Auerswald, K., Schröder, W., Filli, F., Hertwig, S., Schnyder, H., 2009. Analysing the isotopic life history of the alpine ungulates Capra ibex and Rupicapra rupicapra rupicapra through their horns. Rapid Commun. Mass Spectrom. 23, 2347–2356.

Barbour, M.M., 2007. Stable oxygen isotope composition of plant tissue: a review. Funct. Plant Biol. 34, 83–94. https://doi.org/10.1071/FP06228

Bassett, T.J., 1986. Fulani Herd Movements. Geogr. Rev. 76, 233–248. https://doi.org/10.2307/214143

Bataille, C.P., Bowen, G.J., 2012. Mapping $^{87}Sr/^{86}Sr$ variations in bedrock and water for large scale provenance studies. Chem. Geol. 304, 39–52. https://doi.org/10.1016/j.chemgeo.2012.01.028

Bataille, C.P., Brennan, S.R., Hartmann, J., Moosdorf, N., Wooller, M.J., Bowen, G.J., 2014. A geostatistical framework for predicting variations in strontium concentrations and isotope ratios in Alaskan rivers. Chem. Geol. 389, 1–15. https://doi.org/10.1016/j.chemgeo.2014.08.030

Bataille, C.P., Holstein, I.C.C. von, Laffoon, J.E., Willmes, M., Liu, X.-M., Davies, G.R., 2018. A bioavailable strontium isoscape for Western Europe: A machine learning approach. PLOS ONE 13, e0197386. https://doi.org/10.1371/journal.pone.0197386

Bataille, C.P., Laffoon, J., Bowen, G.J., 2012. Mapping multiple source effects on the strontium isotopic signatures of ecosystems from the circum-Caribbean region. Ecosphere 3, 1–24.

Bell, L.S., Lee-Thorp, J.A., Dobney, K., 2006. Mapping Human Movement using Stable Oxygen Isotopic Ratio Mass Spectrometry: Potential Application to Forensic Science Demonstrated by a Modern Horse-Human Study. Can. Soc. Forensic Sci. J. 39, 47–54. https://doi.org/10.1080/00085030.2006.10757136

Bendrey, R., Hayes, T.E., Palmer, M.R., 2009. Patterns of Iron Age Horse Supply: An Analysis of Strontium Isotope Ratios in Teeth. Archaeometry 51, 140–150. https://doi.org/10.1111/j.1475-4754.2008.00419.x

Bendrey, R., Lepetz, S., Zazzo, A., Balasse, M., Turbat, T., Giscard, P.H., Vella, D., Zaitseva, G.I., Chugunov, K.V., Ughetto, J., others, 2017. 18. Nomads, horses and mobility: an assessment of geographic origins of Iron Age horses found at Tsengel Khairkhan and Baga Turgen Gol (Mongolian Altai) based on oxygen isotope compositions of tooth enamel. Archaeozoology East 262.

Bendrey, R., Vella, D., Zazzo, A., Balasse, M., Lepetz, S., 2015. Exponentially decreasing tooth growth rate in horse teeth: implications for isotopic analyses. Archaeometry 57, 1104–1124. https://doi.org/10.1111/arcm.12151

Bentley, R.A., 2006. Strontium isotopes from the earth to the archaeological skeleton: a review. J. Archaeol. Method Theory 13, 135–187.

Bentley, R.A., Knipper, C., 2005. Transhumance at the early Neolithic settlement at Vaihingen (Germany). Antiquity 79, 1–3.

Bernard, A., Daux, V., Lécuyer, C., Brugal, J.-P., Genty, D., Wainer, K., Gardien, V., Fourel, F., Jaubert, J., 2009. Pleistocene seasonal temperature variations recorded in the $\delta^{18}O$ of *Bison priscus teeth*. Earth Planet. Sci. Lett. 283, 133–143. https://doi.org/10.1016/j.epsl.2009.04.005

Birch, S.E.P., Miracle, P.T., Stevens, R.E., O'Connell, T.C., 2016. Late Pleistocene/Early Holocene Migratory Behavior of Ungulates Using Isotopic Analysis of Tooth Enamel and Its Effects on Forager Mobility. PLOS ONE 11, e0155714. https://doi.org/10.1371/journal.pone.0155714

Blumenthal, S.A., Cerling, T.E., Chritz, K.L., Bromage, T.G., Kozdon, R., Valley, J.W., 2014. Stable isotope time-series in mammalian teeth: *In situ* $\delta^{18}O$ from the innermost enamel layer. Geochim. Cosmochim. Acta 124, 223–236. https://doi.org/10.1016/j.gca.2013.09.032

Blumenthal, S.A., Cerling, T.E., Smiley, T.M., Badgley, C.E., Plummer, T.W., 2019. Isotopic records of climate seasonality in equid teeth. Geochim. Cosmochim. Acta 260, 329–348. https://doi.org/10.1016/j.gca.2019.06.037

Bowen, G.J., Wilkinson, B., 2002. Spatial distribution of $\delta^{18}O$ in meteoric precipitation. Geology 30, 315–318.

Brennan, S.R., Fernandez, D.P., Zimmerman, C.E., Cerling, T.E., Brown, R.J., Wooller, M.J., 2015. Strontium isotopes in otoliths of a non-migratory fish (slimy sculpin): Implications for provenance studies. Geochim. Cosmochim. Acta 149, 32–45. https://doi.org/10.1016/j.gca.2014.10.032

Britton, K., Grimes, V., Dau, J., Richards, M.P., 2009. Reconstructing faunal migrations using intra-tooth sampling and strontium and oxygen isotope analyses: a case study of modern caribou (*Rangifer tarandus granti*). J. Archaeol. Sci. 36, 1163–1172. https://doi.org/10.1016/j.jas.2009.01.003

Britton, K., Grimes, V., Niven, L., Steele, T.E., McPherron, S., Soressi, M., Kelly, T.E., Jaubert, J., Hublin, J.-J., Richards, M.P., 2011. Strontium isotope evidence for migration in late Pleistocene *Rangifer*: Implications for Neanderthal hunting strategies at the Middle Palaeolithic site of Jonzac, France. J. Hum. Evol. 61, 176–185. https://doi.org/10.1016/j.jhevol.2011.03.004

Broderick, L., Houle, J.-L., Bayarsaikhan, Jamsranjav, Seitsonen, O., Bayarsaikhan, J, 2014. The mystery of the missing caprines: Stone circles at the great khirigsuur in the Khanuy Valley, in: Arkheologiin Suudal. Mongolian Academy of Sciences., Ulaanbaatar, pp. 164–174.

Broderick, L.G., Seitsonen, O., Bayarsaikhan, J., Houle, J.-L., 2016. Lambs to the Slaughter: A Zooarchaeological Investigation of Stone Circles in Mongolia. Int. J. Osteoarchaeol. 26, 537–543. https://doi.org/10.1002/oa.2425

Brosseder, U., 2009. Xiongnu terrace tombs and their interpretation as elite burials. Curr. Archaeol. Res. Mong. 247–280.

Bruun, O., 2006. Precious steppe: Mongolian nomadic pastoralists in pursuit of the market. Lexington Books.

Bryant, J.D., Froelich, P.N., 1995. A model of oxygen isotope fractionation in body water of large mammals. Geochim. Cosmochim. Acta 59, 4523–4537. https://doi.org/10.1016/0016-7037(95)00250-4

Bryant, J.D., Luz, B., Froelich, P.N., 1994. Oxygen isotopic composition of fossil horse tooth phosphate as a record of continental paleoclimate. Palaeogeogr. Palaeoclimatol. Palaeoecol. 107, 303–316.

Burke, A., Castanet, J., 1995. Histological Observations of Cementum Growth in Horse Teeth and their Application to Archaeology. J. Archaeol. Sci. 22, 479–493. https://doi.org/10.1006/jasc.1995.0047

Burnik Šturm, M., Ganbaatar, O., Voigt, C.C., Kaczensky, P., 2016. Sequential stable isotope analysis reveals differences in dietary history of three sympatric equid species in the Mongolian Gobi. J. Appl. Ecol. n/a-n/a. https://doi.org/10.1111/1365-2664.12825

Burnik Šturm, M., Pukazhenthi, B., Reed, D., Ganbaatar, O., Sušnik, S., Haymerle, A., Voigt, C.C., Kaczensky, P., 2015. A protocol to correct for intra- and interspecific variation in tail hair growth to align isotope signatures of segmentally cut tail hair to a common time line. Rapid Commun. Mass Spectrom. 29, 1047–1054. https://doi.org/10.1002/rcm.7196

Calenge, C., 2006. The package “adehabitat” for the R software: A tool for the analysis of space and habitat use by animals. Ecol. Model. 197, 516–519. https://doi.org/10.1016/j.ecolmodel.2006.03.017

Capo, R.C., Stewart, B.W., Chadwick, O.A., 1998. Strontium isotopes as tracers of ecosystem processes: theory and methods. Geoderma 82, 197–225. https://doi.org/10.1016/S0016-7061(97)00102-X

Carter, R.J., 2001. Dental indicators of seasonal hunan presence at the Danish Boreal sites of Holmegaard I, IV and V and Mullerup and the Atlantic sites of Tybrind Vig and Ringkloster. The Holocene 11, 359–365. https://doi.org/10.1191/095968301667543765

Cavagnaro, J.B., 1988. Distribution of C3 and C4 grasses at different altitudes in a temperate arid region of Argentina. Oecologia 76, 273–277. https://doi.org/10.1007/BF00379962

Cerling, T.E., Harris, J.M., 1999. Carbon isotope fractionation between diet and bioapatite in ungulate mammals and implications for ecological and paleoecological studies. Oecologia 120, 347–363. https://doi.org/10.1007/s004420050868

Cerling, T.E., Passey, B.H., Ayliffe, L.K., Cook, C.S., Ehleringer, J.R., Harris, J.M., Dhidha, M.B., Kasiki, S.M., 2004. Orphans’ tales: seasonal dietary changes in elephants from Tsavo National Park, Kenya. Palaeogeogr. Palaeoclimatol. Palaeoecol., Incremental Growth in Vertebrate Skeletal Tissues: Paleobiological and Paleoenvironmental Implications 206, 367–376. https://doi.org/10.1016/j.palaeo.2004.01.013

Cerling, T.E., Wittemyer, G., Ehleringer, J.R., Remien, C.H., Douglas-Hamilton, I., 2009. History of animals using isotope records (HAIR): a 6-year dietary history of one family of African elephants. Proc. Natl. Acad. Sci. 106, 8093–8100.

Cerling, T.E., Wittemyer, G., Rasmussen, H.B., Vollrath, F., Cerling, C.E., Robinson, T.J., Douglas-Hamilton, I., 2006. Stable isotopes in elephant hair document migration patterns and diet changes. Proc. Natl. Acad. Sci. U. S. A. 103, 371–373. https://doi.org/10.1073/pnas.0509606102

Cernusak, L.A., Barbour, M.M., Arndt, S.K., Cheesman, A.W., English, N.B., Feild, T.S., Helliker, B.R., Holloway-Phillips, M.M., Holtum, J.A., Kahmen, A., others, 2016. Stable isotopes in leaf water of terrestrial plants. Plant Cell Environ. 39, 1087–1102.

Chase, B., Meiggs, D., Ajithprasad, P., Slater, P.A., 2018. What is left behind: Advancing interpretation of pastoral land-use in Harappan Gujarat using herbivore dung to examine biosphere strontium isotope (87Sr/86Sr) variation. J. Archaeol. Sci. 92, 1–12. https://doi.org/10.1016/j.jas.2018.01.007

Chau, T.H., Tipple, B.J., Hu, L., Fernandez, D.P., Cerling, T.E., Ehleringer, J.R., Chesson, L.A., 2017. Reconstruction of travel history using coupled $\delta^{18}O$ and $^{87}Sr/^{86}Sr$ measurements of hair. Rapid Commun. Mass Spectrom. 31, 583–589. https://doi.org/10.1002/rcm.7822

Chazin, H., Gordon, G.W., Knudson, K.J., 2019. Isotopic perspectives on pastoralist mobility in the Late Bronze Age South Caucasus. J. Anthropol. Archaeol. 54, 48–67. https://doi.org/10.1016/j.jaa.2019.02.003

Cloern, J.E., Canuel, E.A., Harris, D., 2002. Stable carbon and nitrogen isotope composition of aquatic and terrestrial plants of the San Francisco Bay estuarine system. Limnol. Oceanogr. 47, 713–729. https://doi.org/10.4319/lo.2002.47.3.0713

Codron, J., Codron, D., Lee-Thorp, J.A., Sponheimer, M., Bond, W.J., de Ruiter, D., Grant, R., 2005. Taxonomic, anatomical, and spatio-temporal variations in the stable carbon and nitrogen isotopic compositions of plants from an African savanna. J. Archaeol. Sci. 32, 1757–1772. https://doi.org/10.1016/j.jas.2005.06.006

Copeland, S.R., Cawthra, H.C., Fisher, E.C., Lee-Thorp, J.A., Cowling, R.M., le Roux, P.J., Hodgkins, J., Marean, C.W., 2016. Strontium isotope investigation of ungulate movement patterns on the Pleistocene Paleo-Agulhas Plain of the Greater Cape Floristic Region, South Africa. Quat. Sci. Rev. 141, 65–84. https://doi.org/10.1016/j.quascirev.2016.04.002

Cornevin, C., Lesbre, F.-X., 1894. Traité de l'âge des animaux domestiques d'après les dents et les productions épidermiques. J.-B. Baillière et fils, Paris.

Coûteaux, M.M., Sarmiento, L., Bottner, P., Acevedo, D., Thiéry, J.M., 2002. Decomposition of standard plant material along an altitudinal transect (65–3968m) in the tropical Andes. Soil Biol. Biochem. 34, 69–78. https://doi.org/10.1016/S0038-0717(01)00155-9

Craine, J.M., Brookshire, E.N.J., Cramer, M.D., Hasselquist, N.J., Koba, K., Marin-Spiotta, E., Wang, L., 2015. Ecological interpretations of nitrogen isotope ratios of terrestrial plants and soils. Plant Soil 396, 1–26. https://doi.org/10.1007/s11104-015-2542-1

Craine, J.M., Elmore, A.J., Aidar, M.P.M., Bustamante, M., Dawson, T.E., Hobbie, E.A., Kahmen, A., Mack, M.C., McLauchlan, K.K., Michelsen, A., Nardoto, G.B., Pardo, L.H., Peñuelas, J., Reich, P.B., Schuur, E.A.G., Stock, W.D., Templer, P.H., Virginia, R.A., Welker, J.M., Wright, I.J., 2009. Global patterns of foliar nitrogen isotopes and their relationships with climate, mycorrhizal fungi, foliar nutrient concentrations, and

nitrogen availability. New Phytol. 183, 980–992. https://doi.org/10.1111/j.1469-8137.2009.02917.x

Cribb, R., 2004. Nomads in Archaeology. Cambridge University Press.

Crowell-Davis, S.L., Houpt, K.A., Carnevale, J., 1985. Feeding and Drinking Behavior of Mares and Foals with Free Access to Pasture and Water. J. Anim. Sci. 60, 883–889. https://doi.org/10.2527/jas1985.604883x

Crowley, B.E., Miller, J.H., Bataille, C.P., 2017. Strontium isotopes ($^{87}Sr/^{86}Sr$) in terrestrial ecological and palaeoecological research: empirical efforts and recent advances in continental-scale models. Biol. Rev. 92, 43–59. https://doi.org/10.1111/brv.12217

Crubézy, E., Martin, H., Giscard, P.-H., Batsaikhan, Z., Erdenebaatar, D., Maureille, B., Verdier, J.-P., 1996. Pratiques funéraires et sacrifices d'animaux en Mongolie á la période proto-historique. Du Perçu au signifié à propos d'une sépulture xiongnu de la vallée d'Egyin Gol (Région Péri-Baïkal). Paléorient 89–107.

Dansgaard, W., 1964. Stable isotopes in precipitation. Tellus A 16, 438–468.

Darling, W.G., Bath, A.H., Talbot, J.C., 2003. The O and H stable isotope composition of freshwaters in the British Isles. 2. Surface waters and groundwater. Hydrol. Earth Syst. Sci. 7, 183–195. https://doi.org/10.5194/hess-7-183-2003

Dash, M., 1966. Mongol Orny Bilcheeriin Mal Mallagaany Arga Turshlaga [Experience of Pastoralism in Mongolian]. Ulsyn Khevlelijn Khereg Erkhlekh Khoroo, Ulaanbataar, Mongolia.

Dashtseren, A., Ishikawa, M., Iijima, Y., Jambaljav, Y., 2014. Temperature Regimes of the Active Layer and Seasonally Frozen Ground under a Forest-Steppe Mosaic, Mongolia. Permafr. Periglac. Process. 25, 295–306. https://doi.org/10.1002/ppp.1824

de Barros Damgaard, P., Martiniano, R., Kamm, J., Moreno-Mayar, J.V., Kroonen, G., Peyrot, M., Barjamovic, G., Rasmussen, S., Zacho, C., Baimukhanov, N., others, 2018. The first horse herders and the impact of early Bronze Age steppe expansions into Asia. Science 360, eaar7711.

Deniro, M.J., Epstein, S., 1981. Influence of diet on the distribution of nitrogen isotopes in animals. Geochim. Cosmochim. Acta 45, 341–351. https://doi.org/10.1016/0016-7037(81)90244-1

DeNiro, M.J., Epstein, S., 1978. Influence of diet on the distribution of carbon isotopes in animals. Geochim. Cosmochim. Acta 42, 495–506. https://doi.org/10.1016/0016-7037(78)90199-0

Diefendorf, A.F., Mueller, K.E., Wing, S.L., Koch, P.L., Freeman, K.H., 2010. Global patterns in leaf ^{13}C discrimination and implications for studies of past and future climate. Proc. Natl. Acad. Sci. 107, 5738–5743. https://doi.org/10.1073/pnas.0910513107

Dobney, K., Ervynck, A., Albarella, U., Rowley-Conwy, P., 2004. The chronology and frequency of a stress marker (linear enamel hypoplasia) in recent and archaeological populations of Sus scrofa in north-west Europe, and the effects of early domestication. J. Zool. 264, 197–208. https://doi.org/10.1017/S0952836904005679

Dodd, M.B., Lauenroth, W.K., Welker, J.M., 1998. Differential water resource use by herbaceous and woody plant life-forms in a shortgrass steppe community. Oecologia 117, 504–512. https://doi.org/10.1007/s004420050686

Dong, S., Wen, L., Liu, S., Zhang, X., Lassoie, J., Yi, S., Li, X., Li, J., Li, Y., 2011. Vulnerability of worldwide pastoralism to global changes and interdisciplinary strategies for sustainable pastoralism. Ecol. Soc. 16.

Douglas, T.A., Blum, J.D., Guo, L., Keller, K., Gleason, J.D., 2013. Hydrogeochemistry of seasonal flow regimes in the Chena River, a subarctic watershed draining discontinuous permafrost in interior Alaska (USA). Chem. Geol. 335, 48–62. https://doi.org/10.1016/j.chemgeo.2012.10.045

Douglas, T.A., Chamberlain, C.P., Blum, J.D., 2002. Land use and geologic controls on the major elemental and isotopic ($\delta^{15}N$ and $^{87}Sr/^{86}Sr$) geochemistry of the Connecticut River watershed, USA. Chem. Geol. 189, 19–34. https://doi.org/10.1016/S0009-2541(02)00047-5

Drewnik, M., 2006. The effect of environmental conditions on the decomposition rate of cellulose in mountain soils. Geoderma 132, 116–130. https://doi.org/10.1016/j.geoderma.2005.04.023

Dufour, E., Goepfert, N., Léon, B.G., Chauchat, C., Jordán, R.F., Sánchez, S.V., 2014. Pastoralism in Northern Peru during Pre-Hispanic Times: Insights from the Mochica Period (100–800 AD) Based on Stable Isotopic Analysis of Domestic Camelids. PLOS ONE 9, e87559. https://doi.org/10.1371/journal.pone.0087559

Duncan, P., 1992. Horses and Grasses: The Nutritional Ecology of Equids and Their Impact on the Camargue, Ecological Studies. Springer-Verlag, New York.

Dunnett, M., 2005. The diagnostic potential of equine hair: A comparative review of hair analysis for assessing nutritional status, environmental poisoning, and drug use and abuse. Adv. Equine Nutr.-III 85–106.

Ebling, F.J.G., 1988. The hair cycle and its regulation. Clin. Dermatol. 6, 67–73. https://doi.org/10.1016/0738-081X(88)90068-5

Ehleringer, J.R., 2005. The influence of atmospheric CO_2, temperature, and water on the abundance of C3/C4 taxa, in: A History of Atmospheric CO2 and Its Effects on Plants, Animals, and Ecosystems. Springer, New York, NY, pp. 214–231.

Ehleringer, J.R., Dawson, T.E., 1992. Water uptake by plants: perspectives from stable isotope composition. Plant Cell Environ. 15, 1073–1082.

Eisma, D., 2012. Agriculture on the Mongolian Steppe. Silk Road 10, 123–135.

El Adli, J.J., Fisher, D.C., Vartanyan, S.L., Tikhonov, A.N., 2017. Final years of life and seasons of death of woolly mammoths from Wrangel Island and mainland Chukotka, Russian Federation. Quat. Int., VIth International Conference on Mammoths and their Relatives, Part 3 445, 135–145. https://doi.org/10.1016/j.quaint.2016.07.017

Ellenberger, F., 1996. Le présent, clef du passé. Trav. Com. Fr. Hist. Géologie 3ème série, 65–71.

Elliott, J.C., 2002. Calcium Phosphate Biominerals. Rev. Mineral. Geochem. 48, 427–453. https://doi.org/10.2138/rmg.2002.48.11

Elliott, S., Bendrey, R., Whitlam, J., Aziz, K.R., Evans, J., 2015. Preliminary ethnoarchaeological research on modern animal husbandry in Bestansur, Iraqi Kurdistan: Integrating animal, plant and environmental data. Environ. Archaeol. 20, 283–303. https://doi.org/10.1179/1749631414Y.0000000025

Ervynck, A., 2005. Detecting the Seasonal Slaughtering of Domestic Mammals: Inferences from the Detailed Recording of Tooth Eruption and Wear. Environ. Archaeol. 10, 153–169. https://doi.org/10.1179/env.2005.10.2.153

European Commission Copernicus Land Monitoring Service - Global Component. Accessible at: https://land.copernicus.eu/global, 2018.

Evans, J., Parker Pearson, M., Madgwick, R., Sloane, H., Albarella, U., 2019. Strontium and oxygen isotope evidence for the origin and movement of cattle at Late Neolithic Durrington Walls, UK. Archaeol. Anthropol. Sci. https://doi.org/10.1007/s12520-019-00849-w

Evans, J.A., Montgomery, J., Wildman, G., 2009. Isotope domain mapping of $^{87}Sr/^{86}Sr$ biosphere variation on the Isle of Skye, Scotland. J. Geol. Soc. 166, 617–631. https://doi.org/10.1144/0016-76492008-043

Farquhar, G.D., Ehleringer, J.R., Hubick, K.T., 1989. Carbon isotope discrimination and photosynthesis. Annu. Rev. Plant Biol. 40, 503–537.

Farquhar, G.D., O'Leary, M.H., Berry, J.A., 1982. On the Relationship Between Carbon Isotope Discrimination and the Intercellular Carbon Dioxide Concentration in Leaves. Funct. Plant Biol. 9, 121–137. https://doi.org/10.1071/pp9820121

Feranec, R.S., Hadly, E.A., Paytan, A., 2007. Determining landscape use of Holocene mammals using strontium isotopes. Oecologia 153, 943–950.

Fernandez-Gimenez, M.E., 2000. The Role of Mongolian Nomadic Pastoralists' Ecological Knowledge in Rangeland Management. Ecol. Appl. 10, 1318–1326. https://doi.org/10.1890/1051-0761(2000)010[1318:TROMNP]2.0.CO;2

Fernández-Giménez, M.E., Batkhishig, B., Batbuyan, B., 2012. Cross-boundary and cross-level dynamics increase vulnerability to severe winter disasters (dzud) in Mongolia. Glob. Environ. Change 22, 836–851. https://doi.org/10.1016/j.gloenvcha.2012.07.001

Fernández-Giménez, M.E., Febre, S.L., 2006. Mobility in pastoral systems: Dynamic flux or downward trend? Int. J. Sustain. Dev. World Ecol. 13, 341–362. https://doi.org/10.1080/13504500609469685

Ferret, C., 2014. Discontinuités spatiales et pastoralisme nomade en Asie intérieure au tournant des XIXe et XXe siècles. Ann. Hist. Sci. Soc. 69, 957–996.

Ferret, C., 2009. Une civilisation du cheval. Les usages de l'équidé de la steppe à la taïga. Belin, Paris.

Finke, P., 2004. Le pastoralisme dans l'ouest de la Mongolie: contraintes, motivations et variations. Cah. D'Asie Cent. 245–265.

Fisher, D.C., Fox, D.L., 2007. Season of death of the Dent mammoths. Dent Prairie Peaks Rock. Recent Paleoindian Res. Colo. 123–153.

Fisher, D.C., Fox, D.L., Agenbroad, L.D., 2003a. Tusk growth rate and season of death of Mammuthus columbi from Hot Springs, South Dakota, USA. Deinsea 9, 117–134.

Fisher, D.C., Fox, D.L., Laub, R.S., 2003b. Season of death and terminal growth histories of Hiscock mastodons. Hiscock Site Late Pleistocene Holocene Paleoecol. Archaeol. West. N. Y. State Bull. Buffalo Soc. Nat. Hist. 37, 83–101.

Fisher, J.L., Valentine, B., 2013. Resource depression, climate change, and mountain sheep in the eastern Great Basin of western North America. Archaeol. Anthropol. Sci. 5, 145–157. https://doi.org/10.1007/s12520-013-0124-9

Fitzhugh, W., 2009. The mongolian deer stone-khirigsuur complex : dating and organisation of a late bronze age Menagerie, in: Current Archaeological Research in Mongolia, Department of Anthropology Staff Publications. pp. 183–199.

Flanagan, L.B., Farquhar, G.D., 2014. Variation in the carbon and oxygen isotope composition of plant biomass and its relationship to water-use efficiency at the leaf- and ecosystem-scales in a northern Great Plains grassland. Plant Cell Environ. 37, 425–438. https://doi.org/10.1111/pce.12165

Flockhart, D.T., Kyser, T.K., Chipley, D., Miller, N.G., Norris, D.R., 2015. Experimental evidence shows no fractionation of strontium isotopes ($^{87}Sr/^{86}Sr$) among soil, plants, and herbivores: implications for tracking wildlife and forensic science. Isotopes Environ. Health Stud. 51, 372–381.

Frachetti, M.D., 2008. Variability and dynamic landscapes of mobile pastoralism in ethnography and prehistory. Archeol. Mobil.

Frachetti, M.D., Smith, C.E., Traub, C.M., Williams, T., 2017. Nomadic ecology shaped the highland geography of Asia's Silk Roads. Nature 543, 193–198. https://doi.org/10.1038/nature21696

Fraser, R.A., Grün, R., Privat, K., Gagan, M.K., 2008. Stable-isotope microprofiling of wombat tooth enamel records seasonal changes in vegetation and environmental conditions in eastern Australia. Palaeogeogr. Palaeoclimatol. Palaeoecol. 269, 66–77. https://doi.org/10.1016/j.palaeo.2008.08.004

Frei, K.M., Frei, R., 2011. The geographic distribution of strontium isotopes in Danish surface waters – A base for provenance studies in archaeology, hydrology and agriculture. Appl. Geochem. 26, 326–340. https://doi.org/10.1016/j.apgeochem.2010.12.006

Frei, K.M., Frei, R., Mannering, U., Gleba, M., Nosch, M.L., Lyngstrøm, H., 2009. Provenance of Ancient Textiles—a Pilot Study Evaluating the Strontium Isotope System in Wool. Archaeometry 51, 252–276. https://doi.org/10.1111/j.1475-4754.2008.00396.x

Fricke, H.C., Clyde, W.C., O'Neil, J.R., 1998. Intra-tooth variations in $\delta^{18}O$ (PO_4) of mammalian tooth enamel as a record of seasonal variations in continental climate variables. Geochim. Cosmochim. Acta 62, 1839–1850. https://doi.org/10.1016/S0016-7037(98)00114-8

Fricke, H.C., O'Neil, J.R., 1999. The correlation between $^{18}O/^{16}O$ ratios of meteoric water and surface temperature: its use in investigating terrestrial climate change over geologic time. Earth Planet. Sci. Lett. 170, 181–196.

Fricke, H.C., O'Neil, J.R., 1996. Inter-and intra-tooth variation in the oxygen isotope composition of mammalian tooth enamel phosphate: implications for palaeoclimatological and palaeobiological research. Palaeogeogr. Palaeoclimatol. Palaeoecol. 126, 91–99.

Fuller, B.T., Fuller, J.L., Sage, N.E., Harris, D.A., O'Connell, T.C., Hedges, R.E.M., 2005. Nitrogen balance and $\delta^{15}N$: why you're not what you eat during nutritional stress. Rapid Commun. Mass Spectrom. 19, 2497–2506. https://doi.org/10.1002/rcm.2090

Fuller, B.T., Fuller, J.L., Sage, N.E., Harris, D.A., O'Connell, T.C., Hedges, R.E.M., 2004. Nitrogen balance and $\delta^{15}N$: why you're not what you eat during pregnancy. Rapid Commun. Mass Spectrom. 18, 2889–2896. https://doi.org/10.1002/rcm.1708

Galvin, K.A., Little, M.A., 1999. Dietary intake and nutritional status. Turkana Herders Dry Savanna Ecol. Biobehav. Response Nomads Uncertain Environ. Oxf. Univ. Press N. Y. 125–145.

Garten, C.T., 1993. Variation in Foliar 15N Abundance and the Availability of Soil Nitrogen on Walker Branch Watershed. Ecology 74, 2098–2113. https://doi.org/10.2307/1940855

Gat, J.R., 1996. Oxygen and Hydrogen Isotopes in the Hydrologic Cycle. Annu. Rev. Earth Planet. Sci. 24, 225–262. https://doi.org/10.1146/annurev.earth.24.1.225

Gaunitz, C., Fages, A., Hanghøj, K., Albrechtsen, A., Khan, N., Schubert, M., Seguin-Orlando, A., Owens, I.J., Felkel, S., Bignon-Lau, O., others, 2018. Ancient genomes revisit the ancestry of domestic and Przewalski's horses. Science 360, 111–114.

Gibson, J.J., Aggarwal, P., Hogan, J., Kendall, C., Martinelli, L.A., Stichler, W., Rank, D., Goni, I., Choudhry, M., Gat, J., Bhattacharya, S., Sugimoto, A., Fekete, B., Pietroniro, A., Maurer, T., Panarello, H., Stone, D., Seyler, P., Maurice-Bourgoin, L., Herczeg, A., 2002. Isotope studies in large river basins: A new global research focus. Eos Trans. Am. Geophys. Union 83, 613–617. https://doi.org/10.1029/2002EO000415

Gigleux, C., Grimes, V., Tütken, T., Knecht, R., Britton, K., 2019. Reconstructing caribou seasonal biogeography in Little Ice Age (late Holocene) Western Alaska using intra-tooth strontium and oxygen isotope analysis. J. Archaeol. Sci. Rep. 23, 1043–1054. https://doi.org/10.1016/j.jasrep.2017.10.043

Giscard, P.-H., Turbat, T., Crubézy, É. (Eds.), 2013. LE PREMIER EMPIRE DES STEPPES EN MONGOLIE : histoire du peuple Xiongnu et étude pluridisciplinaire de l'ensemble funéraire d'Egyin Gol. Editions Faton, Dijon, France.

Glassburn, C.L., Potter, B.A., Clark, J.L., Reuther, J.D., Bruning, D.L., Wooller, M.J., 2018. Strontium and Oxygen Isotope Profiles of Sequentially Sampled Modern Bison (*Bison bison bison*) Teeth from Interior Alaska as Proxies of Seasonal Mobility. Arctic 71.

Goepfert, N., Dufour, E., Gutiérrez, B., Chauchat, C., 2013. Origen geográfico de camélidos en el periodo mochica (100-800 AD) y análisis isotópico secuencial del esmalte dentario: enfoque metodológico y aportes preliminares. Bull. Inst. Fr. Détudes Andin. 25–48. https://doi.org/10.4000/bifea.869

Gonfiantini, R., Roche, M.-A., Olivry, J.-C., Fontes, J.-C., Zuppi, G.M., 2001. The altitude effect on the isotopic composition of tropical rains. Chem. Geol. 181, 147–167. https://doi.org/10.1016/S0009-2541(01)00279-0

Gourichon, L., Parmigiani, V., 2016. Preliminary analysis of dental cementum of Lama guanicoe for the estimation of age and season at death: Studies of modern specimens and further archaeological applications. J. Archaeol. Sci. Rep. 6, 856–861. https://doi.org/10.1016/j.jasrep.2016.01.001

Grant, A., 1982. The Use of Tooth Wear as a Guide to the Age of Domestic Ungulates. Ageing Sexing Anim. Bones Archaeol. Sites Ed Bob Wilson Al 91–108.

Green, D.R., Green, G.M., Colman, A.S., Bidlack, F.B., Tafforeau, P., Smith, T.M., 2017. Synchrotron imaging and Markov Chain Monte Carlo reveal tooth mineralization patterns. PLOS ONE 12, e0186391. https://doi.org/10.1371/journal.pone.0186391

Green, D.R., Olack, G., Colman, A.S., 2018a. Determinants of blood water $\delta^{18}O$ variation in a population of experimental sheep: Implications for paleoclimate reconstruction. Chem. Geol. 485, 32–43. https://doi.org/10.1016/j.chemgeo.2018.03.034

Green, D.R., Smith, T.M., Green, G.M., Bidlack, F.B., Tafforeau, P., Colman, A.S., 2018b. Quantitative reconstruction of seasonality from stable isotopes in teeth. Geochim. Cosmochim. Acta 235, 483–504. https://doi.org/10.1016/j.gca.2018.06.013

Greenfield, H., Moore, N., Steppan, K., 2015. Estimating the Age- and Season-of-Death for Wild Equids: a Comparison of Techniques Utilising a Sample from the Late Neolithic Site of Bad Buchau-Dullenried, Germany. Open Quat. 1, Art. 3. https://doi.org/10.5334/oq.ac

Greenfield, H.J., Arnold, E.R., 2008. Absolute age and tooth eruption and wear sequences in sheep and goat: determining age-at-death in zooarchaeology using a modern control sample. J. Archaeol. Sci. 35, 836–849. https://doi.org/10.1016/j.jas.2007.06.003

Grine, F.E., 1986. Dental evidence for dietary differences in Australopithecus and Paranthropus: a quantitative analysis of permanent molar microwear. J. Hum. Evol. 15, 783–822. https://doi.org/10.1016/S0047-2484(86)80010-0

Gron, K.J., Montgomery, J., Nielsen, P.O., Nowell, G.M., Peterkin, J.L., Sørensen, L., Rowley-Conwy, P., 2016. Strontium isotope evidence of early Funnel Beaker Culture movement of cattle. J. Archaeol. Sci. Rep. 6, 248–251. https://doi.org/10.1016/j.jasrep.2016.02.015

Grue, H., Jensen, B., 1976. Annual cementum structures in canine teeth in arctic foxes (*Alopex lagopus* (L.)) from Greenland and Denmark.

Grupe, G., Price, T.D., Söllner, F., 1999. Mobility of Bell Beaker people revealed by strontium isotope ratios of tooth and bone: a study of southern Bavarian skeletal remains. A reply to the comment by Peter Horn and Dieter Müller-Sohnius. Appl. Geochem. 14, 271–275.

Halder, J., Terzer, S., Wassenaar, L.I., Araguás-Araguás, L.J., Aggarwal, P.K., 2015. The Global Network of Isotopes in Rivers (GNIR): integration of water isotopes in watershed observation and riverine research. Hydrol. Earth Syst. Sci. 19, 3419–3431. https://doi.org/10.5194/hess-19-3419-2015

Hammer, E.L., Arbuckle, B.S., 2017. 10,000 years of pastoralism in Anatolia: a review of evidence for variability in pastoral lifeways. Nomadic Peoples 21, 214–267.

Handley, L.L., Austin, A.T., Stewart, G.R., Robinson, D., Scrimgeour, C.M., Raven, J.A., Heaton, T.H.E., Schmidt, S., 1999. The 15N natural abundance (δ15N) of ecosystem samples reflects measures of water availability. Funct. Plant Biol. 26, 185–199. https://doi.org/10.1071/pp98146

Hartman, G., Danin, A., 2010. Isotopic values of plants in relation to water availability in the Eastern Mediterranean region. Oecologia 162, 837–852. https://doi.org/10.1007/s00442-009-1514-7

Helmer, D., Gourichon, L., Sidi Maamar, H., Vigne, J.-D., 2005. L'élevage des caprinés néolithiques dans le sud-est de la France: saisonnalité des abattages, relations entre grottes-bergeries et sites de plein air. Anthropozoologica 40, 167–189.

Henton, E., 2012. The combined use of oxygen isotopes and microwear in sheep teeth to elucidate seasonal management of domestic herds: the case study of Çatalhöyük, central Anatolia. J. Archaeol. Sci. 39, 3264–3276. https://doi.org/10.1016/j.jas.2012.05.020

Henton, E., Martin, L., Garrard, A., Jourdan, A.-L., Thirlwall, M., Boles, O., 2017a. Gazelle seasonal mobility in the Jordanian steppe: The use of dental isotopes and microwear as environmental markers, applied to Epipalaeolithic Kharaneh IV. J. Archaeol. Sci. Rep. 11, 147–158. https://doi.org/10.1016/j.jasrep.2016.11.031

Henton, E., MCorriston, J., Martin, L., Oches, E.A., 2014. Seasonal aggregation and ritual slaughter: Isotopic and dental microwear evidence for cattle herder mobility in the

Arabian Neolithic. J. Anthropol. Archaeol. 33, 119–131. https://doi.org/10.1016/j.jaa.2013.12.004

Henton, E., Meier-Augenstein, W., Kemp, H.F., 2010. The Use of Oxygen Isotopes in Sheep Molars to Investigate Past Herding Practices at the Neolithic Settlement of Çatalhöyük, Central Anatolia. Archaeometry 52, 429–449. https://doi.org/10.1111/j.1475-4754.2009.00492.x

Henton, E., Ruben, I., Palmer, C., Martin, L., Garrard, A., Thirlwall, M., Jourdan, A.-L., 2017b. The Seasonal Mobility of Prehistoric Gazelle Herds in the Azraq Basin, Jordan: Modelling Alternative Strategies Using Stable Isotopes. Environ. Archaeol. 0, 1–13. https://doi.org/10.1080/14614103.2017.1316432

Hermes, T., Pederzani, S., Makarewicz, C.A., 2017. Ahead of the curve?: Implications for isolating vertical transhumance in seasonal montane environments using sequential oxygen isotope analyses of tooth enamel, in: Isotopic Investigations of Pastoralism in Prehistory. Routledge, pp. 57–76.

Hesse, B., 1982. Slaughter Patterns and Domestication: The Beginnings of Pastoralism in Western Iran. Man 17, 403–417. https://doi.org/10.2307/2801705

Higgins, P., MacFadden, B.J., 2004. "Amount Effect" recorded in oxygen isotopes of Late Glacial horse (*Equus*) and bison (*Bison*) teeth from the Sonoran and Chihuahuan deserts, southwestern United States. Palaeogeogr. Palaeoclimatol. Palaeoecol., Incremental Growth in Vertebrate Skeletal Tissues: Paleobiological and Paleoenvironmental Implications 206, 337–353. https://doi.org/10.1016/j.palaeo.2004.01.011

Hijmans, R.J., 2018. raster: Geographic Data Analysis and Modeling.

Hillson, S., 2005. Teeth. Cambridge university press.

Hobson, K.A., 2008. Applying Isotopic Methods to Tracking Animal Movements, in: Tracking Animal Migration with Stable Isotopes, Terrestrial Ecology. K. A Hobson and L. I Wassenaar, London, UK, pp. 45–78. https://doi.org/10.1016/S1936-7961(07)00003-6

Honeychurch, W., 2015a. Inner Asia and the Spatial Politics of Empire: Archaeology, Mobility, and Culture. Springer, New York.

Honeychurch, W., 2015b. The Late and Final Bronze Age Cultures of Mongolia, 1400–700 BC, in: Honeychurch, W. (Ed.), Inner Asia and the Spatial Politics of Empire: Archaeology, Mobility, and Culture Contact. Springer, New York, NY, pp. 109–156. https://doi.org/10.1007/978-1-4939-1815-7_5

Honeychurch, W., 2013. The Nomad as State Builder: Historical Theory and Material Evidence from Mongolia. J. World Prehistory 26, 283–321. https://doi.org/10.1007/s10963-013-9069-2

Honeychurch, W., 2010. Pastoral nomadic voices: a Mongolian archaeology for the future. World Archaeol. 42, 405–417. https://doi.org/10.1080/00438243.2010.497389

Honeychurch, W., Makarewicz, C.A., 2016. The Archaeology of Pastoral Nomadism. Annu. Rev. Anthropol. 45, 341–359. https://doi.org/10.1146/annurev-anthro-102215-095827

Hoppe, K.A., Koch, P.L., Carlson, R.W., Webb, S.D., 1999. Tracking mammoths and mastodons: Reconstruction of migratory behavior using strontium isotope ratios. Geology 27, 439–442. https://doi.org/10.1130/0091-7613(1999)027<0439:TMAMRO>2.3.CO;2

Hoppe, K.A., Stover, S.M., Pascoe, J.R., Amundson, R., 2004. Tooth enamel biomineralization in extant horses: implications for isotopic microsampling. Palaeogeogr. Palaeoclimatol. Palaeoecol., Incremental Growth in Vertebrate Skeletal Tissues: Paleobiological and Paleoenvironmental Implications 206, 355–365. https://doi.org/10.1016/j.palaeo.2004.01.012

Hoppe, K.A., Stuska, S., Amundson, R., 2005. The implications for paleodietary and paleoclimatic reconstructions of intrapopulation variability in the oxygen and carbon isotopes of teeth from modern feral horses. Quat. Res. 64, 138–146. https://doi.org/10.1016/j.yqres.2005.05.007

Horstwood, M.S.A., Evans, J.A., Montgomery, J., 2008. Determination of Sr isotopes in calcium phosphates using laser ablation inductively coupled plasma mass spectrometry and their application to archaeological tooth enamel. Geochim. Cosmochim. Acta 72, 5659–5674. https://doi.org/10.1016/j.gca.2008.08.016

Houle, J.-L., 2017. Long-term occupation and seasonal mobility in Mongolia: a comparative study of two mobile pastoralist comunities, in: Fitful Histories and Unruly Publics: Rethinking Temporality and Community in Eurasian Archaeology. Kathryn O. Weber Emma Hite Lori Khatchadourian Adam T. Smith, Leiden, The Netherland, pp. 155–174.

Houle, J.-L., 2016. Bronze Age Mongolia. https://doi.org/10.1093/oxfordhb/9780199935413.013.20

Houle, J.-L., 2015. Occupation de longue durée et mobilité saisonnière en Mongolie, in: Les systèmes de mobilité de la Préhistoire au Moyen-Âge XXXV^{e} rencontres internationales d'archéologie et d'histoire d'Antibes. Naudinot, N., Meignen, L., Binder, D., Querré, G., Antibes, p. 442.

Houle, J.-L., Broderick, L., 2011. Settlement patterns and domestic economy of the Xiongnu in Khanui Valley, Mongolia. Xiongnu Archaeol. Multidiscip. Perspect. First Steppe Emp. Inn. Asia 137–152.

Iacumin, P., Bocherens, H., Mariotti, A., Longinelli, A., 1996. Oxygen isotope analyses of co-existing carbonate and phosphate in biogenic apatite: a way to monitor diagenetic alteration of bone phosphate? Earth Planet. Sci. Lett. 142, 1–6. https://doi.org/10.1016/0012-821X(96)00093-3

Iacumin, P., Davanzo, S., Nikolaev, V., 2006. Spatial and temporal variations in the ^{13}C / ^{12}C and ^{15}N / ^{14}N ratios of mammoth hairs: Palaeodiet and palaeoclimatic implications. Chem. Geol. 231, 16–25. https://doi.org/10.1016/j.chemgeo.2005.12.007

Iacumin, P., Davanzo, S., Nikolaev, V., 2005. Short-term climatic changes recorded by mammoth hair in the Arctic environment. Palaeogeogr. Palaeoclimatol. Palaeoecol. 218, 317–324. https://doi.org/10.1016/j.palaeo.2004.12.021

InfoClimat, 2019. Infoclimat.fr Version 5.4. Accessible at: https://www.infoclimat.fr.

Ivanova, L.A., Ivanov, L.A., Ronzhina, D.A., Yudina, P.K., Migalina, S.V., Shinehuu, T., Tserenkhand, G., Voronin, P.Yu., Anenkhonov, O.A., Bazha, S.N., Gunin, P.D., 2019. Leaf traits of C_3- and C_4-plants indicating climatic adaptation along a latitudinal gradient in Southern Siberia and Mongolia. Flora, Functional Traits Explaining Plant Responses to Past and Future Climate Changes 254, 122–134. https://doi.org/10.1016/j.flora.2018.10.008

Jacobson-Tepfer, E., 2012. The image of the wheeled vehicle in the Mongolian Altai: Instability and ambiguity. Silk Road 10, 1–28.

Jensen, P., 2009. The Ethology of Domestic Animals: An Introductory Text. CABI.

Jin, Z., You, C.-F., Yu, J., Wu, L., Zhang, F., Liu, H.-C., 2011. Seasonal contributions of catchment weathering and eolian dust to river water chemistry, northeastern Tibetan Plateau: Chemical and Sr isotopic constraints. J. Geophys. Res. Earth Surf. 116. https://doi.org/10.1029/2011JF002002

Jones, G.G., 2006. Tooth eruption and wear observed in live sheep from Butser Hill, the Cotswold Farm Park and five farms in the Pentland Hills, UK, in: Recent Advances in Ageing and Sexing Animal Bones. Oxbow Books, pp. 155–178.

Jones, R.J., Ludlow, M.M., Troughton, J.H., Blunt, C.G., 1981. Changes in the natural carbon isotope ratios of the hair from steers fed diets of C4, C3 and C4 species in sequence. J. Aust. N. Z. Assoc. Adv. Sci. 12, 85–87.

Julien, M.-A., 2009. Chasseurs de bisons : apports de l'archéozoologie et de la biogéochimie isotopique à l'étude palethnographique et paléoéthologique du gisement épigravettien d'Amvrosievka (Ukraine). Thèse de doctorat. Muséum national d'Histoire naturelle, Paris (France) et Université de Montréal, Montréal (Canada).

Julien, M.-A., Bocherens, H., Burke, A., Drucker, D.G., Patou-Mathis, M., Krotova, O., Péan, S., 2012. Were European steppe bison migratory? ^{18}O, ^{13}C and Sr intra-tooth isotopic variations applied to a palaeoethological reconstruction. Quat. Int. 271, 106–119.

Julien, M.-A., Rivals, F., Serangeli, J., Bocherens, H., Conard, N.J., 2015. A new approach for deciphering between single and multiple accumulation events using intra-tooth isotopic variations: Application to the Middle Pleistocene bone bed of Schöningen 13 II-4. J. Hum. Evol., Special Issue: Excavations at Schöningen: New Insights into Middle Pleistocene Lifeways in Northern Europe 89, 114–128. https://doi.org/10.1016/j.jhevol.2015.02.012

Kern, Z., Kohán, B., Leuenberger, M., 2014. Precipitation isoscape of high reliefs: interpolation scheme designed and tested for monthly resolved precipitation oxygen isotope records of an Alpine domain. Atmospheric Chem. Phys. 14, 1897–1907. https://doi.org/10.5194/acp-14-1897-2014

Kerven, C., Alimaev, I.I., Behnke, R., Davidson, G., Malmakov, N., Smailov, A., Wright, I., 2006. Fragmenting pastoral mobility: Changing grazing patterns in Post-Soviet Kazakhstan. Bedunah Donald J McArthur E Durant Fernandez-Gimenez Maria Comps 2006 Rangel. Cent. Asia Proc. Conf. Transform. Issues Future Chall. 2004 January 27 Salt Lake City UT Proceeding RMRS-P-39 Fort Collins CO US Dep. Agric. For. Serv. Rocky Mt. Res. Stn. P 99-110 039.

Kerven, C., Robinson, S., Behnke, R., Kushenov, K., Milner-Gulland, E.J., 2016. Horseflies, wolves and wells: biophysical and socio-economic factors influencing livestock distribution in Kazakhstan's rangelands. Land Use Policy 52, 392–409. https://doi.org/10.1016/j.landusepol.2015.12.030

King, S.R.B., 2002. Home range and habitat use of free-ranging Przewalski horses at Hustai National Park, Mongolia. Appl. Anim. Behav. Sci., Equine Behavior 78, 103–113. https://doi.org/10.1016/S0168-1591(02)00087-4

Knipper, C., Paulus, S., Uerpmann, M., Uerpmann, H.-P., 2008. Seasonality and land use in Bronze and Iron Age Kakhetia (Georgia). Oxygen and strontium isotope analyses on horse and cattle teeth. Archäol. Mitteilungen Aus Iran Turan 40, 149–168.

Knockaert, J., Balasse, M., Rendu, C., Burens, A., Campmajo, P., Carozza, L., Bousquet, D., Fiorillo, D., Vigne, J.-D., 2018. Mountain adaptation of caprine herding in the eastern Pyrenees during the Bronze Age: A stable oxygen and carbon isotope analysis of

teeth. Quat. Int., Casting a glance over the mountain – multi-proxy approaches to the understanding of vertical mobility 484, 60–74. https://doi.org/10.1016/j.quaint.2017.05.029

Koch, P.L., Fisher, D.C., Dettman, D., 1989. Oxygen isotope variation in the tusks of extinct proboscideans: A measure of season of death and seasonality. Geology 17, 515–519. https://doi.org/10.1130/0091-7613(1989)017<0515:OIVITT>2.3.CO;2

Koch, P.L., Michener, R., Lajtha, K., 2007. Isotopic study of the biology of modern and fossil vertebrates. Stable Isot. Ecol. Environ. Sci. 2, 99–154.

Koch, P.L., Tuross, N., Fogel, M.L., 1997. The Effects of Sample Treatment and Diagenesis on the Isotopic Integrity of Carbonate in Biogenic Hydroxylapatite. J. Archaeol. Sci. 24, 417–429. https://doi.org/10.1006/jasc.1996.0126

Kohn, M.J., 2010. Carbon isotope compositions of terrestrial C3 plants as indicators of (paleo) ecology and (paleo) climate. Proc. Natl. Acad. Sci. 107, 19691–19695.

Kohn, M.J., 2004. Comment: tooth enamel mineralization in ungulates: implications for recovering a primary isotopic time-series, by BH Passey and TE Cerling (2002). Geochim. Cosmochim. Acta 68, 403–405.

Kohn, M.J., 1996. Predicting animal $\delta^{18}O$: accounting for diet and physiological adaptation. Geochim. Cosmochim. Acta 60, 4811–4829.

Kohn, M.J., Cerling, T.E., 2002. Stable Isotope Compositions of Biological Apatite. Rev. Mineral. Geochem. 48, 455–488. https://doi.org/10.2138/rmg.2002.48.12

Kohn, M.J., Schoeninger, M.J., Valley, J.W., 1996. Herbivore tooth oxygen isotope compositions: effects of diet and physiology. Geochim. Cosmochim. Acta 60, 3889–3896.

Kohn, M.J., Welker, J.M., 2005. On the temperature correlation of $\delta^{18}O$ in modern precipitation. Earth Planet. Sci. Lett. 231, 87–96. https://doi.org/10.1016/j.epsl.2004.12.004

Konstantinov, N., Soenov, V., Trifanova, S., Svyatko, S., 2018. History and culture of the early Türkic period: A review of archaeological monuments in the Russian Altai from the 4th–6th century AD. Archaeol. Res. Asia 16, 103–115. https://doi.org/10.1016/j.ara.2018.06.002

Kootker, L.M., van Lanen, R.J., Kars, H., Davies, G.R., 2016. Strontium isoscapes in The Netherlands. Spatial variations in $^{87}Sr/^{86}Sr$ as a proxy for palaeomobility. J. Archaeol. Sci. Rep. 6, 1–13.

Körner, C., Farquhar, G.D., Roksandic, Z., 1988. A global survey of carbon isotope discrimination in plants from high altitude. Oecologia 74, 623–632. https://doi.org/10.1007/BF00380063

Körner, C., Farquhar, G.D., Wong, S.C., 1991. Carbon isotope discrimination by plants follows latitudinal and altitudinal trends. Oecologia 88, 30–40. https://doi.org/10.1007/BF00328400

Kovalev, A.A., Erdenebaatar, D., 2009. Discovery of new cultures of the Bronze Age in Mongolia according to the data obtained by the International Central Asian Archaeological Expedition. Bemmann Al 149–170.

Kradin, N.N., 2011. Heterarchy and hierarchy among the ancient Mongolian nomads. Soc. Evol. Hist. 10.

Landon, D., 2014. The Potential Applications of Tooth Cement Increment Analysis in Historical Archaeology. Northeast Hist. Archaeol. 17. https://doi.org/10.22191/neha/vol17/iss1/5

Lavielle, M., 2005. Using penalized contrasts for the change-point problem. Signal Process. 85, 1501–1510. https://doi.org/10.1016/j.sigpro.2005.01.012

Lavielle, M., 1999. Detection of multiple changes in a sequence of dependent variables. Stoch. Process. Their Appl. 83, 79–102. https://doi.org/10.1016/S0304-4149(99)00023-X

Lazzerini, N., Coulon, A., Simon, L., Marchina, C., Noost, B., Lepetz, S., Zazzo, A., 2019. Grazing high and low: Can we detect horse altitudinal mobility using high-resolution isotope ($\delta^{13}C$ and $\delta^{15}N$ values) time series in tail hair? A case study in the Mongolian Altai. Rapid Commun. Mass Spectrom. 33, 1512–1526. https://doi.org/10.1002/rcm.8496

Lazzerini, N., Zazzo, A., Coulon, A., Turbat, T., Marchina, C., Lepetz, S., 2020. Date of death of domestic caprines assessed by oxygen isotopic analysis of developing molars: implications for deciphering the calendar of pastoral activities in prehistory. J. Archaeol. Sci.

Le Roux, P.J., Lee-Thorp, J.A., Copeland, S.R., Sponheimer, M., de Ruiter, D.J., 2014. Strontium isotope analysis of curved tooth enamel surfaces by laser-ablation multi-collector ICP-MS. Palaeogeogr. Palaeoclimatol. Palaeoecol., Bone and enamel diagenesis: From the crystal to the environment - A tribute to Jean-François Saliège 416, 142–149. https://doi.org/10.1016/j.palaeo.2014.09.007

Lee-Thorp, J.A., 2008. On Isotopes and Old Bones. Archaeometry 50, 925–950. https://doi.org/10.1111/j.1475-4754.2008.00441.x

Legrand, J., 2011. Mongols et Nomades: Société, Histoire, Culture /Mongolchuud, nüüdelchin: niigem, tüüh, soyol. Textes, communications, articles (1973-2011). ADMON, Ulaanbaatar.

Lepetz, S., Decanter, F., 2013. Les restes osseux animaux du site d'Egyin Gol., in: Etude Du Cimetière Xongniou d'Egyin Gol. P.-H. Giscard and T. Turbat, p. 15.

Lepetz, S., Zazzo, A., Bernard, V., de Larminat, S., Magail, J., Gantulga, J.-O., 2019. Customs, rites, and sacrifices relating to a mortuary complex in Late Bronze Age Mongolia (Tsatsyn Ereg, Arkhangai). Anthropozoologica 54, 151–177.

Lewis, J., Pike, A.W.G., Coath, C.D., Evershed, R.P., 2017. Strontium concentration, radiogenic ($^{87}Sr/^{86}Sr$) and stable ($\delta^{88}Sr$) strontium isotope systematics in a controlled feeding study. STAR Sci. Technol. Archaeol. Res. 3, 45–57. https://doi.org/10.1080/20548923.2017.1303124

Li, C., Zhang, X., Liu, X., Luukkanen, O., Berninger, F., 2006. Leaf morphological and physiological responses of *Quercus aquifolioides* along an altitudinal gradient. Silva Fenn. 40, 5–13.

Li, J., Wang, G., Liu, XianZhao, Han, J., Liu, M., Liu, XiaoJuan, 2009. Variations in carbon isotope ratios of C3 plants and distribution of C4 plants along an altitudinal transect on the eastern slope of Mount Gongga. Sci. China Ser. Earth Sci. 52, 1714–1723. https://doi.org/10.1007/s11430-009-0170-4

Li, J., Zhang, S., Bunn, H.T., Sarathi, A., Gao, X., 2017. A preliminary application of dental cementum incremental analysis to determine the season-of-death of equids from the

Xujiayao site, China. Sci. China Earth Sci. 60, 1183–1188. https://doi.org/10.1007/s11430-016-9028-x

Li, M., Liu, H., Li, L., Yi, X., Zhu, X., 2007. Carbon isotope composition of plants along altitudinal gradient and its relationship to environmental factors on the Qinghai-Tibet Plateau. Pol. J. Ecol. 55, 67–78.

Liechti, K., Biber, J.-P., 2016. Pastoralism in Europe: characteristics and challenges of highland-lowland transhumance. Rev. Sci. Tech. Int. Off. Epizoot. 35, 561–575.

Little, M.A., 2015. Chapter 24 - Pastoralism, in: Muehlenbein, M.P. (Ed.), Basics in Human Evolution. Academic Press, Boston, pp. 337–347. https://doi.org/10.1016/B978-0-12-802652-6.00024-4

Liu, J., Song, X., Yuan, G., Sun, X., Yang, L., 2014. Stable isotopic compositions of precipitation in China. Tellus B Chem. Phys. Meteorol. 66, 22567. https://doi.org/10.3402/tellusb.v66.22567

Liu, X., Gao, C., Su, Q., Zhang, Y., Song, Y., 2016. Altitudinal trends in $\delta^{13}C$ value, stomatal density and nitrogen content of Pinus tabuliformis needles on the southern slope of the middle Qinling Mountains, China. J. Mt. Sci. 13, 1066–1077. https://doi.org/10.1007/s11629-015-3532-8

Liu, Xiaoning, Ma, J., Sun, W., Cui, Y., Duan, Z., 2010. Advances in Mechanisms Underlying the Responses of δ∼(13) C in Alpine Plants to the Altitudinal Gradients. J. Mt. Sci. 1.

Liu, X., Wang, G., 2010. Measurements of nitrogen isotope composition of plants and surface soils along the altitudinal transect of the eastern slope of Mount Gongga in southwest China. Rapid Commun. Mass Spectrom. 24, 3063–3071. https://doi.org/10.1002/rcm.4735

Liu, XianZhao, Wang, G., Li, J., Wang, Q., 2010. Nitrogen isotope composition characteristics of modern plants and their variations along an altitudinal gradient in Dongling Mountain in Beijing. Sci. China Ser. Earth Sci. 53, 128–140. https://doi.org/10.1007/s11430-009-0175-z

Liu, X., Zhao, L., Gasaw, M., Gao, D., Qin, D., Ren, J., 2007. Foliar $\delta^{13}C$ and $\delta^{15}N$ values of C3 plants in the Ethiopia Rift Valley and their environmental controls. Chin. Sci. Bull. 52, 1265–1273. https://doi.org/10.1007/s11434-007-0165-5

Lkhagvadorj, D., Hauck, M., Dulamsuren, Ch., Tsogtbaatar, J., 2013. Pastoral nomadism in the forest-steppe of the Mongolian Altai under a changing economy and a warming climate. J. Arid Environ. 88, 82–89. https://doi.org/10.1016/j.jaridenv.2012.07.019

Longinelli, A., 1984. Oxygen isotopes in mammal bone phosphate: a new tool for paleohydrological and paleoclimatological research? Geochim. Cosmochim. Acta 48, 385–390.

Lubinski, P.M., 2001. Estimating age and season of death of pronghorn antelope (Antilocapra americana Ord) by means of tooth eruption and wear. Int. J. Osteoarchaeol. 11, 218–230. https://doi.org/10.1002/oa.536

Lugli, F., Cipriani, A., Peretto, C., Mazzucchelli, M., Brunelli, D., 2017. In situ high spatial resolution $^{87}Sr/^{86}Sr$ ratio determination of two Middle Pleistocene (c.a. 580ka) Stephanorhinus hundsheimensis teeth by LA–MC–ICP–MS. Int. J. Mass Spectrom. 412, 38–48. https://doi.org/10.1016/j.ijms.2016.12.012

Luz, B., Kolodny, Y., 1985. Oxygen isotope variations in phosphate of biogenic apatites, IV. Mammal teeth and bones. Earth Planet. Sci. Lett. 75, 29–36. https://doi.org/10.1016/0012-821X(85)90047-0

Luz, B., Kolodny, Y., Horowitz, M., 1984. Fractionation of oxygen isotopes between mammalian bone-phosphate and environmental drinking water. Geochim. Cosmochim. Acta 48, 1689–1693. https://doi.org/10.1016/0016-7037(84)90338-7

Lynch, T.F., 1983. Camelid pastoralism and the emergence of Tiwanaku civilization in the South-Central Andes. World Archaeol. 15, 1–14. https://doi.org/10.1080/00438243.1983.9979881

Mainland, I., Towers, J., Ewens, V., Davis, G., Montgomery, J., Batey, C., Card, N., Downes, J., 2016. Toiling with teeth: An integrated dental analysis of sheep and cattle dentition in Iron Age and Viking–Late Norse Orkney. J. Archaeol. Sci. Rep. 6, 837–855. https://doi.org/10.1016/j.jasrep.2015.12.002

Mainland, I.L., 1998. Dental Microwear and Diet in Domestic Sheep (Ovis aries) and Goats (Capra Hircus): Distinguishing Grazing and Fodder-fed Ovicaprids using a Quantitative Analytical Approach. J. Archaeol. Sci. 25, 1259–1271. https://doi.org/10.1006/jasc.1998.0301

Makarewicz, C., 2011. Xiongnu pastoral systems: Integrating economies of subsistence and scale. Xiongnu Archaeol. Multidiscip. Perspect. First Steppe Emp. Inn. Asia Rheinische Friedrich-Wilhelms-Univ. Bonn 181–192.

Makarewicz, C., Tuross, N., 2012. Finding fodder and tracking transhumance: isotopic detection of goat domestication processes in the Near East. Curr. Anthropol. 53, 495–505.

Makarewicz, C., Tuross, N., 2006. Foddering by Mongolian pastoralists is recorded in the stable carbon ($\delta^{13}C$) and nitrogen ($\delta^{15}N$) isotopes of caprine dentinal collagen. J. Archaeol. Sci. 33, 862–870.

Makarewicz, C.A., 2017. Sequential $\delta^{13}C$ and $\delta^{18}O$ analyses of early Holocene bovid tooth enamel: Resolving vertical transhumance in Neolithic domesticated sheep and goats. Palaeogeogr. Palaeoclimatol. Palaeoecol. https://doi.org/10.1016/j.palaeo.2017.01.028

Makarewicz, C.A., 2015. Winter is coming: seasonality of ancient pastoral nomadic practices revealed in the carbon ($\delta^{13}C$) and nitrogen ($\delta^{15}N$) isotopic record of Xiongnu caprines. Archaeol. Anthropol. Sci. 1–14.

Makarewicz, C.A., 2014. Winter pasturing practices and variable fodder provisioning detected in nitrogen ($\delta^{15}N$) and carbon ($\delta^{13}C$) isotopes in sheep dentinal collagen. J. Archaeol. Sci. 41, 502–510. https://doi.org/10.1016/j.jas.2013.09.016

Makarewicz, C.A., Arbuckle, B.S., Öztan, A., 2017. Vertical transhumance of sheep and goats identified by intra-tooth sequential carbon ($\delta^{13}C$) and oxygen ($\delta^{18}O$) isotopic analyses: Evidence from Chalcolithic Köşk Höyük, central Turkey. J. Archaeol. Sci. 86, 68–80. https://doi.org/10.1016/j.jas.2017.01.003

Makarewicz, C.A., Pederzani, S., 2017. Oxygen ($\delta^{18}O$) and carbon ($\delta^{13}C$) isotopic distinction in sequentially sampled tooth enamel of co-localized wild and domesticated caprines: Complications to establishing seasonality and mobility in herbivores. Palaeogeogr. Palaeoclimatol. Palaeoecol. https://doi.org/10.1016/j.palaeo.2017.01.010

Makarewicz, C.A., Winter-Schuh, C., Byerly, H., Houle, J.-L., 2018. Isotopic evidence for ceremonial provisioning of Late Bronze age khirigsuurs with horses from diverse geographic locales. Quat. Int. 476, 70–81. https://doi.org/10.1016/j.quaint.2018.02.030

Männel, T.T., Auerswald, K., Schnyder, H., 2007. Altitudinal gradients of grassland carbon and nitrogen isotope composition are recorded in the hair of grazers. Glob. Ecol. Biogeogr. 16, 583–592. https://doi.org/10.1111/j.1466-8238.2007.00322.x

Marchina, C., 2019. Nomad's land. Éleveurs, animaux et paysage chez les peuples mongols, Zones sensibles. ed. Bruxelles.

Marchina, C., 2016. "Follow the horse": The complexities of collaboration between the lasso-pole horse (uurgach mor') and his rider among Mongolian horse herders, in: The Meaning of Horses. Routledge, pp. 116–128.

Marchina, C., Lepetz, S., Salicis, C., Magail, J., 2017. The skull on the hill. Anthropological and osteological investigation of contemporary horse skull ritual practices in central Mongolia (Arkhangai province). Anthropozoologica 52, 171–184. https://doi.org/10.5252/az2017n2a3

Marciniak, A., Evans, J., Henton, E., Pearson, J., Lisowski, M., Bartkowiak, M., Sobkowiak-Tabaka, I., 2017. Animal husbandry in the Early and Middle Neolithic settlement at Kopyd\lowo in the Polish lowlands. A multi-isotope perspective. Archaeol. Anthropol. Sci. 9, 1461–1479.

Martín, P., García-González, R., Nadal, J., Vergès, J.M., 2016. Perinatal ovicaprine remains and evidence of shepherding activities in Early Holocene enclosure caves: El Mirador (Sierra De Atapuerca, Spain). Quat. Int. 414, 316–329. https://doi.org/10.1016/j.quaint.2015.08.024

Martinelli, L.A., Piccolo, M.C., Townsend, A.R., Vitousek, P.M., Cuevas, E., McDowell, W., Robertson, G.P., Santos, O.C., Treseder, K., 1999. Nitrogen stable isotopic composition of leaves and soil: Tropical versus temperate forests. Biogeochemistry 46, 45–65. https://doi.org/10.1023/A:1006100128782

Mashkour, M., 2003. TRACING ANCIENT "NOMADS": ISOTOPIC RESEARCH ON THE ORIGINS OF VERTICAL "TRANSHUMANCE" IN THE ZAGROS REGION. Nomadic Peoples 7, 36–47.

Mashkour, M., Abdi, K., 2002. The question of mobile pastoralist campsites in archaeology: the case of Tuwah Khoshkeh.

Mashkour, M., Bocherens, H., Moussa, I., 2005. Long distance movement of sheep and of Bakhtiari nomads tracked with intra-tooth variations of stable isotopes (^{13}C and ^{18}O). Health Diet Past Anim. Popul. Curr. Res. Future Dir. Davies J Al Eds 113–122.

Maurer, A.-F., Galer, S.J.G., Knipper, C., Beierlein, L., Nunn, E.V., Peters, D., Tütken, T., Alt, K.W., Schöne, B.R., 2012. Bioavailable $^{87}Sr/^{86}Sr$ in different environmental samples — Effects of anthropogenic contamination and implications for isoscapes in past migration studies. Sci. Total Environ. 433, 216–229. https://doi.org/10.1016/j.scitotenv.2012.06.046

McKinney, C.R., McCrea, J.M., Epstein, S., Allen, H.A., Urey, H.C., 1950. Improvements in Mass Spectrometers for the Measurement of Small Differences in Isotope Abundance Ratios. Rev. Sci. Instrum. 21, 724–730. https://doi.org/10.1063/1.1745698

Meiggs, D.C., 2007. Visualizing the seasonal round: a theoretical experiment with strontium isotope profiles in ovicaprine teeth. Anthropozoologica 42, 107–127.

Meiggs, D.C., Arbuckle, B.S., Öztan, A., 2017. The pixelated shepherd: Identifying detailed local land-use practices at Chalcolithic Köşk Höyük, central Turkey, using a strontium isotope (87Sr/86Sr) isoscape, in: Isotopic Investigations of Pastoralism in Prehistory. Routledge, pp. 77–95.

Menard, C., Duncan, P., Fleurance, G., Georges, J.-Y., Lila, M., 2002. Comparative foraging and nutrition of horses and cattle in European wetlands. J. Appl. Ecol. 39, 120–133. https://doi.org/10.1046/j.1365-2664.2002.00693.x

Milhaud, G., Nezit, J., 1991. Molar development in sheep: morphology, radiography, microhardness. Recl. Med. Veterinaire 167, 121–127.

Mohammat, A., Wang, X., Xu, X., Peng, L., Yang, Y., Zhang, X., Myneni, R.B., Piao, S., 2013. Drought and spring cooling induced recent decrease in vegetation growth in Inner Asia. Agric. For. Meteorol., Special Issue:Drought Inner Asia 178–179, 21–30. https://doi.org/10.1016/j.agrformet.2012.09.014

Montgomery, J., Evans, J.A., Horstwood, M.S.A., 2010. Evidence for long-term averaging of strontium in bovine enamel using TIMS and LA-MC-ICP-MS strontium isotope intra-molar profiles. Environ. Archaeol. 15, 32–42. https://doi.org/10.1179/146141010X12640787648694

Morecroft, M.D., Woodward, F.I., 1990. Experimental Investigations on the Environmental Determination of $\delta^{13}C$ at Different Altitudes. J. Exp. Bot. 41, 1303–1308. https://doi.org/10.1093/jxb/41.10.1303

Moritz, M., Galehouse, Z., Hao, Q., Garabed, R.B., 2012. Can one animal represent an entire herd? Modeling pastoral mobility using GPS/GIS technology. Hum. Ecol. 40, 623–630.

Müller, W., Nava, A., Evans, D., Rossi, P.F., Alt, K.W., Bondioli, L., 2019. Enamel mineralization and compositional time-resolution in human teeth evaluated via histologically-defined LA-ICPMS profiles. Geochim. Cosmochim. Acta. https://doi.org/10.1016/j.gca.2019.03.005

Murphy, B.P., Bowman, D.M., 2009. The carbon and nitrogen isotope composition of Australian grasses in relation to climate. Funct. Ecol. 23, 1040–1049.

Naji, S., Colard, T., Blondiaux, J., Bertrand, B., d'Incau, E., Bocquet-Appel, J.-P., 2016. Cementochronology, to cut or not to cut? Int. J. Paleopathol. 15, 113–119. https://doi.org/10.1016/j.ijpp.2014.05.003

Nandintsetseg, B., Shinoda, M., 2011. Seasonal change of soil moisture in Mongolia: its climatology and modelling. Int. J. Climatol. 31, 1143–1152.

Nazarov, A.N., Solomina, O.N., Myglan, V.S., 2012. Variations of the tree line and glaciers in the Central and Eastern Altai regions in the Holocene. Dokl. Earth Sci. 444, 787–790. https://doi.org/10.1134/S1028334X12060244

Negi, G.C.S., Rikhari, H.C., Ram, J., Singh, S.P., 1993. Foraging Niche Characteristics of Horses, Sheep and Goats in an Alpine Meadow of the Indian Central Himalaya. J. Appl. Ecol. 30, 383–394. https://doi.org/10.2307/2404180

Newesely, H., 1989. Fossil bone apatite. Appl. Geochem. 4, 233–245. https://doi.org/10.1016/0883-2927(89)90023-1

Niamir-Fuller, M., Turner, M.D., 1999. A review of recent literature on pastoralism and transhumance in Africa, in: Managing Mobility in African Rangelands: The Legitimization of Transhumance. Practical Action Publishing, pp. 18–46.

Noddle, B., 1974. Ages of epiphyseal closure in feral and domestic goats and ages of dental eruption. J. Archaeol. Sci. 1, 195–204. https://doi.org/10.1016/0305-4403(74)90042-9

Nývltová Fišáková, M., 2013. Seasonality of Gravettian sites in the Middle Danube Region and adjoining areas of Central Europe. Quat. Int. 294, 120–134. https://doi.org/10.1016/j.quaint.2011.08.017

O'Connell, T.C., Hedges, R.E.M., Healey, M.A., Simpson, A.H.R.W., 2001. Isotopic Comparison of Hair, Nail and Bone: Modern Analyses. J. Archaeol. Sci. 28, 1247–1255. https://doi.org/10.1006/jasc.2001.0698

Ogutu, J.O., Piepho, H.-P., Reid, R.S., Rainy, M.E., Kruska, R.L., Worden, J.S., Nyabenge, M., Hobbs, N.T., 2010. Large herbivore responses to water and settlements in savannas. Ecol. Monogr. 80, 241–266. https://doi.org/10.1890/09-0439.1

O'Leary, M.H., 1988. Carbon Isotopes in Photosynthesis. BioScience 38, 328–336. https://doi.org/10.2307/1310735

Outram, A.K., Stear, N.A., Bendrey, R., Olsen, S., Kasparov, A., Zaibert, V., Thorpe, N., Evershed, R.P., 2009. The earliest horse harnessing and milking. Science 323, 1332–1335.

Passey, B.H., Cerling, T.E., 2002. Tooth enamel mineralization in ungulates: implications for recovering a primary isotopic time-series. Geochim. Cosmochim. Acta 66, 3225–3234. https://doi.org/10.1016/S0016-7037(02)00933-X

Passey, B.H., Cerling, T.E., Schuster, G.T., Robinson, T.F., Roeder, B.L., Krueger, S.K., 2005. Inverse methods for estimating primary input signals from time-averaged isotope profiles. Geochim. Cosmochim. Acta 69, 4101–4116. https://doi.org/10.1016/j.gca.2004.12.002

Payne, S., 1973. Kill-off Patterns in Sheep and Goats: the Mandibles from Aşvan Kale. Anatol. Stud. 23, 281–303. https://doi.org/10.2307/3642547

Pebesma, E.J., 2004. Multivariable geostatistics in S: the gstat package. Comput. Geosci. 683–691.

Pederzani, S., Britton, K., 2019. Oxygen isotopes in bioarchaeology: Principles and applications, challenges and opportunities. Earth-Sci. Rev. 188, 77–107. https://doi.org/10.1016/j.earscirev.2018.11.005

Pellegrini, M., Donahue, R.E., Chenery, C., Evans, J., Lee-Thorp, J., Montgomery, J., Mussi, M., 2008. Faunal migration in late-glacial central Italy: implications for human resource exploitation. Rapid Commun. Mass Spectrom. 22, 1714–1726. https://doi.org/10.1002/rcm.3521

Pettorelli, N., Gaillard, J.-M., Mysterud, A., Duncan, P., Chr. Stenseth, N., Delorme, D., Van Laere, G., Toïgo, C., Klein, F., 2006. Using a proxy of plant productivity (NDVI) to find key periods for animal performance: the case of roe deer. Oikos 112, 565–572. https://doi.org/10.1111/j.0030-1299.2006.14447.x

Piao, S., Mohammat, A., Fang, J., Cai, Q., Feng, J., 2006. NDVI-based increase in growth of temperate grasslands and its responses to climate changes in China. Glob. Environ. Change 16, 340–348. https://doi.org/10.1016/j.gloenvcha.2006.02.002

Pike-Tay, A., 1995. Variability and Synchrony of Seasonal Indicators in Dental Cementum Microstructure of the Kaminiriak Caribou Population. Archaeofauna 0, 273–284.

Poage, M.A., Chamberlain, C.P., 2001a. Empirical Relationships Between Elevation and the Stable Isotope Composition of Precipitation and Surface Waters: Considerations for Studies of Paleoelevation Change. Am. J. Sci. 301, 1–15. https://doi.org/10.2475/ajs.301.1.1

Poage, M.A., Chamberlain, C.P., 2001b. Empirical Relationships Between Elevation and the Stable Isotope Composition of Precipitation and Surface Waters: Considerations for Studies of Paleoelevation Change. Am. J. Sci. 301, 1–15. https://doi.org/10.2475/ajs.301.1.1

Podlesak, D.W., Torregrossa, A.-M., Ehleringer, J.R., Dearing, M.D., Passey, B.H., Cerling, T.E., 2008. Turnover of oxygen and hydrogen isotopes in the body water, CO_2, hair, and enamel of a small mammal. Geochim. Cosmochim. Acta 72, 19–35. https://doi.org/10.1016/j.gca.2007.10.003

Pollard, A.M., Pellegrini, M., Lee-Thorp, J.A., 2011. Technical note: Some observations on the conversion of dental enamel $\delta^{18}o_p$ values to $\delta^{18}o_w$ to determine human mobility. Am. J. Phys. Anthropol. 145, 499–504. https://doi.org/10.1002/ajpa.21524

Polosmak, N.V., Bogdanov, E.S., Tseveendorj, D., Erdene-Ochir, N., 2008. THE BURIAL CONSTRUCTION OF NOIN ULA MOUND 20, MONGOLIA. Archaeol. Ethnol. Anthropol. Eurasia 34, 77–87. https://doi.org/10.1016/j.aeae.2008.07.007

Porter, A., 2012. Mobile Pastoralism and the Formation of Near Eastern Civilizations: Weaving Together Society. Cambridge University Press.

Price, T.D., Burton, J.H., Bentley, R.A., 2002. The Characterization of Biologically Available Strontium Isotope Ratios for the Study of Prehistoric Migration. Archaeometry 44, 117–135. https://doi.org/10.1111/1475-4754.00047

Price, T.D., Meiggs, D., Weber, M.-J., Pike-Tay, A., 2017. The migration of Late Pleistocene reindeer: isotopic evidence from northern Europe. Archaeol. Anthropol. Sci. 9, 371–394. https://doi.org/10.1007/s12520-015-0290-z

Putman, R.J., Pratt, R.M., Ekins, J.R., Edwards, P.J., 1987. Food and Feeding Behaviour of Cattle and Ponies in the New Forest, Hampshire. J. Appl. Ecol. 24, 369–380. https://doi.org/10.2307/2403881

Pyankov, V.I., Gunin, P.D., Tsoog, S., Black, C.C., 2000. C4 plants in the vegetation of Mongolia: their natural occurrence and geographical distribution in relation to climate. Oecologia 123, 15–31.

Raich, J.W., Russell, A.E., Vitousek, P.M., 1997. Primary Productivity and Ecosystem Development Along an Elevational Gradient on Mauna Loa, Hawai‘i. Ecology 78, 707–721. https://doi.org/10.1890/0012-9658(1997)078[0707:PPAEDA]2.0.CO;2

Rao, Z., Guo, W., Cao, J., Shi, F., Jiang, H., Li, C., 2017. Relationship between the stable carbon isotopic composition of modern plants and surface soils and climate: A global review. Earth-Sci. Rev. 165, 110–119. https://doi.org/10.1016/j.earscirev.2016.12.007

Reynolds, A.C., Quade, J., Betancourt, J.L., 2012. Strontium isotopes and nutrient sourcing in a semi-arid woodland. Geoderma 189–190, 574–584. https://doi.org/10.1016/j.geoderma.2012.06.029

Rivals, F., Deniaux, B., 2005. Investigation of human hunting seasonality through dental microwear analysis of two Caprinae in late Pleistocene localities in Southern France. J. Archaeol. Sci. 32, 1603–1612. https://doi.org/10.1016/j.jas.2005.04.014

Rivals, F., Prignano, L., Semprebon, G.M., Lozano, S., 2015. A tool for determining duration of mortality events in archaeological assemblages using extant ungulate microwear. Sci. Rep. 5, 17330. https://doi.org/10.1038/srep17330

Rivals, F., Schulz, E., Kaiser, T.M., 2009. A new application of dental wear analyses: estimation of duration of hominid occupations in archaeological localities. J. Hum. Evol. 56, 329–339. https://doi.org/10.1016/j.jhevol.2008.11.005

Robinson, C., Kirkham, J., Brookes, S.J., Bonass, W.A., Shore, R.C., 1995. The chemistry of enamel development. Int. J. Dev. Biol. 39, 145–152. https://doi.org/10.1387/ijdb.7626401

Rodríguez-Hidalgo, A., Rivals, F., Saladié, P., Carbonell, E., 2016. Season of bison mortality in TD10.2 bone bed at Gran Dolina site (Atapuerca): Integrating tooth eruption, wear, and microwear methods. J. Archaeol. Sci. Rep. 6, 780–789. https://doi.org/10.1016/j.jasrep.2015.11.033

Rose, S., Fullagar, P.D., 2005. Strontium isotope systematics of base flow in Piedmont Province watersheds, Georgia (USA). Appl. Geochem. 20, 1571–1586. https://doi.org/10.1016/j.apgeochem.2005.04.015

Rozanski, K., Araguás-Araguás, L., Gonfiantini, R., 1993. Isotopic patterns in modern global precipitation. Clim. Change Cont. Isot. Rec. 78, 1–36. https://doi.org/10.1029/GM078p0001

Rysava, K., McGill, R. a. R., Matthiopoulos, J., Hopcraft, J.G.C., 2016. Re-constructing nutritional history of Serengeti wildebeest from stable isotopes in tail hair: seasonal starvation patterns in an obligate grazer. Rapid Commun. Mass Spectrom. 30, 1461–1468. https://doi.org/10.1002/rcm.7572

Saby, N., Arrouays, D., Boulonne, L., Jolivet, C., Pochot, A., 2006. Geostatistical assessment of Pb in soil around Paris, France. Sci. Total Environ. 367, 212–221. https://doi.org/10.1016/j.scitotenv.2005.11.028

Salter, R.E., Hudson, R.J., 1979. Feeding Ecology of Feral Horses in Western Alberta. J. Range Manag. 32, 221–225. https://doi.org/10.2307/3897127

Salzman, P.C., 2002. Pastoral Nomads: Some General Observations Based on Research in Iran. J. Anthropol. Res. 58, 245–264. https://doi.org/10.1086/jar.58.2.3631038

Sambuu, J., 1945. Mal Azu Aqui Deger-e-Ben Jagakizu Azillaqu Tuqai Arad-Du Ögkü Sanagulg-a Surgal [Advice to Herders on How to Improve Their Husbandry Practices]. Ulaanbataar, Mongolia.

Samec, C.T., Yacobaccio, H.D., Panarello, H.O., 2018. Stable isotope compositions of South American camelids in the Dry Puna of Argentina: A frame of reference for the study of prehistoric herding and hunting strategies. J. Archaeol. Sci. Rep. 18, 628–636. https://doi.org/10.1016/j.jasrep.2017.10.042

Samec, C.T., Yacobaccio, H.D., Panarello, H.O., 2017. Carbon and nitrogen isotope composition of natural pastures in the dry Puna of Argentina: a baseline for the study of prehistoric herd management strategies. Archaeol. Anthropol. Sci. 9, 153–163. https://doi.org/10.1007/s12520-015-0263-2

Schmaus, T.M., Doumani Dupuy, P.N., Frachetti, M.D., 2019. Variability in seasonal mobility patterns in Bronze and Iron Age Kazakhstan through cementum analysis. Quat. Int. https://doi.org/10.1016/j.quaint.2019.04.018

Schmid, E., 1972. Atlas of animal bones, Elsevier Publishing Company. ed. Amsterdam, Oxford, New-York.

Schnyder, H., Schwertl, M., Auerswald, K., Schäufele, R., 2006. Hair of grazing cattle provides an integrated measure of the effects of site conditions and interannual weather variability on $\delta^{13}C$ of temperate humid grassland. Glob. Change Biol. 12, 1315–1329. https://doi.org/10.1111/j.1365-2486.2006.01169.x

Schweissing, M.M., Grupe, G., 2003. Stable strontium isotopes in human teeth and bone: a key to migration events of the late Roman period in Bavaria. J. Archaeol. Sci. 30, 1373–1383. https://doi.org/10.1016/S0305-4403(03)00025-6

Seitsonen, O., Houle, J.-L., Broderick, L.G., 2014. GIS approaches to past mobility and accessibility: An example from the Bronze Age Khanuy Valley, Mongolia. Past Mobilities Archaeol. Approaches Mov. Mobil. 79–110.

Sharp, Z., 2007. Principles of stable isotope geochemistry. Pearson education Upper Saddle River, NJ.

Sharp, Z.D., Atudorei, V., Panarello, H.O., Fernández, J., Douthitt, C., 2003. Hydrogen isotope systematics of hair: archeological and forensic applications. J. Archaeol. Sci. 30, 1709–1716. https://doi.org/10.1016/S0305-4403(03)00071-2

Silver, I.A., 1963. The Ageing of Domestic Animals. Sci. Archaeol. Compr. Surv. Prog. Res. 250.

Slivinska, K., Kopij, G., 2011. Diet of the Przewalski's horse Equus przewalskii in the Chernobyl exclusion zone. Pol. J. Ecol. 59, 841–847.

Slovak, N.M., Paytan, A., 2012. Applications of Sr Isotopes in Archaeology, in: Baskaran, M. (Ed.), Handbook of Environmental Isotope Geochemistry, Advances in Isotope Geochemistry. Springer Berlin Heidelberg, pp. 743–768. https://doi.org/10.1007/978-3-642-10637-8_35

Smedley, M.P., Dawson, T.E., Comstock, J.P., Donovan, L.A., Sherrill, D.E., Cook, C.S., Ehleringer, J.R., 1991. Seasonal carbon isotope discrimination in a grassland community. Oecologia 85, 314–320. https://doi.org/10.1007/BF00320605

Smith, T.M., Tafforeau, P., 2008. New visions of dental tissue research: Tooth development, chemistry, and structure. Evol. Anthropol. Issues News Rev. 17, 213–226. https://doi.org/10.1002/evan.20176

Snoeck, C., Ryan, S., Pouncett, J., Pellegrini, M., Claeys, P., Wainwright, A.N., Mattielli, N., Lee-Thorp, J.A., Schulting, R.J., 2019. Towards a biologically available strontium isotope baseline for Ireland. Sci. Total Environ. 136248. https://doi.org/10.1016/j.scitotenv.2019.136248

Söllner, F., Toncala, A., Hölzl, S., Grupe, G., 2016. Determination of Geo-dependent Bioavailable $^{87}Sr/^{86}Sr$ Isotopic Ratios for Archaeological Sites from the Inn Valley (Austria): A Model Calculation, in: Isotopic Landscapes in Bioarchaeology. Springer, Berlin, Heidelberg, pp. 123–140. https://doi.org/10.1007/978-3-662-48339-8_7

Solounias, N., Semprebon, G., 2002. Advances in the Reconstruction of Ungulate Ecomorphology with Application to Early Fossil Equids. Am. Mus. Novit. 225, 1–49. https://doi.org/10.1206/0003-0082(2002)366<0001:AITROU>2.0.CO;2

Sponheimer, M., Robinson, T., Ayliffe, L., Passey, B., Roeder, B., Shipley, L., Lopez, E., Cerling, T., Dearing, D., Ehleringer, J., 2003a. An experimental study of carbon-isotope fractionation between diet, hair, and feces of mammalian herbivores. Can. J. Zool. 81, 871–876. https://doi.org/10.1139/z03-066

Sponheimer, M., Robinson, T., Ayliffe, L., Roeder, B., Hammer, J., Passey, B., West, A., Cerling, T., Dearing, D., Ehleringer, J., 2003b. Nitrogen isotopes in mammalian herbivores: hair $\delta^{15}N$ values from a controlled feeding study. Int. J. Osteoarchaeol. 13, 80–87. https://doi.org/10.1002/oa.655

Stacy, E.M., 2009. Stable Isotopic Analysis of Equid (Horse) Teeth from Mongolia. University of Pittsburgh.

Stépanoff, C., Ferret, C., Lacaze, G., Thorez, J., 2013. Nomadismes d'Asie centrale et septentrionale. Armand Colin.

Stewart, G.R., Turnbull, M.H., Schmidt, S., Erskine, P.D., 1995. 13C Natural Abundance in Plant Communities Along a Rainfall Gradient: a Biological Integrator of Water Availability. Funct. Plant Biol. 22, 51–55. https://doi.org/10.1071/pp9950051

Still, C.J., Berry, J.A., Collatz, G.J., DeFries, R.S., 2003. Global distribution of C3 and C4 vegetation: Carbon cycle implications. Glob. Biogeochem. Cycles 17, 6-1-6–14. https://doi.org/10.1029/2001GB001807

Straight, W.H., Barrick, R.E., Eberth, D.A., 2004. Reflections of surface water, seasonality and climate in stable oxygen isotopes from tyrannosaurid tooth enamel. Palaeogeogr. Palaeoclimatol. Palaeoecol., Incremental Growth in Vertebrate Skeletal Tissues: Paleobiological and Paleoenvironmental Implications 206, 239–256. https://doi.org/10.1016/j.palaeo.2004.01.006

Stuart-Williams, H.L.Q., Schwarcz, H.P., 1997. Oxygen isotopic determination of climatic variation using phosphate from beaver bone, tooth enamel, and dentine. Geochim. Cosmochim. Acta 61, 2539–2550. https://doi.org/10.1016/S0016-7037(97)00112-9

Stutz, A.J., 2002. Polarizing Microscopy Identification of Chemical Diagenesis in Archaeological Cementum. J. Archaeol. Sci. 29, 1327–1347. https://doi.org/10.1006/jasc.2001.0805

Suess, H.E., 1955. Radiocarbon Concentration in Modern Wood. Science 122, 415–417.

Suga, S., 1982. Progressive mineralization pattern of developing enamel during the maturation stage. J. Dent. Res. Spec No, 1532–1542.

Suga, S., Murayama, Y., Musashi, T., 1970. A study of the mineralization process in the developing enamel of guinea pigs. Arch. Oral Biol. 15, 597-IN15. https://doi.org/10.1016/0003-9969(70)90129-9

Szpak, P., 2014. Complexities of nitrogen isotope biogeochemistry in plant-soil systems: implications for the study of ancient agricultural and animal management practices. Front. Plant Sci. 5. https://doi.org/10.3389/fpls.2014.00288

Szpak, P., White, C.D., Longstaffe, F.J., Millaire, J.-F., Sánchez, V.F.V., 2013. Carbon and Nitrogen Isotopic Survey of Northern Peruvian Plants: Baselines for Paleodietary and Paleoecological Studies. PLOS ONE 8, e53763. https://doi.org/10.1371/journal.pone.0053763

Tafforeau, P., Bentaleb, I., Jaeger, J.-J., Martin, C., 2007. Nature of laminations and mineralization in rhinoceros enamel using histology and X-ray synchrotron microtomography: Potential implications for palaeoenvironmental isotopic studies. Palaeogeogr. Palaeoclimatol. Palaeoecol. 246, 206–227. https://doi.org/10.1016/j.palaeo.2006.10.001

Taylor, W., 2017. Horse demography and use in Bronze Age Mongolia. Quat. Int. 436, 270–282. https://doi.org/10.1016/j.quaint.2015.09.085

Taylor, W., Jargalan, B., Lowry, K., Clark, J., Tuvshinjargal, T., Bayarsaikhan, J., 2017. A Bayesian chronology for early domestic horse use in the Eastern Steppe. J. Archaeol. Sci. 81, 49–58. https://doi.org/10.1016/j.jas.2017.03.006

Teaford, M.F., 2007. What do we know and not know about dental microwear and diet, in: Evolution of the Human Diet: The Known, the Unknown and the Unknowable. Oxford University Press, pp. 106–132.

Tejada-Lara Julia V., MacFadden Bruce J., Bermudez Lizette, Rojas Gianmarco, Salas-Gismondi Rodolfo, Flynn John J., 2018. Body mass predicts isotope enrichment in

herbivorous mammals. Proc. R. Soc. B Biol. Sci. 285, 20181020. https://doi.org/10.1098/rspb.2018.1020

Thomsen, E., Andreasen, R., 2019. Agricultural lime disturbs natural strontium isotope variations: Implications for provenance and migration studies. Sci. Adv. 5, eaav8083. https://doi.org/10.1126/sciadv.aav8083

Tieszen, L.L., Senyimba, M.M., Imbamba, S.K., Troughton, J.H., 1979. The distribution of C<Subscript>3</Subscript> and C<Subscript>4</Subscript> grasses and carbon isotope discrimination along an altitudinal and moisture gradient in Kenya. Oecologia 37, 337–350. https://doi.org/10.1007/BF00347910

Tornero, C., Aguilera, M., Ferrio, J.P., Arcusa, H., Moreno-García, M., Garcia-Reig, S., Rojo-Guerra, M., 2018. Vertical sheep mobility along the altitudinal gradient through stable isotope analyses in tooth molar bioapatite, meteoric water and pastures: A reference from the Ebro valley to the Central Pyrenees. Quat. Int., Casting a glance over the mountain – multi-proxy approaches to the understanding of vertical mobility 484, 94–106. https://doi.org/10.1016/j.quaint.2016.11.042

Tornero, C., Balasse, M., Bălăşescu, A., Chataigner, C., Gasparyan, B., Montoya, C., 2016. The altitudinal mobility of wild sheep at the Epigravettian site of Kalavan 1 (Lesser Caucasus, Armenia): Evidence from a sequential isotopic analysis in tooth enamel. J. Hum. Evol. 97, 27–36. https://doi.org/10.1016/j.jhevol.2016.05.001

Towers, J., Jay, M., Mainland, I., Nehlich, O., Montgomery, J., 2011. A calf for all seasons? The potential of stable isotope analysis to investigate prehistoric husbandry practices. J. Archaeol. Sci. 38, 1858–1868. https://doi.org/10.1016/j.jas.2011.03.030

Towers, J., Montgomery, J., Evans, J., Jay, M., Pearson, M.P., 2010. An investigation of the origins of cattle and aurochs deposited in the Early Bronze Age barrows at Gayhurst and Irthlingborough. J. Archaeol. Sci. 37, 508–515. https://doi.org/10.1016/j.jas.2009.10.012

Trautz, O.R., 1967. Crystalline organization of dental mineral, in: Structural and Chemical Organization of Teeth. Elsevier, pp. 165–200.

Trayler, R.B., Kohn, M.J., 2017. Tooth enamel maturation reequilibrates oxygen isotope compositions and supports simple sampling methods. Geochim. Cosmochim. Acta 198, 32–47. https://doi.org/10.1016/j.gca.2016.10.023

Trentacoste, A., Lightfoot, E., Le Roux, P., Buckley, M., Kansa, S.W., Esposito, C., Gleba, M., 2020. Heading for the hills? A multi-isotope study of sheep management in first-millennium BC Italy. J. Archaeol. Sci. Rep. 29, 102036. https://doi.org/10.1016/j.jasrep.2019.102036

Tucker, L., Favreau, J., Itambu, M., Larter, F., Mollel, N., Mwambwiga, A., Patalano, R., Roberts, P., Soto, M., Mercader, J., 2020. Initial assessment of bioavailable strontium at Oldupai Gorge, Tanzania: Potential for early mobility studies. J. Archaeol. Sci. 114, 105066. https://doi.org/10.1016/j.jas.2019.105066

Unkelbach, J., Dulamsuren, C., Punsalpaamuu, G., Saindovdon, D., Behling, H., 2018. Late Holocene vegetation, climate, human and fire history of the forest-steppe-ecosystem inferred from core G2-A in the ‘Altai Tavan Bogd’ conservation area in Mongolia. Veg. Hist. Archaeobotany 27, 665–677. https://doi.org/10.1007/s00334-017-0664-5

Upex, B., Dobney, K., 2012. Dental enamel hypoplasia as indicators of seasonal environmental and physiological impacts in modern sheep populations: a model for interpreting the zooarchaeological record. J. Zool. 287, 259–268.

van Dam, J.A., Reichart, G.J., 2009. Oxygen and carbon isotope signatures in late Neogene horse teeth from Spain and application as temperature and seasonality proxies. Palaeogeogr. Palaeoclimatol. Palaeoecol. 274, 64–81. https://doi.org/10.1016/j.palaeo.2008.12.022

van de Water, P.K., Leavitt, S.W., Betancourt, J.L., 2002. Leaf $\delta^{13}C$ variability with elevation, slope aspect, and precipitation in the southwest United States. Oecologia 132, 332–343. https://doi.org/10.1007/s00442-002-0973-x

Ventresca Miller, A.R., Bragina, T.M., Abil, Y.A., Rulyova, M.M., Makarewicz, C.A., 2018. Pasture usage by ancient pastoralists in the northern Kazakh steppe informed by carbon and nitrogen isoscapes of contemporary floral biomes. Archaeol. Anthropol. Sci. https://doi.org/10.1007/s12520-018-0660-4

Ventresca Miller, A.R., Makarewicz, C.A., 2017. Isotopic approaches to pastoralism in prehistory : Diet, mobility, and isotopic reference sets, in: Isotopic Investigations of Pastoralism in Prehistory. Routledge, London, pp. 9–22. https://doi.org/10.4324/9781315143026-1

Ventresca Miller, A.R., Winter-Schuh, C., Usmanova, E.R., Logvin, A., Shevnina, I., Makarewicz, C.A., 2017. Pastoralist Mobility in Bronze Age Landscapes of Northern Kazakhstan: $^{87}Sr/^{86}Sr$ and $\delta^{18}O$ Analyses of Human Dentition from Bestamak and Lisakovsk. Environ. Archaeol. 0, 1–15. https://doi.org/10.1080/14614103.2017.1390031

Vigne, J.-D., 2017. Les débuts de l'élevage. Humensis.

Vigne, J.-D., Helmer, D., 2007. Was milk a "secondary product" in the Old World Neolithisation process? Its role in the domestication of cattle, sheep and goats. Anthropozoologica 42, 9–40.

Viner, S., Evans, J., Albarella, U., Pearson, M.P., 2010. Cattle mobility in prehistoric Britain: strontium isotope analysis of cattle teeth from Durrington Walls (Wiltshire, Britain). J. Archaeol. Sci. 37, 2812–2820.

Vitousek, P.M., Shearer, G., Kohl, D.H., 1989. Foliar 15N natural abundance in Hawaiian rainforest: patterns and possible mechanisms. Oecologia 78, 383–388.

Vroon, P.Z., van der Wagt, B., Koornneef, J.M., Davies, G.R., 2008. Problems in obtaining precise and accurate Sr isotope analysis from geological materials using laser ablation MC-ICPMS. Anal. Bioanal. Chem. 390, 465–476. https://doi.org/10.1007/s00216-007-1742-9

Wang, C., Liu, D., Luo, W., Fang, Y., Wang, X., Lü, X., Jiang, Y., Han, X., Bai, E., 2016. Variations in leaf carbon isotope composition along an arid and semi-arid grassland transect in northern China. J. Plant Ecol. 9, 576–585. https://doi.org/10.1093/jpe/rtw006

Wang, G., Jia, Y., Li, W., 2015. Effects of environmental and biotic factors on carbon isotopic fractionation during decomposition of soil organic matter. Sci. Rep. 5, 11043. https://doi.org/10.1038/srep11043

Weber, M., Lugli, F., Jochum, K.P., Cipriani, A., Scholz, D., 2018. Calcium Carbonate and Phosphate Reference Materials for Monitoring Bulk and Microanalytical Determination of Sr Isotopes. Geostand. Geoanalytical Res. 42, 77–89. https://doi.org/10.1111/ggr.12191

Weinreb, M.M., Sharav, Y., 1964. Tooth development in sheep. Am. J. Vet. Res. 25, 891–908.

West, A.G., Ayliffe, L.K., Cerling, T.E., Robinson, T.F., Karren, B., Dearing, M.D., Ehleringer, J.R., 2004. Short-term diet changes revealed using stable carbon isotopes in horse tail-hair. Funct. Ecol. 18, 616–624.

West, A.G., February, E.C., Bowen, G.J., 2014. Spatial analysis of hydrogen and oxygen stable isotopes ("isoscapes") in ground water and tap water across South Africa. J. Geochem. Explor. 145, 213–222. https://doi.org/10.1016/j.gexplo.2014.06.009

Widga, C., Walker, J.D., Boehm, A., 2017. Variability in bioavailable $^{87}Sr/^{86}Sr$ in the north american midcontinent. Open Quat. 3. http://dx.doi.org/10.5334/oq.32

Widga, C., Walker, J.D., Stockli, L.D., 2010. Middle Holocene Bison diet and mobility in the eastern Great Plains (USA) based on $\delta^{13}C$, $\delta^{18}O$, and $^{87}Sr/^{86}Sr$ analyses of tooth enamel carbonate. Quat. Res. 73, 449–463. https://doi.org/10.1016/j.yqres.2009.12.001

Willmes, M., Bataille, C.P., James, H.F., Moffat, I., McMorrow, L., Kinsley, L., Armstrong, R.A., Eggins, S., Grün, R., 2018. Mapping of bioavailable strontium isotope ratios in France for archaeological provenance studies. Appl. Geochem. 90, 75–86. https://doi.org/10.1016/j.apgeochem.2017.12.025

Wilson, A.S., Tobin, D.J., 2010. Hair After Death, in: Trüeb, R.M., Tobin, D.J. (Eds.), Aging Hair. Springer, Berlin, Heidelberg, pp. 249–261. https://doi.org/10.1007/978-3-642-02636-2_24

Wingard, G.J., Harris, R.B., Pletscher, D.H., Bedunah, D.J., Mandakh, B., Amgalanbaatar, S., Reading, R.P., 2011. Argali food habits and dietary overlap with domestic livestock in Ikh Nart Nature Reserve, Mongolia. J. Arid Environ. 75, 138–145.

Winter, N.J. de, Snoeck, C., Claeys, P., 2016. Seasonal Cyclicity in Trace Elements and Stable Isotopes of Modern Horse Enamel. PLOS ONE 11, e0166678. https://doi.org/10.1371/journal.pone.0166678

Winter-Schuh, C., 2017. Investigating seasonal changes of cattle diet in terrestrial C_3 biomes through the isotopic analysis of serially sampled tooth enamel, in: Isotopic Investigations of Pastoralism in Prehistory. Routledge, pp. 29–39.

Wittemyer, G., Cerling, T.E., Douglas-Hamilton, I., 2009. Establishing chronologies from isotopic profiles in serially collected animal tissues: An example using tail hairs from African elephants. Chem. Geol., Combined Ecological and Geologic Perspectives in Ecosystem Studies 267, 3–11. https://doi.org/10.1016/j.chemgeo.2008.08.010

Wood, S., Scheipl, F., 2017. gamm4: Generalized Additive Mixed Models using mgcv and lme4. R.

Wooller, M., Smallwood, B., Scharler, U., Jacobson, M., Fogel, M., 2003. A taphonomic study of $\delta^{13}C$ and $\delta^{15}N$ values in Rhizophora mangle leaves for a multi-proxy approach to mangrove palaeoecology. Org. Geochem. 34, 1259–1275. https://doi.org/10.1016/S0146-6380(03)00116-5

Wright, J., 2007. Organizational principles of Khirigsuur monuments in the lower Egiin Gol valley, Mongolia. J. Anthropol. Archaeol. 26, 350–365. https://doi.org/10.1016/j.jaa.2007.04.001

Wright, J., Honeychurch, W., Amartuvshin, C., 2009. The Xiongnu settlements of Egiin Gol, Mongolia. Antiquity 83, 372–387. https://doi.org/10.1017/S0003598X00098495

Wright, J., Makarewicz, C., 2015. Perceptions of pasture: the role of skill and networks in maintaining stable pastoral nomadic systems in Inner Asia, in: Climate and Ancient Societies. S Kerner, R Dann, PB Jensen, Copenhagen, pp. 267–288.

Yi, X.F., Yang, Y.Q., others, 2006. Enrichment of stable carbon and nitrogen isotopes of plant populations and plateau pikas along altitudes. J. Anim. Feed Sci. 15, 661.

Zazzo, A., Balasse, M., Passey, B.H., Moloney, A.P., Monahan, F.J., Schmidt, O., 2010. The isotope record of short- and long-term dietary changes in sheep tooth enamel: Implications for quantitative reconstruction of paleodiets. Geochim. Cosmochim. Acta 74, 3571–3586. https://doi.org/10.1016/j.gca.2010.03.017

Zazzo, A., Balasse, M., Patterson, W.P., 2005. High-resolution $\delta^{13}C$ intratooth profiles in bovine enamel: Implications for mineralization pattern and isotopic attenuation. Geochim. Cosmochim. Acta 69, 3631–3642. https://doi.org/10.1016/j.gca.2005.02.031

Zazzo, A., Bendrey, R., Vella, D., Moloney, A.P., Monahan, F.J., Schmidt, O., 2012. A refined sampling strategy for intra-tooth stable isotope analysis of mammalian enamel. Geochim. Cosmochim. Acta 84, 1–13. https://doi.org/10.1016/j.gca.2012.01.012

Zazzo, A., Cerling, T.E., Ehleringer, J.R., Moloney, A.P., Monahan, F.J., Schmidt, O., 2015. Isotopic composition of sheep wool records seasonality of climate and diet. Rapid Commun. Mass Spectrom. 29, 1357–1369.

Zazzo, A., Harrison, S.M., Bahar, B., Moloney, A.P., Monahan, F.J., Scrimgeour, C.M., Schmidt, O., 2007. Experimental determination of dietary carbon turnover in bovine hair and hoof. Can. J. Zool. 85, 1239–1248.

Zazzo, A., Lécuyer, C., Mariotti, A., 2004. Experimentally-controlled carbon and oxygen isotope exchange between bioapatites and water under inorganic and microbially-mediated conditions. Geochim. Cosmochim. Acta 68, 1–12. https://doi.org/10.1016/S0016-7037(03)00278-3

Zazzo, A., Lepetz, S., Magail, J., Gantulga, J.-O., 2019. High-precision dating of ceremonial activity around a large ritual complex in Late Bronze Age Mongolia. Antiquity 93, 80–98. https://doi.org/10.15184/aqy.2018.175

Zazzo, A., Mariotti, A., Lécuyer, C., Heintz, E., 2002. Intra-tooth isotope variations in late Miocene bovid enamel from Afghanistan: paleobiological, taphonomic, and climatic implications. Palaeogeogr. Palaeoclimatol. Palaeoecol. 186, 145–161.

Zazzo, A., Moloney, A.P., Monahan, F.J., Scrimgeour, C.M., Schmidt, O., 2008. Effect of age and food intake on dietary carbon turnover recorded in sheep wool. Rapid Commun. Mass Spectrom. 22, 2937–2945. https://doi.org/10.1002/rcm.3693

Zeder, M.A., 2006. Reconciling rates of long bone fusion and tooth eruption and wear in sheep (*Ovis*) and goat (*Capra*), in: Recent Advances in Ageing and Sexing Animal Bones. pp. 87–118.

Zhang, Y., Qi, W., Zhou, C., Ding, M., Liu, L., Gao, J., Bai, W., Wang, Z., Zheng, D., 2014. Spatial and temporal variability in the net primary production of alpine grassland on the Tibetan Plateau since 1982. J. Geogr. Sci. 24, 269–287. https://doi.org/10.1007/s11442-014-1087-1

ANNEXE

ILLUSTRATIONS DES ÉLEVEURS ET DE LEURS TROUPEAUX

Éleveur 1 : DL

Cet éleveur nomadise peu dans l'année et uniquement entre deux vallées situées à plus de 2000 m d'altitude et distantes d'un peu moins de 10 km. Ce schéma de mobilité est assez différent de ce qui est généralement observé dans la région où la mobilité altitudinale est plus prononcée et les éleveurs nomadisent plus souvent. Le troupeau de cet éleveur a été suivi par GPS de septembre 2016 à juillet 2018.

Planche 1 : (**A**) vue du camp de Dl (2380 m) dans une vallée de haut altitude ; (**B, C et D**) un bouc, un cheval et un mouton équipés d'un collier GPS (Photos : C. Marchina & A. Zazzo – Sept. 2016).

Éleveur 2 : JK

Cet éleveur nomadise régulièrement dans l'année sur un axe est-ouest (voir figure 5) entre des pâtures de plaines, vers une zone humide, jusqu'aux pâtures de haute altitude, en passant par des campements en bas des vallées de montagne. Son troupeau a été suivi par GPS de juin 2015 à juillet 2018.

Planche 2 : (**A, B & D**) le cheval, un mouton et un bouc équippés d'un collier GPS en septembre 2016. (**C**) vue du troupeau gardé par l'éleveur ; (**E**) vue du camp en septembre se situant dans la plaine proche de la zone humide juxtant le village de Nogoonnuur (Photos : C. Marchina, A. Zazzo & N. Lazzerini – Sept. 2016).

Éleveur 3 : KB

Cet éleveur nomadise régulièrement également sur un axe est-ouest entre des pâtures de plaines vers une zone humide, jusqu'aux pâtures de haute altitude, en passant par des campements en bas des vallées de montagne. Son troupeau a été suivi par GPS de juin 2015 à juillet 2018.

Planche 3 : (**A, B**) caprinés équippés de colliers GPS avant leur échantillonnage en septembre 2016. (**C**) l'éleveur avec son cheval, qui a été monitoré, en novembre 2017 dans à son campement d'hiver. (**D**) le troupeau à côté du campement en plaine, au petit matin, avant d'être envoyé pâturer – sept. 2016. (Photos : © C. Marchina, A. Zazzo & N. Lazzerini).

Éleveur 4 : KJ

Cet éleveur nomadise régulièrement dans l'année sur un axe est-ouest (voir figure 5) plus au nord que les éleveurs Jk et Kb. Son troupeau a été suivi par GPS de juin 2015 à juillet 2018.

Planche 4 : (**A, B**) le même mouton en juin 2015 et septembre 2016 avant son abattage. (**C & D**) vue du campement d'hiver en novembre 2017. (**E**) cheval de monte équippé d'un collier GPS en juin 2015. (Photos : © C. Marchina & A. Zazzo).

Eleveur 5 : ZK

Cet éleveur nomadise régulièrement dans l'année sur un axe NE-SO entre les deux provinces, établit un campment d'été en altitude au SO de la zone d'étude. Son troupeau a été suivi par GPS de septembre 2016 à novembre 2017.

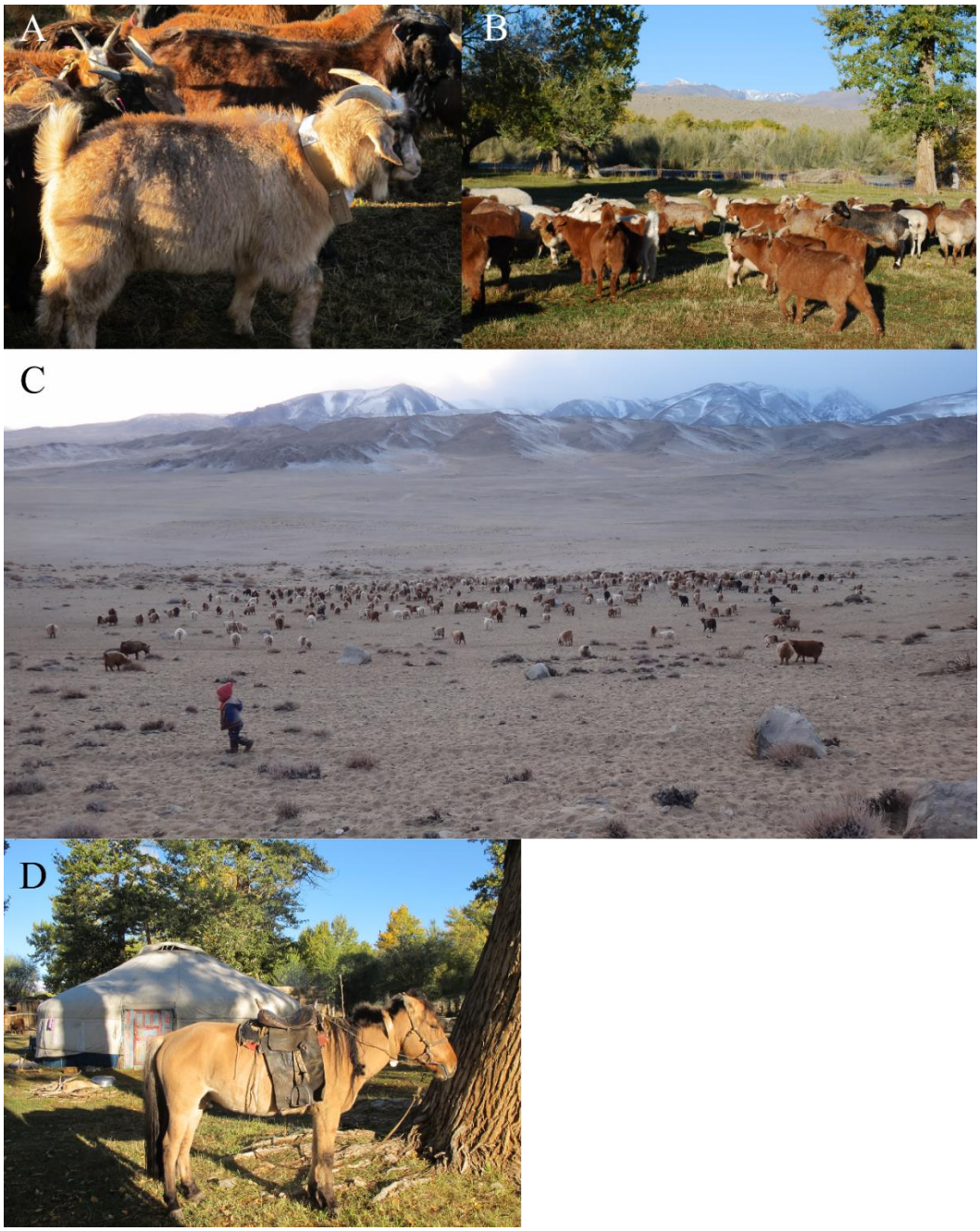

Planche 5 : (**A, B**) troupeau de caprinés en septembre 2016 proche de la rivière séparant les deux provicnesz. (**C**) troupeau en novembre 2017 proche du campement d'hiver que l'éleveur ZK partage avec l'éleveur KJ car ils font partie de la même famille. (**D**) le cheval attaché au campement en septembre 2016.

Résumé

Les sociétés pastorales laissent des marques discrètes dans le registre archéologique. De ce fait, la description et la caractérisation fines des interactions homme-animal-environnement dans le passé au sein de ces sociétés est difficile. L'analyse isotopique des tissus biologiques des animaux d'élevage est une clé d'entrée pour comprendre ces interactions car elle livre des informations sur l'histoire alimentaire, la mobilité et l'environnement de ces animaux. Cette approche nécessite néanmoins la mise en place de référentiels actuels de qualité afin d'interpréter correctement les résultats obtenus en contexte archéologique. Le présent travail a pour objectif de valider des marqueurs isotopiques (C, N, O, Sr) de la mobilité pastorale et de la date de mort du bétail. Nous avons pour cela équipé de colliers GPS le bétail (cheval, mouton, chèvre) de plusieurs troupeaux appartenant à des éleveurs nomades de l'Altaï mongol et exploité les données issues de l'analyse isotopique séquentielle des tissus biologiques à croissance continue ou prolongée (poil, dent) de ces animaux.

Nos résultats montrent que les déplacements fréquents des animaux compliquent l'interprétation des variations isotopiques enregistrées par les crins des chevaux. En revanche, la valeur moyenne de $\delta^{13}C$ du poil et de l'émail ainsi que l'anticovariation entre les valeurs de $\delta^{13}C$ et $\delta^{18}O$ mesurées dans l'émail peuvent être exploitées pour inférer la mobilité altitudinale des animaux et le taux d'occupation des étages alpins. La cartographie isotopique en strontium de la zone d'étude nous a permis de discuter l'utilisation des variations isotopiques en Sr de l'émail pour retracer l'origine géographique et les déplacements des animaux. Enfin, la modélisation des séquences saisonnières enregistrées par le $\delta^{18}O$ de l'émail donne accès à la date de mort des caprinés avec une précision de l'ordre du mois. L'analyse isotopique de l'émail des chevaux archéologiques trouvés en contexte rituel et funéraire dans la zone d'étude conduit à proposer une origine locale couplée à une utilisation des pâtures d'altitude dès l'âge du Bronze. Elle révèle également l'existence d'un calendrier de subsistance favorisant un abattage hivernal des chevaux.

Mots clés : pastoralisme ; bétail ; cheval ; caprinés ; émail ; kératine ; saison d'abattage ; GPS ; âge du Bronze ; période Türk ; ablation laser ; isoscape.

Abstract

Pastoral societies leave discrete marks in the archaeological record. As a result, the fine description and characterisation of past interactions between human-animal-environment within these societies is difficult. The isotopic analysis of the biological tissues of herd animals is a key entry point for understanding these interactions because it provides information on their feeding history, mobility and environment. However, this approach requires the establishment of robust reference sets in order to correctly interpret the results obtained on the archaeological material. The aim of this work was to validate isotope markers (C, N, O, Sr) of pastoral mobility and of the date of death of livestock. To this end, we equipped modern livestock (horse, sheep, goat) belonging to nomadic herders in the Mongolian Altai with GPS collars and analysed the isotopic composition of their biological tissues (hair, teeth) using sequential sampling.

Our results show that frequent animal movements complicate the interpretation of isotope variations recorded by horse hair. On the other hand, the average $\delta^{13}C$ value of hair and enamel and the anticovariation between $\delta^{13}C$ and $\delta^{18}O$ values measured in enamel can be used to infer the altitudinal mobility of the animals and the occupancy rate of alpine pastures. Strontium isotope mapping of the study area allowed us to discuss the use of Sr isotope variations in enamel to trace the geographical origin and movements of animals. Finally, modelling of the oxygen isotope time series in tooth enamel gives access to the date of death of caprines with an accuracy of a month. The isotopic analysis of the archaeological horses found in ritual and funerary contexts of the study area suggests a local origin together with the use of high altitude pastures as early as the Bronze Age. It also reveals the existence of a subsistence calendar favouring the winter slaughter of these horses.

Keywords : pastoralism ; livestock ; horse; caprines; enamel ; keratin ; slaughtering season ; GPS ; Bronze age ; Turkic period ; laser ablation.; isoscape.